MODEL APPLICATIONS IN WASTEWATER TREATMENT

MODEL APPLICATIONS ON NITROGEN AND MICROPLASTIC REMOVAL IN NOVEL WASTEWATER TREATMENT

By

Ahmed Tarek Fawzy Elsayed

B.Sc., M.Sc.

A Thesis Submitted to the School of Graduate Studies in Partial Fulfillment of the Requirements for the Degree of Doctor of Philosophy

McMaster University DOCTOR OF PHILOSOPHY (2021)

Hamilton, Ontario (Civil Engineering)

TITLE: Model applications on nitrogen and microplastic removal in novel wastewater treatment

AUTHOR: Ahmed Tarek Fawzy Elsayed, B.Sc., M.Sc., (Cairo University)

SUPERVISOR: Dr. Younggy Kim

NUMBER OF PAGES: xxi, 196.

Lay Abstract

Nitrogen and microplastic (MP) are serious contaminants in wastewater that can cause critical environmental and public health problems. Nitrogen can cause algal blooms, threatening the aquatic ecosystem while MP can be ingested by the biota (e.g., fish and seabirds), causing serious damage in the food chain. Nitrogen removal in the conventional biological wastewater treatment is relatively expensive, requiring high energy cost and large footprint for the wastewater treatment facilities. MP removal is also difficult in the conventional wastewater and sludge treatment processes. Therefore, new technologies, including membrane aerated biofilm reactor (MABR), anaerobic ammonia oxidation (Anammox) and hydrolytic enzymes processes, are implemented to improve the nitrogen and MP removal with a reduced energy and resources consumption in wastewater and sludge treatment processes. Numerical models are considered as an efficient tool for better understanding of these novel technologies and the competitive biological reaction in these technologies coupled with accurate estimation of process rates of the reactions. In this thesis, different numerical models were developed and calibrated to estimate the important model parameters, assess the effect of operational conditions on the removal mechanisms and determine the dominant parameters on the removal of nitrogen and MP in the wastewater treatment processes. These numerical models can be used for better understanding of the removal mechanisms of nitrogen and MP, helping in the design and operation of removal systems and addressing novel technologies in large-scale nitrogen and MP removal applications.

Abstract

Excessive release of nitrogen (e.g., ammonia and organic nitrogen) into natural water systems can cause serious environmental problems such as algal blooms and eutrophication in lakes and rivers, threating the aquatic life and ecosystem balance. Membrane aerated biofilm reactor (MABR) and anaerobic ammonia oxidation (Anammox) are new technologies for wastewater treatment with an emphasis on energy-efficient nitrification and denitrification. Microplastic (MP) is an emerging contaminant in wastewater and sludge treatment that has a negative effect on the environment and public health. For these relatively new technologies and contaminants, mathematical models can enhance our understanding of the removal mechanisms, such as reaction kinetics and mass transport. In this study, mathematical models were developed and utilized to simulate the removal of nitrogen and MP in biological reactions in wastewater treatment processes. Firstly, a comprehensive MABR model was developed and calibrated using a pilot-scale MABR operation data to estimate the important process parameters where it was found that biofilm thickness, liquid film thickness and C/N ratio are key parameters on nitrification and denitrification. Secondly, a mathematical model for Anammox process was developed and calibrated using previous experimental results to simulate the wastewater treatment using Anammox process, reflecting the importance of dissolved oxygen on the nitrogen removal using Anammox bacteria. Thirdly, a granule-based Anammox mathematical model was built and calibrated using other simulation results from previous Anammox studies, showing the significance of operational conditions (e.g., granule diameter and dissolved oxygen) on the success of Anammox enrichment process. Fourthly, an enzyme kinetic mathematical model was constructed and calibrated with lab-scale experiments to simulate the MP reduction using hydrolytic enzymes under various experimental conditions where it was found that

anaerobic digesters can be an innovative solution for MP removal during the wastewater treatment processes. Based on the main findings in this study, it can be concluded that mathematical models calibrated with various experimental results are efficient tools for determining the important operational parameters on the nitrogen and MP removal and helping in the design and operation of large-scale removal applications.

Preface

This thesis has been prepared in accordance with the guidelines of the sandwich thesis format from the School of graduate studies at McMaster University. Four papers are included in this thesis as listed below.

- Elsayed, A., Hurdle, M., Kim, Y., 2021. Comprehensive model applications for better understanding of pilot-scale membrane-aerated biofilm reactor performance. Journal of Water Process Engineering. 40, 101894.
- Elsayed, A., Kim, Y. Estimation of rate kinetic constants in microplastic degradation using hydrolytic enzymes.
- Elsayed, A., Kim, Y. Mathematical model application for real-time aeration based on nitrite level in Anammox process.
- Elsayed, A., Kim, Y. Sensitivity analysis on important kinetic constants in Anammox bacteria enrichment process using a mathematical model.

The first manuscript is presented in Chapter 2. The work was started in September 2017. The manuscript was submitted in October 2020 and accepted in April 2020. The work was conducted under the supervision of Dr. Younggy Kim. The manuscript is included in this thesis as it provided a novel nitrogen removal technology with a reduced energy cost. Michael Hurdle was responsible for operating the pilot site and collecting the MABR operation data. My contributions include:

- Model development and calibration with the pilot-scale operation data.
- Writing the manuscript.

The second manuscript is presented in Chapter 3. The work was started in January 2020. The work was conducted under the supervision of Dr. Younggy Kim. The manuscript is included in this thesis as it provided a novel microplastic technology using hydrolytic enzymes. My contributions include:

- Designing and building the reactors.
- Conducting the experiments.
- Data collection and analysis.
- Model development and calibration with the experimental results.
- Writing the manuscript.

The third manuscript is presented in Chapter 4. The work was started in March 2019. The work was conducted under the supervision of Dr. Younggy Kim. The manuscript is included in this thesis as it provided a novel nitrogen removal technology with a reduced organic carbon supply. My contributions include:

- Model development and calibration with the experimental results of previous studies.
- Writing the manuscript.

The fourth manuscript is presented in Chapter 5. The work was started in March 2019. The work was conducted under the supervision of Dr. Younggy Kim. The manuscript is included in this thesis as it provided a novel technology for the enrichment of Anammox bacteria. My contributions include:

- Model development and calibration with the experimental results of previous studies.
- Writing the manuscript.

Copyright permission

I have secured permission to include copyright material in this Ph.D. thesis from the copyright holder. The permission includes a grant of an irrevocable, non-exclusive license to McMaster University and to Library and Archives Canada to reproduce the material as part of the thesis.

Acknowledgements

First of all, I would like to express my gratitude to my supervisor Dr. Younggy Kim for his continuous support and guidance through my Ph.D. study. It was a great opportunity to work in his lab under his supervision, helping me to formulate a strong background in the wastewater treatment area. Thank you for sharing your academic experience with me and helping me to achieve this success. I would also like to thank my supervisory committee members Dr. Wael El-Dakhakhni, Dr. Zoe Li and Dr. Spencer Snowling for their valuable advices and feedback during the Ph.D. journey. A special thanks to Dr. El-Dakhakhni who always provides time, support and guidance for me in my academic and personal life. I would also like to thank the community of Civil Engineering Department at McMaster University for the beautiful time and amazing moments that I lived during my four years as a Ph.D. student. Of course, I can't forget my home university "Cairo University" and all my professors in Irrigation and Hydraulics Department as they prepared and formulated my academic and research skills at the beginning of my career.

I want also to thank my lifelong friends in McMaster University Dr. Maysara Ghaith, Dr. Ahmed Yosri, and Ahmed Ragaey for their inspiration and continuous support when I was depressed to continue this rough route. Also, I would like to thank the circumstances that allowed me to meet Dr. Yasser Al-Anany, Dr. Mohamed Yasser, Dr. Mohamed El-sefy, Dr. Ahmad Siam, Mohamed Salah Abou-youssief, Mohamed Gamal Ahmed and Mohamed El-ganzory during my accommodation in Hamilton. They were all available during my difficult times and tough stages in my life, so thank you for being here. I would like to thank my lifelong friend and brother Hazem Omar for his dedication and continuous support. Despite of being in two different continents, you are and will be always irreplaceable, my brother.

I want to finalize my acknowledgment with mentioning the most important persons in my life because they endured many difficulties to live this amazing moment with me and I know they have waited for a long time to see my success. I want to thank my wife “Nesma” for sharing the beautiful and stressful moments with me during my Ph.D.; she was always available and ready to hear me with love, passion and support. Thank you for your infinite motivation and for being here, my beloved wife. I want to thank my daughter “Laureen” for the love she gave to me and cheerful moments that I lived with her. You will remain the main source of my pleasure and happiness. I know that you are too young to recognize this right now, but one day you will definitely be proud of your father. Also, I would like to thank my second family “Nesma’s family” for their continuous support and motivation. I would like to thank my mother “Fatma” and my sister “Nourhan” for encouraging me with kind words and positive altitude during my hard times and critical moments. You are and will be always my backbone and main supporters in this tough life. Finally, I want to thank my father who passed away just four months before my final defense. He literally gave me everything: love, kindness, care and support. I wish that you were here to share this amazing moment with me and I know that you were always eager for attending my Ph.D. final defense. I promise that I will do my best to make you proud of me. You are always missed, my beloved father.

Table of contents

List of Figures

List of Tables

List of Symbols and nomenclatures

ΔP_{O2}	difference between inlet and exhaust oxygen partial pressure
θ_i	temperature correction factor for kinetic constant i
AD	anaerobic digestion
Anammox	anaerobic ammonia oxidation
ASM	activated sludge model
B_f	biofilm thickness
C/N	carbon-to-nitrogen
COD	chemical oxygen demand
D_i	diffusivity of soluble substrate i
DO	dissolved oxygen concentration
E_i	concentration of enzyme i
GS	granule size (diameter)
IWA	international water association
$k_{1,i}$	kinetic constant of MP reduction by enzyme i
$k_{2,ii}$	self-decay constant of enzyme i
$k_{2,CP}$	interactive-decay constant of cellulase and protease
K_H	Henry's law constant
L_f	liquid film thickness
L_{fence}	lower fence
MABR	membrane aerated biofilm reactor
MP	microplastic
NH_4-N	ammonia-nitrogen concentration
NO_2-N	nitrite-nitrogen concentration
NO_3-N	nitrate-nitrogen concentration
P_{O2}	oxygen partial pressure
PE	polyethylene

Q_1	first quartile
Q_2	second quartile
r	distance from the center of granule
RAS	returned activated sludge
RT	retention time
S_i	substrate of soluble component i
S_{COD}	COD concentration
S_{NH4}	ammonia concentration
S_{NO2}	nitrite concentration
$S_{NO_2}\|_{ON}$	nitrite threshold concentration
S_{NO3}	nitrate concentration
S_{O2}	oxygen concentration
SBR	sequence batch reactor
SEM	scanning electron microscope
SND	simultaneous nitrification and denitrification
TSS	total suspended solids
U_{fence}	upper fence
VSS	volatile suspended solids
x	distance from membrane surface
X_i	particulate component i
X_{AOB}	ammonia oxidizing bacteria
X_{ANA}	anaerobic ammonia oxidizing bacteria
X_H	heterotrophic bacteria
X_I	inert biomass
X_{NOB}	nitrite oxidizing bacteria
X_S	particulate COD

Declaration of Academic Achievement

Ahmed Elsayed was the main contributor to the four presented manuscripts in this thesis. The contributions from the co-authors are detailed at the beginning of each chapter.

1. Introduction

1.1 Overview

Excessive release of nitrogen nutrients (e.g., ammonia, nitrate, and organic nitrogen) into natural water systems can cause critical environmental problems such as algal blooms and eutrophication that can damage the aquatic ecosystem (Rodriguez-Sanchez et al., 2016; Tang et al., 2017; Ge et al., 2019). Therefore, nitrogen nutrient removal is important in modern biological wastewater treatment systems. In the conventional municipal wastewater treatment, ammonia and organic nitrogen are aerobically converted into nitrate by nitrifiers through nitrification process and further into nitrogen gas through denitrification processes by heterotrophs under anoxic conditions (Pereira et al., 2017; Ma et al., 2020). However, nitrification and denitrification requires high oxygen demands (increasing the aeration cost) coupled with an additional organic carbon supply (Martin and Nerenberg, 2012). Also, long solids retention time (increasing the pumping cost) and large footprint are necessary for successful nitrogen removal (Terada et al., 2003). The sludge production rate (disposal cost) and greenhouse gases emission rate (environmental aspect) are relatively high in the conventional biological wastewater treatment processes (Eskicioglu et al., 2018; Conthe et al., 2019). Therefore, nitrogen removal in the biological wastewater treatment processes is a key challenge, requiring novel technologies for efficient removal with a reduced energy cost. Membrane aerated biofilm reactor (MABR) and anaerobic ammonia oxidation (Anammox) are two innovative technologies for nitrogen removal and can be used as promising alternatives for conventional treatment methods with a reduced

operation cost, greenhouse gases emission and facility size (Xu et al., 2015; Perez-Calleja et al., 2017; Goswami et al., 2018; Guo et al., 2020).

Microplastic (MP) is considered as an emerging contaminant in wastewater treatment processes. MP can cause critical environmental problem to the biota (e.g., fish and seabirds) and public health problem (Auta et al., 2017; Silva et al., 2018). Wastewater treatment plants are considered as an active source for discharging MP to the environment (Mason et al., 2016; Gies et al., 2018). MP removal is a key challenge in biological wastewater treatment due to difficulties in MP degradation during the treatment processes. Also, potential bypass of MP from wastewater to sludge treatment process is one of the common challenges in MP removal applications (Edo et al., 2020). Therefore, a novel MP removal technique using hydrolytic enzymes was proposed and examined in this study and can be implemented in sludge treatment process where enzymes are rich in concentration.

Mathematical modeling of the novel technologies for nitrogen and MP removal is essential to comprehensively describe the rate mechanisms and identify the complex correlation between the process parameters in the removal reactions (Vannecke et al., 2015; Baeten et al., 2019). Mathematical models can also be used for assessing the performance of these technologies under various operational conditions. Moreover, models calibration using experimental/pilot-scale data is essential to determine realistic ranges of the important process parameters. Therefore, mathematical modeling coupled with experimental work can lead to better conceptual understanding for the nitrogen and MP removal as the level of complexity can be selected based on the resources availability and aimed accuracy (Liu et al., 2016; Wang et al., 2016).

1.2 Nitrogen removal using membrane aerated biofilm reactor (MABR)

MABR is a promising technology for simultaneous nitrification and denitrification where air is provided through gas-permeable membrane fibers to form a biofilm on the membrane surface (Lin et al., 2016; Xu et al., 2020). As a result, the inner layers of the biofilm become aerobic zone for nitrification while the outer layers of the biofilm are anoxic zone for denitrification (Shanahan and Semmens 2015; Chaali et al., 2018). The soluble components, except of oxygen, are diffused from the bulk solution to the biofilm while the oxygen is transported through the membrane fibers, causing a counter diffusion mechanism that prevents the competition between heterotrophic bacteria and nitrifiers for oxygen (Satoh et al., 2004; Nerenberg, 2016).

In previous MABR studies, lab-scale experiments were conducted to examine the nitrification (Satoh et al., 2000; Terada et al., 2006), simultaneous nitrification and denitrification (Liu et al., 2010; Lin et al., 2016), simultaneous COD and nitrogen removal (Hibiya et al., 2003; Hu et al., 2008) and high-strength wastewater treatment (e.g., animal manure waste) (Brindle et al., 1999; Terada et al., 2003). Also, mathematical models were developed in previous MABR model studies to assess the effect of the operational conditions on nitrogen removal in MABR (Shanahan and Semmens, 2004; Li et al., 2018), describe the microbial communities in the biofilm (van Loosdrecht et al., 2002) and identify the removal mechanisms in MABR operation (Nicolella et al., 2000; Syron and Casey, 2008a). Moreover lab-scale experimental work and mathematical modeling were combined in previous MABR studies to highlight the importance of oxygen concentration (Hwang et al., 2009; Wang et al., 2009), C/N (carbon-to-nitrogen)

ratio and biofilm thickness (Matsumoto et al., 2007), and pH (Shanahan and Semmens, 2015) on the removal of nitrogen in MABR.

Operational conditions play a dominant role in COD and nitrogen removal in MABR. In other MABR studies, it was found that the oxygen concentration at the membrane surface and bulk solution is a governing factor on the nitrogen removal efficiency in MABR (Gonzalez – Brambila et al., 2006; Terada et al., 2006; Downing and Nerenberg, 2008). Also, the influent ammonia loading rate, C/N ratio and influent COD concentration controlled the competition between the different involved microbes (e.g., autotrophs and heterotrophs) and nitrogen removal in MABR biofilms (LaPara et al., 2006; Lackner et al., 2010). Moreover, denitrification can be significantly enhanced by correlating the oxygen flux with the influent COD and ammonia concentrations (Matsumoto et al., 2007). However, there are no systematic studies to investigate the effect of the C/N ratio on nitrification for high-strength wastewater (e.g., downstream liquid from dewatering processes with higher levels of ammonia nitrogen than typical municipal wastewater) in MABR. Also, the effect of liquid film thickness (i.e., boundary diffusive layer between the biofilm and bulk) on simultaneous nitrification and denitrification in MABR has not been well investigated.

Comprehensive mathematical models, describing the biological reactions and mass transport in the biofilm, biological reactions in the bulk solution and the oxygen partial pressure along the membrane fiber, are an efficient tool to detect the complicated relations between various model parameters in the MABR operation. The models calibration with MABR pilot-scale operation data is significantly important as some model parameters (e.g., diffusivity of soluble substrates and liquid film thickness) are

difficult to be measured during the MABR operation (Arcangeli and Arvin, 1999; Syron and Casey, 2008b). Therefore, calibration process can lead to robust models for determining realistic ranges of these model parameters. However, there are no previous model calibration studies using MABR pilot-scale operation data to estimate the important parameters in MABR (e.g., biofilm thickness and liquid film thickness).

1.3 Microplastic (MP) removal using hydrolytic enzymes

MP is an emerging contaminant in wastewater with a particle size smaller than 5 mm (Blair et al., 2019; Magni et al., 2019). MP is highly mobile in the aquatic environment because of its light-weight and insolubility in water (Holland et al., 2016; Murphy et al., 2016). They can cause critical environmental and public health problems (Pettipas et al., 2016; Wright and Kelly, 2017) such as releasing plastic additives and toxic monomers and in the organs of biota (Anderson et al., 2017), damaging the respiratory and digestive system of humans (Revel et al., 2018) and accumulating heavy metals (e.g., zinc and lead) and hydrophobic organics pollutants (e.g., pesticides) (Gatidou et al., 2019; Sun et al., 2019).

MP can reach to the wastewater treatment plants through the raw wastewater, including synthetic fibers of clothes laundry and microbeads from personal care products (Cheung and Fok, 2017; Alvim et al., 2020). Also, MP is present in the sludge treatment process where MP concentration can be up to 56,000 MP particles per kg of dry sludge depending on the community lifestyle, wastewater source and treatment method (Mahon et al., 2017; Peng et al., 2017). Although there are various types of MP such as polyvinylchloride and polypropylene (Horton et al., 2017; Rezania et al., 2018),

polyethylene (PE) is the most common type of MP in wastewater and sludge treatment processes (Alimi et al., 2018; Wei et al., 2019). Therefore, the main focus was oriented towards PE-based MP beads in this study.

There are various MP removal mechanisms in the wastewater treatment processes, including chemical removal by coagulation (Hidayaturrahman and Lee, 2019), removal by ozone technology (Poerio et al., 2019), removal by rapid sand filtration (Michielssen et al., 2016) and removal by membrane disc-filter system (Talvitie et al., 2017). However, potential by-passing of small MP beads through the sand filtration and membrane clogging are considered as two of the key challenges on applying these technologies on large-scale removal applications. In biological wastewater treatment, it is difficult to remove MP beads because they are transported to the anaerobic digesters (Mintenig et al., 2017; Raju et al., 2020).

Although there are different applications for hydrolytic enzymes in wastewater and sludge treatment processes such as increasing the hydrolysis rate in anaerobic digestion process (Domingues et al., 2015; Odnell et al., 2016), limited systematic studies implemented these enzymes in the MP degradation applications (Othman et al., 2021). Moreover, there are no reported studies on the effect of operational conditions (e.g., temperature and enzyme dose) on the MP degradation. There is also a lack of numerical models for determining the MP removal mechanisms and the governing parameters using hydrolytic enzymes. Thus, the reaction kinetic constants of the MP degradation are unknown, resulting in an absence of prediction models for better understanding of MP degradation in anaerobic digesters and other biological treatment systems. Also, calibration of numerical models with experimental results is important for simulating the

MP degradation by hydrolytic enzymes, resulting in accurate determination of the reaction kinetics ranges.

1.4 Nitrogen removal by anaerobic ammonia oxidation (Anammox) process

Anammox is a relatively new technology for nitrogen removal by converting ammonia and nitrite into nitrogen gas without expensive aeration systems (Hauck et al., 2016; You et al., 2020). However, the biological reactions in the Anammox process are sensitive to the operational conditions, including dissolved oxygen (DO) concentration (Lotti et al., 2014; Yue et al., 2018), C/N ratio (Ni et al., 2012; Chen et al., 2016) and nitrite concentration (Lackner et al., 2008; Connan et al., 2016). Also, the competition between Anammox bacteria (X_{ANA}) and nitrite oxidizing bacteria (X_{NOB}) for nitrite is a dominant parameter on successful nitrogen removal by Anammox process (Ali and Okabe, 2015; Cao et al., 2017). However, there are no systematic modeling studies for describing this microbial competition for nitrogen compounds.

Different lab-scale Anammox studies proposed and examined potential experimental techniques to limit the competition between X_{ANA} and X_{NOB} such as intermittent aeration (Miao et al., 2017; Miao et al., 2018), wash-out of X_{NOB} (Gilmore et al., 2013; Laureni et al., 2016), maintaining residual ammonia concentration (Regmi et al., 2014) and sludge age (Kanders et al., 2018; Jiang et al., 2018). However, there are no systematic studies on the real-time schematic aeration based on nitrite concentration where DO concentration is correlated to the nitrite level to provide favorable conditions for successful Anammox process. Real-time monitoring of nitrite concentration can limit

the competition between X_{ANA} and X_{NOB} for nitrite as high nitrite concentration can stimulate the growth of nitrite oxidizing bacteria, resulting in an inhibition of Anammox bacteria. In the real-time schematic aeration, if nitrite level is higher than a specific nitrite threshold concentration, the aeration system is automatically turned off to allow the growth of Anammox bacteria under anaerobic conditions.

Mathematical modeling of nitrogen removal during Anammox process is essential to comprehensively analyze the removal mechanisms and determine the governing parameters in the biological wastewater treatment processes. Also, mathematical models can be implemented for detecting the sophisticated relations between the process parameters and evaluating the effect of numerous operational conditions and aeration schemes on the nitrogen removal efficiency. Therefore, mathematical modeling can lead to better understanding of the Anammox process operation and system design based on the available resources and determined accuracy.

1.5 Enrichment of anaerobic ammonia oxidation (Anammox) bacteria

Nitrogen removal by Anammox process is a cost-efficient technology with a reduced energy, operational cost and greenhouse gases emission (Du et al., 2015; Guo et al., 2020). However, the doubling time ranges from 10 to 20 days depending on the operational conditions (Isanta et al., 2015; Marie et al., 2015), indicating slow growth rate of Anammox bacteria. Also, the competition between X_{ANA} and X_{NOB} for nitrite is a key challenge on the success of Anammox bacteria enrichment process. In this study, the main scope is to evaluate the Anammox granulation approach as a potential technique for efficient Anammox enrichment processes. Granulation is an innovative solution for

limiting the activity of X_{AOB} and X_{NOB} and providing a sufficient retention time for complete growth of Anammox bacteria (Laureni et al., 2015; Xu et al., 2019). In an Anammox granule, X_{AOB} grows in the aerobic zone (i.e., the outer layer of the granule) where DO is supplied from the bulk solution while Anammox bacteria grow at in the anoxic zone (i.e., the inner layer of the granule).

Many previous Anammox studies experimentally investigated the enrichment of Anammox bacteria using granules (Vlaeminck et al., 2010; Wang et al., 2020; Li et al., 2021); however, limited studies focused on the mathematical modeling of Anammox granules to describe the mass transport and microbial communities in the granules. In previous lab-scale enrichment studies using Anammox granulation, it was demonstrated that operational conditions are important in Anammox enrichment, including the DO concentration (Perez et al., 2014; Zekker et al., 2018), granule diameter (Liu et al., 2017; Luo et al., 2017; Chen et al., 2019) and influent COD concentration (Li et al., 2017; Zhang et al., 2020). The competition between Anammox bacteria and the involved microbes also plays an important role on the Anammox granulation process (Pellicer-Nacher et al., 2014; Cao et al., 2017). However, there are no systematic studies on the effect of liquid film thickness on the enrichment of Anammox bacteria by granulation.

Numerical models are an efficient tool to diagnose the competition between X_{AOB} and X_{ANA} for ammonia, X_{ANA} and X_{NOB} for nitrite and X_{AOB} and X_{NOB} for DO under various operational conditions during the Anammox enrichment processes. Also, numerical models can be applied for identifying the governing microorganisms and kinetic constants on the Anammox granules. Numerical modeling can be implemented to analyze the failure mechanisms of Anammox enrichment (e.g., rapid growth rate of X_{NOB}

compared to X_{ANA} and granule diameter). However, there are no systematic investigations based on numerical modeling to describe the role of kinetic constants of the involved microbes on the difficulty of Anammox enrichment granulation.

1.6 Research objectives

The research work presented in this thesis aims to describe novel technologies for nitrogen and MP removal in wastewater treatment. In this thesis, the examined technologies for nitrogen removal were MABR and Anammox processes while MP removal was performed using hydrolytic enzymes. The main objectives of this thesis are to:

- Chapter 2: develop a comprehensive mathematical model for simulating the biological reactions in the MABR biofilm, bulk solution and along the membrane height; determine the important model parameters by calibrating the mathematical model using pilot-scale operation data; evaluate the effect of operational conditions (e.g., liquid film thickness and biofilm thickness) on the performance of MABR system; and identify the governing parameters on the simultaneous nitrification and denitrification in MABR for low and high-strength wastewater.
- Chapter 3: investigate the MP degradation by hydrolytic enzymes using experimentation; evaluate the effect of experimental operational conditions (e.g., temperature and enzyme dose) on the MP removal; develop a kinetic mathematical model to simulate the MP degradation by enzymes; and estimate

the model kinetic constants by calibrating the mathematical model using the experimental results.

- Chapter 4: develop a mathematical model to simulate the biological reactions during wastewater treatment using Anammox process; estimate the important model parameters by calibrating the model using previous Anammox lab-scale experimental results; evaluate the effect of operational conditions (e.g., nitrite concentration) on the nitrogen removal; and propose/examine the effect of real-time schematic aeration based on the nitrite level on the nitrogen removal mechanisms.
- Chapter 5: develop a one-dimensional mathematical model using spherical coordinates to describe the competition between different microbes; calibrate the model using pervious Anammox studies to estimate the important mode parameters; determine the governing parameters on the Anammox bacteria enrichment using sensitivity analysis on the kinetic constants of microbes; and evaluate the effect of operational conditions (e.g., granule diameter and dissolved oxygen concentration) on the Anammox enrichment process.

References

Ali, M., Okabe, S., 2015. Anammox-based technologies for nitrogen removal : Advances in process start-up and remaining issues. Chemosphere. 141, 144–153.

Alimi, O.S., Budarz, J.F., Hernandez, L.M., Tufenkji, N., 2018. Microplastics and Nanoplastics in Aquatic Environments: Aggregation, Deposition, and Enhanced Contaminant Transport. Environmental Science and Technology. 52(4), 1704–1724.

Alvim, B.C., Mendoza-Roca, J.A., Bes-Piá, A., 2020. Wastewater treatment plant as microplastics release source – Quantification and identification techniques. Journal of Environmental Management. 255, 109739.

Anderson, P.J., Warrack, S., Langen, V., Challis, J.K., Hanson, M.L., Rennie, M.D., 2017. Microplastic contamination in Lake Winnipeg, Canada. Environmental Pollution. 225, 223–231.

Arcangeli, J.P, Arvin, E., 1999. Modeling the growth of a methanotrophic biofilm : Estimation of parameters and variability. Biodegradation. 10, 177–191.

Auta, H.S., Emenike, C.U., Fauziah, S.H., 2017. Distribution and importance of microplastics in the marine environment: A review of the sources, fate, effects, and potential solutions. Environment International, 102, 165–176.

Baeten, J.E., Batstone, D.J., Schraa, O.J., van Loosdrecht, M.C.M., Volcke, E.I.P., 2019. Modelling anaerobic, aerobic and partial nitritation-anammox granular sludge reactors - A review. Water Research. 149, 322–341.

Blair, R.M., Waldron, S., Gauchotte-Lindsay, C., 2019. Average daily flow of microplastics through a tertiary wastewater treatment plant over a ten-month period. Water Research. 163, 114909.

Brindle, K., Stephenson, T., Semmens, M.J., 1999. Pilot plant treatment of a high-strength brewery wastewater using a membrane-aeration bioreactor. Water Environment Research. 71, 1197-1204.

Cao, Y., van Loosdrecht, M.C.M., Daigger, G.T., 2017. Mainstream partial nitritation – anammox in municipal wastewater treatment : status, bottlenecks, and further studies. Applied Microbiology and Biotechnology. 101, 1365–1383.

Chaali, M., Naghdi, M., Brar, K., 2018. A review on the advances in nitrifying biofilm reactors and their removal rates in wastewater treatment. Journal of Chemical Technology and Biotechnology. 93, 3113–3124.

Chen, C., Sun, F., Zhang, H., Wang, J., Shen, Y., Liang, X., 2016. Evaluation of COD effect on anammox process and microbial communities in the anaerobic baffled reactor (ABR). Bioresource Technology. 216, 571–578.

Chen, R., Ji, J., Chen, Y., Takemura, Y., Liu, Y., Kubota, K., Ma, H., Li, Y., 2019. Successful operation performance and syntrophic micro-granule in partial nitritation and anammox reactor treating low-strength ammonia wastewater. Water Research. 155, 288–299.

Cheung, P.K., Fok, L., 2017. Characterisation of plastic microbeads in facial scrubs and their estimated emissions in Mainland China. Water Research. 122, 53–61.

Connan, R., Dabert, P., Khalil, H., Bridoux, G., Béline, F., Magrí, A., 2016. Batch enrichment of anammox bacteria and study of the underlying microbial community dynamics. Chemical Engineering Journal. 297(3), 217–228.

Conthe, M., Lycus, P., Arntzen, M.Ø., Ramos, A., Frostegård, Å., Bakken, L.R., Kleerebezem, R., van Loosdrecht, M.C.M., 2019. Denitrification as an N_2O sink. Water Research. 151, 381–387.

Domingues, R.F., Sanches, T., Silva, G.S., Bueno, B.E., Ribeiro, R., Kamimura, E.S., Franzolin Neto, R., Tommaso, G., (2015). Effect of enzymatic pretreatment on the anaerobic digestion of milk fat for biogas production. Food Research International. 73, 26–30.

Downing, L.S., & Nerenberg, R., 2008. Effect of oxygen gradients on the activity and microbial community structure of a nitrifying membrane-aerated biofilm. Biotechnology and Bioengineering. 101 (6), 1193-1204.

Du, R., Peng, Y., Cao, S., Wang, S., Wu, C., 2015. Advanced nitrogen removal from wastewater by combining anammox with partial denitrification. Bioresource Technology. 179, 497–504.

Edo, C., González-Pleiter, M., Leganés, F., Fernández-Piñas, F., Rosal, R., 2020. Fate of microplastics in wastewater treatment plants and their environmental dispersion with effluent and sludge. Environmental Pollution, 259, 113837.

Eskicioglu, C., Galvagno, G., Cimon, C., 2018. Approaches and processes for ammonia removal from side-streams of municipal effluent treatment plants. Bioresource Technology. 268, 797–810.

Gatidou, G., Arvaniti, O.S., Stasinakis, A.S., 2019. Review on the occurrence and fate of microplastics in Sewage Treatment Plants. Journal of Hazardous Materials. 367, 504–512.

Ge, C., Dong, Y., Li, H., Li, Q., Ni, S., Gao, B., 2019. Nitritation-anammox process – A realizable and satisfactory way to remove nitrogen from high saline wastewater. Bioresource Technology, 275, 86–93.

Gies, E.A., LeNoble, J.L., Noël, M., Etemadifar, A., Bishay, F., Hall, E.R., Ross, P.S., 2018. Retention of microplastics in a major secondary wastewater treatment plant in Vancouver, Canada. Marine Pollution Bulletin. 133, 553–561.

Gilmore, K.R., Terada, A., Smets, B.F., Love, N.G., Garland, J.L., 2013. Autotrophic Nitrogen Removal in a Membrane-Aerated Biofilm Reactor Under Continuous Aeration: A Demonstration, Environmental Engineering Science. 30(1), 38–45.

González-Brambila, M., Monroy, O., López-isunza, F., 2006. Experimental and theoretical study of membrane-aerated biofilm reactor behavior under different modes of oxygen supply for the treatment of synthetic wastewater. Chemical Engineering Science. 61, 5268–5281.

Goswami, L., Kumar, R.V., Borah, S.N., Manikandan, N.A., Pakshirajan, K., Pugazhenthi, G. 2018. Membrane bioreactor and integrated membrane bioreactor systems for micropollutant removal from wastewater: a review. Journal of Water Process Engineering. 26, 314-328.

Guo, Y., Chen, Y., Webeck, E., Li, Y., 2020. Towards more efficient nitrogen removal and phosphorus recovery from digestion effluent : Latest developments in the anammox-based process from the application perspective. Bioresource Technology. 299, 122560.

Hauck, M., Maalcke-luesken, F.A., Jetten, M.S.M., Huijbregts, M.A.J., 2016. Removing nitrogen from wastewater with side stream anammox : What are the trade-offs between environmental impacts . Resources, Conservation and Recycling. 107, 212–219.

Hibiya, K., Terada, A., Tsuneda, S., Hirata, A., 2003. Simultaneous nitrification and denitrification by controlling vertical and horizontal microenvironment in a membrane- aerated biofilm reactor. Journal of Biotechnology. 100, 23–32.

Hidayaturrahman, H., Lee, T.G., 2019. A study on characteristics of microplastic in wastewater of South Korea: Identification, quantification, and fate of microplastics during treatment process. Marine Pollution Bulletin. 146, 696–702.

Holland, E.R., Mallory, M.L., Shutler, D., 2016. Plastics and other anthropogenic debris in freshwater birds from Canada. Science of the Total Environment. 571, 251–258.

Horton, A.A., Svendsen, C., Williams, R.J., Spurgeon, D.J., Lahive, E., 2017. Large microplastic particles in sediments of tributaries of the River Thames, UK – Abundance, sources and methods for effective quantification. Marine Pollution Bulletin. 114(1), 218–226.

Hu, S., Yang, F., Sun, C., Zhang, J., Wang, T., 2008. Simultaneous removal of COD and nitrogen using a novel carbon-membrane aerated biofilm reactor. Journal of Environmental Science. 20 (2), 142–148.

Hwang, J.H., Cicek, N., Oleszkiewicz, J., 2009. Effect of loading rate and oxygen supply on nitrification in a non-porous membrane biofilm reactor. Water Research. 43, 3301- 3307.

Isanta, E., Bezerra, T., Fernández, I., Suárez-Ojeda, M.E., Pérez, J., Carrera, J., 2015. Microbial community shifts on an anammox reactor after a temperature shock using 454-pyrosequencing analysis. Bioresource Technology, 181, 207–213.

Jiang, H., Liu, G., Ma, Y., Xu, X., Chen, J., Yang, Y., Liu, X., Wang, H., 2018. A pilot-scale study on start-up and stable operation of mainstream partial nitrification-

anammox biofilter process based on online pH-DO linkage control. Chemical Engineering Journal. 350, 1035–1042.

Kanders, L., Beier, M., Nogueira, R., Nehrenheim, E., 2018. Sinks and sources of anammox bacteria in a wastewater treatment plant – screening with qPCR. Water Science and Technology. 78.2, 441–451.

Lackner, S., Terada, A., Smets, B.F., 2008. Heterotrophic activity compromises autotrophic nitrogen removal in membrane-aerated biofilms : Results of a modeling study. Water Research. 42(3), 1102–1112.

Lackner, S., Terada, A., Horn, H., Henze, M., & Smets, B.F., 2010. Nitration performance in membrane-aerated biofilm reactors differs from conventional biofilm systems. Water Research, 44(20), 6073–6084.

LaPara, T.M., Cole, A.C., Shanahan, J.W., Semmens, M.J., 2006. The effects of organic carbon, ammoniacal-nitrogen, and oxygen partial pressure on the stratification of membrane-aerated biofilms. Journal of Industrial Microbiology and Biotechnology. 33, 315–323.

Laureni, M., Weissbrodt, D.G., Sziv, I., Robin, O., Lund, J., Morgenroth, E., Joss, A., 2015. Activity and growth of anammox biomass on aerobically pre-treated municipal wastewater. Water Research. 80, 325–336

Laureni, M., Falås, P., Robin, O., Wick, A., Weissbrodt, D.G., Lund, J., Ternes, T.A., Morgenroth, E., Joss, A., 2016. Mainstream partial nitritation and anammox : long-term process stability and effluent quality at low temperatures. Water Research. 101, 628–639.

Li, J., Zhang, L., Peng, Y., Zhang, Q., 2017. Effect of low COD/N ratios on stability of single-stage partial nitritation/anammox (SPN/A) process in a long-term operation. Bioresource Technology. 244, 192–197.

Li, M., Du, C., Liu, J., Quan, X., Lan, M., 2018. Mathematical modeling on the nitrogen removal inside the membrane- aerated biofilm dominated by ammonia-oxidizing archaea (AOA): Effects of temperature, aeration pressure and COD/N ratio. Chemical Engineering Journal. 338, 680–687.

Li, J., Peng, Y., Zhang, Q., Li, X., Yang, S., Li, S., 2021. Rapid enrichment of anammox bacteria linked to floc aggregates in a single-stage partial nitritation-anammox process : Providing the initial carrier and anaerobic microenvironment. Water Research. 191, 116807.

Lin, J., Zhang, P., Li, G., Yin, J., Li, J., Zhao, X., 2016. Effect of COD/N ratio on nitrogen removal in a membrane-aerated biofilm reactor. International Biodeterioration & Biodegradation. 113, 74–79.

Liu, H., Yang, F., Shi, S., Liu, X., 2010. Effect of substrate COD/N ratio on performance and microbial community structure of a membrane aerated biofilm reactor. Journal of Environmental Sciences. 22 (4), 540–546.

Liu, Y., Hao, H., Guo, W., Peng, L., Pan, Y., Guo, J., Chen, X., Ni, B., 2016. Autotrophic nitrogen removal in membrane-aerated biofilms : Archaeal ammonia oxidation versus bacterial ammonia oxidation. Chemical Engineering Journal. 302, 535–544.

Liu, T., Ma, B., Chen, X., Ni, B., Peng, Y., Guo, J., 2017. Evaluation of mainstream nitrogen removal by simultaneous partial nitrification, anammox and denitrification (SNAD) process in a granule-based reactor. Chemical Engineering Journal. 327, 973–981.

Lotti, T., Kleerebezem, R., Lubello, C., van Loosdrecht, M.C.M., 2014. Physiological and kinetic characterization of a suspended cell anammox culture. Water Research. 60, 1–14.

Luo, J., Chen, H., Han, X., Sun, Y., Yuan, Z., Guo, J., 2017. Microbial community structure and biodiversity of size-fractionated granules in a partial nitritation – anammox process. FEMS Microbiology Ecology. 93, 1–10.

Ma, B., Xu, X., Wei, Y., Ge, C., Peng, Y., 2020. Recent advances in controlling denitritation for achieving denitritation/anammox in mainstream wastewater treatment plants. Bioresource Technology. 299, 122697.

Magni, S., Binelli, A., Pittura, L., Avio, C. G., Della Torre, C., Parenti, C.C., Gorbi, S., Regoli, F., 2019. The fate of microplastics in an Italian Wastewater Treatment Plant. Science of the Total Environment. 652, 602–610.

Mahon, A.M., O'Connell, B., Healy, M.G., O'Connor, I., Officer, R., Nash, R., Morrison, L., 2017. Microplastics in sewage sludge: Effects of treatment. Environmental Science and Technology. 51(2), 810–818.

Marie, P.S, Pumpel, T., Markt, R., Murthy, S., Bott, C., Wett, B., 2015. Comparative evaluation of multiple methods to quantify and characterise granular anammox biomass. Water Research. 68, 194–205.

Martin, K.J., Nerenberg, R., 2012. The membrane biofilm reactor (MBfR) for water and wastewater treatment : Principles, applications, and recent developments. Bioresource Technology. 122, 83–94.

Mason, S.A., Garneau, D., Sutton, R., Chu, Y., Ehmann, K., Barnes, J., Fink, P., Papazissimos, D., Rogers, D. L., 2016. Microplastic pollution is widely detected in US municipal wastewater treatment plant effluent. Environmental Pollution. 218, 1045–1054.

Matsumoto, S., Terada, A., Tsuneda, S., 2007. Modeling of membrane-aerated biofilm : Effects of C/N ratio, biofilm thickness and surface loading of oxygen on feasibility of simultaneous nitrification and denitrification. Biochemical Engineering Journal. 37, 98–107.

Miao, Y., Zhang, L., Li, B., Zhang, Q., Wang, S., Peng, Y., 2017. Enhancing ammonium oxidizing bacteria activity was key to single- stage partial nitrification-anammox system treating low-strength sewage under intermittent aeration condition. Bioresource Technology. 231, 36–44.

Miao, Y., Peng, Y., Zhang, L., Li, B., Li, X., Wu, L., Wang, S., 2018. Partial nitrification-anammox (PNA) treating sewage with intermittent aeration mode : Effect of influent C/N ratios. Chemical Engineering Journal. 334, 664–672.

Michielssen, M.R., Michielssen, E.R., Ni, J., Duhaime, M.B., 2016. Fate of microplastics and other small anthropogenic litter (SAL) in wastewater treatment plants depends on unit processes employed. Environmental Science: Water Research and Technology. 2(6), 1064–1073.

Mintenig, S.M., Int-Veen, I., Löder, M.G.J., Primpke, S., Gerdts, G., 2017. Identification of microplastic in effluents of waste water treatment plants using focal plane array-based micro-Fourier-transform infrared imaging. Water Research. 108, 365–372.

Murphy, F., Ewins, C., Carbonnier, F., Quinn, B., 2016. Wastewater Treatment Works (WwTW) as a Source of Microplastics in the Aquatic Environment. Environmental Science and Technology. 50(11), 5800–5808.

Nerenberg, R., 2016. The membrane-biofilm reactor (MBfR) as a counter-diffusional biofilm process. Current Opinion in Biotechnology. 38, 131–136.

Ni, S., Sung, S., Yue, Q., Gao, B., 2012. Substrate removal evaluation of granular anammox process in a pilot-scale upflow anaerobic sludge blanket reactor. Ecological Engineering. 38(1), 30–36.

Nicolella, C., Pavasant, P., Livingston, A.G., 2000. Substrate counter diffusion and reaction in membrane-attached biofilms : mathematical analysis of rate limiting mechanisms. Chemical Engineering Science. 55, 1385–1398.

Odnell, A., Recktenwald, M., Stensén, K., Jonsson, B.H., Karlsson, M., 2016. Activity, life time and effect of hydrolytic enzymes for enhanced biogas production from sludge anaerobic digestion. Water Research. 103, 462–471.

Othman, A.R., Hasan, H.A., Muhamad, M.H., Ismail, N. 'Izzati, Abdullah, S.R.S., (2021). Microbial degradation of microplastics by enzymatic processes: a review. Environmental Chemistry Letters.

Pellicer-Nàcher, C., Franck, S., Ruscalleda, M., Terada, A., Al-soud, A., Hansen, M.A., Søren, J., Smets, B.F., 2013. Sequentially aerated membrane biofilm reactors for autotrophic nitrogen removal : microbial community composition and dynamics. Microbial Biotechnology. 7, 32–43.

Peng, G., Zhu, B., Yang, D., Su, L., Shi, H., Li, D., 2017. Microplastics in sediments of the Changjiang Estuary. China. Environmental Pollution. 225, 283–290.

Pereira, A.D., Cabezas, A., Etchebehere, Chernicharo, C.A.D.L., Araújo, J.C.D, 2017. Microbial communities in anammox reactors : a review. Environmental Technology Reviews. 6(1), 74–93.

Pérez, J., Lotti, T., Kleerebezem, R., Picioreanu, C., van Loosdrecht, M.C.M., 2014. Outcompeting nitrite-oxidizing bacteria in single- stage nitrogen removal in sewage treatment plants : A model-based study. Water Research. 66, 208–218.

Perez-Calleja, P., Aybar, M., Picioreanu, C., Esteban-Garcia, A.L., Martin, K.J., Nerenberg, R., 2017. Periodic venting of MABR lumen allows high removal rates and high gas-transfer efficiencies. Water Research. 121, 349–360.

Pettipas, S., Bernier, M., Walker, T.R., 2016. A Canadian policy framework to mitigate plastic marine pollution. Marine Policy. 68, 117–122.

Poerio, T., Piacentini, E., Mazzei, R., 2019. Membrane processes for microplastic removal. Molecules, 24(22). Rodriguez-Sanchez, A., Purswani, J., Lotti, T., van Loosdrecht, M.C.M., Vahala, R., Gonzalez-Martinez, A., 2016. Distribution and microbial community structure analysis of a single-stage partial nitritation / anammox granular sludge bioreactor operating at low temperature. Environmental Technology, 37(18), 2281–2291.

Raju, S., Carbery, M., Kuttykattil, A., Senthirajah, K., Lundmark, A., Rogers, Z., SCB, S., Evans, G., Palanisami, T., 2020. Improved methodology to determine the fate and transport of microplastics in a secondary wastewater treatment plant. Water Research. 173, 115549.

Regmi, P., Miller, M.W., Holgate, B., Bunce, R., Park, H., Chandran, K., Wett, B., Murthy, S., Bott, C.B., 2014. Control of aeration, aerobic SRT and COD input for mainstream nitritation/denitritation. Water Research. 57, 162–171.

Revel, M., Châtel, A., Mouneyrac, C., 2018. Micro (nano) plastics: A threat to human health? Current Opinion in Environmental Science and Health. 1, 17–23.

Rezania, S., Park, J., Md Din, M. F., Mat Taib, S., Talaiekhozani, A., Kumar Yadav, K., Kamyab, H., 2018. Microplastics pollution in different aquatic environments and biota: A review of recent studies. Marine Pollution Bulletin. 133, 191–208.

Satoh, H., Okabe, S., Norimatsu, N., Watanabe, Y., 2000. Significance of substrate C / N ratio on structure and activity of nitrifying biofilms determined by in situ hybridization and the use of microelectrodes. Water Science & Technology. 41 (4-5), 317–321.

Satoh, H., Ono, H., Rulin, B., Kamo, J., Okabe, S., 2004. Macroscale and microscale analyses of nitrification and denitrification in biofilms attached on membrane aerated biofilm reactors. Water Research. 38, 1633–1641.

Shanahan, J.W, Semmens, M.J., 2004. Multipopulation Model of Membrane-Aerated Biofilms. Environmental Science and Technology. 38(11), 3176–3183.

Shanahan, J. W., Semmens, M.J., 2015. Alkalinity and pH effects on nitrification in a membrane aerated bioreactor : An experimental and model analysis. Water Research. 4, 10–22.

Silva, A.B., Bastos, A.S., Justino, C.I.L., da Costa, J.P., Duarte, A.C., Rocha-Santos, T.A.P., 2018. Microplastics in the environment: Challenges in analytical chemistry - A review. Analytica Chimica Acta. 1017, 1–19.

Sun, J., Dai, X., Wang, Q., van Loosdrecht, M.C.M., Ni, B.J., 2019. Microplastics in wastewater treatment plants: Detection, occurrence and removal. Water Research. 152, 21–37.

Syron, E., Casey, E., 2008a. Model-Based Comparative Performance Analysis of Membrane Aerated Biofilm Reactor Configurations. Biotechnology and Bioengineering. 99 (6), 1361–1373.

Syron, E., Casey, E., 2008b. Membrane-Aerated Biofilms for High Rate biotreatment : Performance Appraisal, Engineering Principles, Scale-up, and Development Requirements. Environmental Science and Technology. 42 (6), 1833–1844.

Talvitie, J., Mikola, A., Koistinen, A., Setälä, O., 2017. Solutions to microplastic pollution – Removal of microplastics from wastewater effluent with advanced wastewater treatment technologies. Water Research. 123, 401–407.

Tang, C., Duan, C., Yu, C., Song, Y., 2017. Removal of nitrogen from wastewaters by anaerobic ammonium oxidation (ANAMMOX) using granules in upflow reactors. Environmental Chemistry Letters. 15(2), 311–328.

Terada, A., Hibiya, K., Nagai, J., Tsuneda, S., Hirata, A., 2003. Nitrogen Removal Characteristics and Biofilm Analysis of a Membrane-Aerated Biofilm Reactor Applicable to High-Strength Nitrogenous Wastewater Treatment. Journal of Bioscience and Bioengineering. 95 (2), 170–178.

Terada, A., Yamamoto, T., Igarashi, R., Tsuneda, S., Hirata, A., 2006. Feasibility of a membrane-aerated biofilm reactor to achieve controllable nitrification. Biochemical Engineering Journal. 28, 123–130.

Van Loosdrecht, M.C.M., Heijnen, J.J., Eberl, H., Kreft, J., Picioreanu, C., 2002. Mathematical modeling of biofilm structures. Antonie van Leeuwenhoek. 81, 245–256.

Vannecke, T.P.W., Wells, G., Hubaux, N., Morgenroth, E., Volcke, E.I.P., 2015. Considering microbial and aggregate heterogeneity in biofilm reactor models : how far do we need to go ?. Water Science and Technology. 72.10, 1692–1699.

Vlaeminck, S.E., Terada, A., Smets, B.F., Clippeleir, D., Schaubroeck, T., Bolca, S., Demeestere, L., Mast, J., Boon, N., Carballa, M., Verstraete, W., 2010. Aggregate Size and Architecture Determine Microbial Activity Balance for One-Stage Partial Nitritation and Anammox. Applied and Environmental Microbiology. 76(3), 900–909.

Wang, R., Terada, A., Lackner, S., Smets, B.F., Henze, M., Xia, S., Zhao, J. 2009. Nitritation performance and biofilm development of co- and counter-diffusion biofilm reactors : Modeling and experimental comparison. Water Research. 43(10), 2699–2709.

Wang, R., Xiao, F., Wang, Y., Lewandowski, Z., 2016. Determining the optimal trans-membrane gas pressure for nitrification in membrane-aerated biofilm reactors based on oxygen profile analysis. Applied Microbiology and Biotechnology. 100, 7699–7711.

Wang, X., Yang, H., Su, Y., Liu, X., 2020. Characteristics and mechanism of anammox granular sludge with different granule size in high load and low rising velocity sewage treatment. Bioresource Technology. 312, 123608.

Wei, W., Huang, Q.S., Sun, J., Dai, X., Ni, B.J., 2019. Revealing the Mechanisms of Polyethylene Microplastics Affecting Anaerobic Digestion of Waste Activated Sludge. Environmental Science and Technology. 53(16), 9604–9613.

Wright, S.L., Kelly, F.J., 2017. Plastic and Human Health: A Micro Issue?. Environmental Science and Technology. 51(12), 6634–6647.

Xu, G., Zhou, Y., Yang, Q., Lee, Z.M., 2015. The challenges of mainstream deammonification process for municipal used water treatment. Applied Microbial Biotechnology. 99, 2485–2490.

Xu, D., Kang, D., Yu, T., Ding, A., Lin, Q., Zhang, M., Hu, Q., Zheng, P., 2019. A secret of high-rate mass transfer in anammox granular sludge : “Lung-like breathing”. Water Research. 154, 189–198.

Xu, Y., Peng, L., Liu, Y., Xie, G., Song, S., Ni, B., 2020. Modelling melamine biodegradation in a membrane aerated biofilm reactor. Journal of Water Process Engineering. 38, 101626.

You, Q., Wang, J., Qi, G., Zhou, Y., 2020. Anammox and partial denitrification coupling : a review. RSC Advances. 12554–12572.

Yue, X., Yu, G., Lu, Y., Liu, Z., Li, Q., Tang, J., Liu, J., 2018. Effect of dissolved oxygen on nitrogen removal and the microbial community of the completely autotrophic nitrogen removal over nitrite process in a submerged aerated biological filter. Bioresource Technology. 254, 67–74.

Zekker, I., Kiviru, A., Mandel, A., Jaagura, M., Tenno, T., 2019. Enhanced Efficiency of Nitritating-Anammox Sequencing Batch Reactor Achieved at Low Decrease Rates of Oxidation–Reduction Potential. Environmental Engineering Science. 36(3), 1–11.

Zhang, X., Liu, Y., Zhang, J., Chen, Y., Wang, Q., 2020. Impact of COD/N on anammox granular sludge with different biological carriers. Science of the Total Environment. 728, 138557.

2. Comprehensive model applications for better understanding of pilot-scale membrane-aerated biofilm reactor performance

Membrane aerated biofilm reactor (MABR) is an innovative technology for simultaneous nitrification and denitrification with a reduced aeration demand and operation cost. Although many previous MABR studies investigated the nitrification and denitrification in MABR and assessed the effect of numerous operational conditions (e.g., oxygen concentration) on the system performance using experimental work, there are no reported studies for mathematical models calibration with a MABR pilot-scale operation data. In this study, a comprehensive mathematical model was developed and calibrated to estimate the important model parameters (e.g., biofilm thickness and liquid film thickness) and describe the effect of operational conditions (e.g., C/N ratio) on the nitrification and denitrification during the wastewater treatment.

The following published journal article is included in this chapter.

- Elsayed, A., Hurdle, M., Kim, Y., 2021. Comprehensive model applications for better understanding of pilot-scale membrane-aerated biofilm reactor performance. Journal of Water Process Engineering. 40, 101894.

The co-author’s contributions include:

Michael Hurdle: MABR pilot operation, data collection.

Younggy Kim: supervision, funding acquisition, technical support, manuscript revision.

Abstract

In membrane aerated biofilm reactors (MABR), simultaneous nitrification and denitrification (SND) are achieved by complicated biological reactions and mass transport in and between highly heterogeneous media: the air-permeable membrane; layered biofilms; liquid film; and bulk. To better understand large-scale MABR performance under real operation conditions, a comprehensive MABR model was developed and model calibration was completed with a pilot-scale MABR system. For the pilot system operated with municipal wastewater mixed with return activated sludge, the biofilm thickness was 1000 - 2000 μm, the liquid film thickness was 200 - 300 μm, and the diffusivity of the soluble components in the biofilm was 10 - 45% of that in the infinite dilute solution. In the pilot operation, the ammonia removal rate was more rapid for higher ammonia loading rate, higher oxygen supply and lower pH conditions. Based on the model simulation results, we recommend that the biofilm be maintained thicker than 600 μm for SND. Thin liquid films (i.e., sufficient mixing conditions) are necessary for active denitrification as the slow transport of soluble organics through the liquid film limits denitrification; however, nitrification was hardly affected by thick liquid films because ammonia transport was sufficiently fast both in the liquid film and biofilm. A lower carbon-to-nitrogen (C/N) ratio enhanced nitrification only for high-strength wastewater (e.g., ammonia > 100 mg-N/L) because of more dominant growth of ammonia oxidizing bacteria (X_{AOB}) compared to heterotrophic bacteria (X_H). On the other hand, the C/N ratio does not affect nitrification when MABR is used for municipal wastewater treatment. Using the comprehensive model calibrated with pilot-scale MABR

operation, the complicated biological reactions and material transport was elucidated for large scale MABR applications.

Keywords

Membrane aerated biofilm reactor; simultaneous nitrification and denitrification; liquid film thickness; carbon-to-nitrogen ratio; model calibration

2.1 Introduction

High levels of nitrogen nutrients (e.g., ammonia, nitrate, and organic nitrogen) can be present in various wastewater streams, including domestic wastewater, agricultural wastewater, and animal manure waste. Excessive release of nitrogen nutrients into natural water systems can cause serious environmental problems such as algal bloom formation and eutrophication that threaten the aquatic ecosystem (Tchobanoglous and Burton, 1991; Wan et al., 2014; Chaali et al., 2018). Therefore, nitrogen nutrient removal is essential in modern wastewater treatment systems (Hibiya et al., 2003; Lackner et al., 2010; Lin et al., 2016). Conventional activated sludge is widely used in municipal wastewater treatment for ammonia and organic nitrogen removal by nitrification; however, it requires high oxygen demands (increasing the aeration cost) coupled with a long solids retention time (increasing the pumping cost) (Hao et al., 2002; Matsumoto et al., 2007; Martin and Nerenberg, 2012). Also, additional reactors are necessary for complete denitrification, requiring a large footprint for wastewater treatment facilities (Terada et al., 2003). Biological nitrification and denitrification can also be achieved using attached growth bioreactors, such as trickling filters, moving bed biofilm reactors, and rotating biological contactors. Membrane aerated biofilm reactors (MABRs) are a relatively new treatment

method which is considered as a promising alternative for conventional attached growth reactors for simultaneous nitrification and denitrification (SND) with a significant reduction of the facility size and operation cost (Casey et al., 1999; Syron and Casey, 2008a; Shanahan and Semmens, 2015; Nerenberg, 2016; Perez-Calleja et al., 2017; Goswami et al., 2018; Xu et al., 2020). In MABR operation, oxygen is provided through gas-permeable membranes to the biofilm; as a result, the aerobic zone is formed in the inner layers of the biofilm for nitrification while the anoxic zone is created in the outer layers of the biofilm for denitrification (Casey et al., 1999; Terada et al., 2003; Syron and Casey, 2008a; Lin et al., 2016; Chaali et al., 2018). Since soluble organics are readily diffused from the bulk solution to the outer biofilm, MABRs are known to achieve more efficient denitrification compared to conventional attached growth reactors (Matsumoto et al., 2007; Syron and Casey, 2008a; Martin and Nerenberg, 2012; Nerenberg, 2016).

Numerical modeling of MABR is important to comprehensively describe the rate mechanisms and identify the complex correlation between the process parameters. Numerical models can also be used for assessing the performance of MABR under various operational conditions (Li et al., 2018). Therefore, numerical modeling leads to better conceptual understanding for the MABR operation as the level of complexity can be selected based on the resources availability and aimed accuracy (Picioreanu et al., 2004; Liu et al., 2016; Wang et al., 2016). Numerical comprehensive model, including the biological reactions in the biofilm, oxygen partial pressure along the membrane fiber and biological reactions in the bulk solution, is essential to detect the sophisticated relations between model parameters in the MABR operation. Also, model calibration with pilot-scale operation data is significantly important as it forms robust models to

reflect realistic values for the model parameters compared to those determined using lab-scale results.

Most of other MABR studies have examined the feasibility of MABR based on lab-scale experiments with specific focuses on nitrification (Yamagiwa et al., 1994; Brindle et al., 1998; Yamagiwa et al., 1998; Satoh et al., 2000; Terada et al., 2006), COD (chemical oxygen demand) removal (Pankhania et al., 1999), simultaneous nitrification and denitrification (Liu et al., 2010; Lin et al., 2016), simultaneous COD and nitrogen removal (Hibiya et al., 2003; Semmens et al., 2003; Satoh et al., 2004; Hu et al., 2008), treatment of wastewater with high ammonia concentration (e.g., animal manure waste) (Brindle et al., 1999; Terada et al., 2003), and the C/N (carbon-to-nitrogen) ratio on the performance of MABR (Liu et al., 2010; Lin et al., 2016). Moreover, other model studies introduced mathematical models to investigate the effect of the operational conditions on nitrogen removal (Shanahan and Semmens, 2004; Liu et al., 2016; Li et al., 2018), describe the microbial community in the biofilm (van Loosdrecht et al., 2002) and determine the removal mechanisms in MABR (Nicolella et al., 2000; Syron and Casey, 2008a). Also, other MABR studies combined lab-scale experimental work with numerical modeling to show the importance of oxygen concentration (Gonzalez – Brambila et al., 2006; Downing and Nerenberg, 2008; Hwang et al., 2009; Wang et al., 2009), C/N ratio and biofilm thickness (Matsumoto et al., 2007), and pH and alkalinity (Shanahan and Semmens, 2015) on COD and nitrogen removal in MABR. The calibration of numerical models with MABR pilot-scale operation data is significantly important because some model parameters are difficult to be measured during the complicated system operation (Arcangeli and Arvin, 1999; Syron and Casey, 2008b). However, there is no previous

model calibration study with MABR pilot-scale operation to determine the important parameters in MABR (e.g., biofilm thickness, liquid film thickness (i.e., boundary diffusive layer between the biofilm and bulk) and diffusion coefficient of soluble components).

Operational conditions play an important role in COD and nitrogen removal in MABRs. In other MABR studies, the oxygen concentration at the membrane surface and bulk solution was found to govern the efficiency of nitrification in MABR (Brindle et al., 1998; Hibiya et al., 2003; Gonzalez – Brambila et al., 2006; Terada et al., 2006; Downing and Nerenberg, 2008). It was also found that the influent ammonia loading rate controls ammonia removal in MABR (Hwang et al., 2009; Lackner et al., 2010). Two other critical operational factors are the C/N ratio and influent COD concentration as they affect the microbial competition between autotrophic bacteria for nitrification and heterotrophic bacteria for denitrification in MABR biofilms (Satoh et al., 2000; LaPara et al., 2006; Liu et al., 2010; Lin et al., 2016; Li et al., 2018). Especially, denitrification can be dramatically improved by adjusting the oxygen flux as a function of the influent COD and ammonia loadings (Matsumoto et al., 2007). However, the effect of the C/N ratio on nitrification for high-strength wastewater (e.g., downstream liquid from dewatering processes with higher levels of ammonia nitrogen than typical municipal wastewater) has not been investigated in MABR. Also, there were no systematic investigations on the liquid film thickness for simultaneous nitrification and denitrification.

In this study, the main objectives are to: (1) develop a comprehensive model to simulate the mass transport and biological reactions in the MABR biofilm and bulk solution, including the oxygen partial pressure changes along the membrane fiber; (2)

calibrate the comprehensive model with MABR pilot-scale operation data to estimate the important model parameters; (3) identify the rate-limiting parameters on nitrification and denitrification in MABR for low and high-strength wastewater; and (4) assess the effect of operational conditions (e.g., biofilm thickness, liquid film thickness and C/N ratio) on nitrification and denitrification in MABR.

2.2 Pilot MABR experiments

2.2.1 Pilot MABR installation and operation

A pilot MABR reactor was built in a container with an effective wastewater volume of 16.5 m^3 where a MABR cassette (3.0 m in length; 1.75 m in width and 2.15 m in depth) was immersed (ZeeLung MABR module, SUEZ Water Technologies & Solutions, Canada) (Fig. A1). The MABR cassette contained 300,000 cords and each cord consisted of a central string (providing mechanical strength) and 40 gas permeable membrane fibers (length: 2.0 m, inner diameter: 70 μm, outer diameter: 95 μm). Each membrane fiber provided an effective surface area of 4.4×10^{-4} m^2 for biofilm attachment, resulting in a total surface area of 1,920 m^2 in the pilot rector.

The MABR pilot reactor was installed in a local municipal wastewater treatment facility between the primary clarifiers and aeration tanks of conventional activated sludge (Adelaide Wastewater Treatment Plant, London, Ontario, Canada). The primary clarifier effluent mixed with the return activated sludge (RAS) was continuously introduced into the pilot reactor to examine the nitrification and denitrification capacity with an extra nitrate input from RAS (Table 2.1). The wastewater flow rate was 45 ± 4.7 m^3/hr, resulting in a very short mean hydraulic retention time in the MABR reactor (22 min).

The pilot operation was initiated in February 2017 and operated for 14 months until March 2018.

During the pilot operation, fresh air was continuously provided to the MABR cassette and the air traveled from the top to the bottom of individual gas permeable membrane fibers. As the air flew inside the membrane fiber, oxygen was transported from the membrane surface into the attached biofilm only by diffusion, requiring a significantly low pressure (0.34 atm) and low air flow rate (8 m^3/hr). The oxygen partial pressure of the inlet and exhaust air was monitored every weekday using a hand-held oxygen partial pressure sensor (Max O_2^+AE by Maxtec, USA) to estimate the rate of oxygen consumption. The exhaust air from the MABR cassette was collected in separate air pockets beneath the MABR cassette and the collected exhaust air was released every 90 sec. to provide a partial mixing condition (Cote and Pedersen, 2014).

The influent and effluent samples were collected and analyzed for COD (chemical oxygen demand), NH_4-N (ammonia), NO_3-N (nitrate) and TSS (total suspended solids) every weekday according to the standard methods (APHA/AWWA/WEF, 2012). On the other hand, NO_2-N (nitrite) and VSS (volatile suspended solids) were analyzed once a week (APHA/AWWA/WEF, 2012). The influent and effluent were also monitored for temperature and pH using real-time thermometers (Endress and Hauser, Switzerland) and pH probes (George Fisher, Switzerland), respectively.

Table 2.1. Average influent and effluent characteristics over the 14-month MABR pilot operation.

Parameter (Unit)	Influent	Effluent
Soluble COD (mg-COD/L)	29.2 ± 8.76	22.0 ± 7.15
Ammonia (mg-N/L)	13.5 ± 2.70	9.80 ± 2.12
Nitrite (mg-N/L)	0.30 ± 0.26	0.25 ± 0.26
Nitrate (mg-N/L)	4.51 ± 2.49	4.20 ± 2.05
Wastewater temperature (°C)	17.0 ± 3.06	16.9 ± 3.07
pH condition (-)	7.30 ± 0.08	7.20 ± 0.10
TSS (kg-TSS/ m^3)	1.27 ± 0.21	1.26 ± 0.18
VSS (kg-VSS/ m^3)	0.96 ± 0.17	0.97 ± 0.15

2.2.2 MABR pilot operation data

The raw pilot operation measurements (ammonia, nitrite, nitrate and COD concentrations, temperature, pH and oxygen partial pressure) were statistically processed to exclude outlier data points using the box and whiskers method (Tukey, 1977). In the box and whiskers method, the upper fence (U_{fence}) and lower fence (L_{femce}), defined in Eq. 2.1 and 2.2 using the first quartile (Q_1) and third quartile (Q_3), were applied to the measured pilot data (Table A1).

$$U_{fence} = Q_3 + 1.5 \times (Q_3 - Q_1) \qquad (Eq\ 2.1)$$

$$L_{fence} = Q_1 - 1.5 \times (Q_3 - Q_1) \qquad (Eq\ 2.2)$$

2.3 Numerical model development and calibration

2.3.1 Biological reaction kinetics and mass transport in biofilm

A steady-state one-dimensional model was developed to simulate the biological reactions in the MABR biofilm based on IWA-ASM3 (International Water Association Activated Sludge Model No.3) (Henze et al., 2000) and the biological reactions in another MABR model study (Matsumoto et al., 2007). The model includes the biological reaction kinetics and diffusive mass transport in the biofilms attached on MABR membrane surfaces (Table 2.2). The biological reactions on the nitrogenous compounds were: ammonia (S_{NH_4}) oxidation by ammonia oxidizing bacteria (X_{AOB}); nitrite (S_{NO_2}) oxidation into nitrate (S_{NO_3}) by nitrite oxidizing bacteria (X_{NOB}); and denitrification by heterotrophic bacteria (X_H) (Table A2). The effect of pH on nitrification was reflected on the maximum specific growth rate of X_{AOB} (μ_{AOB}) (Table 2.2). The reaction kinetics for soluble COD (S_{COD}) utilization by X_H, particulate COD (X_S) hydrolysis into S_{COD} and microbial respiration reactions are also included in the model (Table A2). The daily temperature condition in the pilot operation data was reflected for the individual biological reactions using temperature correction factor (θ) (Table 2.2). In the biofilm, the soluble components (S_{NH_4}, S_{NO_2}, S_{NO_3}, S_{O_2} and S_{COD}) were mobile by diffusion, while the particulate components (X_{AOB} ,X_{NOB}, X_H and X_S) were assumed to be immobile.

2.3.2 Boundary conditions

The concentration of soluble components at the interface between the liquid film and bulk was defined using the measured effluent concentration during the pilot operation

(Table 2.1). Soluble components except for oxygen diffused from the bulk to biofilm in the liquid film where biological reactions were assumed to be negligible. On the membrane surface ($x = 0$), it was assumed that there is no flux for each of the soluble components except for oxygen (Eq. 2.3) while the oxygen concentration (S_{O_2}) at the membrane surface was defined by Henry's law (Eq. 2.4).

$$\left.\frac{dS_i}{dx}\right|_{x=0} = 0 \qquad (Eq\ 2.3)$$

where S_i is an individual soluble component except for oxygen and x is the distance from the membrane surface.

$$S_{O_2} = \frac{P_{O_2}}{K_H} \qquad (Eq\ 2.4)$$

where S_{O_2} is the oxygen concentration (mg-O_2/L), P_{O_2} is the oxygen partial pressure (atm) and K_H is the Henry's law constant (K_H = 0.024 atm/ mg-O_2/L at 25°C). Note that the Henry's law constant was corrected for pilot operation temperature conditions using van't Hoff equation (Krug et al., 1976).

2.3.3 Numerical solution methods and model verification

The nine steady-state mass balance equations for individual soluble ($S_{NH_4}, S_{NO_2}, S_{NO_3}, S_{O_2}$ and S_{COD}) and particulate (X_{AOB}, X_{NOB}, X_H and X_S) components were discretized by the finite difference methods (Table A2) (Chapra and Canale, 1998). In the finite difference method, the biofilm was evenly divided into fifty grids regardless of the biofilm thickness. The 450 discretized mass-balance equations (50 grids × 9

components) were solved numerically by the fixed-point iteration approach (Chapra and Canale, 1998). The built numerical model was validated by comparing simulation results with another MABR model study (Fig. A2) (Matsumoto et al., 2007).

Table 2.2. Model parameters at T = 20°C and pH = 7.0.

Model Parameter	Symbol	Value	Unit	Reference
Heterotrophic Bacteria (X_H)				
Maximum specific growth rate	μ_H	6.0	1/d	Henze et al., (2000)
Maximum endogenous respiration rate	b_H	0.4	1/d	Henze et al., (2000)
Anoxic reduction factor for μ_H	η_d	0.8	-	Henze et al., (2000)
Oxygen saturation constant	$K_{O_2}^H$	0.2	mg-O_2/L	Henze et al., (2000)
Substrate saturation constant	K_{COD}^H	4.0	mg-COD/L	Henze et al., (2000)
Ammonium saturation constant	$K_{NH_4}^H$	0.05	mg-N/L	Henze et al., (2000)
Nitrite saturation constant	$K_{NO_2}^H$	0.5	mg-N/L	Henze et al., (2000)
Nitrate saturation constant	$K_{NO_3}^H$	0.5	mg-N/L	Henze et al., (2000)
Ammonia Oxidizing Bacteria (X_{AOB})				
Maximum specific growth rate	μ_{AOB}	2.05 [b]	1/d	Wiesmann, (1994)
Maximum endogenous respiration rate	b_{AOB}	0.13	1/d	Wiesmann, (1994)
Oxygen saturation constant	$K_{O_2}^{AOB}$	0.6	mg-O_2/L	Wiesmann, (1994)
Ammonium saturation constant	$K_{NH_4}^{AOB}$	2.4	mg-N/L	Wiesmann, (1994)
Nitrite saturation constant	$K_{NO_2}^{AOB}$	5.5	mg-N/L	Matsumoto et al., (2007
Nitrate saturation constant	$K_{NO_3}^{AOB}$	0.1	mg-N/L	Matsumoto et al., (2007
Nitrite Oxidizing Bacteria (X_{NOB})				
Maximum specific growth rate	μ_{NOB}	1.45	1/d	Wiesmann, (1994)
Maximum endogenous respiration rate	b_{NOB}	0.06	1/d	Wiesmann, (1994)
Oxygen saturation constant	$K_{O_2}^{NOB}$	2.20	mg-O_2/L	Wiesmann, (1994)
Ammonium saturation constant	$K_{NH_4}^{NOB}$	0.01	mg-N/L	Matsumoto et al., (2007)
Nitrite saturation constant	$K_{NO_2}^{NOB}$	5.5	mg-N/L	Wiesmann, (1994)
Nitrate saturation constant	$K_{NO_3}^{NOB}$	0.1	mg-N/L	Matsumoto et al., (2007
Hydrolysis				
Hydrolysis rate constant	q_H	3.0	1/d	Henze et al., (2000)
Saturation constant for particulate COD	K_X	0.1	g-X_S/ g-X_H	Henze et al., (2000)
Anoxic reduction for q_H	η_H	0.6	-	Henze et al., (2000)
Stoichiometric Parameters				
Yield of X_H on substrate	Y_H	0.63	g-COD/g-COD	Henze et al., (2000)
Yield of X_{AOB} on ammonium	Y_{AOB}	0.15	g-COD/g-N	Wiesmann, (1994)
Yield of X_{NOB} on nitrite	Y_{NOB}	0.041	g-COD/g-N	Wiesmann, (1994)
Nitrogen content in biomass	i_{NBM}	0.07	g-N/g-COD	Henze et al., (2000)
Inert content in lysis biomass	f_i	0.1	g-COD/g-COD	Henze et al., (2000)
Temperature correction factor (θ)				
Maximum specific growth rate (μ_H)	θ_{μ_H}	1.07[a]	-	Henze et al., (2000)
Maximum endogenous respiration rate (b_H)	θ_{b_H}	1.07 [a]	-	Henze et al., (2000)
Maximum specific growth rate (μ_{AOB})	$\theta_{\mu_{AOB}}$	1.11 [a]	-	Henze et al., (2000)
Maximum endogenous respiration rate (b_{AOB})	$\theta_{b_{AOB}}$	1.11 [a]	-	Henze et al., (2000)
Maximum specific growth rate (μ_{NOB})	$\theta_{\mu_{NOB}}$	1.11 [a]	-	Henze et al., (2000)
Maximum endogenous respiration rate (b_{NOB})	$\theta_{b_{NOB}}$	1.11 [a]	-	Henze et al., (2000)
Hydrolysis rate constant (q_H)	θ_{q_H}	1.04 [a]	-	Henze et al., (2000)
Saturation constant for particulate COD (k_X)	θ_{K_X}	0.89 [a]	-	Henze et al., (2000)

[a] Arrhenius equation: $k_{T_1} = k_{T_2} \times \theta^{(T_1 - T_2)}$ (k is a kinetic constant, T is wastewater temperature and θ is temperature correction factor).

[b] μ_{AOB} = 2.05 d^{-1} at pH of 6.5. For other pH conditions: $\mu_{AOB} = 2.05 \times \frac{1}{1+10^{6.5-pH}}$.

2.3.4 Model expansion for 2.0-m long MABR membrane

The one-dimensional biofilm model was expanded to reflect the changes in the oxygen partial pressure (P_{O_2}) along the air flow direction from the top to the bottom of an individual MABR fiber. In the pilot operation, the average oxygen partial pressure decreased from 0.209 atm (inlet P_{O_2}) to 0.157 ± 0.01 atm (exhaust P_{O_2}) along the air flow direction in the 2.0-meter long air-permeable hollow membrane fiber. The 2.0-m long membrane was discretized into ten segments in the direction of air flow, and it was assumed that the oxygen partial pressure changes linearly from the inlet to exhaust P_{O_2} along the membrane height. The oxygen partial pressure in each membrane segment was then applied to the Henry's law equation (Eq. 2.4) to determine the oxygen concentration at the membrane surface.

2.3.5 Biological reactions in bulk solution

The biological reactions in the bulk solution (pilot reactor effective volume of 16.5 m^3) were combined with the biofilm biological reactions to build a comprehensive MABR model. The rates of individual biological reactions were calculated based on the effluent characteristics of the daily pilot operation (Table 2.1) using ASM3 (Table 2.2 and Table A2) (Henze et al., 2000; Matsumoto et al., 2007). The biomass fractions were assumed as: 13.60% for X_H; 0.027% for X_{AOB}; 0.018% for X_{NOB}; 50% for X_S and the rest for X_I (Henze, 1992; Yang et al., 2009). The daily wastewater temperature and pH conditions were reflected on the biological reactions in the bulk and biofilm (Table 2.2).

2.3.6 Model calibration using pilot operation data

The comprehensive model, including the biological reactions in the bulk solution and the biofilms on the 2.0-m long fibers, was calibrated using the daily pilot operation data over 14 months to determine the biofilm thickness, liquid film thickness and the diffusion coefficient of soluble components in the biofilm (Table 2.3). The model simulation results were compared with the pilot operation data to match the same trend and values of the removal rates of ammonia, nitrate and COD. The daily operation data of the pilot reactor (effluent concentrations of ammonia, nitrite, nitrate, COD, inlet and exhaust oxygen partial pressure, wastewater temperature and pH) were used in the model calibration.

Table 2.3. Calibrated diffusivity in the biofilm

Biofilm thickness (μm)	1000	1250	1500	1750	2000	Literature Range (Stewart, 1998; Stewart,2003)
Diffusivity of S_{COD}, $\boldsymbol{D_{COD}}$ (cm^2/day)	0.18	0.15	0.12	0.12	0.10	0.04 – 0.49
Diffusivity of S_{O2}, $\boldsymbol{D_{O_2}}$ (cm^2/day)	0.45	0.45	0.55	0.60	0.65	0.44 – 1.36
Diffusivity of S_{NH4}, $\boldsymbol{D_{NH_4}}$ (cm^2/day)	0.40	0.50	0.60	0.65	0.75	0.57 – 1.38
Diffusivity of S_{NO2}, $\boldsymbol{D_{NO_2}}$ (cm^2/day)	0.40	0.50	0.60	0.65	0.75	0.56 – 1.35
Diffusivity of S_{NO3}, $\boldsymbol{D_{NO_3}}$ (cm^2/day)	0.40	0.50	0.60	0.65	0.75	0.55 – 1.34

The liquid film thickness (L_f) was 250 μm.

Diffusion coefficients of soluble components in the biofilm were estimated at 25°C.

2.4 Results and discussion

2.4.1 The MABR pilot operation results

In the pilot MABR operation, the ammonia removal rate was enhanced with the increasing influent ammonia loading rate (Fig. 2.1a) and increasing oxygen supply rate

(Fig. 2.1b). The ammonia removal rate increased linearly with the increasing ammonia loading rate up to 1.25 kg-N/m^3/day (Fig. 2.1a), indicating that MABR can effectively handle high ammonia loading conditions. This finding is consistent with another MABR study where efficient ammonia removal at high ammonia loading rates (up to 1.50 kg-N/m^3/day) was demonstrated (Terada et al., 2006). Efficient oxygen transfer from the membrane to biofilms was critical for enhanced ammonia removal (Fig. 2.1b). Note that the membrane material of the MABR pilot was SUEZ ZeeLung media. The membrane material is known to control the oxygen transfer efficiency through the membrane surface. In other MABR studies, hollow fiber membranes made of polydimethyl siloxane (Syron et al., 2015) and silicone-based membranes (Casey et al., 1999) were examined for efficient oxygen transfer in ammonia removal. Moreover, the oxygen supply pressure through the membrane fibers is an important factor in efficient ammonia removal in the MABR (Tian et al., 2015; Chaali et al., 2018).

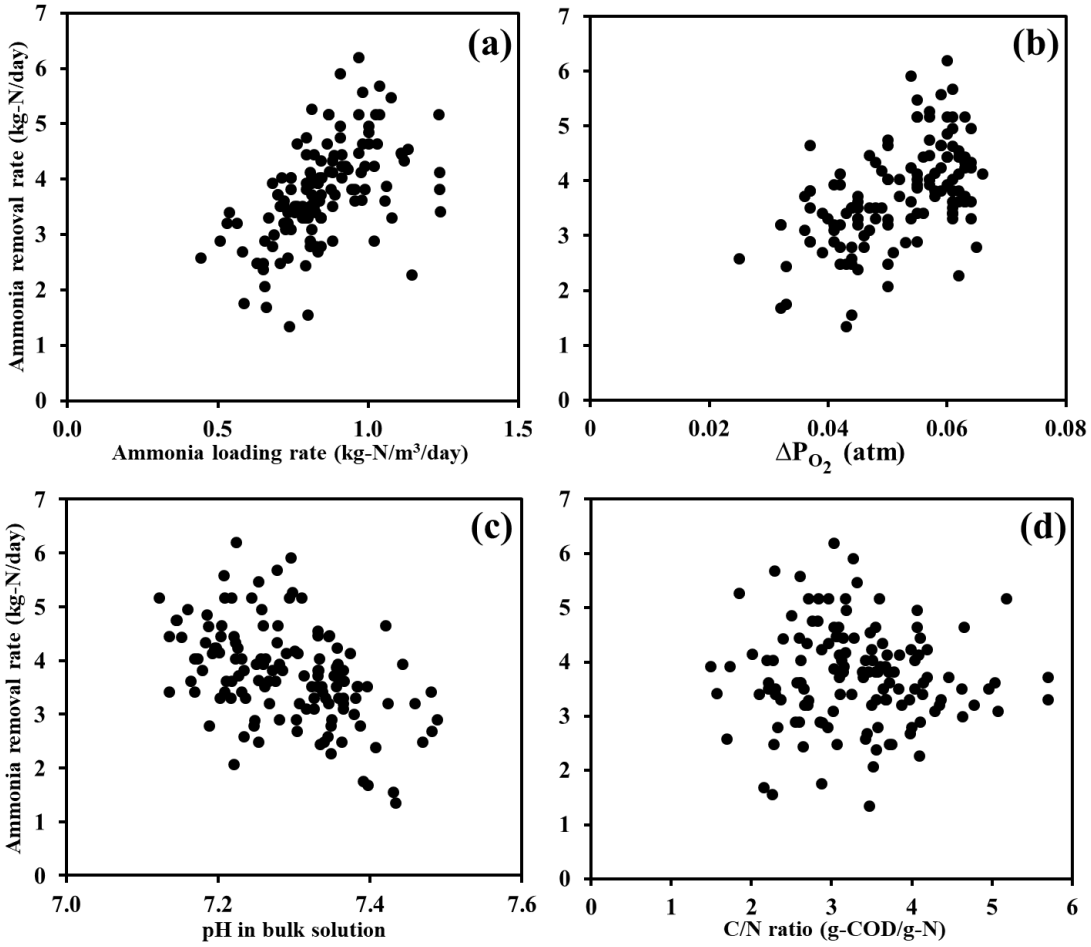

Fig. 2.1. Effect of various operation conditions on ammonia removal: (a) influent ammonia loading rate, (b) difference between inlet and exhaust oxygen partial pressure at the membrane (oxygen supply), (c) effluent pH and (d) influent C/N ratio. Pilot operation data were recorded from February 2017 to March 2018.

The ammonia removal rate was enhanced with the decreasing effluent pH (Fig. 2.1c) while the influent C/N ratio hardly affected the ammonia removal rate in the pilot MABR operation (Fig. 2.1d). Although the range of bulk solution pH was narrow (7.1 to 7.5), low pH was correlated to enhanced ammonia removal during the pilot operation (Fig. 2.1c). This finding is not consistent with the well-known low pH inhibition on nitrification (Metcalf and Eddy, 2003; Grady et al., 2011), indicating that the bulk solution pH does not represent the pH condition in the MABR biofilm as previously

claimed (Flora et al., 1999). It was also found in other MABR studies that nitrification reaction in biofilms can affect the bulk pH significantly (Park et al., 2015; Shanahan and Semmens, 2015). During the pilot operation, the influent C/N ratio varied in a wide range from 1.5 to 5.7 g-COD/g-N; however, there were no clear relationships between the influent C/N ratio and ammonia removal rate because the growth rate of X_{AOB} was insensitive to the influent C/N ratio within the operated range of C/N ratio (Fig. 2.1d). This finding is consistent with the results of other MABR studies where it was reported that ammonia removal was independent of the C/N ratio (Matsumoto et al., 2007; Lin et al., 2016; Li et al., 2018; Li and Zhang, 2018).

A clear seasonal dependency of the removal rate of ammonia, nitrate and COD was observed during the pilot operation as high wastewater temperature enhanced the biological reactions in the MABR (Fig.2.2 and Table A3). The ammonia removal rate ranged between 1.55 and 6.20 kg-N/d with an annual average rate of 3.75 kg-N/d (Fig. 2.2a). At the beginning of the MABR pilot operation (February – August), biofilms were thin on the membrane surface, indicating sufficient oxygen transport throughout the biofilm thickness. While the ammonia removal rate increased quickly during this period (February – August), there was limited nitrate removal until August because anoxic zones were not established in the biofilm (Fig. 2.2b). After the first seven months of the operation (August and thereafter), the nitrate removal rate increased rapidly as the biofilm was thick enough to have the outer anoxic layer for active denitrification (Fig. 2.2b). This trend of the nitrate removal rate was consistent with that of the COD removal rate during the pilot operation (Fig. 2.2b and 2.2c). For the first seven months of the MABR operation (February– August), the average COD removal rate was relatively low

at 6.45 kg-COD/day and then it increased to 12.25 kg-COD/day between September and March with active denitrification (Fig. 2.2c).

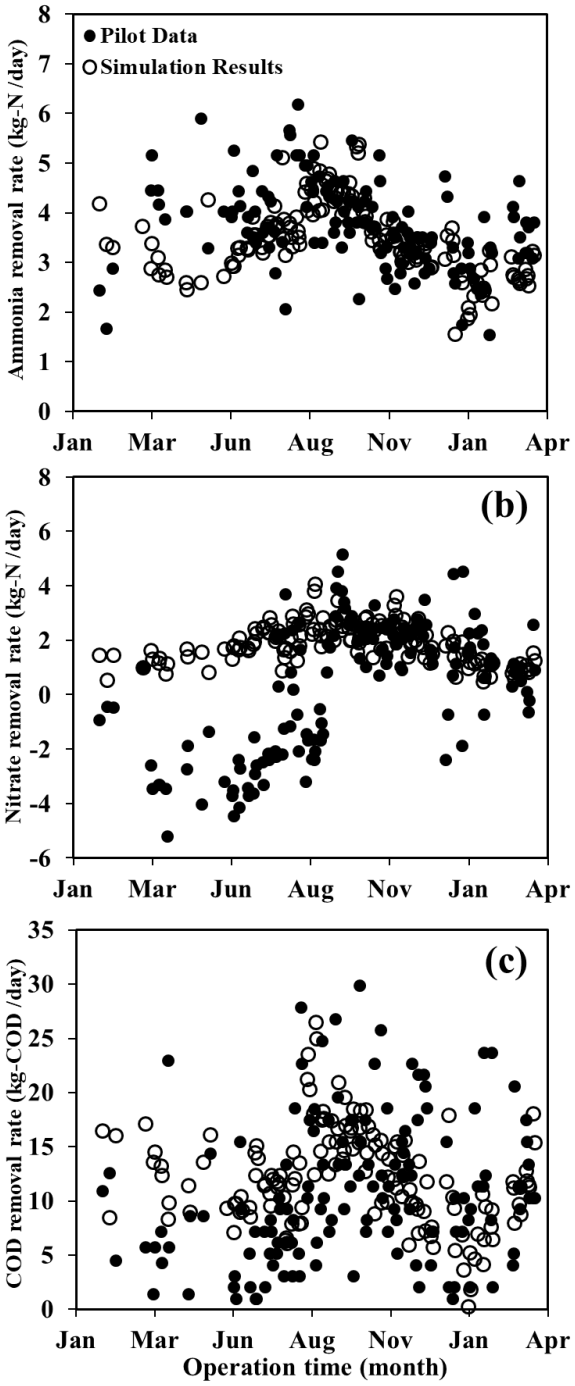

Fig. 2.2. Comparison between pilot operational data and the model simulation results: (a) ammonia removal, (b) nitrate removal and (c) COD removal. (Simulation conditions: biofilm thickness = 1500 μm, liquid film thickness = 250 μm, other conditions were assumed based on parameters in Tables 2.1, 2.2 and 2.3. The simulation results included the biological reactions in the biofilm and the bulk solution. In Fig. 2.2b, negative values of nitrate removal indicate net creation of nitrate.

2.4.2 Model calibration with the pilot operation results

The biofilm thickness, liquid film thickness and diffusion coefficient of soluble components in the numerical model were determined using the pilot operation data (more emphasis on the data collected from August to March) (Fig. 2.2, Table 2.3). Based on the comprehensive model calibration, the biofilm thickness was found to range from 1000 to 2000 μm (Fig. A3, A4, A5, and A6). Note that the scanning electron microscope (SEM) image of the biofilms and MABR membrane fibers in Fig. A7 was taken after the biofilms shrank and partially fell off while the membrane sample was processed and dried for the SEM analysis. Also, the determined biofilm thickness range is consistent with those observed or used in other MABR studies (LaPara et al., 2006; Matsumoto et al., 2007; Peng et al., 2015; Peng et al., 2016; Perez-Calleja et al., 2017; Xu et al., 2020). Based on the model calibration in Fig. 2.2, 1500 μm (average of the calibrated range) was used for the biofilm thickness in the study although the estimated biofilm thickness ranged from 1000 to 2000 μm (Figs. A3, A4, A5, and A6). The calibrated liquid film thickness (approximately 250 μm) using the comprehensive model was also consistent with assumed values in other MABR model studies (Bishop et al., 1997; Wäsche et al., 2002; Martin et al., 2017; Li et al., 2018). Although it was reported in another MABR study that the liquid film thickness should be smaller than 100 μm under a sufficient

mixing condition in MABR reactors (Matsumoto et al., 2007), the liquid film thickness in the pilot MABR was expected to be thicker than 100 µm during our pilot operation due to the relatively mild mixing condition using exhaust air from the MABR cassette (Cote and Pedersen, 2014).

2.4.3 Biological reactions in biofilm versus bulk

In the model calibration with the pilot data, the ammonia removal in the biofilm represented 77% of the total ammonia removal during the pilot operation while 23% of the total ammonia (0.8 kg-N/day) was removed in the bulk solution (Table 2.4). This result is consistent with another lab-scale experimental study where the ammonia removal in the biofilm was higher than that in the bulk solution (Terada et al., 2006). Although the nitrification rate in the biofilm was considerable (0.27 kg-N/day), nitrification was limited in the bulk solution due to the absence of dissolved oxygen. On the other hand, denitrification in the bulk solution was substantial (82% of the total nitrate removal) and only 18% was denitrified in the biofilm (Table 2.4). As a result of active denitrification in the bulk solution, 40% of the total COD removal (5.0 out of 12.7 kg-COD/day) was achieved in the bulk solution. This finding clearly indicates that that the biological reactions in the bulk solution should not be ignored in MABR operation while there are no previously studies reporting the importance of the biological reactions in the bulk solution.

Table 2.4. Comparison between the average removal/creation rate of ammonia, nitrate and COD in biofilm and bulk.

Removal/creation of soluble component	Biofilm	Bulk
Ammonia removal rate (kg-N/day)	2.7 ± 0.65	0.8 ± 0.16
Nitrate creation rate (kg-N/day)	0.27 ± 0.2	0
Nitrate removal rate (kg-N/day)	0.4 ± 0.28	1.8 ± 0.4
COD removal rate (kg-COD/day)	7.2 ± 2.6	5.0 ± 2.5

2.4.4 Distribution of soluble components in the biofilm

In the model simulation with 1500-μm thick biofilms (other model parameters in Tables 2.1, 2.2 and 2.3), oxygen diffused up to 600 μm from the membrane surface, forming an inner aerobic layer for nitrification (Fig. 2.3a). This aerobic layer thickness is comparable with previously reported ranges in lab-scale MABR systems (300 – 700 μm) (Picioreanu et al., 1997; LaPara et al., 2006; Wang et al., 2016; Kinh et al., 2017). The oxygen concentration became practically zero (< 0.01 mg/L) at 600 μm from the membrane surface, creating an outer anoxic layer of the biofilm for denitrification. Based on the comprehensive model simulation results, the biofilm thickness must be at least 600 μm for simultaneous nitrification and denitrification in MABR. This model result is consistent with the suggested range in another MABR study for optimal biofilm thickness to achieve simultaneous nitrification and denitrification in MABR (600 - 1200 μm) (Matsumoto et al., 2007).

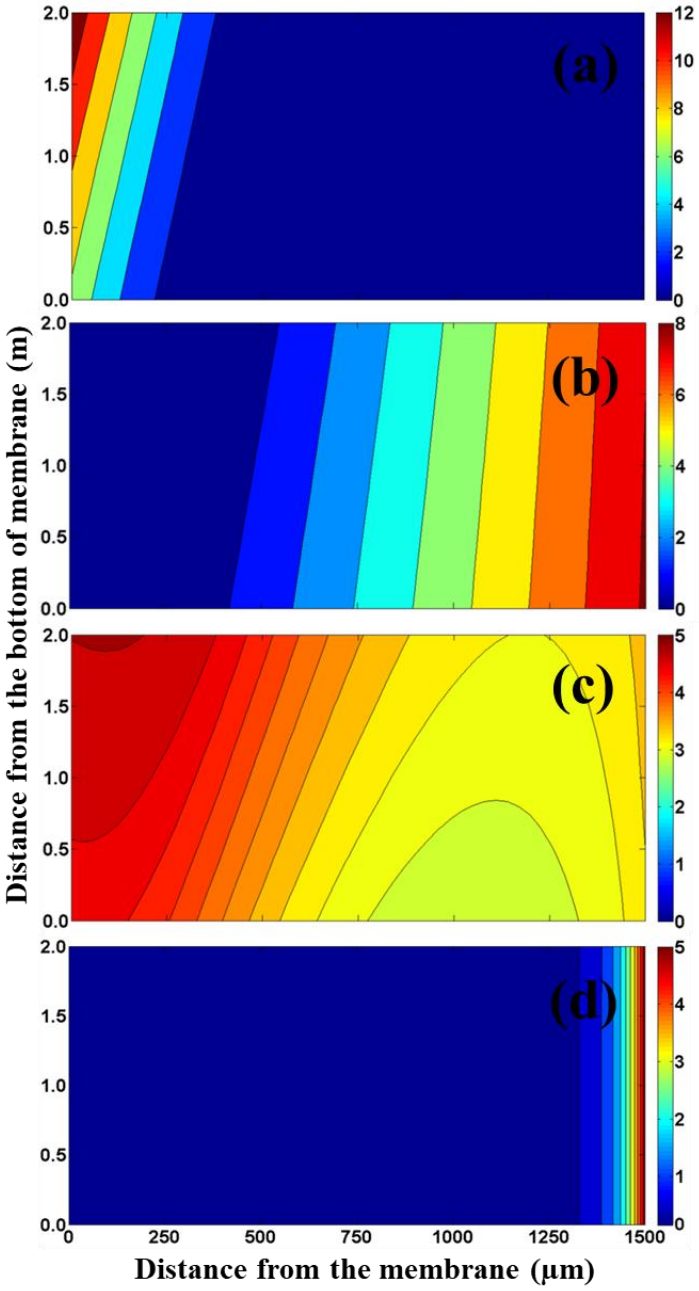

Fig. 2.3. Two-dimensional distribution of the model soluble components: (a) oxygen, (b) ammonia, (c) nitrate and (d) soluble COD. (Simulation conditions: biofilm thickness = 1500 μm, liquid film thickness = 250 μm, other conditions were assumed based on the parameters in Tables 2.1, 2.2 and 2.3).

Ammonia concentration in the biofilm decreased gradually from 8 mg-N/L at the interface between the biofilm and liquid film to 0 mg-N/L at the membrane surface,

creating a concentration gradient for the diffusive transport of ammonia to the inner layer of biofilm where ammonia is oxidized to nitrite and nitrate (Fig. 2.3b and 2.3c). It should be noted that there was no considerable residual ammonia concentration near the membrane due to active ammonia removal, indicating that oxygen transport from the membrane surface was sufficient for ammonia oxidation in the MABR simulation. The importance of oxygen in ammonia removal is consistent with other studies that emphasized the role of oxygen transport for efficient nitrification in MABR (Satoh et al., 2004; Lackner et al., 2010; Liu et al., 2016). Therefore, it is recommended that MABR membrane fibers be manufactured or coated with materials of high oxygen selectivity for enhanced nitrification.

Although nitrate was consistently high across the biofilms (> 3.0 mg-N/L) and oxygen concentration was negligible beyond 600 μm (Fig. 2.3a), active denitrification was driven only in the narrow range of 1300 to 1500 μm (i.e., 200 μm from the interface with the liquid film) (Fig. 2.3c) because of the limited soluble COD concentration in the biofilm (Fig. 2.3d). This finding indicates that soluble COD transport is the rate-limiting factor for denitrification in the biofilm due to relatively low soluble COD concentration in the bulk (S_{COD} = 22 mg-COD/L with C/N ratio = 2.2 g-COD/g-N). This limited denitrification result is consistent with the results of another MABR study where it was mentioned that the C/N ratio should be maintained higher than 5 g-COD/g-N to allow efficient denitrification (Liu et al., 2010). Therefore, soluble COD availability in the biofilm is the rate-limiting factor for the rapid denitrification in MABR systems. In an addition model simulation with a doubled soluble COD concentration in the bulk (from 22 to 44 mg-COD/L), the denitrification rate was increased nine times (from 0.1 to 0.9

kg-N/m^3). Therefore, high soluble COD is recommended for enhanced denitrification in MABR.

Although fresh air was introduced from the top of the membrane fibers and travelled down to the bottom end of the membrane fibers, it was noticed that there were not significant changes in the removal rate of ammonia, nitrite and COD and the microbial population along the air flow direction. For example, the ammonia removal rate at the bottom of the membrane was lower than that at the membrane top by only 8% (from 0.282 to 0.260 kg-N/day). On the other hand, the nitrate removal rate changed along the fiber height where the nitrate creation was dominant in the upper part of the MABR membrane and the nitrate removal was dominant in the lower part of the membrane (0.025 kg-N/day) because of oxygen diffusion along the membrane height. Based on this model simulation result, it is recommended to use longer membrane fibers (> 2 m) to achieve more efficient oxygen utilization in MABR operation.

2.4.5 Effect of biofilm thickness

Thin biofilms were suitable for efficient ammonia removal and it was noticed that the highest ammonia removal rate (7.1 kg-N/day) occurred at biofilm thickness of 300 μm (Fig. 2.4a). For the biofilm thickness greater than 300 μm, the ammonia removal rate decreased gradually with the increasing biofilm thickness because of ammonia diffusion through thick biofilms. When the ammonia concentration in the bulk was doubled from 10 mg-N/L to 20 mg-N/L, the ammonia removal rate at 300-μm thick biofilm was also the highest (12.4 kg-N/day) and decreased gradually to 3.9 kg-N/day at biofilm thickness of 2000 μm, indicating that the ammonia removal rate increased by 76% compared to

ammonia concentration of 10 mg-N/L case. This finding asserts that the ammonia loading rate (i.e., ammonia concentration in the bulk solution) governs the rate of nitrification in MABR. The importance of the ammonia loading rate in ammonia removal is consistent with the pilot MABR operation (Fig. 2.1a). Nitrite creation was dominant in MABR for biofilm thickness less than 700 µm due to the high ammonia oxidation rate and the high activity of AOB over NOB near the membrane surface (Fig. 2.4a). For thick biofilms (> 700 µm), nitrite removal became balanced with nitrite creation, resulting in a relatively low nitrite average removal rate ≤ 0.35 kg-N/day.

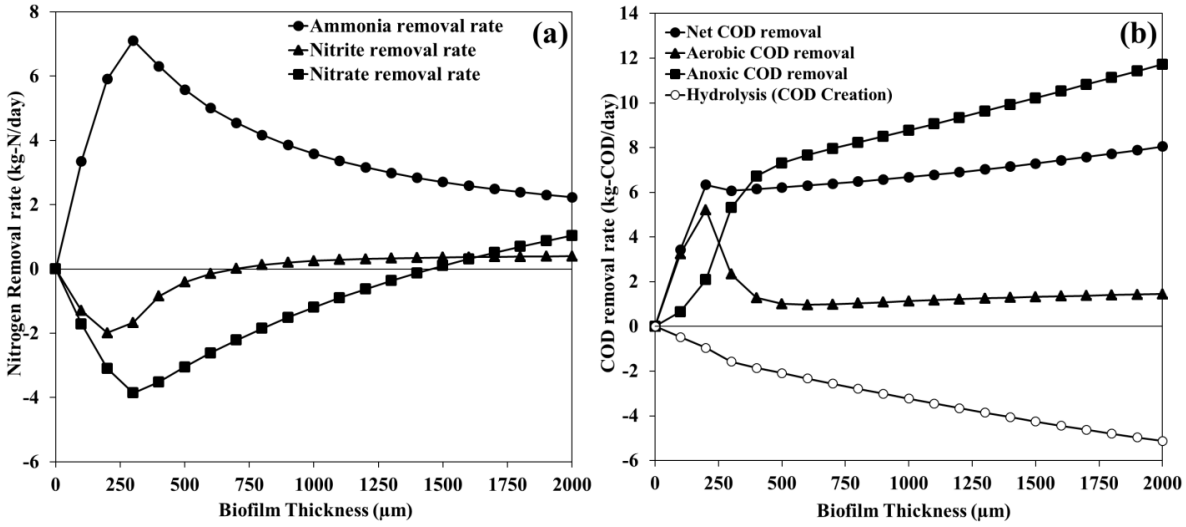

Fig. 2.4. Effect of biofilm thickness on the biological reactions: (a) nitrogen removal and (b) net COD removal through aerobic, anoxic and hydrolysis reactions. (Simulation conditions: liquid film thickness = 250 µm, other conditions were assumed based on the parameters in Tables 2.1, 2.2 and 2.3). The negative rate in the figure means a net creation rate.

At a biofilm thickness of 1400 µm, there was a balance between the nitrate creation and removal rates (Fig. 2.4a). Although the outer anoxic layer was thick enough for denitrification, nitrate creation was dominant up to a biofilm thickness of 1400 µm because the soluble COD concentration in the bulk solution was the governing factor on

denitrification in MABR (S_{COD} = 22 mg-COD/L). The maximum nitrate creation rate was observed at a biofilm thickness of 300 µm (3.9 kg-N/day), corresponding to the highest ammonia oxidation rate (7.1 kg-N/day) due to the absence of the anoxic layer for denitrification. For a biofilm thickness larger than 1400 µm, the net nitrate removal rate increased gradually to 1.1 kg-N/day (biofilm thickness of 2000 µm). When soluble COD concentration in the bulk is doubled (S_{COD} = 44 mg-COD/L), the balance between the nitrate creation and removal occurred at biofilm thickness of 1000 µm and the maximum denitrification rate was 1.9 kg-N/day at a biofilm thickness of 2000 µm (increasing by 73%).

These model simulation results are consistent with those results of the calibrated comprehensive model where it was recommended to maintain the biofilm thickness thicker than 600 µm for simultaneous nitrification and denitrification. In other studies, it was also found that the optimal biofilm thickness to achieve simultaneous nitrification and denitrification in MABR was 1600 µm (Terada et al., 2003), 600 - 1200 µm (Matsumoto et al., 2007) and 750 – 1500 µm (Peng et al., 2015). As a result, the determination of optimal biofilm thickness in MABR is highly dependent on the operational conditions (e.g., C/N ratio, ammonia loading rate, liquid film thickness and membrane material); however, a relative thick biofilm thickness (> 600 µm) is generally preferred.

It was observed that the biofilm thickness should be at least 500 µm to minimize the contribution of aerobic COD removal in MABR (Fig. 2.4b). Aerobic COD removal had a significant contribution to the total COD removal up to biofilm thickness of 200 µm (5.2 kg-COD/day), representing 80% of total COD removal because of the absence of

sufficient anoxic layer for denitrification. However, it became negligible and constant for biofilms thicker than 400 μm (1.2 kg-COD/day) where only 11% of COD was utilized under aerobic conditions. On the other hand, the anoxic COD removal enhanced with the increasing biofilm thickness due to the formation of a wide anoxic layer, allowing better removal of nitrate in the MABR. For biofilms thicker than 800 μm, anoxic COD removal represented 89% of the total COD removal.

2.4.6 Effect of liquid film thickness

The liquid film thickness hardly affected the ammonia oxidation rate up to 300 μm (Fig. 2.5a) because ammonia transport from the bulk solution to biofilm was sufficiently high (Table 2.3). However, ammonia oxidation was governed by the bulk ammonia concentration; thus, the increasing ammonia concentration enhanced the ammonia oxidation rate in the biofilm up to 100 mg-N/L (Fig. 2.5a), indicating that the examined MABR operation conditions are suitable for municipal wastewater treatment where TKN ranges up to 100 mg-N/L (Metcalf and Eddy, 2003; Lotti et al., 2015; Yuan et al., 2016; Gwak et al., 2019). For high-strength wastewater (e.g., liquid downstream from dewatering processes) (Ledda et al., 2015; Ge and Champagne, 2016; Ge et al., 2018); however, the ammonia oxidation rate did not increase beyond 22.3 kg-N/day with the increasing bulk-phase ammonia concentration above 200 mg-N/L (Fig. 2.5a).

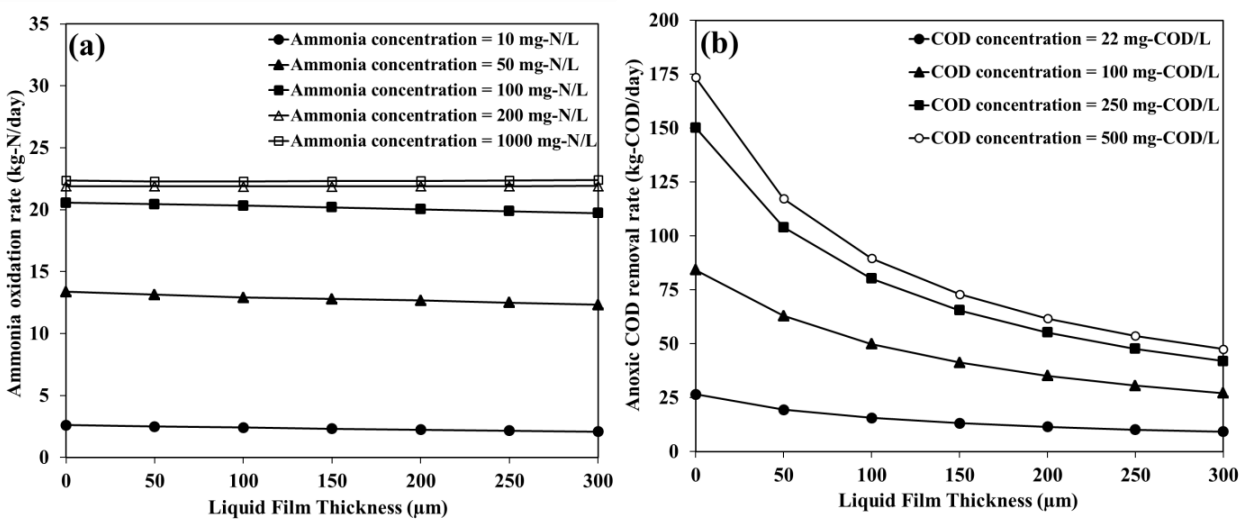

Fig. 2.5. Effect of liquid film thickness on (a) ammonia oxidation and (b) anoxic COD removal. (Simulation conditions: biofilm thickness = 1500 µm, other conditions were assumed based on the average daily pilot operational data (Tables 2.1 and 2.2 and 2.3)).

Thin liquid films (i.e., turbulent mixing conditions in the bulk solution) significantly enhanced anoxic COD removal (i.e., denitrification) (Fig. 2.5b). The anoxic COD removal rate increased by 230% with the decreasing liquid film thickness from 300 to 50 µm because thin liquid films allowed rapid transport of soluble COD from the bulk to biofilm. This finding is consistent with the results of other studies that demonstrated a negative correlation between the liquid film thickness and COD removal in a bench-scale submerged rotating disc biofilm reactor (Boltz and Daigger, 2010) and a lab-scale moving bed biofilm reactor (Nogueira et al., 2015). Denitrification was enhanced with the increasing soluble COD in the bulk (Fig. 2.5b), indicating that denitrification in the biofilm is limited by soluble COD. Thus, it can be concluded that denitrification is sensitive to the liquid film thickness while ammonia oxidation can hardly be affected by the mass transport resistance in the liquid film. Based on the model simulation results, it

is highly recommended that turbulent mixing conditions be established for effective denitrification although nitrification will be achieved regardless of mixing conditions.

2.4.7 Effect of C/N ratio

The decreasing C/N ratio enhanced the ammonia oxidation rate for the bulk ammonia concentration higher than 100 mg-N/L; however, the C/N ratio did not affect ammonia oxidation for ammonia concentration from 10 to 100 mg-N/L (Fig. 2.6). This finding (negligible effect of the C/N ratio for low ammonia concentration) is consistent with the pilot operation results (Fig. 2.1d), indicating sufficient oxygen supply and thus no competition between X_H and X_{AOB} for oxygen at the membrane surface. On the other hand, the ammonia oxidation rate decreased substantially with the increasing C/N ratio for ammonia concentration of 200 - 1000 mg-N/L (high-strength wastewater) due to the competition between X_H and X_{AOB} for oxygen. For bulk ammonia concentration higher than 400 mg-N/L, the ammonia removal rate was insensitive to the change in the C/N ratio from 4 to 10 g-COD/g-N because of the large amount of organics in the biofilm, resulting in a greater growth rate of X_H compared to X_{AOB}. Although the C/N ratio is not an important parameter in MABR operation for municipal wastewater, the C/N ratio must be reflected in MABR operation for high-strength wastewater.

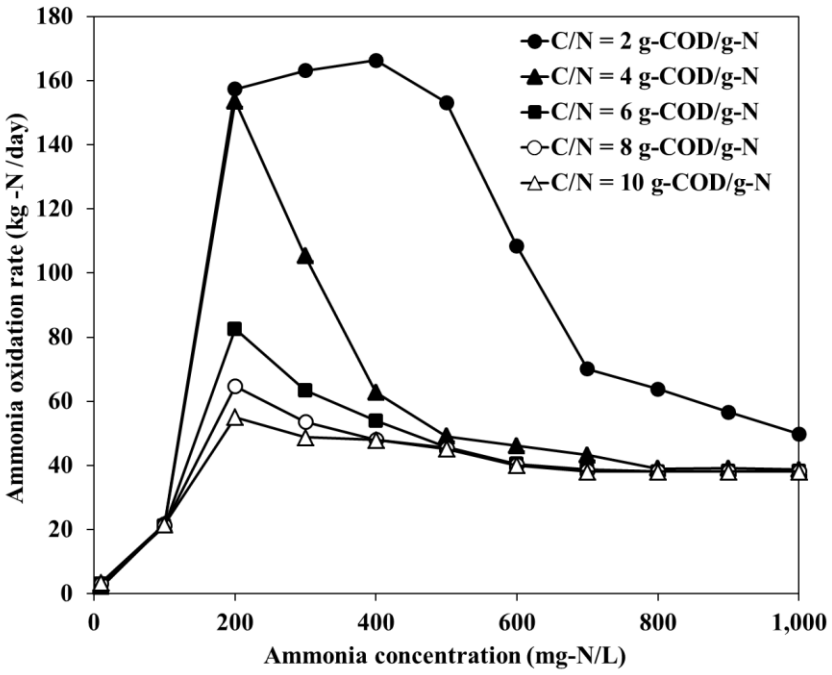

Fig. 2.6. Effect of C/N ratio on ammonia oxidation at different ammonia concentrations. (Simulation conditions: biofilm thickness = 1500 μm, liquid film thickness = 250 μm, other conditions were assumed based on the average daily pilot operational data (Tables 2.1, 2.2 and 2.3)).

2.5 Conclusions

A comprehensive MABR model was established to simulate the mass transport and biological reactions in the MABR biofilm. The model was further extended to include the oxygen partial pressure along the MABR membrane fiber and the biological reactions in the bulk solution because active denitrification in the bulk solution cannot be neglected in MABR operation. Also, a pilot-scale MABR cassette was operated in a municipal wastewater treatment facility with an emphasis on enhanced denitrification. In the pilot operation, the increasing influent ammonia loading rate and increasing oxygen supply rate enhanced the ammonia removal rate; however, the influent C/N ratio hardly affected the ammonia removal rate. Moreover, active nitrification in the MABR biofilm caused

decreases in the effluent pH. The pilot operation data over 14 months were used to calibrate the comprehensive numerical model by determining the biofilm thickness, liquid film thickness and diffusivity of soluble components. The numerical simulation results indicated that the bulk ammonia concentration is a dominant parameter on efficient nitrification in the MABR biofilm for municipal wastewater while the bulk ammonia concentration showed insignificant effects on nitrification for high-strength wastewater. Moreover, low soluble COD can limit active denitrification in the MABR biofilm. Based on the model simulation results, the biofilm thickness should be maintained at 600 μm or thicker to house both the aerobic and anoxic zones in the biofilm. It was also found that the liquid film thickness is not an important factor for nitrification; however, thick liquid films limit denitrification because of the slow transport of soluble COD through the liquid film. The C/N ratio becomes an important parameter in MABR operation only for high-strength wastewater due to the competition between X_H and X_{AOB} for oxygen. Therefore, numerical modeling of MABR coupled with pilot-scale calibration is essential for better understanding of the complex removal mechanisms and relations between numerous model parameters in MABR.

References

APHA, AWWA, WEF, 2012. Standard methods for the examination of water and wastewater. Standard Methods, 541.

Arcangeli, J.P, Arvin, E., 1999. Modeling the growth of a methanotrophic biofilm : Estimation of parameters and variability. Biodegradation. 10, 177–191.

Bishop, P.L., Gibbs, J.T., Cunningham, B.E., 1997. Relationship between concentration and hydrodynamic boundary layers over biofilms. Environmental Technology. 18, 375- 385.

Boltz, J.P., Daigger, G.T., 2010. Uncertainty in bulk-liquid hydrodynamics and biofilm dynamics creates uncertainties in biofilm reactor design. Water Science and Technology. 61 (2), 307–316.

Brindle, K., Stephenson, T., Semmens, M.J., 1998. Nitrification and oxygen utilization in a membrane aeration bioreactor. Journal of Membrane Science. 144, 197-209.

Brindle, K., Stephenson, T., Semmens, M.J., 1999. Pilot plant treatment of a high-strength brewery wastewater using a membrane-aeration bioreactor. Water Environment Research. 71, 1197-1204.

Casey, E., Glennon, B., Hamer, G., 1999. Review of membrane aerated biofilm reactors. Resources, Conservation and Recycling. 27 (1-2), 203–215.

Chaali, M., Naghdi, M., Brar, K., 2018. A review on the advances in nitrifying biofilm reactors and their removal rates in wastewater treatment. Journal of Chemical Technology and Biotechnology. 93, 3113–3124.

Chapra, S.C., Canale, P.R., 1998. Numerical Methods for Engineers with Software and Programming Applications, third Ed. McGrawHill, America.

Cote, P.L., Pedersen, S.K., 2014. Membrane assembly for supporting a biofilm. WO 2014/130043 A1. World Intellectual Property Organization. International Bureau.

Downing, L.S., & Nerenberg, R., 2008. Effect of oxygen gradients on the activity and microbial community structure of a nitrifying membrane-aerated biofilm. Biotechnology and Bioengineering. 101 (6), 1193-1204.

Flora, E.M.C.V., Suidan, M.T., Flora, J.R.V., Kim, B.J., 1999. Speciation and chemical interactions in nitrifying biofilms. I: Model development. Journal of Environmental Engineering. 125(9), 871–877.

Ge, S., Champagne, P., 2016. Nutrient removal, microalgal biomass growth, harvesting and lipid yield in response to centrate wastewater loadings. Water Research. 88, 604–612.

Ge, S., Qiu, S., Tremblay, D., Viner, K., Champagne, P., Jessop, P. G., 2018. Centrate wastewater treatment with Chlorella vulgaris : Simultaneous enhancement of nutrient removal, biomass and lipid production. Chemical Engineering Journal. 342, 310–320.

González-Brambila, M., Monroy, O., López-isunza, F., 2006. Experimental and theoretical study of membrane-aerated biofilm reactor behavior under different modes of oxygen supply for the treatment of synthetic wastewater. Chemical Engineering Science. 61, 5268–5281.

Goswami, L., Kumar, R.V., Borah, S.N., Manikandan, N.A., Pakshirajan, K., Pugazhenthi, G. 2018. Membrane bioreactor and integrated membrane bioreactor systems for micropollutant removal from wastewater: a review. Journal of Water Process Engineering. 26, 314-328.

Grady, C.P.L., Daigger, G.T., Love, N.G., Filipe, C.D.M., 2011.Biological Wastewater Treatment, third ed. CRC Press (Taylor &Francis Group), Boca Raton, FL, U.S.

Gwak, J., Jung, J.G.M., Hong, H., Quan, J.K.Z., Spasov, E., Neufeld, J.D., Wagner, M., Rhee, S., 2019. Archaeal nitrification is constrained by copper complexation with organic matter in municipal wastewater treatment plants. The ISME Journal, 335–346.

Hao, X., Heijnen, J. J., van Loosdrecht, M.C.M., 2002. Sensitivity Analysis of a Biofilm Model Describing a One-Stage Completely Autotrophic Nitrogen Removal (CANON) Process. Biotechnology and Bioengineering. 77(3), 266-277.

Henze, M., 1992. Characterization of wastewater for modeling of activated sludge processes. Water Science and Technology. 25 (6), 1–15.

Henze, M., Gujer, W., Mino, T., van Loosdrecht, M.C.M., 2000. Activated Sludge Models ASM1, ASM2, ASM2d and ASM3. IWA Scientific and Technical Report No. 9, London, UK.

Hibiya, K., Terada, A., Tsuneda, S., Hirata, A., 2003. Simultaneous nitrification and denitrification by controlling vertical and horizontal microenvironment in a membrane- aerated biofilm reactor. Journal of Biotechnology. 100, 23–32.

Hu, S., Yang, F., Sun, C., Zhang, J., Wang, T., 2008. Simultaneous removal of COD and nitrogen using a novel carbon-membrane aerated biofilm reactor. Journal of Environmental Science. 20 (2), 142–148.

Hwang, J.H., Cicek, N., Oleszkiewicz, J., 2009. Effect of loading rate and oxygen supply on nitrification in a non-porous membrane biofilm reactor. Water Research. 43, 3301- 3307.

Kinh, C.T., Suenaga, T., Hori, T., Riya, S., Hosomi, M., Smets, B.F., Terada, A., 2017.Counter-diffusion biofilms have lower N_2O emissions than co-diffusion biofilms during simultaneous nitrification and denitrification: Insights from depth-profile analysis. Water Research. 124, 363-371.

Krug, R., Hunter, W., Grieger, R., 1976. Enthalpy–entropy compensation. 1. Some fundamental statistical problems associated with the analysis of van't Hoff and Arrhenius data. Journal of Physical Chemistry. 80, 2335–234.

Lackner, S., Terada, A., Horn, H., Henze, M., & Smets, B.F., 2010. Nitration performance in membrane-aerated biofilm reactors differs from conventional biofilm systems. Water Research, 44(20), 6073–6084.

LaPara, T.M., Cole, A.C., Shanahan, J.W., Semmens, M.J., 2006. The effects of organic carbon, ammoniacal-nitrogen, and oxygen partial pressure on the stratification of membrane-aerated biofilms. Journal of Industrial Microbiology and Biotechnology. 33, 315–323.

Ledda, C., Villegas, G.I.R., Adani, F., Fernández, F.G.A., Grima, E.M., 2015. Utilization of centrate from wastewater treatment for the outdoor production of Nannochloropsis gaditana biomass at pilot-scale. Algal, 12, 17–25.

Li, M., Du, C., Liu, J., Quan, X., Lan, M., 2018. Mathematical modeling on the nitrogen removal inside the membrane- aerated biofilm dominated by ammonia-oxidizing archaea (AOA): Effects of temperature, aeration pressure and COD/N ratio. Chemical Engineering Journal. 338, 680–687.

Li, Y., Zhang, K., 2018. Pilot scale treatment of polluted surface waters using membrane-aerated biofilm reactor (MABR). Biotechnology & Biotechnological Equipment.32 (2), 376- 386.

Lin, J., Zhang, P., Li, G., Yin, J., Li, J., Zhao, X., 2016. Effect of COD/N ratio on nitrogen removal in a membrane-aerated biofilm reactor. International Biodeterioration & Biodegradation. 113, 74–79.

Liu, H., Yang, F., Shi, S., Liu, X., 2010. Effect of substrate COD/N ratio on performance and microbial community structure of a membrane aerated biofilm reactor. Journal of Environmental Sciences. 22 (4), 540–546.

Liu, Y., Hao, H., Guo, W., Peng, L., Pan, Y., Guo, J., Chen, X., Ni, B., 2016. Autotrophic nitrogen removal in membrane-aerated biofilms : Archaeal ammonia oxidation versus bacterial ammonia oxidation. Chemical Engineering Journal. 302, 535–544.

Lotti, T., Kleerebezem, R., Hu, Z., Kartal, B., Kreuk, M. K. De, Taalman, C.V.E., Kruit, J., Hendrickx, T.L.G., van Loosdrecht M.C.M., 2015. Pilot-scale evaluation of anammox-based mainstream nitrogen removal from municipal wastewater. Environmental Technology. 36 (9), 1167- 1177.

Martin, K.J., Nerenberg, R., 2012. The membrane biofilm reactor (MBfR) for water and wastewater treatment : Principles, applications, and recent developments. Bioresource Technology. 122, 83–94.

Martin, K., Sathyamoorthy, S., Houweling, D., Long, Z., Peeters, J., Snowling, S., 2017. A Sensitivity Analysis of Model Parameters Influencing the Biofilm Nitrification Rate : Comparison between the Aerated Biofilm Reactor (MABR) and Integrated

Fixed Film Activated Sludge (IFAS) Process. Water Environment Federation, 257-265.

Matsumoto, S., Terada, A., Tsuneda, S., 2007. Modeling of membrane-aerated biofilm : Effects of C/N ratio, biofilm thickness and surface loading of oxygen on feasibility of simultaneous nitrification and denitrification. Biochemical Engineering Journal. 37, 98–107.

Metcalf, E., Eddy, E., 2003. Wastewater Engineering: Treatment and Reuse. McGrawHill. Inc., New York.

Nerenberg, R., 2016. The membrane-biofilm reactor (MBfR) as a counter-diffusional biofilm process. Current Opinion in Biotechnology. 38, 131–136.

Nicolella, C., Pavasant, P., Livingston, A.G., 2000. Substrate counter diffusion and reaction in membrane-attached biofilms : mathematical analysis of rate limiting mechanisms. Chemical Engineering Science. 55, 1385–1398.

Nogueira, B.L., Perez, J., van Loosdrecht, M.C.M., Secchi, A.R., Dezotti, M., Biscaia Jr., E.C., 2015. Determination of the external mass transfer coefficient and influence of mixing intensity in moving bed biofilm reactors for wastewater treatment. Water Research. 80, 90- 98.

Pankhania, M., Brindle, K., Stephenson, T., 1999. Membrane aeration bioreactors for wastewater treatment : completely mixed and plug-flow operation. Chemical Engineering Journal. 73, 131–136.

Park, S., Chung, J., Rittmann, B.E., Bae, W., 2015. Nitrite Accumulation from Simultaneous Free-Ammonia and Free-Nitrous-Acid Inhibition and Oxygen Limitation in a Continuous-Flow Biofilm Reactor. Biotechnology and Bioengineering. 112 (1), 43–52.

Peng, L., Chen, X., Xu, Y., Liu, Y., Gao, S., Ni, B., 2015. Biodegradation of pharmaceuticals in membrane aerated biofilm reactor for autotrophic nitrogen removal : A model-based evaluation. Journal of Membrane Science. 494, 39–47.

Peng, L., Liu, Y., Ni, B., 2016. Nitrous oxide production in completely autotrophic nitrogen removal biofilm process : A simulation study. Chemical Engineering Journal. 287, 217–224.

Perez-Calleja, P., Aybar, M., Picioreanu, C., Esteban-Garcia, A.L., Martin, K.J., Nerenberg, R., 2017. Periodic venting of MABR lumen allows high removal rates and high gas-transfer efficiencies. Water Research. 121, 349–360.

Picioreanu, C., Van Loosdrecht, M.C.M, Heijnen, J., 1997. Modelling the effect of oxygen concentration on nitrite accumulation in a biofilm airlift suspension reactor. Water Science and Technology. 36 (1), 147-156.

Picioreanu, C., Kreft, J., Van Loosdrecht, M.C.M., 2004. Particle-Based Multidimensional Multispecies Biofilm Model. Applied and Environmental Microbiology. 70 (5), 3024–3040.

Satoh, H., Okabe, S., Norimatsu, N., Watanabe, Y., 2000. Significance of substrate C / N ratio on structure and activity of nitrifying biofilms determined by in situ hybridization and the use of microelectrodes. Water Science & Technology. 41 (4-5), 317–321.

Satoh, H., Ono, H., Rulin, B., Kamo, J., Okabe, S., 2004. Macroscale and microscale analyses of nitrification and denitrification in biofilms attached on membrane aerated biofilm reactors. Water Research. 38, 1633–1641.

Semmens, M.J., Dahm, K., Shanahan, J., Christianson, A., 2003. COD and nitrogen removal by biofilms growing on gas permeable membranes. Water Research. 37, 4343–4350.

Shanahan, J.W, Semmens, M.J., 2004. Multipopulation Model of Membrane-Aerated Biofilms. Environmental Science and Technology. 38(11), 3176–3183.

Shanahan, J. W., Semmens, M.J., 2015. Alkalinity and pH effects on nitrification in a membrane aerated bioreactor : An experimental and model analysis. Water Research. 4, 10–22.

Stewart, P. S., 1998. A Review of Experimental Measurements of Effective Diffusive Permeabilities and Effective Diffusion Coefficients in Biofilms. Biotechnology and Bioengineering. 59 (3), 261 -272.

Stewart, P.S., 2003. Diffusion in Biofilms. Journal of bacteriology. 185 (5), 1485–1491.

Syron, E., Casey, E., 2008a. Model-Based Comparative Performance Analysis of Membrane Aerated Biofilm Reactor Configurations. Biotechnology and Bioengineering. 99 (6), 1361–1373.

Syron, E., Casey, E., 2008b. Membrane-Aerated Biofilms for High Rate biotreatment : Performance Appraisal, Engineering Principles, Scale-up, and Development Requirements. Environmental Science and Technology. 42 (6), 1833–1844.

Syron, E., Semmens, M.J., Casey, E., 2015. Performance analysis of a pilot-scale membrane aerated biofilm reactor for the treatment of landfill leachate. Chemical Engineering Journal. 273, 120–129.

Tchobanoglous, G., Burton, F.L., 1991. Advanced Wastewater Treatment. Wastewater Engineering, Treatment, Disposal, and Reuse. McGraw-Hill. Inc., Singapore, 711-726.

Terada, A., Hibiya, K., Nagai, J., Tsuneda, S., Hirata, A., 2003. Nitrogen Removal Characteristics and Biofilm Analysis of a Membrane-Aerated Biofilm Reactor Applicable to High-Strength Nitrogenous Wastewater Treatment. Journal of Bioscience and Bioengineering. 95 (2), 170–178.

Terada, A., Yamamoto, T., Igarashi, R., Tsuneda, S., Hirata, A., 2006. Feasibility of a membrane-aerated biofilm reactor to achieve controllable nitrification. Biochemical Engineering Journal. 28, 123–130.

Tian, H., Zhang, H., Li, P., Sun, L., Hou, F., & Li, B., 2015.Treatment of pharmaceutical wastewater for reuse by coupled membrane-aerated biofilm reactor. RSC Advances. RSC advances. 5, 69829–69838.

Tukey, J.W., 1977. Exploratory data analysis (Vol. 2). Reading Mass.

Van Loosdrecht, M.C.M., Heijnen, J.J., Eberl, H., Kreft, J., Picioreanu, C., 2002. Mathematical modeling of biofilm structures. Antonie van Leeuwenhoek. 81, 245–256.

Wäsche, S., Horn, H., Hempel, D.C., 2002. Influence of growth conditions on biofilm development and mass transfer at the bulk/biofilm interface. Water Research. 36 (19), 4775–4784.

Wan, T., Zhang, G., Du, F., He, J., Wu, P., 2014. Combined biological aerated filter and Sulfur /ceramisite autotrophic denitrification for advanced wastewater nitrogen removal in low temperatures. Frontiers of Environmental Science and Engineering. 8 (6), 967-972.

Wang, R., Terada, A., Lackner, S., Smets, B.F., Henze, M., Xia, S., Zhao, J. 2009. Nitritation performance and biofilm development of co- and counter-diffusion biofilm reactors : Modeling and experimental comparison. Water Research. 43(10), 2699–2709.

Wang, R., Xiao, F., Wang, Y., Lewandowski, Z., 2016. Determining the optimal trans-membrane gas pressure for nitrification in membrane-aerated biofilm reactors based on oxygen profile analysis. Applied Microbiology and Biotechnology. 100, 7699–7711.

Wiesmann, U., 1994. Biological nitrogen removal from wastewater. Advances in Biochemical Engineering & Biotechnology. 51, 113–154.

Xu, Y., Peng, L., Liu, Y., Xie, G., Song, S., Ni, B., 2020. Modelling melamine biodegradation in a membrane aerated biofilm reactor. Journal of Water Process Engineering. 38, 101626.

Yamagiwa, K., Ohkawa, A., Hirasa, O., 1994. Simultaneous organic carbon removal and nitrification by biofilm formed on oxygen enrichment membrane. Journal of Chemical Engineering. 27,638-643.

Yamagiwa, K., Yoshida, M., Ito, A., Ohkawa, A., 1998. A new oxygen supply method for simultaneous organic carbon removal and nitrification by a one-stage biofilm process. Water Science & Technology. 37, 117-124.

Yang, S., Yang, F., Fu, Z., Lei, R., 2009. Comparison between a moving bed membrane bioreactor and a conventional membrane bioreactor on organic carbon and nitrogen removal. Bioresource Technology. 100 (8), 2369–2374.

Yuan, Q., Jia, H., Poveda, M., 2016. Study on the effect of landfill leachate on nutrient removal from municipal wastewater. Journal of Environmental Sciences. 43, 153–158.

3. Estimation of rate kinetic constants in microplastic degradation using hydrolytic enzymes

Microplastic (MP) is an emerging contaminant in wastewater and can cause serious environmental and public health problems. MP removal is difficult in conventional biological wastewater treatment. Therefore, lab-scale experiments were conducted to describe the MP degradation using hydrolytic enzymes under various experimental conditions (e.g., temperature and enzyme dose). Also, a mathematical model was developed and calibrated using the experimental results to estimate the rate kinetic constants of MP degradation and enzyme self-decay. The mathematical model can be used for approximating the MP removal in anaerobic digestion process.

This paper is prepared for future journal publication.

- Elsayed, A., Kim, Y. Estimation of rate kinetic constants in microplastic degradation using hydrolytic enzymes.

The co-author's contributions include:

- Funding acquisition.
- Supervision and technical support.
- Manuscript review and revision.

Abstract

Microplastic (MP) is an emerging contaminant that can cause serious environmental and public health problems. There are many challenges (e.g., potential bypass of MP particles to sludge treatment systems) of MP removal in conventional wastewater treatment that make wastewater treatment plants an active source for MP release to the environment. Moreover, there are no systematic studies on MP degradation by hydrolytic enzymes that are rich in concentration within the sludge treatment process, such as anaerobic digestion. In this study, therefore, lab-scale experiments were implemented to investigate the degradation of polyethylene beads by hydrolytic enzymes (i.e., lipase, cellulase and protease) under various experimental conditions (e.g., enzyme concentration and temperature). In a 3-day batch experiment, protease was most effective in MP degradation as 4.0% of the initial MP mass was removed at an enzyme concentration of 88 mg/L under thermophilic temperature (55°C). It was also found that the increasing enzyme concentration enhanced the MP degradation for the three examined enzymes. Also, high temperature increased the reduction of MP and the temperature correction factor (θ) was found to be 1.016 to 1.019, indicating strong dependency on temperature. In a separate 7-day experiment with repeated doses of protease, 23.3% of the initial MP mass was removed at thermophilic temperature, indicating that anaerobic digestion with a long retention time (e.g., 20 days) and heated temperature (e.g., thermophilic digestion) has a significant potential for MP degradation. A mathematical model was developed and calibrated using the experimental results to estimate the kinetic constant of MP reduction by an enzyme ($k_{1,i}$) and enzyme self-decay constant ($k_{2,ii}$). The calibrated $k_{1,i}$ ranged from 5.0 to 8.1 × 10^{-4} L/mg/hr while $k_{2,ii}$ was

0.44 – 1.10 L/mg/hr. Using the calibrated model, MP degradation using multiple enzymes (i.e., cellulase and protease) was simulated, considering the interactive-decay reaction between the two enzymes. The interactive-decay constant of cellulase and protease ($k_{2,CP}$) was estimated to be 0.51 L/mg/hr where 3.8% of the initial MP mass was removed after 3 days of the experiment. The calibrated model was also used to simulate the MP degradation in anaerobic digestion where 70 – 95% of the initial MP mass was removed at typical retention time (e.g., 15 – 20 days) under mesophilic digestion (37.5°C). Also, it was found that the temperature has a negligible effect on the MP degradation while retention time is dominant on MP removal in anaerobic digestion. Based on the experimental and simulation results, it can be concluded that hydrolytic enzymes can be used as an efficient technology for large-scale MP removal applications.

Keywords

Microplastic; hydrolytic enzyme; enzyme concentration; model calibration; protease; kinetic constant.

3.1 Introduction

Microplastic (MP) is an emerging contaminant with a particle size smaller than 5 mm (Ziajahromi et al., 2017; Blair et al., 2019; Magni et al., 2019). MP is highly mobile in the aquatic environment because of its insolubility in water and light-weight (Holland et al., 2016; Murphy et al., 2016), causing serious environmental and public health problems (Pettipas et al., 2016; Auta et al., 2017; Wright and Kelly, 2017; Silva et al., 2018). MP can release toxic monomers and plastic additives (e.g., phthalates and

bisphenol A) in the bodies of biota (e.g., fishes and seabirds) (Wardrop et al., 2016; Anderson et al., 2017; Lu et al., 2018; Pitt et al., 2018). Also, MP can cause critical problems in the digestive and respiratory system of humans (Rochman et al., 2015; Ferreira et al., 2016; Miranda and Carvalho-Souza, 2016; Revel et al., 2018). MP can adsorb and accumulate heavy metals (e.g., nickel, zinc, lead and cadmium) (Koelmans et al., 2016; Sun et al., 2019; Wu et al., 2020) and hydrophobic organics pollutants (e.g., pesticides and polychlorinated biphenyls) (Wu et al., 2016; Gatidou et al., 2019; Zhou et al., 2021), leading to serious environmental disasters for the aquatic habitats and ecosystem balance.

Limited MP removal during wastewater treatment process is an active source of discharging MP to the environment (Mason et al., 2016; Gies et al., 2018; Edo et al., 2020; Li et al., 2020). MP is transported to the wastewater treatment plants with raw wastewater, including synthetic fibers of clothes washing, microbeads from toothpastes, and microparticles from tire fragments (Pirc et al., 2016; Cheung and Fok, 2017; Alvim et al., 2020). MP concentration in wastewater sludge can be up to 56×10^3 MP particles per kg of dry sludge depending on the WWTP capacity, sludge source and serving population (Mahon et al., 2017; Peng et al., 2017; Wang et al., 2017). In wastewater and sludge treatment processes, MP includes polyethylene (PE), polyvinylchloride (PVC), polypropylene (PP), polyamide (PA), polystyrene (PS), polyethylene terephthalate (PET), polyolefin, acrylic fibers, alkyd resins, rubber and acetyl (Avio et al., 2016; Horton et al., 2017; Rezania et al., 2018; Xu et al., 2019). PE is the most abundant type of MP in wastewater and sludge treatment processes (Tagg et al., 2015; Alimi et al., 2018; Wei et al., 2019). Therefore, the main focus in this study was oriented towards PE-based MP.

Chemical removal of MP through coagulation process using inorganic coagulants is one of the potential techniques for MP removal (Hidayaturrahman and Lee, 2019). Moreover, ozone technology is a promising way for efficient MP removal because ozone can change the physical, ionic, mechanical and adhesion properties of MP (Chen et al., 2018; Poerio et al., 2019). Membrane disc-filter can also be used for MP removal in the wastewater treatment process; however, it is suitable for low influent concentration of MP to avoid membrane clogging (Talvitie et al., 2017a). Although rapid sand filtration can be applied for MP removal through trapping the plastic particles between the sand grains, MP should have a particle size larger than the diameter of grains to avoid potential passing through the sand filtration (Michielssen et al., 2016; Talvitie et al., 2017a; Hidayaturrahman and Lee, 2019). It was also emphasized in other MP studies that biological wastewater treatment can decrease the concentration of MP in wastewater using sequence batch reactor, anaerobic-anoxic-aerobic and membrane systems (Carr et al., 2016; Lares et al., 2018; Lee and Kim, 2018; Li et al., 2018). However, the removed MP particles in the biological wastewater treatment process are transferred to the sludge treatment process (i.e., anaerobic digestion) (Mintenig et al., 2017; Raju et al., 2020; Zhang et al., 2020). Moreover, a combination of mechanical, biological and chemical treatment can achieve reasonable MP removal rate in the sludge treatment process (Talvitie et al., 2017b; Song et al., 2017).

There are numerous applications for hydrolytic enzymes in wastewater and sludge treatment processes (e.g., enhancing hydrolysis rate in anaerobic digestion) (Yu et al., 2013; Domingues et al., 2015; Odnell et al., 2016); however, limited studies investigated the MP removal using these enzymes (Othman et al., 2021). Moreover, there are no

systematic studies on the effect of operational conditions (e.g., temperature and enzyme dose) on the MP removal. Also, there is a lack of comprehensive modeling studies about the MP removal mechanisms and the rate-limiting parameters using hydrolytic enzymes. Thus, the kinetic constants of the MP removal reactions using enzymes are unknown, resulting in a lack of prediction mathematical models for determining the MP removal in anaerobic digestion and other biological treatment systems. Therefore, mathematical models coupled with experimentation is essential to simulate the MP removal by hydrolytic enzymes, resulting in accurate determination of the reaction kinetic constants for better understanding of the MP removal rate and the dominant operational parameters.

In this study, the main objectives are to: (1) investigate the MP reduction using hydrolytic enzymes; (2) assess the effect of experimental conditions (e.g., enzyme concentration and temperature) on the degradation of MP; (3) develop a mathematical model to simulate the reduction of MP under different experimental conditions; and (4) calibrate the numerical model with the experimental results to estimate the model kinetic constants.

3.2 *Methods*

3.2.1 Single batch tests

White polyethylene (PE) spherical microplastics with a diameter of 500 - 600 µm were used in the experiment (Cospheric LLC Co., WPMS-1.35 500-600 µm – 10g, USA). The density of the MP was 1.35 g/mL to ensure that the MP particles were submerged in water during the experiment. MP reduction batch tests were carried out in 160-mL air tight glass bottles. Each bottle contained 450 mg/L of MP (initial mass = 70.5

mg ± 3%), 5 mM of NaCl, 3.0 mM of Na_2HPO_4, 1.5 mM of NaH_2PO_4, 0.4 mM of NH_4Cl and 0.1 mM of KCl in the experimental solution (pH = 7.8 ± 0.2). The selected enzyme(s) was added at the beginning of the experiment (Table 3.1). In each test, the bottles were capped with rubber stoppers and metal caps after being purged with nitrogen for 3 minutes to maintain strict anaerobic conditions during the experiment. The bottles were placed in a heated temperature chamber for 1, 3, 7, 24 and 72 hours. All tests were performed in duplicate and control tests were conducted without enzymes to confirm no MP reduction. The remaining MP particles were retrieved, rinsed and dried to determine the reduction in MP mass using a scale with a precision of four decimal points. The MP degradation was estimated based on the difference in MP mass before and after the hydrolysis reaction.

Table 3.1. Summary of the experimental conditions.

Temperature	Enzyme type	Enzyme concentration	Operation
37.5 and 55°C	Lipase only	22 mg/L 44 mg/L 88 mg/L	Single batch over 72 hours
37.5 and 55°C	Cellulase only	22 mg/L 44 mg/L 88 mg/L	Single batch over 72 hours
37.5 and 55°C	Protease only	22 mg/L 44 mg/L 88 mg/L	Single batch over 72 hours
55°C	Cellulase Protease	44 mg/L 44 mg/L	Single batch over 72 hours

3.2.2 Repeated doses of enzyme test

A repeated doses of enzyme experiment was performed using protease to investigate the effect of repetitive cycles of enzyme addition on the reduction of MP. Protease was selected because it was the most effective enzyme on MP reduction among the three examined enzymes. The experimental solution was identical to the one used in the single batch tests (pH = 7.9). In the first cycle, the initial 1.35 g/mL-dense MP mass was 70.5 mg and protease concentration was 88 mg/L. The glass bottle was capped, purged using nitrogen and placed in a temperature chamber at temperature of 55°C. After each cycle, the MP sample was rinsed, dried and weighted to update the initial MP mass for the new cycle. Protease was added every weekday for seven cycles (9 days) with an enzyme concentration of 20% (w/w) of the initial MP mass of each cycle. After the last cycle, the residual MP mass was measured and analyzed under electronic microscope (Nikon Eclipse E200, Japan).

3.2.3 Numerical model development

A non-steady state model was developed to simulate the reduction of MP by hydrolytic enzymes. The model described the MP reduction rate by an enzyme using a MP reduction kinetic constant ($k_{1,i}$) (Eq. 3.1), assuming loss of enzyme during the MP reduction. Also, the model included the self-decay reaction of an enzyme (collision between enzyme particles) where a second order enzyme self-decay constant ($k_{2,ii}$) was defined (Eq. 3.2).

$$\frac{dC_{MP}}{dt} = -k_{1,i}.E_i.C_{MP} \qquad (Eq\ 3.1)$$

$$\frac{dE_i}{dt} = -k_{2,ii}.{E_i}^2 - k_{1,i}.E_i.C_{MP} \qquad (Eq\ 3.2)$$

where C_{MP} is the MP concentration, E_i is the concentration of an enzyme, $k_{1,i}$ is the kinetic constant of MP reduction by an enzyme and $k_{2,ii}$ is the self-decay constant for an enzyme.

In the multiple enzymes simulation, the MP reduction by cellulase and protease was described using two MP reduction kinetic constants ($k_{1,C}$ and $k_{1,P}$) (Eq. 3.3). Eq. 3.2 was also expanded to consider the interaction between cellulase and protease (Eq. 3.4 and 3.5) by adding an interactive-decay constant between the two enzymes ($k_{2,CP}$). In the non-steady state model, the mass balance equations for the enzymes and MP were discretized using the implicit Euler method (Chapra and Canale, 1998) and solved by fixed point iteration (tolerance = 10^{-7}). The time step was assumed to be 10 seconds; however, larger time steps can be used in the temporal discretization with high numerical solution accuracy.

$$\frac{dC_{MP}}{dt} = -k_{1,C}.E_C.C_{MP} - k_{1,P}.E_P.C_{MP} \qquad (Eq\ 3.3)$$

$$\frac{dE_C}{dt} = -k_{2,CC}.{E_C}^2 - k_{1,C}.E_C.C_{MP} - k_{2,CP}.E_C.E_P \qquad (Eq\ 3.4)$$

$$\frac{dE_P}{dt} = -k_{2,PP}.{E_P}^2 - k_{1,P}.E_P.C_{MP} - k_{2,CP}.E_C.E_P \qquad (Eq\ 3.5)$$

where E_C is cellulase concentration, E_P is protease concentration, $k_{1,C}$ is the kinetic constant of MP reduction by cellulase, $k_{1,P}$ is the kinetic constant of MP reduction by protease, $k_{2,CC}$ is the self-decay constant of cellulase, $k_{2,PP}$ is the self-decay constant of protease and $k_{2,CP}$ is the interactive-decay constant of cellulase and protease.

3.3 Results and discussion

3.3.1 Effect of enzyme type and concentration on MP reduction

In the thermophilic batch experiment using three types of hydrolytic enzymes, the reduction of MP was enhanced linearly with the increasing enzyme concentration from 22 to 88 mg/L (Fig. 3.1). This experimental result is consistent with the results obtained from other enzymatic reaction studies, reflecting the importance of enzyme concentration on the removal efficiency (Cirne et al., 2007; Yang et al., 2010; Mlaik et al., 2019). The reduction in the residual MP mass was 1.1 mg for the lipase concentration of 22 mg/L while it increased to 1.4 mg for the enzyme concentration of 44 mg/L and 1.8 mg for the concentration of 88 mg/L (Fig. 3.1a). Also, the removal of MP was improved up to 2.6 mg with cellulase (Fig. 3.1b) and up to 2.8 mg with protease (Fig. 3.1c) for the enzyme concentration of 88 mg/L.

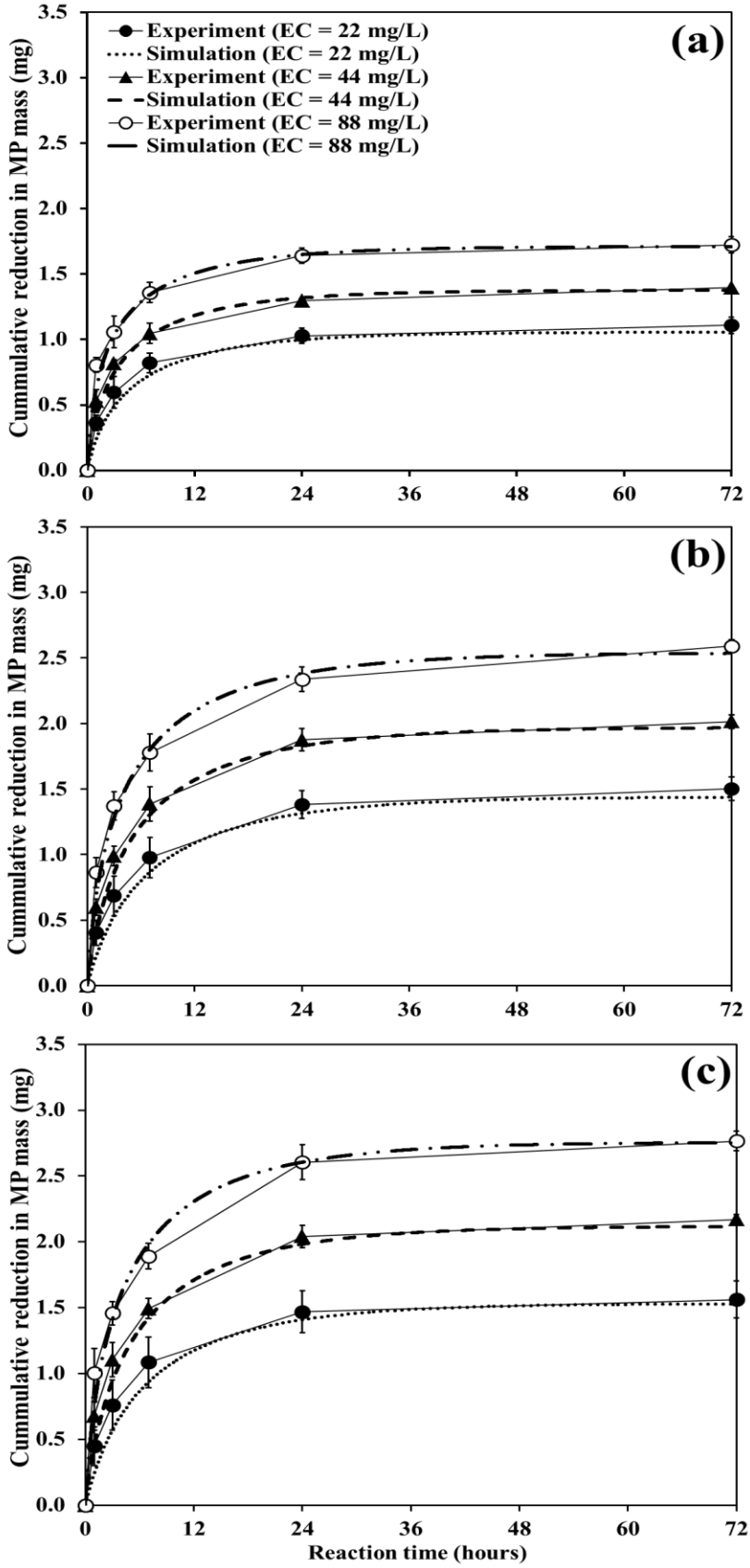
(a)
(b)
(c)
Experiment (EC = 22 mg/L)
Simulation (EC = 22 mg/L)
Experiment (EC = 44 mg/L)
Simulation (EC = 44 mg/L)
Experiment (EC = 88 mg/L)
Simulation (EC = 88 mg/L)
Cummulative reduction in MP mass (mg)
Reaction time (hours)
0.0
0.5
1.0
1.5
2.0
2.5
3.0
3.5
0
12
24
36
48
60
72

Fig. 3.1. Comparison between the experimental results and model simulations for all three hydrolytic enzymes using three different enzyme concentrations (22, 44 and 88 mg/L) under thermophilic conditions (T = 55°C): (a) lipase, (b) cellulase, and (c) protease. Calibrated kinetic constants were used for the model simulations (Table 3.2 and 3.3).

The MP reduction rate was rapid for the first seven hours of the experiment for all three enzymes (Fig. 3.1). After seven hours of the experiment, the reduction in the MP mass was 75% (1.3 out of 1.8 mg) with lipase, 67% (1.7 out of 2.6 mg) with cellulase and 65% (1.8 out of 2.8 mg) with protease for the enzyme concentration of 88 mg/L while the rest was reduced during the latter 65 hours of the experiment. This result is consistent with the results of previous enzyme studies where it was observed that the enzyme activity was the highest within the first 4-8 hours of the experiment based on the enzyme stability, temperature and pressure (Marie-Olive et al., 2000; Daniel et al., 2008; Yang et al., 2010; Luo et al., 2012). It was also noticed that there was no significant change in the MP reduction after 24 hours of the experiment where the MP reduction was 5% (0.09 out of 1.8 mg) with lipase, 6% (0.14 out of 2.6 mg) with cellulase and 7% (0.17 out of 2.8 mg) with protease (Fig. 3.1), reflecting a complete depletion of enzyme activity.

3.3.2 Effect of temperature on MP reduction

The thermophilic condition (55°C) greatly enhanced the MP reduction compared to the mesophilic condition (37.5°C) by 22% (from 1.4 to 1.8 mg) with lipase, 16% (from 2.2 to 2.6 mg) with cellulase and 14% (from 2.4 to 2.8 mg) with protease for the enzyme concentration of 88 mg/L after 3 days of the experiment (Fig. 3.2). The activity of lipase was the most sensitive to the temperature increase while protease was the least sensitive

to the examined temperature conditions (Fig. 3.2a and c). For the mesophilic condition, the MP degradation rate was rapid during the first seven hours of the experiment where the reduction in the MP mass was 72% (1.0 out of 1.4 mg) with lipase, 68% (1.5 out of 2.2 mg) with cellulase and 70% (1.7 out of 2.4 mg) with protease for the enzyme concentration of 88 mg/L (Fig. 3.2). Although the change in MP reduction was minor after 24 hours of the mesophilic experiment, mesophilic condition resulted in higher MP reduction rate during the latter 48 hours of the experiment compared to the thermophilic condition because low temperature provided residual enzyme during the rest of the experiment (from 1 to 3 days). Under mesophilic condition, 10% (lipase), 9% (cellulase) and 8% (protease) of the removed MP was degraded within the latter 48-hours of operation for the enzyme concentration of 88 mg/L.

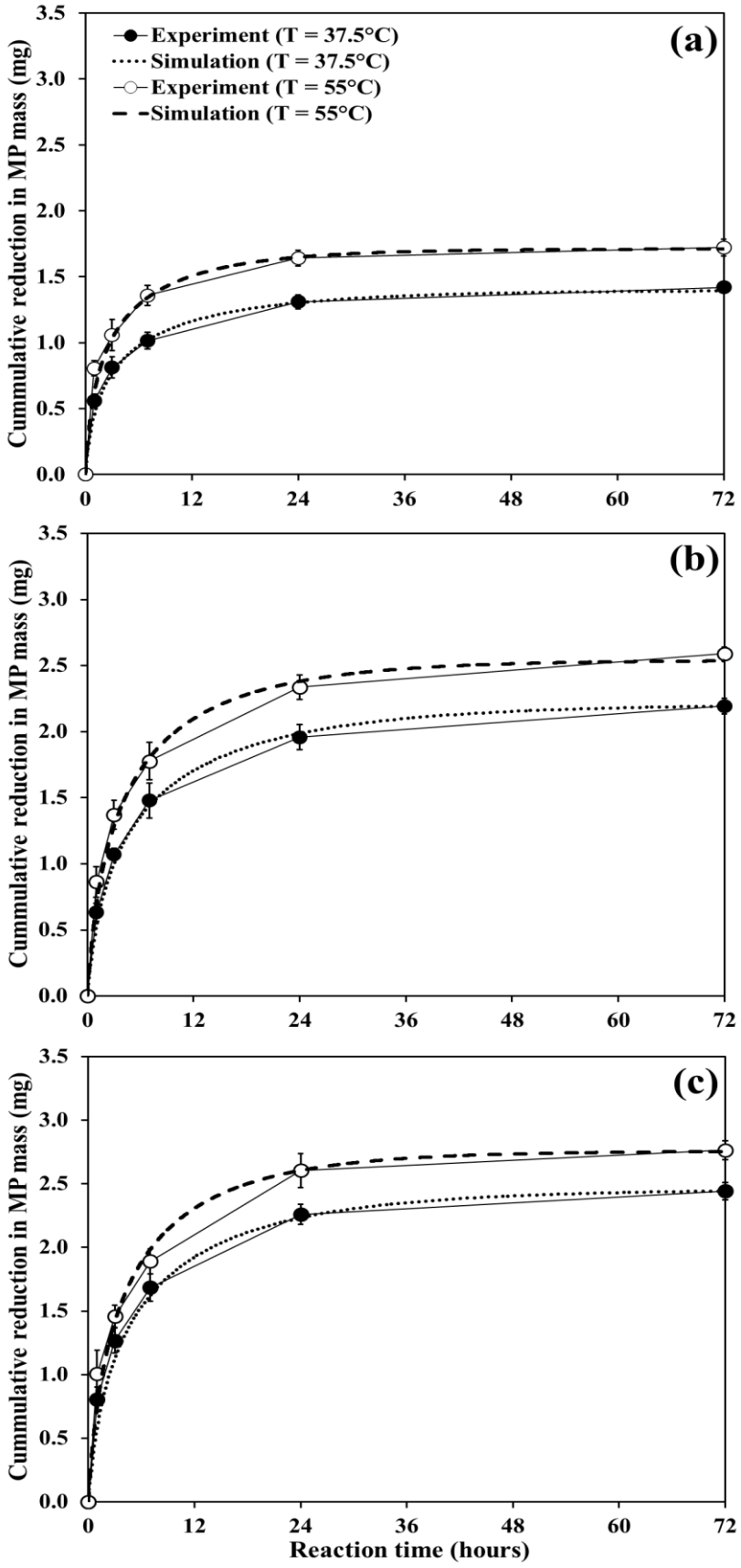
Experiment (T = 37.5°C)
Simulation (T = 37.5°C)
Experiment (T = 55°C)
Simulation (T = 55°C)
(a)
(b)
(c)
Cummulative reduction in MP mass (mg)
Reaction time (hours)
0.0
0.5
1.0
1.5
2.0
2.5
3.0
3.5
0
12
24
36
48
60
72

Fig. 3.2. Comparison between the experimental results and model simulations for all three hydrolytic enzymes under mesophilic and thermophilic conditions for the enzyme concentration of 88 mg/L: (a) lipase, (b) cellulase, and (c) protease. Calibrated kinetic constants were used for the model simulations (Table 3.2 and 3.3).

3.3.3 Model calibration with the experimental results

The developed enzyme kinetic mathematical model for MP reduction was calibrated using the experimental results (Fig. 3.1 and 3.2). The calibrated kinetic constant for MP reduction by an enzyme ($k_{1,i}$) was determined for the three examined enzymes (i.e., lipase, cellulase and protease) under mesophilic and thermophilic conditions (Table 3.2). Under mesophilic conditions, $k_{1,i}$ was 5.8×10^{-4} L/mg/hr (lipase), 5.0×10^{-4} L/mg/hr (cellulase) and 5.5×10^{-4} L/mg/hr (protease) while it increased by 40% for lipase, 36% for cellulase and 33% for protease when the temperature increased from 37.5 to 55°C. These values are comparable with the ranges of kinetic constants that were estimated or mentioned in previous enzyme studies (1.0×10^{-4} – 5.5×10^{-4} L/mg/hr) (Tomei et al., 2008; Leiyu et al., 2009; Luo et al., 2012). It was found that $k_{1,i}$ is sensitive to temperature and its degree of sensitivity is similar to the sensitivity of other kinetic constants in the activated sludge models (ASM) (e.g., growth and decay constants) (Henze et al., 2000; Elsayed et al., 2021). It was also noticed that the degree of sensitivity to the temperature is similar among the three examined enzymes (θ = 1.016 – 1.019).

Table 3.2. Calibrated kinetic constant for MP reduction by an enzyme ($k_{1,i}$) in L/mg/hr for the three examined hydrolytic enzymes under mesophilic and thermophilic conditions.

Enzyme	Thermophilic (55°C) $\times 10^{-4}$	Mesophilic (37.5°C) $\times 10^{-4}$	Temperature correction factor (θ)
Lipase	8.1	5.8	1.019
Cellulase	6.8	5.0	1.018
Protease	7.3	5.5	1.016

The second order enzyme self-decay constant ($k_{2,ii}$) was also estimated to be 1.05 L/mg/hr (lipase), 0.47 L/mg/hr (cellulase) and 0.44 L/mg/hr (protease) under mesophilic conditions (Table 3.3). For high temperature condition (55°C), $k_{2,ii}$ increased by 5% for lipase, 11% for cellulase and 14% for protease. It was demonstrated that the temperature had a negligible effect on the half-life of the three examined enzymes. Based on the determined enzyme self-decay constant, the half-life decreased by a marginal time period with the increased temperature for all three enzymes: from 26 to 24 min (lipase); from 57 to 51 min (cellulase); and 60 to 54 min (protease). The estimated half-life is consistent with the determined and mentioned values in previous enzyme studies where they ranged from 17 to 60 minutes at temperature of 40 -50°C for lipase (Mateos Diaz et al., 2006; Gutarra et al., 2009; Kim et al., 2016), 20 to 32 minutes at temperature of 70 - 80°C for cellulase (Stutzenberger, 1972; Dalal et al., 2007; Perwez et al., 2019) and 55 to 65 minutes at temperature of 60 - 70°C for protease (Atalo and Gashe, 1993; Li et al., 1997; Negi and Banerjee, 2009). This finding also means that the self-decay constant of an

enzyme ($k_{2,ii}$) is less sensitive to temperature for the three examined enzymes (θ = 1.003 - 1.006).

Table 3.3. Calibrated enzyme self-decay constant ($k_{2,ii}$) in L/mg/hr for the three examined hydrolytic enzymes under mesophilic and thermophilic conditions.

Enzyme	Thermophilic (55°C)	Mesophilic (37.5°C)	Temperature correction factor (θ)
Lipase	1.10	1.05	1.003
Cellulase	0.52	0.47	1.006
Protease	0.50	0.44	1.006

3.3.4 MP removal by repeated doses of enzyme

In the repeated enzyme addition experiment, the cumulative MP reduction along the reaction time (9 days) reached to 23.3% (16.4 out of 70.5 mg) while the average MP reduction was 2.35 mg over the seven operational cycles (Fig. 3.3a). The enzyme type (protease), concentration (20% of the residual MP mass) and temperature (55°C) were selected based on the previously mentioned experimental results where high MP reduction was obtained (Fig. 3.1 and 3.2). Repetitive addition of protease and high temperature (55°C) stimulated the enzyme motion, causing high collision rate between enzyme and MP particles coupled with significant changes in the shape of MP particles (Fig. 3.4b). After the first cycle of the experiment, the reduction in MP mass was 2.6 mg while it became 2.05 mg after the seventh cycle due to the decrease in the MP surface area and the drop in the added enzyme concentration (from 88 to 70 mg/L). The degree of MP mass removal after each cycle did not change over the seven cycles (3.70% of the

residual MP mass), reflecting the validity of kinetic constant assumptions for the mathematical model. The degree of MP mass removal in the repeated doses of protease experiment is consistent with the reduction in MP mass after 24 hours in the previously mentioned experimental results (Fig. 3.1c).

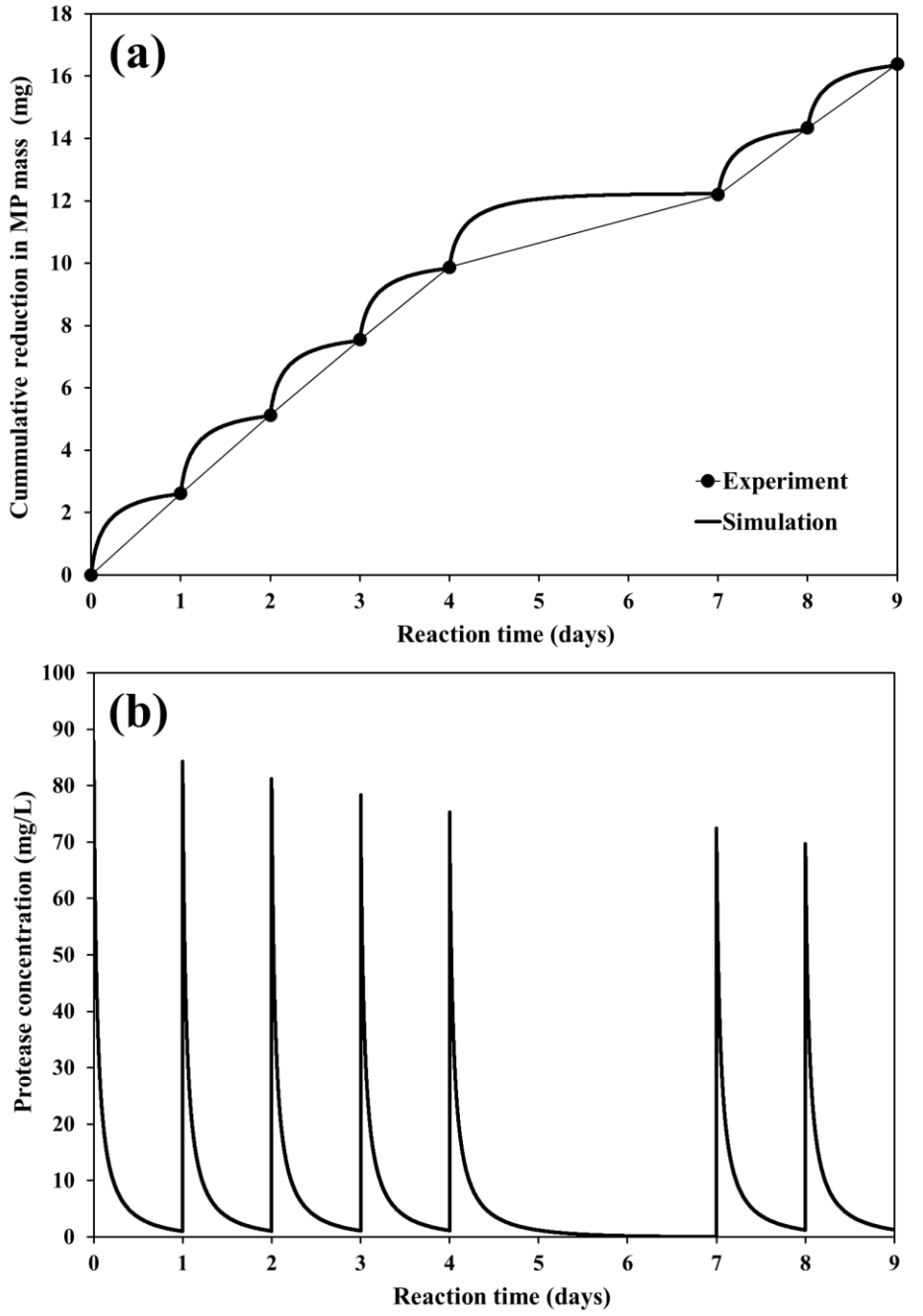

Fig. 3.3. MP removal by repetitive doses of protease: (a) comparison between the experimental data and simulation results of cumulative MP reduction, and (b) modeled enzyme concentration over the time. (Operational conditions: protease concentration = 20% of the residual MP mass, and temperature = 55°C). The sample was rinsed, dried and analyzed each weekday along the experiment duration. (Simulation conditions: the calibrated kinetic constants were adopted from Table 3.2 and 3.3).

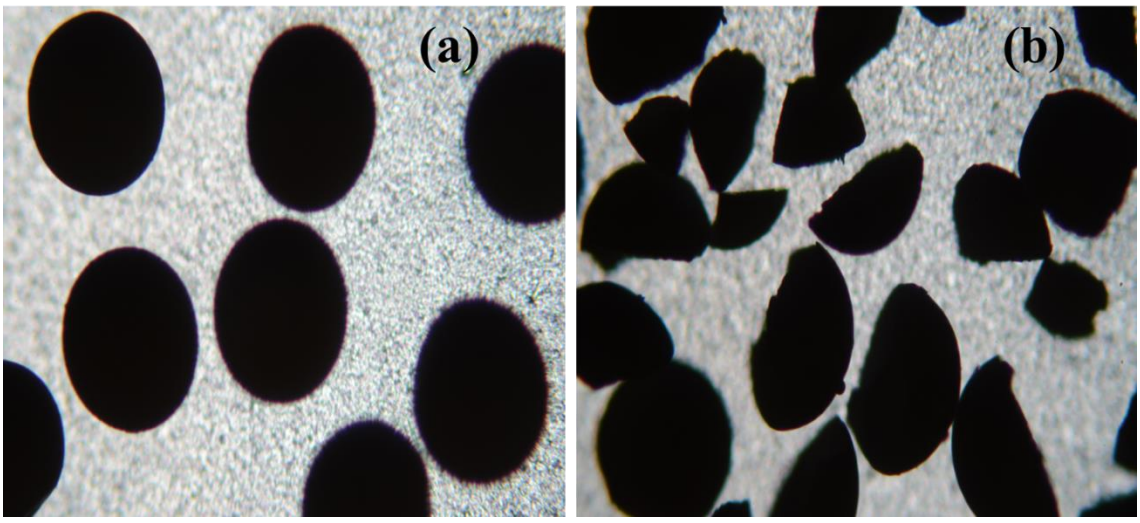

Fig. 3.4. Microscopic images for MP particles before and after protease addition in the repeated feeding experiment: (a) control (clean), and (b) 23.3% reduction of MP by protease. (Operational conditions: protease concentration = 20% of the residual MP mass from the previous cycle, total experiment duration = 9 days, and temperature = 55°C). The sample was rinsed, dried prior to being analyzed using the microscope.

The non-steady state mathematical model was applied to simulate the repeated doses of enzyme experiment where it was able to capture the same trend and values of MP reduction along the operation time using the calibrated model kinetic constant of MP reduction by protease ($k_{1,P}$) and protease self-decay constant ($k_{2,PP}$) (Fig. 3.3a, Table 3.2 and 3.3). Also, it was emphasized that there was a negligible residual enzyme (1-2% of the initial added concentration of protease) after each 1-day cycle (Fig. 3.3b), confirming

that MP reduction after 24 hours is negligible. This simulation result is consistent with the previously mentioned experimental results where most of the reduced MP mass was removed within the first 24 hours of the experiment (Fig. 3.1 and 3.2).

3.3.5 MP removal using multiple enzymes

MP reduction using two enzymes (cellulase and protease) resulted in 3.77% (2.66 out of 70.5 mg) of MP removal in 3 days (Fig. 3.5). It was demonstrated that removal of MP by the two enzymes was higher than that caused by cellulase only (3.62%) and lower than the MP reduction by single protease (3.93%) under the same experimental conditions (Fig. 3.5), indicating that protease was the most effective enzyme on MP reduction. The decay reaction between cellulase and protease was considered (Eq. 3.4 and 3. 5) where the second order interactive-decay constant of cellulase and protease ($k_{2,CP}$) was estimated to be 0.51 L/mg/hr, showing high consistency with the self-decay constant of cellulase ($k_{2,CC}$) and protease ($k_{2,PP}$) under the same temperature condition (Table 3.3). It was also observed that the mathematical model overestimated the MP reduction when no interaction between cellulase and protease was considered where the MP reduction was 5.75% (4.05 out of 70.5 mg) in 3 days (Fig. 3.5), reflecting the importance of interactive decay reaction between the two enzymes.

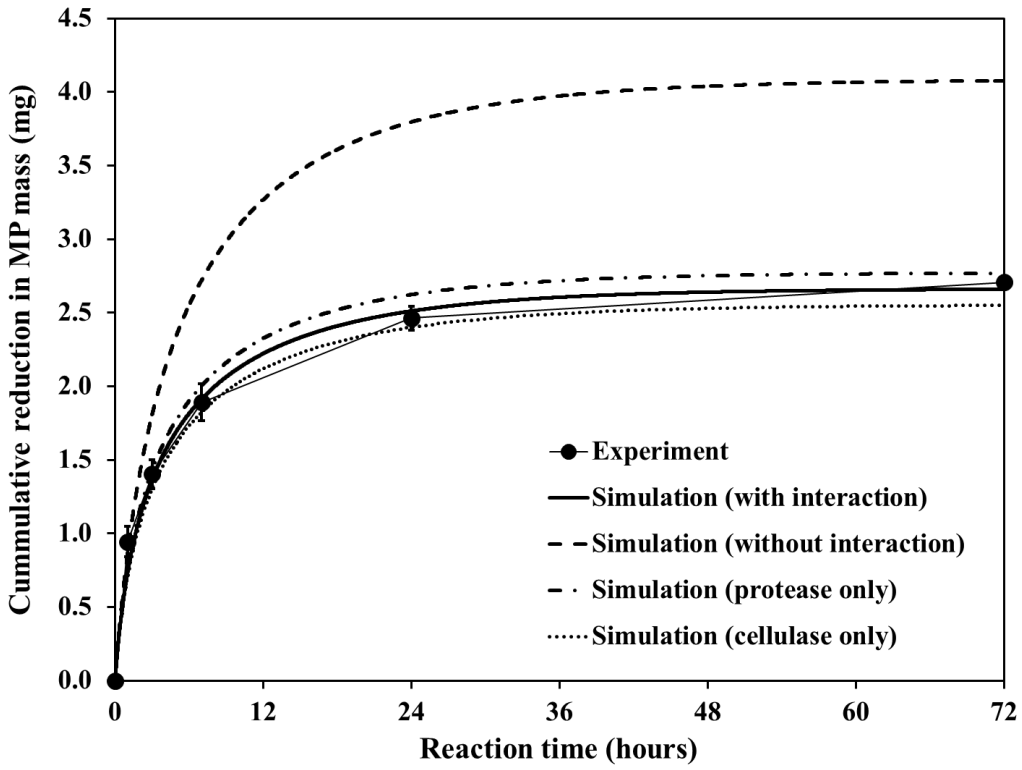

Fig. 3.5. Comparison between the experimental results and model simulations of MP removal using multiple enzymes (cellulase and protease) with and without interaction between the two enzymes. (Operational conditions: cellulase: protease concentration = 1:1 (w/w), total enzymes concentration = 88 mg/L and temperature = 55°C). Calibrated kinetic constants were used for model simulations (Table 3.2 and 3.3).

3.3.6 MP removal by anaerobic digestion enzymes

The calibrated model was used to approximate the MP reduction in anaerobic digestion (AD). The concentration of residual MP was correlated with the retention time, the calibrated kinetic constant of MP reduction by protease ($k_{1,P}$) and the enzyme concentration (E_P) in the reactor (Eq. 3.6). In the model simulations, protease was selected as the hydrolytic enzyme in AD because it was the most efficient enzyme on MP reduction. Protease concentration was assumed to be maintained at 50, 100 and 300 mg/L

in the digester. Note that the hydrolytic enzyme concentration in conventional anaerobic digesters was reported as 50 - 450 mg/L (Yang et al., 2010; Luo et al., 2012).

$$\frac{C_{MP_R}}{C_{MP_o}} = \frac{1}{1 + RT\ .\ k_{1,P}.E_P} \qquad (Eq\ 3.6)$$

where C_{MP_R} is the residual MP concentration, C_{MP_o} is initial MP concentration and RT is the retention time.

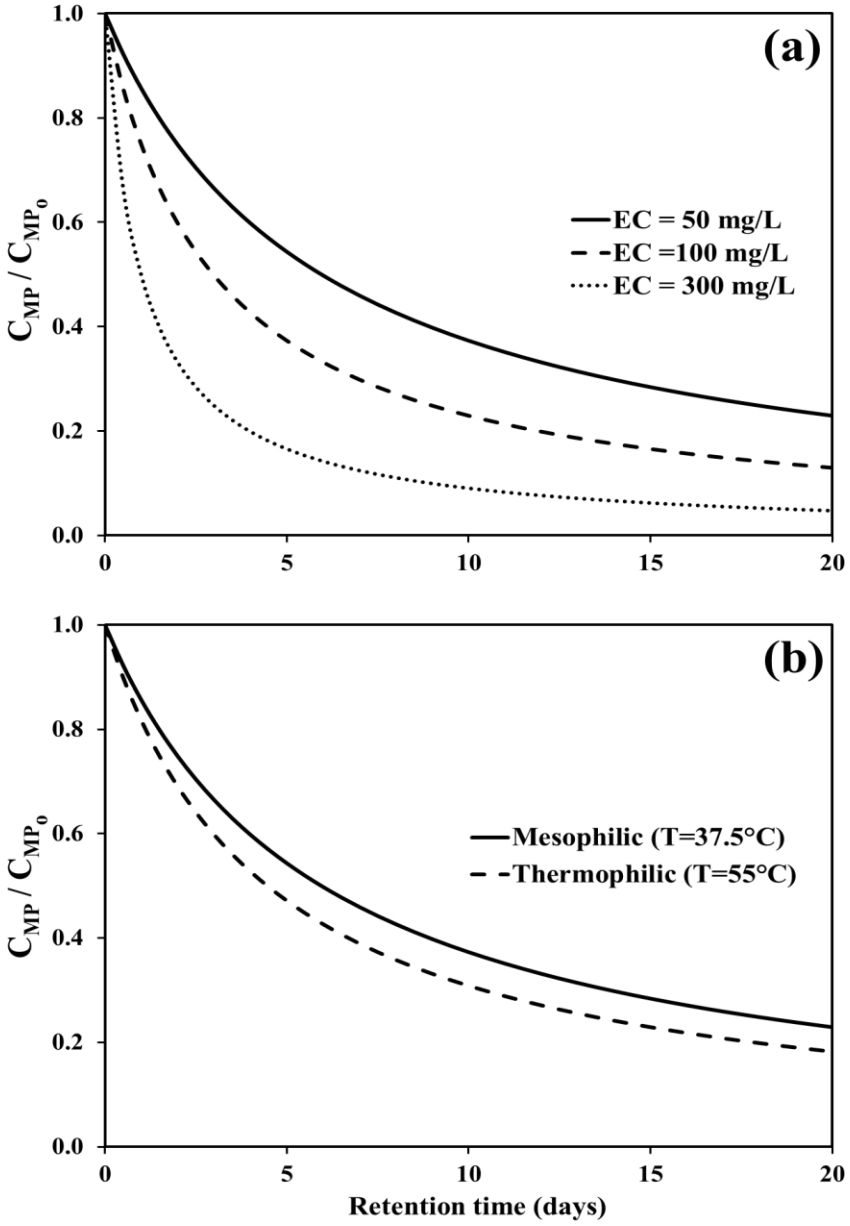

Fig. 3.6. Effect of retention time on MP removal with the variation of: (a) protease concentration (temperature = 37.5°C), (b) temperature (protease concentration = 50 mg/L). (Simulation conditions: the hydrolytic enzyme was protease and MP kinetic constant (k_{1_P}) was adopted from Table 3.2).

Based on the model simulation results, a significant amount of MP was degraded in AD (70 - 95% removal) considering that the typical retention time for mesophilic anaerobic digesters is 15 to 20 days (Fig. 3.6a). For the enzyme concentration in the digester, it was observed that high protease concentration resulted in low residual MP in the digester effluent, reflecting high MP removal at high enzyme concentrations. This simulation result is consistent with the results obtained from previous enzyme studies (Moon and Song, 2011; Dors et al., 2013).

It was also found that the temperature is not a dominant factor on MP reduction while retention time is important for efficient MP removal (Fig. 3.6b). For thermophilic digestion, retention time is not long as it is used mainly for sludge pretreatment, reflecting effective MP reduction during the pretreatment process. Thermophilic condition (55°C) slightly enhanced the MP reduction compared to the mesophilic condition (37.5°C) (Fig. 3.6b) because the kinetic constant of MP reduction by protease (k_{1_P}) was sensitive to the temperature (Table 3.2). However, high MP reduction rate could be obtained in mesophilic anaerobic digesters at typical AD retention time (15 – 20 days). Therefore, it can be concluded that AD process can be an efficient way for MP reduction during the sludge treatment process.

3.4 Conclusions

Lab-scale experiments were conducted to determine the kinetic constants for polyethylene MP destruction using hydrolytic enzymes (i.e., lipase, cellulase and protease) at three different enzyme concentrations (i.e., 22, 44 and 88 mg/L). It was found that protease was the most effective enzyme on MP reduction while lipase was the

least efficient enzyme. Based on the experimental results, the increasing enzyme concentration enhanced the reduction of MP for the three examined enzymes. Also, the high temperature (55°C) increased the MP destruction compared to 37.5°C. In the 3-day batch experiment, the majority of the MP destruction was achieved in the first seven hours while there was no significant MP removal after 24 hours of the experiment. When protease was repetitively dosed at 55°C, the cumulative MP reduction was 23.3% in 9 days (7 doses of protease). When cellulase and protease were dosed simultaneously, the MP reduction was 3.77% after 3 days of the batch experiment where there was interactive destruction between the two enzymes.

A non-steady state mathematical model was developed and calibrated using the lab-scale experimental results. The estimated kinetic constant of MP reduction by an enzyme ($k_{1,i}$) ranged from 5.0 to 8.1 × 10^{-4} L/mg/hr while the range of the enzyme self-decay constant ($k_{2,ii}$) was 0.44 – 1.10 L/mg/hr. The mathematical model was also used to simulate the multiple enzymes (i.e., cellulase and protease) batch experiment, assuming an interaction between the two enzymes using an interactive-decay constant ($k_{2,CP}$) where $k_{2,CP}$ was estimated to be 0.51 L/mg/hr. Using the calibrated kinetic constants at 37.5 and 55°C, the temperature correction factor (θ) for $k_{1,i}$ was determined to be 1.019 (lipase), 1.018 (cellulase) and 1.016 (protease) while θ for $k_{2,ii}$ was 1.003 for lipase and 1.006 for cellulase and protease. The calibrated model kinetic constants were used to approximate the MP reduction in anaerobic digestion where it was found that the retention time is the most dominant parameter on MP removal. For mesophilic temperature (37.5°C), MP removal was up to 95% in 20 days of AD retention time, reflecting the strength of AD in MP removal applications. It can be concluded that

hydrolytic enzymes represent a feasible solution for MP removal in the conventional biological wastewater and sludge treatment processes.

References

Alimi, O.S., Budarz, J.F., Hernandez, L.M., Tufenkji, N., 2018. Microplastics and Nanoplastics in Aquatic Environments: Aggregation, Deposition, and Enhanced Contaminant Transport. Environmental Science and Technology. 52(4), 1704–1724.

Alvim, B.C., Mendoza-Roca, J.A., Bes-Piá, A., 2020. Wastewater treatment plant as microplastics release source – Quantification and identification techniques. Journal of Environmental Management. 255, 109739.

Anderson, P.J., Warrack, S., Langen, V., Challis, J.K., Hanson, M.L., Rennie, M.D., 2017. Microplastic contamination in Lake Winnipeg, Canada. Environmental Pollution. 225, 223–231.

Atalo, K., Gashe, B.A., 1993. Protease production by a thermophilic Bacillus species (P-001A) which degrades various kinds of fibrous proteins. Biotechnology Letters. 15(11), 1151–1156.

Auta, H.S., Emenike, C.U., Fauziah, S.H., 2017. Distribution and importance of microplastics in the marine environment: A review of the sources, fate, effects, and potential solutions. Environment International, 102, 165–176.

Avio, C.G., Gorbi, S., Milan, M., Benedetti, M., Fattorini, D., D'Errico, G., Pauletto, M., Bargelloni, L., Regoli, F., 2015. Pollutants bioavailability and toxicological risk from microplastics to marine mussels. Environmental Pollution. 198, 211–222.

Blair, R.M., Waldron, S., Gauchotte-Lindsay, C., 2019. Average daily flow of microplastics through a tertiary wastewater treatment plant over a ten-month period. Water Research. 163, 114909.

Carr, S.A., Liu, J., Tesoro, A.G., 2016. Transport and fate of microplastic particles in wastewater treatment plants. Water Research. 91, 174–182.

Chen, R., Qi, M., Zhang, G., Yi, C., 2018. Comparative experiments on polymer degradation technique of produced water of polymer flooding oilfield. IOP Conference Series: Earth and Environmental Science. 113(1).

Cheung, P.K., Fok, L., 2017. Characterisation of plastic microbeads in facial scrubs and their estimated emissions in Mainland China. Water Research. 122, 53–61.

Cirne, D.G., Paloumet, X., Björnsson, L., Alves, M.M., & Mattiasson, B., 2007. Anaerobic digestion of lipid-rich waste-Effects of lipid concentration. Renewable Energy. 32(6), 965–975.

Dalal, S., Sharma, A., Gupta, M.N., 2007. A multipurpose immobilized biocatalyst with pectinase, xylanase and cellulase activities. Chemistry Central Journal. 1(1), 1–5.

Daniel, R.M., Danson, M.J., Eisenthal, R., Lee, C.K., Peterson, M.E., 2008. The effect of temperature on enzyme activity: New insights and their implications. Extremophiles. 12(1), 51–59.

Domingues, R.F., Sanches, T., Silva, G.S., Bueno, B.E., Ribeiro, R., Kamimura, E.S., Franzolin Neto, R., Tommaso, G., (2015). Effect of enzymatic pretreatment on the anaerobic digestion of milk fat for biogas production. Food Research International. 73, 26–30.

Dors, G., Mendes, A.A., Pereira, E.B., de Castro, H.F., Furigo, A., 2013. Simultaneous enzymatic hydrolysis and anaerobic biodegradation of lipid-rich wastewater from poultry industry. Applied Water Science. 3(1), 343–349.

Edo, C., González-Pleiter, M., Leganés, F., Fernández-Piñas, F., Rosal, R., 2020. Fate of microplastics in wastewater treatment plants and their environmental dispersion with effluent and sludge. Environmental Pollution, 259, 113837.

Elsayed, A., Hurdle, M., Kim, Y., 2021. Comprehensive model applications for better understanding of pilot-scale membrane-aerated biofilm reactor performance. Journal of Water Process Engineering. 40, 101894.

Ferreira, P., Fonte, E., Soares, M.E., Carvalho, F., Guilhermino, L., 2016. Effects of multi-stressors on juveniles of the marine fish Pomatoschistus microps: Gold nanoparticles, microplastics and temperature. Aquatic Toxicology. 170, 89–103.

Gatidou, G., Arvaniti, O.S., Stasinakis, A.S., 2019. Review on the occurrence and fate of microplastics in Sewage Treatment Plants. Journal of Hazardous Materials. 367, 504–512.

Gies, E.A., LeNoble, J.L., Noël, M., Etemadifar, A., Bishay, F., Hall, E.R., Ross, P.S., 2018. Retention of microplastics in a major secondary wastewater treatment plant in Vancouver, Canada. Marine Pollution Bulletin. 133, 553–561.

Gutarra, M.L.E., Godoy, M.G., Maugeri, F., Rodrigues, M.I., Freire, D.M.G., Castilho, L.R., 2009. Production of an acidic and thermostable lipase of the mesophilic fungus Penicillium simplicissimum by solid-state fermentation. Bioresource Technology. 100(21), 5249–5254.

Henze, M., Gujer, W., Mino, T., van Loosdrecht, M., 2002. Activated Sludge Models ASM1, ASM2, ASM2d and ASM3. Scientific and Technical Report. (No. 9), 130.

Hidayaturrahman, H., Lee, T.G., 2019. A study on characteristics of microplastic in wastewater of South Korea: Identification, quantification, and fate of microplastics during treatment process. Marine Pollution Bulletin. 146, 696–702.

Holland, E.R., Mallory, M.L., Shutler, D., 2016. Plastics and other anthropogenic debris in freshwater birds from Canada. Science of the Total Environment. 571, 251–258.

Horton, A.A., Svendsen, C., Williams, R.J., Spurgeon, D.J., Lahive, E., 2017. Large microplastic particles in sediments of tributaries of the River Thames, UK – Abundance, sources and methods for effective quantification. Marine Pollution Bulletin. 114(1), 218–226.

Kim, S.H., Park, S., Yu, H., Kim, J.H., Kim, H.J., Yang, Y.H., Kim, Y.H., Kim, K.J., Kan. E., Lee, S.H., 2016. Effect of deep eutectic solvent mixtures on lipase activity and stability. Journal of Molecular Catalysis B: Enzymatic. 128, 65–72.

Koelmans, A.A., Bakir, A., Burton, G.A., Janssen, C.R., 2016. Microplastic as a Vector for Chemicals in the Aquatic Environment: Critical Review and Model-Supported Reinterpretation of Empirical Studies. Environmental Science and Technology. 50(7), 3315–3326.

Lares, M., Ncibi, M.C., Sillanpää, M., Sillanpää, M., 2018. Occurrence, identification and removal of microplastic particles and fibers in conventional activated sludge process and advanced MBR technology. Water Research. 133, 236–246.

Lee, H., Kim, Y., 2018. Treatment characteristics of microplastics at biological sewage treatment facilities in Korea. Marine Pollution Bulletin. 137, 1–8.

Leiyu, F., Yuanyuan, Y., Yinguang, C., 2009. Kinetic analysis of waste activated sludge hydrolysis and short-chain fatty acids production at pH 10. Journal of Environmental Sciences. 21(5), 589–594.

Li, D.C., Yang, Y.I.J., Shen, C.Y., 1997. Protease production by the thermophilic fungus Thermomyces Lanuginosus. Mycological Research. 101(1), 18–22.

Li, L., Xu, G., Yu, H., Xing, J., 2018. Dynamic membrane for micro-particle removal in wastewater treatment: Performance and influencing factors. Science of the Total Environment. 627, 332–340.

Li, X., Chen, L., Ji, Y., Li, M., Dong, B., Qian, G., Zhou, J., Dai, X., 2020. Effects of chemical pretreatments on microplastic extraction in sewage sludge and their physicochemical characteristics. Water Research. 171, 115379.

Lu, K., Qiao, R., An, H., Zhang, Y., 2018. Influence of microplastics on the accumulation and chronic toxic effects of cadmium in zebrafish (Danio rerio). Chemosphere. 202, 514–520.

Luo, K., Yang, Q., Li, X., Yang, G., Liu, Y., Wang, D., Zheng, W., Zeng, G., 2012. Hydrolysis kinetics in anaerobic digestion of waste activated sludge enhanced by α-amylase. Biochemical Engineering Journal. 62, 17–21.

Magni, S., Binelli, A., Pittura, L., Avio, C. G., Della Torre, C., Parenti, C.C., Gorbi, S., Regoli, F., 2019. The fate of microplastics in an Italian Wastewater Treatment Plant. Science of the Total Environment. 652, 602–610.

Mahon, A.M., O'Connell, B., Healy, M.G., O'Connor, I., Officer, R., Nash, R., Morrison, L., 2017. Microplastics in sewage sludge: Effects of treatment. Environmental Science and Technology. 51(2), 810–818.

Marie-Olive, M.N., Athes, V., Combes, D., 2000. Combined effects of pressure and temperature on enzyme stability. High Pressure Research. 19(1–6), 317–322.

Mason, S.A., Garneau, D., Sutton, R., Chu, Y., Ehmann, K., Barnes, J., Fink, P., Papazissimos, D., Rogers, D. L., 2016. Microplastic pollution is widely detected in US municipal wastewater treatment plant effluent. Environmental Pollution. 218, 1045–1054.

Mateos Diaz, J.C., Rodríguez, J.A., Roussos, S., Cordova, J., Abousalham, A., Carriere, F., Baratti, J., 2006. Lipase from the thermotolerant fungus Rhizopus homothallicus is more thermostable when produced using solid state fermentation than liquid fermentation procedures. Enzyme and Microbial Technology. 39(5), 1042–1050.

Michielssen, M.R., Michielssen, E.R., Ni, J., Duhaime, M.B., 2016. Fate of microplastics and other small anthropogenic litter (SAL) in wastewater treatment plants depends on unit processes employed. Environmental Science: Water Research and Technology. 2(6), 1064–1073.

Mintenig, S.M., Int-Veen, I., Löder, M.G.J., Primpke, S., Gerdts, G., 2017. Identification of microplastic in effluents of waste water treatment plants using focal plane array-based micro-Fourier-transform infrared imaging. Water Research. 108, 365–372.

Miranda, D. de A., de Carvalho-Souza, G.F., 2016. Are we eating plastic-ingesting fish? Marine Pollution Bulletin. 103(1–2), 109–114.

Mlaik, N., Khoufi, S., Hamza, M., Masmoudi, M.A., Sayadi, S., 2019. Enzymatic pre-hydrolysis of organic fraction of municipal solid waste to enhance anaerobic digestion. Biomass and Bioenergy. 127, 105286.

Moon, H.C., Song, I.S., 2011. Enzymatic hydrolysis of foodwaste and methane production using UASB bioreactor. International Journal of Green Energy. 8(3), 361–371.

Murphy, F., Ewins, C., Carbonnier, F., Quinn, B., 2016. Wastewater Treatment Works (WwTW) as a Source of Microplastics in the Aquatic Environment. Environmental Science and Technology. 50(11), 5800–5808.

Negi, S., Banerjee, R., 2009. Characterization of amylase and protease produced by Aspergillus awamori in a single bioreactor. Food Research International. 42(4), 443–448.

Odnell, A., Recktenwald, M., Stensén, K., Jonsson, B.H., Karlsson, M., 2016. Activity, life time and effect of hydrolytic enzymes for enhanced biogas production from sludge anaerobic digestion. Water Research. 103, 462–471.

Othman, A.R., Hasan, H.A., Muhamad, M.H., Ismail, N. 'Izzati, Abdullah, S.R.S., (2021). Microbial degradation of microplastics by enzymatic processes: a review. Environmental Chemistry Letters.

Peng, G., Zhu, B., Yang, D., Su, L., Shi, H., Li, D., 2017. Microplastics in sediments of the Changjiang Estuary. China. Environmental Pollution. 225, 283–290.

Perwez, M., Mazumder, J.A., Sardar, M., 2019. Preparation and characterization of reusable magnetic combi-CLEA of cellulase and hemicellulase. Enzyme and Microbial Technology. 131, 109389.

Pettipas, S., Bernier, M., Walker, T.R., 2016. A Canadian policy framework to mitigate plastic marine pollution. Marine Policy. 68, 117–122.

Pirc, U., Vidmar, M., Mozer, A., Kržan, A., 2016. Emissions of microplastic fibers from microfiber fleece during domestic washing. Environmental Science and Pollution Research. 23(21), 22206–22211.

Pitt, J.A., Kozal, J.S., Jayasundara, N., Massarsky, A., Trevisan, R., Geitner, N., Wiesner, M., Levin, E.D., Di Giulio, R.T., 2018. Uptake, tissue distribution, and toxicity of polystyrene nanoparticles in developing zebrafish (Danio rerio). Aquatic Toxicology. 194, 185–194.

Poerio, T., Piacentini, E., Mazzei, R., 2019. Membrane processes for microplastic removal. Molecules, 24(22).

Raju, S., Carbery, M., Kuttykattil, A., Senthirajah, K., Lundmark, A., Rogers, Z., SCB, S., Evans, G., Palanisami, T., 2020. Improved methodology to determine the fate and transport of microplastics in a secondary wastewater treatment plant. Water Research. 173, 115549.

Revel, M., Châtel, A., Mouneyrac, C., 2018. Micro (nano) plastics: A threat to human health? Current Opinion in Environmental Science and Health. 1, 17–23.

Rezania, S., Park, J., Md Din, M. F., Mat Taib, S., Talaiekhozani, A., Kumar Yadav, K., Kamyab, H., 2018. Microplastics pollution in different aquatic environments and biota: A review of recent studies. Marine Pollution Bulletin. 133, 191–208.

Rochman, C.M., Tahir, A., Williams, S.L., Baxa, D.V., Lam, R., Miller, J.T., Teh, F., Werorilang, S., Teh, S.J., 2015. Anthropogenic debris in seafood: Plastic debris and fibers from textiles in fish and bivalves sold for human consumption. Scientific Reports. 5, 1–10.

Silva, A.B., Bastos, A.S., Justino, C.I.L., da Costa, J.P., Duarte, A.C., Rocha-Santos, T.A.P., 2018. Microplastics in the environment: Challenges in analytical chemistry - A review. Analytica Chimica Acta. 1017, 1–19.

Song, Y.K., Hong, S.H., Jang, M., Han, G.M., Jung, S.W., Shim, W.J., 2017. Combined Effects of UV Exposure Duration and Mechanical Abrasion on Microplastic Fragmentation by Polymer Type. Environmental Science and Technology. 51(8), 4368–4376.

Stutzenberger, F.J., 1972. Cellulolytic activity of Thermomonospora curvata: nutritional requirements for cellulase production. Applied Microbiology. 24(1), 77–82.

Sun, J., Dai, X., Wang, Q., van Loosdrecht, M.C.M., Ni, B.J., 2019. Microplastics in wastewater treatment plants: Detection, occurrence and removal. Water Research. 152, 21–37.

Tagg, A.S., Sapp, M., Harrison, J.P., Ojeda, J.J., 2015. Identification and Quantification of Microplastics in Wastewater Using Focal Plane Array-Based Reflectance Micro-FT-IR Imaging. Analytical Chemistry. 87(12), 6032–6040.

Talvitie, J., Mikola, A., Koistinen, A., Setälä, O., 2017a. Solutions to microplastic pollution – Removal of microplastics from wastewater effluent with advanced wastewater treatment technologies. Water Research. 123, 401–407.

Talvitie, J., Mikola, A., Setälä, O., Heinonen, M., Koistinen, A., 2017b. How well is microlitter purified from wastewater? – A detailed study on the stepwise removal of microlitter in a tertiary level wastewater treatment plant. Water Research. 109, 164–172.

Tomei, M.C., Braguglia, C.M., Mininni, G., 2008. Anaerobic degradation kinetics of particulate organic matter in untreated and sonicated sewage sludge: Role of the inoculum. Bioresource Technology. 99(14), 6119–6126.

Wang, J., Peng, J., Tan, Z., Gao, Y., Zhan, Z., Chen, Q., Cai, L., 2017. Microplastics in the surface sediments from the Beijiang River littoral zone: Composition, abundance, surface textures and interaction with heavy metals. Chemosphere. 171, 248–258.

Wardrop, P., Shimeta, J., Nugegoda, D., Morrison, P.D., Miranda, A., Tang, M., Clarke, B.O., 2016. Chemical Pollutants Sorbed to Ingested Microbeads from Personal Care Products Accumulate in Fish. Environmental Science and Technology. 50(7), 4037–4044.

Wei, W., Huang, Q.S., Sun, J., Dai, X., Ni, B.J., 2019. Revealing the Mechanisms of Polyethylene Microplastics Affecting Anaerobic Digestion of Waste Activated Sludge. Environmental Science and Technology. 53(16), 9604–9613.

Wright, S.L., Kelly, F.J., 2017. Plastic and Human Health: A Micro Issue?. Environmental Science and Technology. 51(12), 6634–6647.

Wu, C., Zhang, K., Huang, X., Liu, J., 2016. Sorption of pharmaceuticals and personal care products to polyethylene debris. Environmental Science and Pollution Research. 23(9), 8819–8826.

Wu, M., Yang, C., Du, C., Liu, H., 2020. Microplastics in waters and soils: Occurrence, analytical methods and ecotoxicological effects. Ecotoxicology and Environmental Safety. 202, 110910.

Xu, X., Jian, Y., Xue, Y., Hou, Q., Wang, L.P., 2019. Microplastics in the wastewater treatment plants (WWTPs): Occurrence and removal. Chemosphere. 235, 1089–1096.

Yang, Q., Luo, K., Li, X., Wang, D., Zheng, W., Zeng, G., Liu, J., 2010. Enhanced efficiency of biological excess sludge hydrolysis under anaerobic digestion by additional enzymes. Bioresource Technology, 101(9), 2924–2930.

Yu, S., Zhang, G., Li, J., Zhao, Z., Kang, X., 2013. Effect of endogenous hydrolytic enzymes pretreatment on the anaerobic digestion of sludge. Bioresource Technology. 146, 758–761.

Zhang, X., Chen, J., Li, J., 2020. The removal of microplastics in the wastewater treatment process and their potential impact on anaerobic digestion due to pollutants association. Chemosphere. 251.

Zhou, X., Wang, J., Li, H., Zhang, H., Hua-Jiang, Zhang, D.L., 2021. Microplastic pollution of bottled water in China. Journal of Water Process Engineering. 40, 101884.

Ziajahromi, S., Neale, P.A., Rintoul, L., Leusch, F.D.L., 2017. Wastewater treatment plants as a pathway for microplastics: Development of a new approach to sample wastewater-based microplastics. Water Research, 112, 93–99.

4. Mathematical model application for real-time aeration based on nitrite level in Anammox process

Anaerobic ammonia oxidation (Anammox) is an innovative technology for nitrogen removal with a reduced greenhouse gases emission, operation cost and facility size. However, controlling the competition between Anammox and nitrite oxidizing bacteria is an important challenge on successful wastewater treatment using Anammox process. Anammox bacteria are also sensitive to the dissolved oxygen concentration and aeration schemes. Therefore, a mathematical model was developed and calibrated using experimental results of previous Anammox studies to estimate the important model parameters. Also, a real-time aeration scheme based on nitrite concentration was implemented to limit the competition between Anammox and nitrite oxidizing bacteria, providing favorable conditions for the growth of Anammox bacteria. This schematic aeration can be applied in large-scale nitrogen removal applications by Anammox process.

This paper is prepared for future journal publication.

- Elsayed, A., Kim, Y. Mathematical model application for real-time aeration based on nitrite level in Anammox process.

The co-author’s contributions include:

- Funding acquisition.
- Supervision and technical support.
- Manuscript review and revision.

Abstract

Anaerobic ammonia oxidation (Anammox) is an innovative technology for cost-efficient nitrogen removal without intensive aeration. However, controlling the competition between nitrite oxidizing bacteria (X_{NOB}) and Anammox bacteria (X_{ANA}) is a key challenge for broad applications of Anammox processes in real wastewater treatment. In this study, a non-steady state mathematical model was developed and calibrated using previously reported lab-scale Anammox results to investigate the competition between X_{NOB} and X_{ANA} under various Anammox operation conditions. Based on the model simulation results, dissolved oxygen (DO) of about 0.10 mg-O_2/L was found to be ideal for maintaining effective nitrite creation by ammonia oxidizing bacteria (X_{AOB}) while slowing the growth of X_{NOB}. If DO concentration is too low (e.g., 0.01 mg-O_2/L or lower), ammonia removal will be limited due to slow growth of X_{AOB}. Also, relatively high DO (e.g., 1.0 mg-O_2/L or higher) inhibits the growth of X_{ANA}, resulting in dominancy of X_{AOB} and X_{NOB}. It was also found that nitrite concentration can be used as an aeration indicator to enhance the performance of Anammox bacteria. A schematic aeration method based on real-time nitrite concentration was proposed and examined for controlling the competition between X_{ANA} and X_{NOB} for nitrite. In the model simulation, the X_{ANA} activity was successfully maintained because the schematic aeration prevented an outgrowth of X_{NOB}, allowing long-term operation of Anammox processes. The proposed real-time schematic aeration can allow successful operation of Anammox processes for energy-efficient nitrogen removal coupled with broad applications of Anammox processes in biological wastewater treatment.

Keywords

Anaerobic ammonia oxidation; real-time aeration; nitrite-based aeration; mathematical model calibration; nitrite oxidizing bacteria.

4.1 Introduction

Different wastewater streams, including municipal, industrial and agricultural wastewater, contain high levels of nitrogen components (e.g., ammonia, organic nitrogen and nitrate). Excessive discharge of nitrogen components can cause critical environmental problems such as algal blooms and eutrophication in natural water systems, threatening the aquatic ecosystem (Ge et al., 2019; Chen et al., 2020). Therefore, nitrogen removal is important in the modern wastewater treatment processes. In the conventional ammonia removal process, ammonia is oxidized into nitrite and nitrate by nitrifiers under aerobic conditions and nitrate is converted into nitrogen gas by heterotrophs under anoxic conditions with an additional organic carbon supply (Pereira et al., 2017; Ma et al., 2020; Zhang et al., 2020a). However, this process requires availability of organic carbon (resources), high oxygen demand (aeration cost) for complete nitrification (i.e., from ammonia to nitrate), long retention time (pumping cost) and large footprint for denitrification reactors (resources and cost) (Hauck et al., 2016; Chen et al., 2019; Du et al., 2019). Also, the sludge production rate (disposal cost) and greenhouse gases emission rate (environmental aspect) are relatively high in the conventional nitrification and denitrification processes (Gilbert et al., 2015; Eskicioglu et al., 2018; Conthe et al., 2019). Anaerobic ammonia oxidation (Anammox) is a relatively new technology for ammonia removal and is considered as an innovative alternative for

conventional nitrification and denitrification systems in wastewater treatment with a reduced operation cost, greenhouse gases emission and facility size (Du et al., 2015; Xu et al., 2015; Guo et al., 2020). In the Anammox process, ammonia is consumed by Anammox bacteria with nitrite as the terminal electron acceptor (Graham and Jolis et al., 2017; You et al., 2020; Li et al., 2021).

Operational conditions have a dominant role on the biological ammonia removal by Anammox bacteria (He et al., 2018; Qian et al., 2019; Cui et al., 2020). In previous Anammox bacteria studies, it was found that dissolved oxygen concentration is a crucial parameter on the activity of Anammox bacteria as reasonable dissolved oxygen (DO) concentration is required to create sufficient amount of nitrite by ammonia oxidizing bacteria while the DO concentration should be low enough to avoid an inhibition on the growth of Anammox bacteria (Lotti et al., 2014; Lin et al., 2014; Liu et al., 2017a; Yue et al., 2018). It was also demonstrated that the C/N ratio (carbon-to-nitrogen) and influent COD concentration control the ammonia removal in Anammox process as they affect the competition between ammonia oxidizing and heterotrophic bacteria for oxygen, and the competition between Anammox and heterotrophic bacteria for nitrite (Ni et al., 2012; Chen et al., 2016; Li et al., 2017a). Many previous Anammox studies described the nitrite inhibition on Anammox bacteria at high nitrite concentrations (> 100 mg-N/L) using experimentation (Lackner et al., 2008; Lotti et al., 2012; Connan et al., 2016); however, there are no systematic mathematical modeling studies on the effect of nitrite concentration on Anammox bacteria at the non-inhibitory concentration levels. Although the competition between nitrite oxidizing and Anammox bacteria for nitrite is the main key for a successful nitrogen removal by Anammox bacteria (Pellicer-Nàcher et al., 2014;

Ali and Okabe, 2015; Cao et al., 2017), there are no comprehensive mathematical models for describing this competition.

Different Anammox studies suggested potential experimental techniques for controlling the competition between Anammox and nitrite oxidizing bacteria, such as intermittent aeration (Ma et al., 2015; Yang et al., 2015; Miao et al., 2017; Miao et al., 2018), sludge age (van Hulle et al., 2010; Akgul et al., 2013; Kanders et al., 2018; Jiang et al., 2018), maintaining residual ammonia concentration (Perez et al., 2014; Regmi et al., 2014; Li et al., 2018) and wash-out of nitrite oxidizing bacteria (Gilmore et al., 2013; Laureni et al., 2016; Li et al., 2017b). However, there are no investigations on the real-time monitoring of nitrite concentration where DO concentration can be linked with the nitrite concentration for dominating Anammox bacteria over nitrite oxidizing bacteria. Real-time monitoring of nitrite can be an innovative approach to avoid the competition between nitrite oxidation and Anammox bacteria for nitrite with a reduced energy cost for aeration. Real-time monitoring of nitrite concentration can provide favorable conditions for ammonia removal by Anammox bacteria as high nitrite concentration can trigger the nitrite oxidizing bacteria growth, inhibiting the growth of Anammox bacteria. In the real-time schematic aeration, the aeration system is automatically turned off when nitrite concentration becomes high, creating anaerobic conditions for better growth and dominance of Anammox bacteria.

Mathematical modeling of Anammox process is important to describe the competition between ammonia oxidizing and Anammox bacteria for ammonia, nitrite oxidizing, heterotrophic and Anammox bacteria for nitrite, and ammonia oxidizing and nitrite oxidizing bacteria for oxygen coupled with a comprehensive analysis for the

removal mechanisms during the nitrogen removal process (Niu et al., 2016; Agrwal et al., 2018). Also, mathematical models can be applied for identifying the correlation between the process parameters and assessing the effect of various operational conditions on the performance of Anammox bacteria (Baeten et al., 2019; Jia et al., 2020). Therefore, mathematical modeling can lead to more comprehensive understanding of the Anammox process operation and system design based on the available resources and determined accuracy. Mathematical modeling, including various microorganisms (i.e., nitrifiers, heterotrophs and Anammox bacteria), is essential to determine the complicated relations between the model parameters in the Anammox process. Model calibration with previous experimental results can be an efficient tool for estimating realistic ranges of the model parameters.

In this study, the main objectives are to: (1) develop a mathematical model to simulate the biological reactions during Anammox process; (2) calibrate the mathematical model using previous experimental results to determine the important model parameters; (3) assess the effect of operational conditions (e.g., ammonia, nitrite and oxygen concentration) on nitrogen removal during Anammox process; and (4) implement a real-time schematic aeration on Anammox process to maintain high nitrogen removal by Anammox bacteria rather than by nitrite oxidizing bacteria.

4.2 Numerical model development and calibration

4.2.1 Biological reaction kinetics

A non-steady state model was developed to simulate comprehensive biological reactions by Anammox, ammonia oxidizing, nitrite oxidizing and heterotrophic bacteria based on ASM3 (Activated Sludge Model No.3) (Henze et al., 2000; Lackner et al., 2008; Ni et al., 2013) in completely mixed batch reactors. The biological reactions on nitrogen compounds include: the ammonia (S_{NH_4}) oxidation by Anammox bacteria (X_{ANA}) and ammonia oxidizing bacteria (X_{AOB}); nitrite (S_{NO_2}) oxidation into nitrate (S_{NO_3}) by X_{ANA} and nitrite oxidizing bacteria (X_{NOB}); and denitrification by heterotrophic bacteria (X_H) (Table B1). For the carbonaceous compounds, soluble COD (S_{COD}) was utilized by X_H and particulate COD (X_S) was hydrolyzed into S_{COD}. In the mathematical model, it was assumed that the particulate components (X_{AOB} ,X_{NOB}, X_H and X_{ANA}) have microbial decay reactions (Table B1). Also, the biological reaction kinetics were included (Table 4.1), assuming a homogenous suspended biomass completely mixed system.

4.2.2 Numerical solution methods

In the non-steady state model, the ten mass balance equations for individual soluble (S_{NH_4}, S_{NO_2}, S_{NO_3}, $S_{O_2}$and S_{COD}) and particulate (X_{ANA}, X_{AOB}, X_{NOB}, X_H and X_S) components were discretized using the explicit Euler method (Chapra and Canale, 1998). In the explicit Euler method, the time step was evenly assumed to be two seconds regardless of the reaction time. The initial concentration of soluble and particulate components was summarized in Table 4.2.

4.2.3 Model calibration using literature data

The non-steady state model was calibrated using experimental results from previous lab-scale Anammox studies (Ma et al., 2015; Ni et al., 2014; Gong et al., 2007; Li et al., 2020) to determine the kinetic constants of Anammox bacteria. In the model calibration, the simulation conditions (e.g., initial concentration of soluble substrates) were assumed based on the experimental conditions of each study (Table 4.2). The initial concentration of volatile suspended solids (VSS) and the fraction of particulate components (Table 4.1) were assumed based on previous Anammox studies (Beun et al., 2002; Keluskar et al., 2013; Ni et al., 2013; Ni et al., 2014; Chen et al., 2014; Zhang et al., 2020b; Wang et al., 2021). The experimental results in the previous Anammox process papers were digitized and extracted to prepare the changes in soluble components concentration with time.

4.2.4 Real-time schematic aeration

A real-time schematic aeration was proposed to simulate the programmed aeration based on the real-time monitoring of nitrite concentration in Anammox processes. The aeration system is turned on when nitrite concentration becomes less than the threshold concentration ($S_{NO_2}\big|_{ON}$) while dissolved oxygen automatically set at zero if nitrite concentration exceeds the threshold concentration. In the model simulation, nitrite concentration was checked each 10 seconds to determine the dissolved oxygen level for the next 10 seconds of simulation. In a model simulation using the real-time schematic aeration, the initial nitrite concentration was zero while the threshold concentration was set to be 0.05 mg-N/L; therefore, the aeration system was turned on at dissolved oxygen

concentration of 0.5 mg-O_2/L for 10 seconds (Fig. B1b, c). The dissolved oxygen was automatically set to zero After 10 seconds of aeration because nitrite concentration (0.2 mg-N/L) was higher than the threshold concentration ($S_{NO_2}\big|_{ON}$ = 0.05 mg-N/L).

Table 4.1 Model parameters and calibration targets at T = 20°C and pH = 7.0.

Model Parameter	Symbol	Study A	Study B	Study C	Study D	This study	Reference
Heterotrophic Bacteria (X_H)							
Maximum specific growth rate (1/d)	μ_H	6.0	6.0	6.0	6.0	6.0	Henze et al., (2000)
Decay rate (1/d)	b_H	0.4	0.4	0.4	0.4	0.4	Henze et al., (2000)
Anoxic reduction factor for μ_H (-)	η_d	0.8	0.8	0.8	0.8	0.8	Henze et al., (2000)
Oxygen saturation constant (mg-O_2/L)	$K_{O_2}^H$	0.2	0.2	0.2	0.2	0.2	Henze et al., (2000)
Substrate saturation constant (mg-COD/L)	K_{COD}^H	20	20	20	20	20	Henze et al., (2000)
Ammonium saturation constant (mg-N/L)	$K_{NH_4}^H$	0.05	0.05	0.05	0.05	0.05	Henze et al., (2000)
Nitrite saturation constant (mg-N/L)	$K_{NO_2}^H$	0.5	0.5	0.5	0.5	0.5	Henze et al., (2000)
Nitrate saturation constant (mg-N/L)	$K_{NO_3}^H$	0.5	0.5	0.5	0.5	0.5	Henze et al., (2000)
Ammonia Oxidizing Bacteria (X_{AOB})							
Maximum specific growth rate (1/d)	μ_{AOB}	2.05	2.05	2.05	2.05	2.05	Wiesmann, (1994)
Decay rate (1/d)	b_{AOB}	0.13	0.13	0.13	0.13	0.13	Wiesmann, (1994)
Oxygen saturation constant (mg-O_2/L)	$K_{O_2}^{AOB}$	0.6	0.6	0.6	0.6	0.6	Wiesmann, (1994)
Ammonium saturation constant (mg-N/L)	$K_{NH_4}^{AOB}$	2.4	2.4	2.4	2.4	2.4	Wiesmann, (1994)
Nitrite Oxidizing Bacteria (X_{NOB})							
Maximum specific growth rate (1/d)	μ_{NOB}	1.45	1.45	1.45	1.45	1.45	Wiesmann, (1994)
Decay rate (1/d)	b_{NOB}	0.06	0.06	0.06	0.06	0.06	Wiesmann, (1994)
Oxygen saturation constant (mg-O_2/L)	$K_{O_2}^{NOB}$	1.0	1.0	1.0	1.0	1.0	Moussa et al., (2005)
Ammonium saturation constant (mg-N/L)	$K_{NH_4}^{NOB}$	0.20	0.20	0.20	0.20	0.20	Ma et al., (2017)
Nitrite saturation constant (mg-N/L)	$K_{NO_2}^{NOB}$	0.50	0.50	0.50	0.50	0.50	Volcke et al., (2010)
Anammox Bacteria (X_{ANA})							
Maximum specific growth rate (1/d)	μ_{ANA}	0.051	0.07	0.048	0.09	0.10	This study.
Decay rate (1/d)	b_{ANA}	0.003	0.003	0.003	0.003	0.003	This study.
Oxygen saturation constant (mg-O_2/L)	$K_{O_2}^{ANA}$	0.10	0.10	0.10	0.10	0.10	This study.
Ammonium saturation constant (mg-N/L)	$K_{NH_4}^{ANA}$	0.07	0.07	0.07	0.07	0.07	This study.
Nitrite saturation constant (mg-N/L)	$K_{NO_2}^{ANA}$	0.05	0.05	0.05	0.05	0.05	This study.
Hydrolysis							
Hydrolysis rate constant (1/d)	q_H	3	3	3	3	3	Henze et al., (2000)
Saturation constant for particulate COD (g-X_S/ g-X_H)	K_X	0.1	0.1	0.1	0.1	0.1	Henze et al., (2000)
Anoxic reduction for q_H (-)	η_H	0.6	0.6	0.6	0.6	0.6	Henze et al., (2000)
Stoichiometric Parameters							
Yield of X_H on substrate (g-COD/g-COD)	Y_H	0.63	0.63	0.63	0.63	0.63	Henze et al., (2000)
Yield of X_{AOB} on ammonium (g-COD/g-N)	Y_{AOB}	0.15	0.15	0.15	0.15	0.15	Wiesmann, (1994)
Yield of X_{NOB} on nitrite (g-COD/g-N)	Y_{NOB}	0.041	0.041	0.041	0.041	0.041	Wiesmann, (1994)
Yield of X_{ANA} on nitrite (g-COD/g-N)	Y_{ANA}	0.159	0.159	0.159	0.159	0.159	Lackner et al., (2008)
Nitrogen content in biomass (g-N/g-COD)	i_{NBM}	0.07	0.07	0.07	0.07	0.07	Henze et al., (2000)
Inert content in lysis biomass (g-COD/g-COD)	f_i	0.1	0.1	0.1	0.1	0.1	Henze et al., (2000)

Table 4.2. Initial concentration of soluble and particulate components of the calibrated model and the previous Anammox studies.

Figure	Fig. 4.1	Fig. B2	Fig. B3	Fig. B4	Fig. 4.2	Fig. 4.3	Fig. 4.4	Fig. 4.5,4.6,4.7	Fig. B5,B6,B7	Fig. 4.8,4.9,4.10, B1
Reference	Ma et al., 2015	Ni et al., 2014	Gong et al., 2007	Li et al., 2020	This study	This study	This study	This study	This study	This study
S_{NH_4} (mg-N/L)	41	175	95	56	Variable	Variable	100	100	500	Real-time
S_{NO_2} (mg-N/L)	0	1.7	91	0.5	10	10	Variable	10	10	0
S_{NO_3} (mg-N/L)	1.0	0	1.0	3.0	0	0	0	0	0	0
S_{COD} (mg-COD/L)	49	0	0	0	50	50	50	50	50	50
S_{O_2} (mg-O_2/L)	0.15	0.30	0	0.25	Variable	Variable	Variable	0.5	0.50	0.50
VSS (mg-COD/L)	1,200	1,500	900	1,500	5,000	5,000	5,000	5,000	5,000	5,000
X_{ANA} (mg-COD/L)	894	1,050	630	975	3,500	3,500	3,500	3,500	3,500	3,500
X_{AOB} (mg-COD/L)	240	225	112.5	270	500	500	500	500	500	500
X_{NOB} (mg-COD/L)	60	150	112.5	105	500	500	500	500	500	500
X_H (mg-COD/L)	6.0	75	45	150	500	500	500	500	500	500
Reaction time (hr.)	5.417	3.35	96	2	2	Estimated	2	2	2	120
Reactor system	SBR	SBR	MABR	SBR	SBR	SBR	SBR	SBR	SBR	SBR
Aeration scheme	Intermittent	Continuous	No aeration	Intermittent	Continuous	Continuous	Continuous	Real-time	Real-time	Real-time
Aeration time (hr.)	0.5	3.35	0	1.0	2.0	2.0	2.0	Real-time	Real-time	Real-time

* SBR: sequential batch reactor.
MABR: membrane aerated biofilm reactor.
Variable: the parameter was changed at different simulations.
Estimated: the parameter was determined at different simulations.
Real-time: the parameter was determined based on the monitoring of another parameter.

4.3 Results and discussion

4.3.1 Model calibration with previous experimental results

The kinetic constants of Anammox bacteria were determined by calibrating the non-steady state mathematical model using experimental results from previous Anammox studies (Gong et al., 2007; Ni et al., 2014; Ma et al., 2015; Li et al., 2020) (Fig. 4.1, B2, B3, B4, Table 4.1 and 4.2). The simulation results were compared with the experimental results to match the same trend and values of the ammonia, nitrite, nitrate and COD concentrations. The maximum specific growth rate constant of X_{ANA} (μ_{ANA}) ranged from 0.048 to 0.09 d^{-1} while the decay rate constant of X_{ANA} (b_{ANA}) was 0.003 d^{-1}, oxygen half saturation constant of X_{ANA} ($K_{O_2}^{ANA}$) was 0.10 mg-O_2/L, ammonia half saturation constant ($K_{NH_4}^{ANA}$) was 0.07 mg-N/L and nitrite half saturation constant ($K_{NO_2}^{ANA}$) was 0.05 mg-N/L. The determined Anammox bacteria kinetic constant ranges are consistent with those used or estimated in previous Anammox studies (Strous et al., 1998; Koch et al., 2000; Hao et al., 2002; Lackner et al., 2008; van der Star et al., 2008; Volcke et al., 2010; Ni et al., 2013; Mozumender et al., 2014; Ni et al., 2014; Bi et al., 2015; Corbalá-Robles et al., 2016; Ma et al., 2016; Azari et al., 2017; Zhang et al., 2017; Liu et al., 2020).

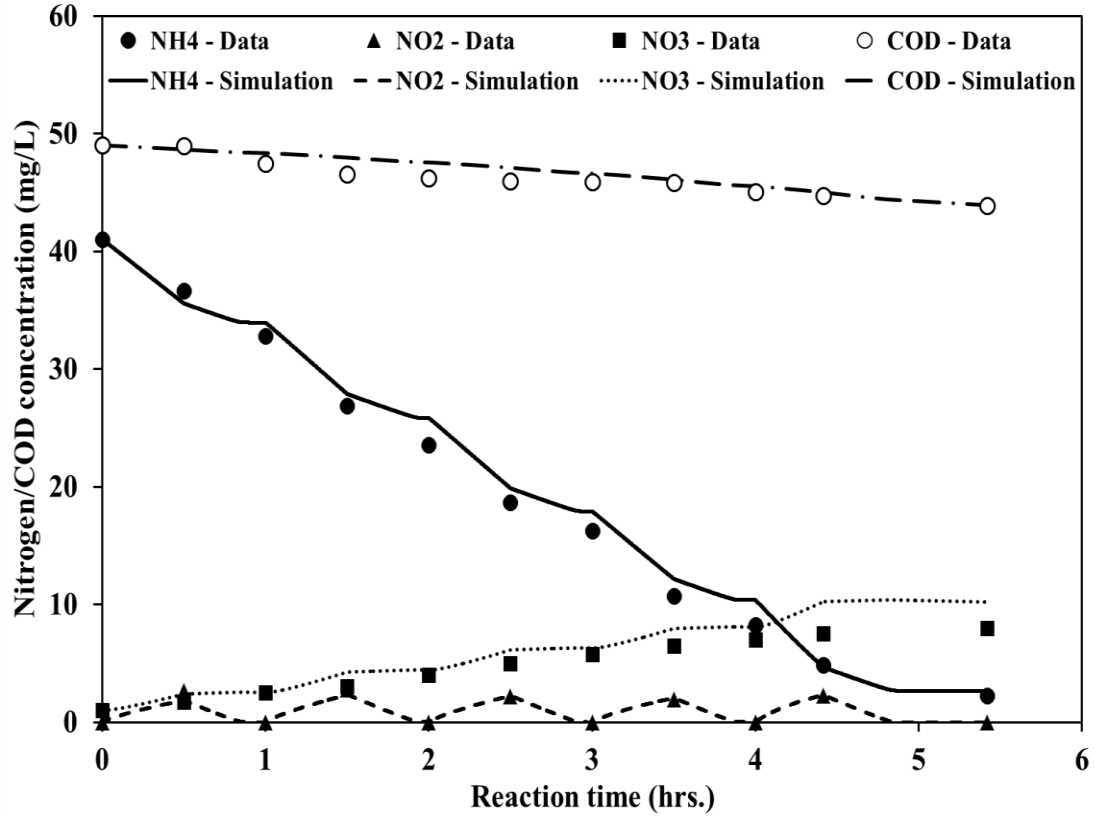

Fig. 4.1. Comparison between the simulation results of the non-steady state model and the experimental data of study A (Ma et al., 2015) for model calibration. (Simulation conditions are mentioned in Table 4.1 and 4.2).

4.3.2 Effect of initial ammonia concentration and DO on ammonia removal

In the model simulation results, it was found that moderate dissolved oxygen concentration (i.e., DO = 0.10 mg-O_2/L) is required for high ammonia removal by of X_{ANA} (Fig. 4.2) as moderate DO allowed ammonia oxidation into nitrite by X_{AOB}, providing sufficient amount of nitrite for ammonia removal by Anammox bacteria. This result is consistent with the results of other Anammox studies (Gong et al., 2007; Joss et al., 2011; Ni et al., 2014; Bi et al., 2015; Li et al., 2016; Liu et al., 2017b; Zhang et al., 2019) where the recommended range of DO concentration was 0.10 – 0.60 mg-O_2/L. For

an initial ammonia concentration of 100 mg-N/L, it was observed that ammonia was completely removed after two hours of operation at moderate DO concentration where 42% of the removed ammonia was utilized by X_{ANA}, 54% by X_{AOB} and the rest was removed by the cell growth reactions, reflecting significant contribution of Anammox bacteria to the total ammonia removal. However, the total ammonia removal rate decreased with the increasing of initial ammonia concentration at the three examined dissolved oxygen concentrations (DO = 0.01, 0.10 and 1.0 mg-O_2/L) (Fig. 4.2) because the reaction time was insufficient for ammonia removal completion by X_{ANA} and X_{AOB} (e.g., 90% ammonia removal).

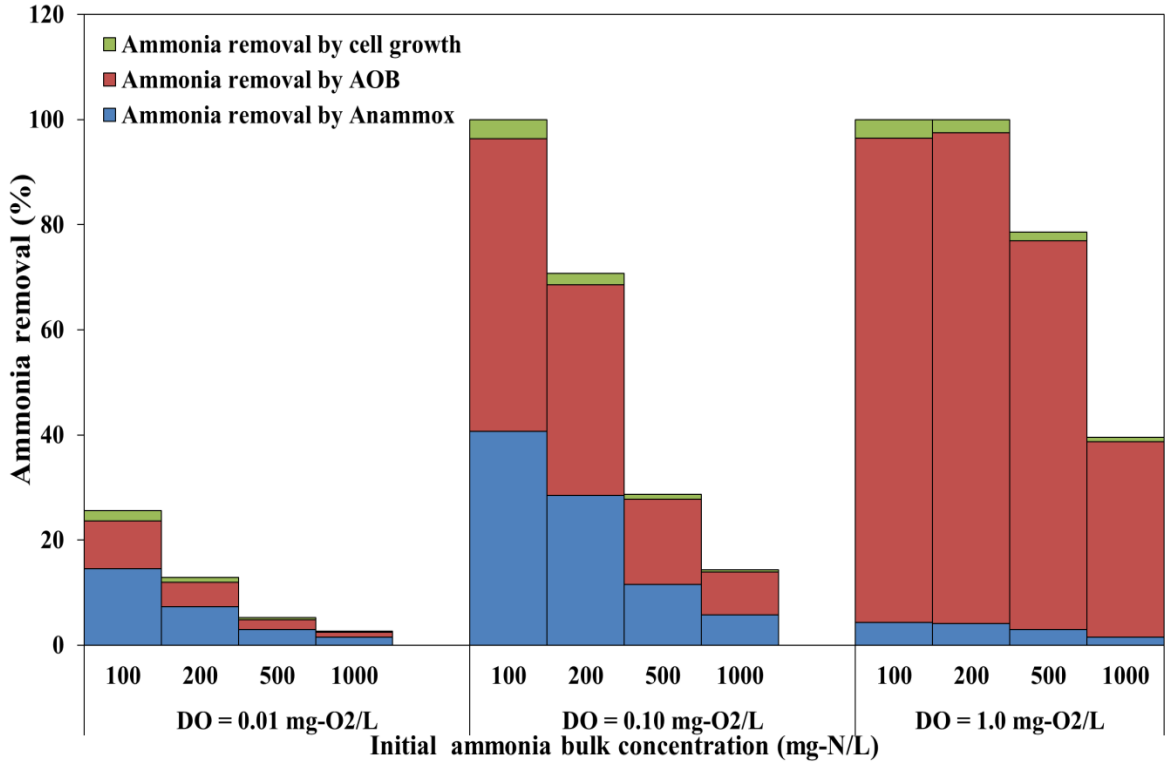

Fig. 4.2. Effect of initial ammonia concentration and dissolved oxygen on the ammonia removal by X_{AOB}, X_{ANA} and cell growth. (Simulation conditions are mentioned in Table 4.1 and 4.2).

It is important to link the ammonia removal efficiency with the initial ammonia concentration and dissolved oxygen concentration because rapid ammonia removal is required in real wastewater treatment systems, challenging the slow reaction of Anammox bacteria growth. Therefore, a balance between ammonia removal by X_{ANA} and X_{AOB} is required for cost-efficient wastewater treatment systems. Based on the model simulation results, the required time for 90% ammonia removal increased with the increasing initial ammonia concentration (Fig. 4.3). For a DO concentration of 0.10 mg-N/L, the required time for 90% ammonia removal increased from 1.3 to 12.4 hours when the initial ammonia concentration increased from 100 to 1000 mg-N/L. It was also noticed that the required time for 90% ammonia removal decreased with the increasing DO concentration (Fig. 4.3) because high oxygen concentration enhanced the ammonia removal by X_{AOB}, providing sufficient nitrite for ammonia removal by X_{ANA}. For an initial ammonia concentration of 100 mg-N/L, the required time for 90% ammonia removal decreased from 9.7 to 0.5 hours when the DO concentration increased from 0.01 to 1.0 mg-O_2/L because of high activity of X_{AOB}, reflecting the importance of DO on the total ammonia removal rate.

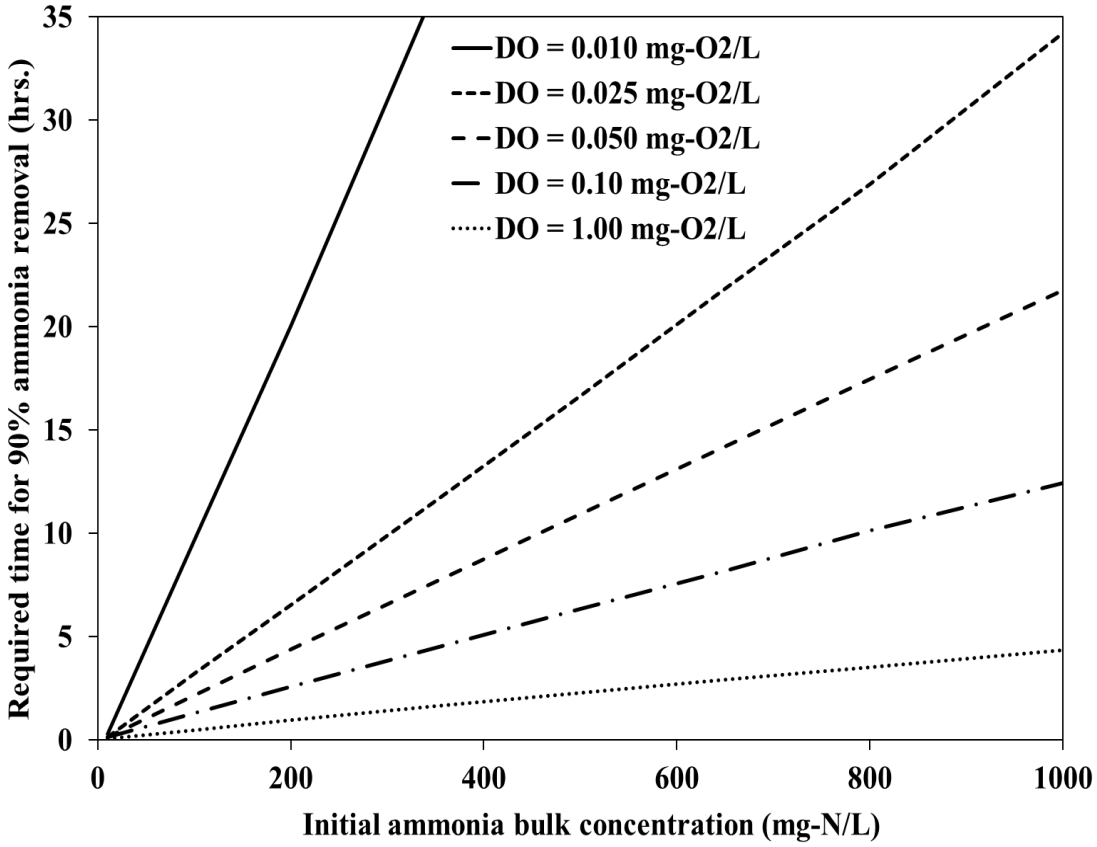

Fig. 4.3. Effect of initial ammonia concentration and dissolved oxygen on the required time for 90% ammonia removal. (Simulation conditions are mentioned in Table 4.1 and 4.2).

For low oxygen concentration (i.e., DO = 0.01 mg-O_2/L), total ammonia removal was the least at the examined range of initial ammonia concentration (100 – 1000 mg-N/L) (Fig. 4.2) because low DO limited the ammonia removal by X_{AOB}, resulting in insufficient nitrite for ammonia removal by X_{ANA}. For an initial ammonia concentration of 100 mg-N/L, the total ammonia removal was 26% (15% by X_{ANA}, 9% by X_{AOB} and 2% by cell growth), reflecting the dependence of X_{ANA} on X_{AOB} for nitrite production. This finding is consistent with the previously reported results in other Anammox studies (Cho et al., 2011; Ma et al., 2015; Val de Rio et al., 2019; Li et al., 2020), confirming the partnership between X_{ANA} and X_{AOB} in ammonia removal. However, the contribution of

ammonia removal by X_{ANA} at low DO concentration was higher than that at relatively high DO concentration (i.e., DO = 1.0 mg-O_2/L) because there was no competition between X_{ANA} and X_{AOB} for ammonia, avoiding Anammox bacteria inhibition by high oxygen concentration. For an initial ammonia concentration of 100 mg-N/L, the required time for 90% ammonia removal at DO concentration of 0.01 mg-O_2/L was 9.7 hours (Fig. 4.3), confirming that relatively low DO concentration has a negative effect on the growth of Anammox bacteria. This finding is consistent with the results of previous Anammox studies (Hao et al., 2002; Lackner et al., 2014) where it was demonstrated that extremely low oxygen concentration (< 0.10 mg-O_2/L) inhibits the Anammox bacteria growth due to absence of nitrite produced by aerobic ammonia oxidation by X_{AOB}.

It was also found that total ammonia removal was the highest at relatively high oxygen concentration because of the high activity of X_{AOB} (Fig. 4.2). This result is consistent with the results of previous ammonia removal studies (Blackburne et al., 2008; Munz et al., 2011; Chaali et al., 2018; Soliman and Eldyasti, 2018; Elsayed et al., 2021), confirming the importance of oxygen for X_{AOB} growth for complete ammonia removal. Thus, short operation time was required for 90% ammonia removal at a DO concentration of 1.0 mg-O_2/L (Fig. 4.3) due to the rapid ammonia removal by X_{AOB}. However, ammonia removal by X_{ANA} decreased with the increasing DO concentration because high oxygen inhibited the growth of X_{ANA}, resulting in X_{AOB} dominancy at the four examined ammonia concentrations. This simulation result is comparable with other Anammox studies (Udert et al., 2008; Corbalá-Robles et al., 2016; Liu et al., 2017; Hoekstra et al., 2018), highlighting the toxicity of high oxygen concentration on X_{ANA} growth. Although 100% of ammonia was removed at the initial ammonia concentration of 100 - 200 mg-

N/L (Fig. 4.2), only 4% of ammonia was removed by X_{ANA}. Therefore, it is highly recommended to maintain moderate oxygen concentration to allow ammonia oxidation into nitrite by X_{AOB} with favorable conditions for Anammox bacteria growth.

4.3.3 Effect of initial nitrite concentration and DO on ammonia removal

Ammonia removal by X_{ANA} was enhanced with the increasing initial nitrite concentration at low and moderate DO concentration (Fig. 4.4) because the availability of nitrite stimulated the growth of X_{ANA} without a competition with X_{AOB} and X_{NOB} under limited oxygen condition. This finding is consistent with the results of previous Anammox studies (Strous et al., 1999; Lotti et al., 2012; Xu et al., 2015; Ma et al., 2017), confirming that nitrite is a rate-limiting parameter on the growth of Anammox bacteria. At a DO concentration of 0.01 mg-O_2/L, ammonia removal by X_{ANA} increased from 8 to 84% when the initial nitrite concentration increased from 0 to 100 mg-N/L. It was also found that ammonia removal by X_{AOB} (9%) was insensitive to the initial nitrite concentration at DO concentration of 0.01 mg-O_2/L, reflecting that the total ammonia removal was completely dependent on Anammox bacteria reactions at low DO concentration. At moderate DO concentration, there was a balance between ammonia removal by X_{ANA} and X_{AOB} where 53% of ammonia was removed by $X_{ANA}$and 43% was utilized by X_{AOB} at an initial nitrite concentration of 100 mg-N/L.

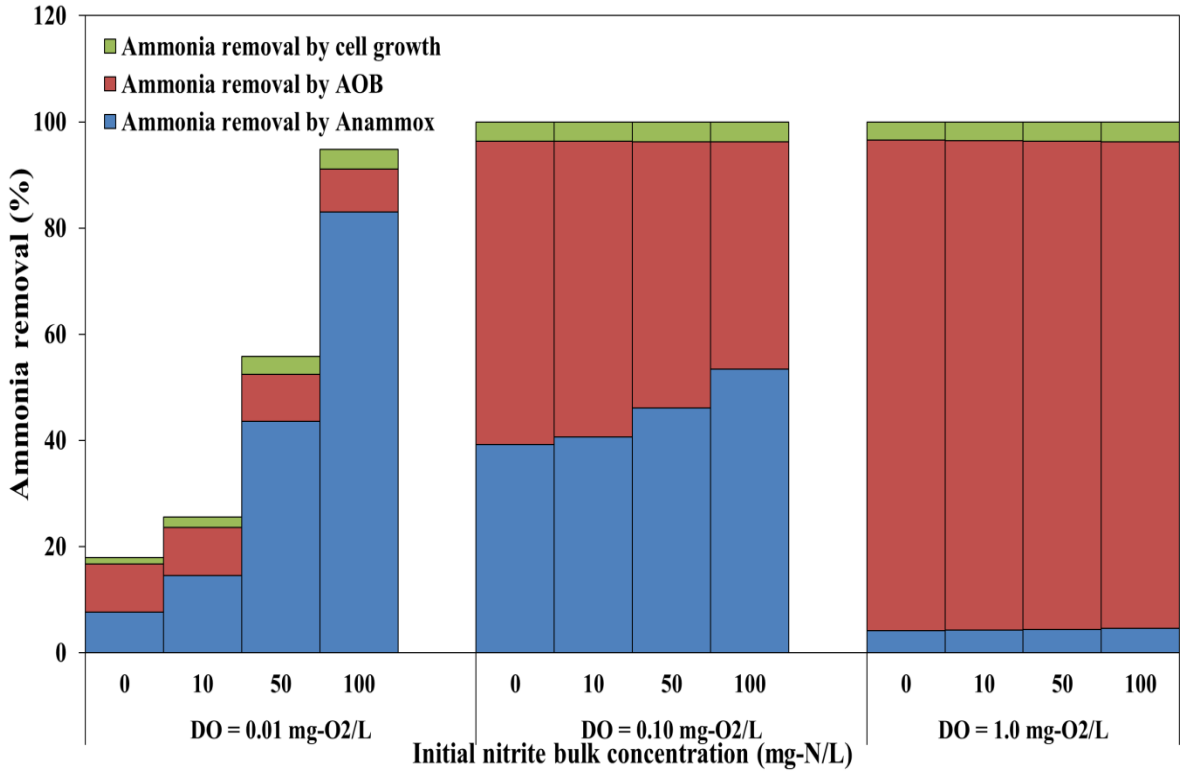

Fig. 4.4. Effect of initial nitrite concentration and dissolved oxygen on the ammonia removal by X_{AOB}, X_{ANA} and cell growth. (Simulation conditions are mentioned in Table 4.1 and 4.2).

At relatively high DO concentration (1.0 mg-O_2/L), ammonia removal by $X_{ANA}$was the least (5%) while ammonia removal by X_{AOB} was the highest (92%) because high oxygen concentration allowed the growth of X_{AOB} and X_{NOB}, inhibiting the activity of Anammox bacteria. This simulation result confirms that total ammonia removal was dominated by the activity of X_{AOB} at high oxygen concentration, highlighting the competition between X_{ANA} and X_{NOB}. For the examined range of initial nitrite concentration (0 – 100 mg-N/L), it was also found that there was a negligible change in the ammonia removal by X_{ANA} and X_{AOB} at relatively high DO concentration due to the high growth rate of X_{AOB} and X_{NOB}, resulting in limited contribution of Anammox bacteria in the total ammonia removal.

4.3.4 Effect of real-time aeration on nitrogen removal

Ammonia removal by Anammox bacteria increased with the decreasing nitrite threshold concentration while ammonia removal by X_{AOB} was enhanced with the increasing threshold concentration for an initial ammonia concentration of 100 mg-N/L (low-strength wastewater) (Fig. 4.5a) because DO concentration controlled the ammonia removal mechanism by X_{ANA} and X_{AOB}. This finding is consistent with the results of previous Anammox studies (Hao et al., 2002; Mozumder et al., 2014; Li et al., 2018) where it was emphasized that the dominance of X_{AOB} over X_{ANA} can be avoided by controlling the oxygen concentration for better Anammox bacteria growth. Ammonia removal by X_{ANA} increased from 16 to 45% for low-strength wastewater treatment when the nitrite threshold concentration decreased from 0.4 to 0.05 mg-N/L (Fig. 4.6), reflecting the importance of automated operation of DO as a function of nitrite concentration in low strength wastewater treatment. For a nitrite threshold concentration of 0.05 mg-N/L, ammonia removal by X_{ANA} and X_{AOB} was in balance where 52% of ammonia was removed by X_{AOB} and 45% was utilized by X_{ANA} for low and high-strength wastewater.

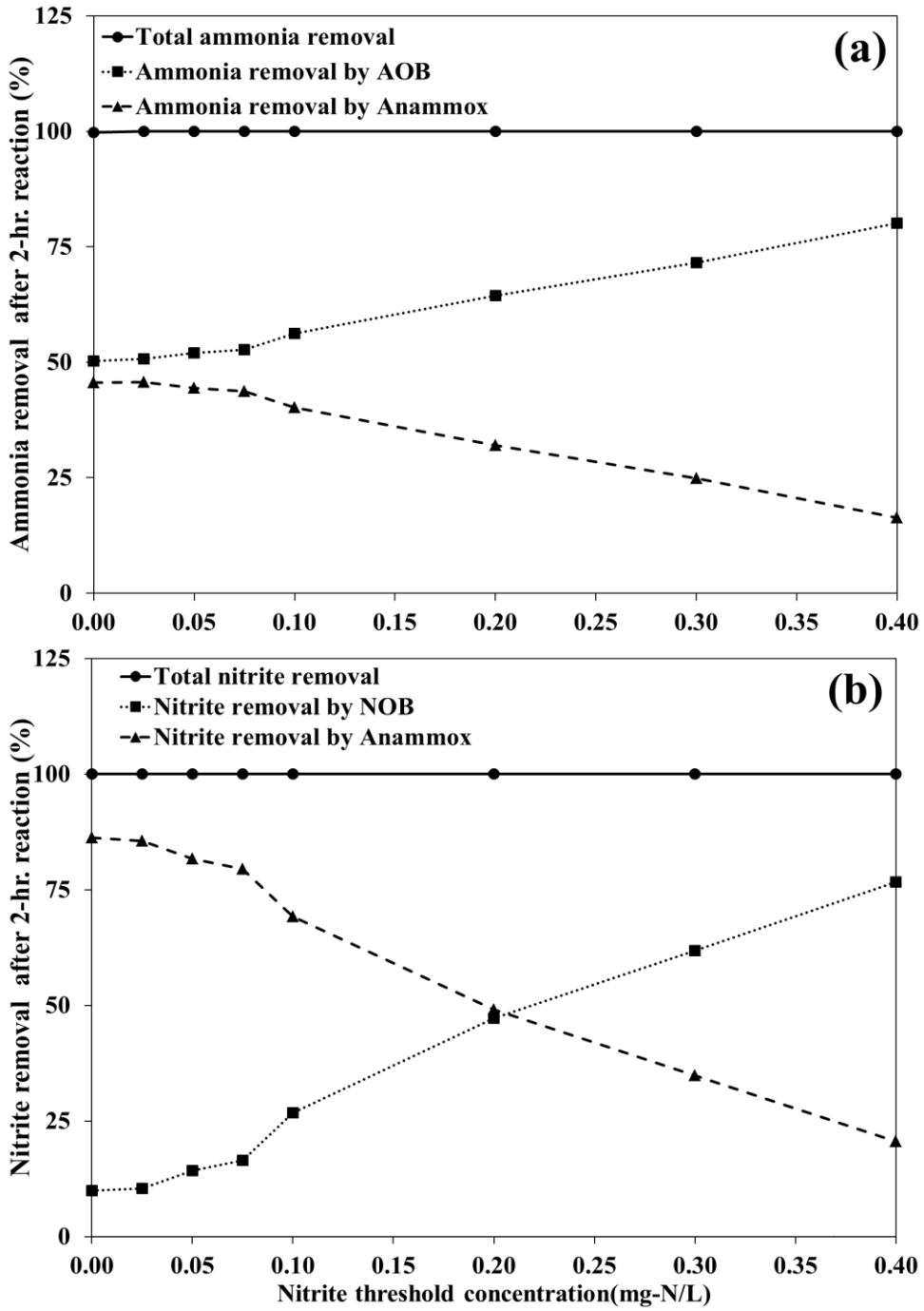

Fig. 4.5. Effect of the nitrite threshold concentration ($S_{NO_2}\big|_{ON}$) for low-strength wastewater on the contribution of: (a) X_{AOB} and X_{ANA} in the ammonia removal, (b) X_{NOB} and X_{ANA} in the nitrite removal. (Simulation conditions are mentioned in Table 4.1 and 4.2, real-time aeration is: If $S_{NO_2} < S_{NO_2}\big|_{ON}$ → DO = 0.5 mg-O_2/L and If $S_{NO_2} > S_{NO_2}\big|_{ON}$ → DO = 0).

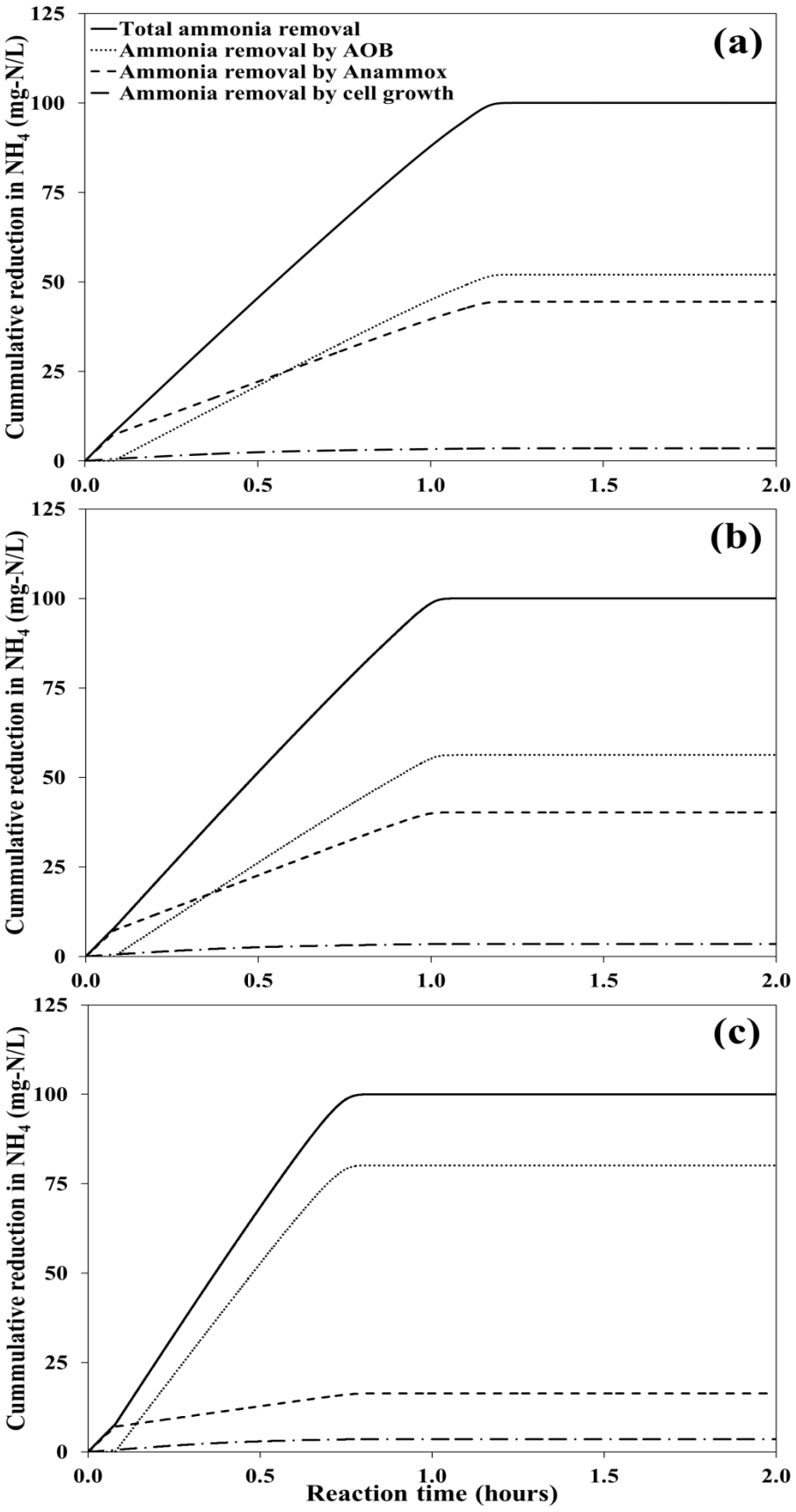
Total ammonia removal
Ammonia removal by AOB
Ammonia removal by Anammox
Ammonia removal by cell growth
(a)
(b)
(c)
Cummulative reduction in NH4 (mg-N/L)
Reaction time (hours)
0
25
50
75
100
125
0.0
0.5
1.0
1.5
2.0

Fig. 4.6. Effect of the nitrite threshold concentration ($S_{NO_2}\big|_{ON}$) on the contribution of X_{AOB}, X_{ANA} and cell growth in the cumulative removal of ammonia concentration for low-strength wastewater at nitrite threshold of: (a) 0.05 mg-N/L, (b) 0.10 mg-N/L, and (c) 0.40 mg-N/L. (Simulation conditions are mentioned in Table 4.1 and 4.2, real-time aeration is: If $S_{NO_2} < S_{NO_2}\big|_{ON}$ → DO = 0.5 mg-O_2/L and If $S_{NO_2} > S_{NO_2}\big|_{ON}$ → DO = 0).

Nitrite removal by X_{ANA} was also enhanced with the decreasing nitrite threshold concentration while nitrite removal by X_{NOB} increased with the increasing threshold concentration for low-strength wastewater (Fig. 4.5b) because the DO concentration and aeration scheme controlled the nitrite utilization mechanism by X_{ANA} and X_{NOB}. The nitrite removal mechanism based on the oxygen availability was described in previous Anammox studies (Perez et al., 2014; Cao et al., 2017; Li et al., 2018), showing the importance of aeration scheme for X_{ANA}. These findings are consistent for high-strength wastewater (initial ammonia concentration = 500 mg-N/L) (Fig. B5, B6). However, ammonia was not completely removed for high-strength wastewater at a threshold concentration less than 0.05 mg-N/L (Fig. B5a), reflecting the importance of selecting a reasonable real-time aeration scheme for better total ammonia removal with a significant contribution of Anammox bacteria.

At a nitrite threshold concentration of 0.4 mg-N/L, ammonia removal by X_{AOB} was dominant where 81% of ammonia was removed by X_{AOB} for low and high-strength wastewater (Fig. 4.6c and B6c), highlighting the effect of the correlation between nitrite and DO concentration on the ammonia removal mechanism. It was also observed that the total ammonia removal rate was rapid at threshold concentration of 0.4 mg-N/L compared to lower threshold concentrations for low and high-strength wastewater

because of the dominance of X_{AOB} by longer aeration time. For the examined nitrite threshold and initial ammonia concentrations, ammonia removal by cell growth was negligible (2 - 3.5%) compared to the contribution of X_{ANA} and X_{AOB} in the total ammonia removal (Fig. 4.6 and Fig. B6).

Based on the model simulation results, it was found that the nitrite removal rate was rapid at nitrite threshold concentration of 0.4 mg-N/L where nitrite removal was 77% by X_{NOB} and 22% by X_{ANA} for low and high-strength wastewater (Fig. 4.7c and Fig. B7c), confirming that nitrite removal by X_{NOB} was the dominant removal mechanism due to availability of DO. On the other hand, nitrite removal by X_{ANA} was dominant at nitrite threshold concentration of 0.05 mg-N/L where 84% of nitrite was removed by X_{ANA} and 15% was utilized by X_{NOB} for low and high-strength wastewater (Fig. 4.7a and Fig. B7a), highlighting the importance of real-time aeration on the nitrite removal mechanism. It was also noticed that nitrite removal by heterotrophs was negligible (2%) compared to the contribution of X_{ANA} and X_{NOB} in the total nitrite removal for the examined range of nitrite threshold and initial ammonia concentrations (Fig. 4.7 and Fig. B7). Based on the model simulation results, it is highly recommended to implement real-time monitoring of nitrite to expand the Anammox process applications in biological wastewater treatment process.

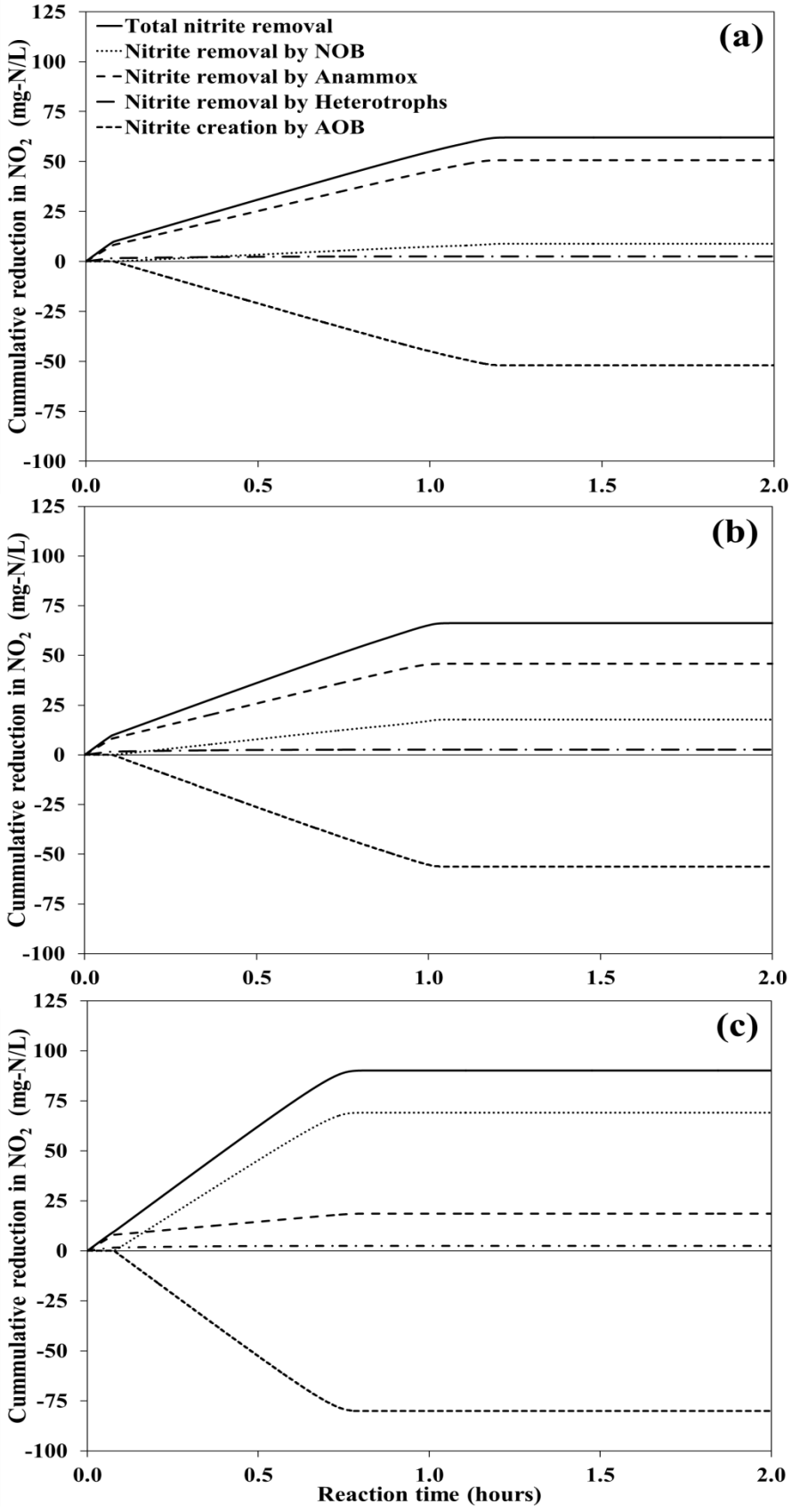
(a)
Total nitrite removal
Nitrite removal by NOB
Nitrite removal by Anammox
Nitrite removal by Heterotrophs
Nitrite creation by AOB
Cummulative reduction in NO2 (mg-N/L)
125
100
75
50
25
0
-25
-50
-75
-100
0.0
0.5
1.0
1.5
2.0
(b)
Cummulative reduction in NO2 (mg-N/L)
(c)
Cummulative reduction in NO2 (mg-N/L)
Reaction time (hours)

Fig. 4.7. Effect of the nitrite threshold concentration ($S_{NO_2}\big|_{ON}$) on the contribution of X_{NOB}, $X_{ANA}$and heterotrophs in the cumulative removal of nitrite concentration for low-strength wastewater at nitrite threshold of: (a) 0.05 mg-N/L, (b) 0.10 mg-N/L, and (c) 0.40 mg-N/L. (Simulation conditions are mentioned in Table 4.1 and 4.2, real-time aeration is: If $S_{NO_2} < S_{NO_2}\big|_{ON}$ → DO = 0.5 mg-O_2/L and If $S_{NO_2} > S_{NO_2}\big|_{ON}$ → DO = 0). Negative values mean creation of nitrite by X_{AOB}.

4.3.5 Comparison between continuous and real-time aeration schemes

In the model simulation of the real-time monitoring of the ammonia and nitrite concentration, ammonia was injected with a concentration of 500 mg-N/L when the ammonia concentration was 25 mg-N/L (i.e., ammonia removal efficiency = 95%) (Fig. B1a) while the continuous or real-time aeration scheme was implemented (Fig. B1b, c). For the continuous aeration with a DO concentration of 0.5 mg-O_2/L, the total ammonia removal rate was extremely rapid (Fig. 4.8a) because of the high activity of X_{AOB}. After one day of reaction, the total injected ammonia concentration was 5500 mg-N/L (11 injection cycles) under continuous aeration scheme (Fig. B1a). However, ammonia was injected six times with total concentration of 3000 mg-N/L under real-time aeration scheme, reflecting that the total ammonia removal rate was slow (Fig. 4.8b) because there was a balance between X_{ANA} and X_{AOB} in ammonia removal rate by the automated DO concentration. After five days of continuous aeration, 200 g-N/L of ammonia was removed where 97.5% of ammonia was removed by X_{AOB}, 1% by X_{ANA} and the rest was utilized by cell growth (Fig. 4.8a), reflecting the dominancy of X_{AOB} at continuous aeration scheme. On the other hand, the total removed ammonia under real-time aeration was 15.5 g-N/L where 58% was removed by X_{AOB}, 40% by X_{ANA} and the rest was consumed by cell growth (Fig. 4.8b). Therefore, it is highly recommended implementing

the real-time monitoring of nitrite concentration for broad Anammox bacteria applications in cost-efficient biological wastewater treatment.

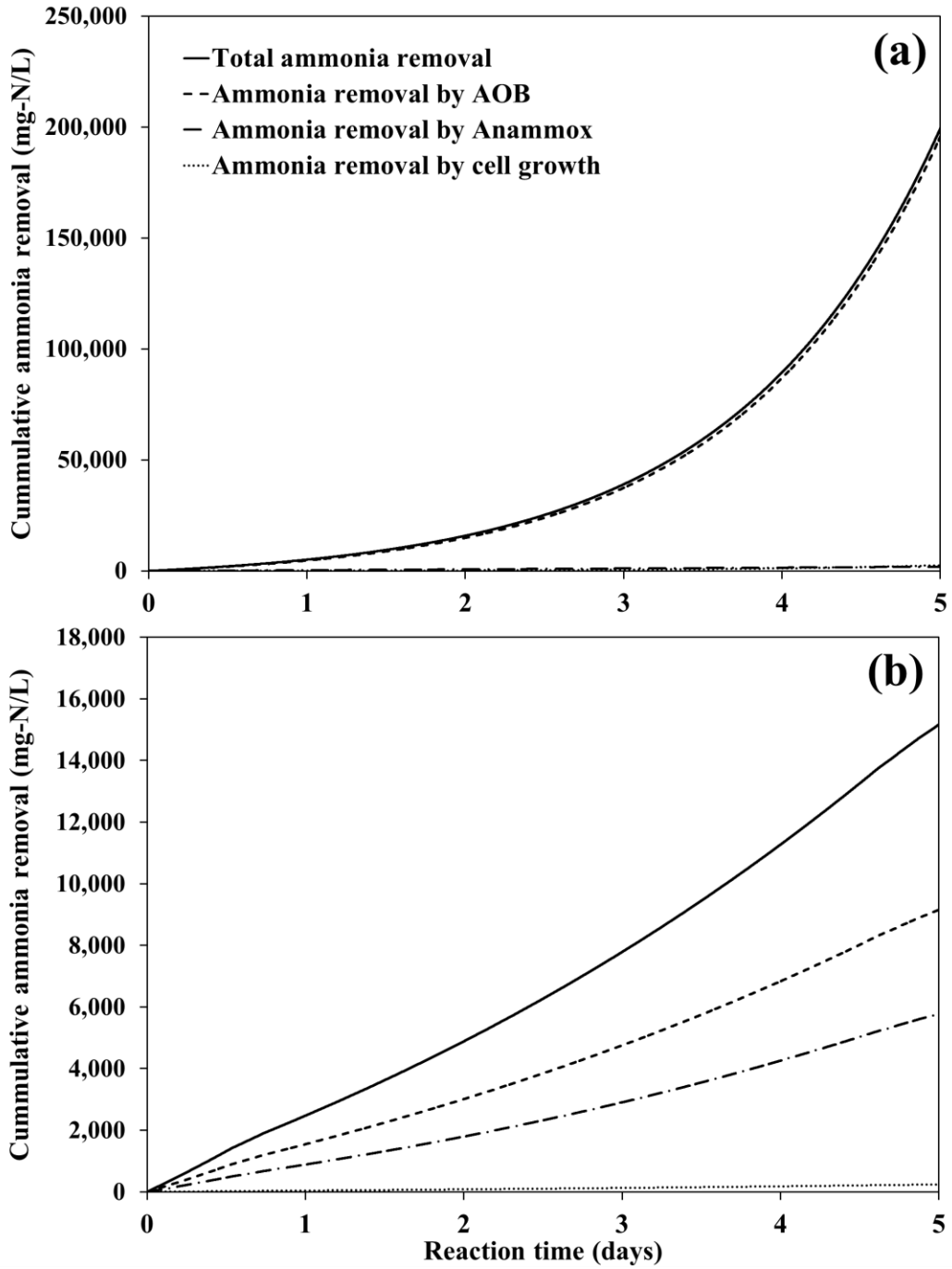

Fig. 4.8. Total ammonia removal, ammonia removal by X_{AOB}, ammonia removal by $X_{ANA}$and ammonia removal by cell growth under: (a) continuous aeration, and (b) real-time aeration. (Simulation conditions are mentioned in Table 4.1 and 4.2, real-time aeration is: If $S_{NO_2} \leq 0.05 \rightarrow$ DO = 0.5 mg-O_2/L for 10 seconds and If $S_{NO_2} > 0.05 \rightarrow$ DO = 0 for 10 seconds).

Anammox bacteria growth rate was enhanced by the real-time aeration scheme (Fig. 4.9a) because there was no competition between X_{AOB} and X_{ANA} for ammonia, and X_{NOB} and X_{ANA} for nitrite under limited DO concentration where the Anammox population increased by 25% after five days of real-time aeration. This result is comparable with the results of previous experimental Anammox studies (Joss et al., 2009; Cao et al., 2017;Wang et al., 2019; Zekker et al., 2019) where it was recommended to maintain reasonable DO concentration for ammonia oxidation by X_{AOB} without toxic effect on Anammox bacteria. On the other hand, the Anammox population increased by only 7% (Fig. 4.9a) when the reactor was operated under continuous aeration because high oxygen concentration and nitrite accumulation inhibited the growth of Anammox bacteria (Fig. 4.10a), resulting in a dominance of X_{AOB} and X_{NOB} over X_{ANA} (Fig. 4.9b, c). This finding is consistent with the results of other Anammox studies (Strous et al., 1999; Wyffels et al., 2004; Lotti et al., 2012; Carvajal-Arroyo et al., 2014; Lackner et al., 2014) where it was demonstrated that inhibition by nitrite can occur at high nitrite concentration (i.e., S_{NO_2} > 100 mg-N/L).

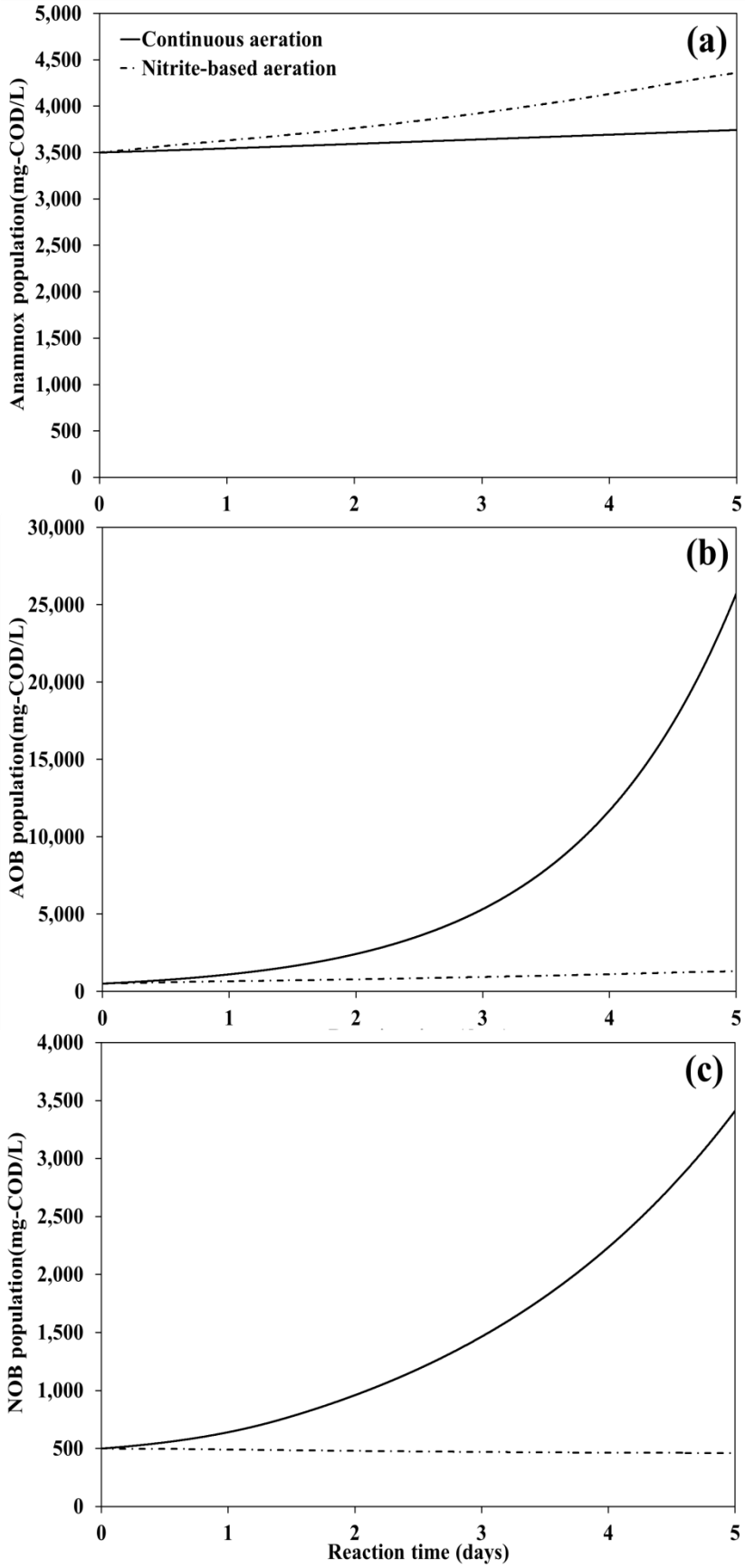
(a)
Continuous aeration
Nitrite-based aeration
Anammox population(mg-COD/L)
5,000
4,500
4,000
3,500
3,000
2,500
2,000
1,500
1,000
500
0
0
1
2
3
4
5
(b)
AOB population(mg-COD/L)
30,000
25,000
20,000
15,000
10,000
5,000
0
0
1
2
3
4
5
(c)
NOB population(mg-COD/L)
4,000
3,500
3,000
2,500
2,000
1,500
1,000
500
0
0
1
2
3
4
5
Reaction time (days)

Fig. 4.9. Comparison between the effect of continuous and real-time aeration on the population of: (a) Anammox bacteria, (b) AOB bacteria and (c) NOB bacteria. (Simulation conditions are mentioned in Table 4.1 and 4.2, real-time aeration is: If $S_{NO_2} \leq 0.05 \rightarrow$ DO = 0.5 mg-O_2/L for 10 seconds and If $S_{NO_2} > 0.05 \rightarrow$ DO = 0 for 10 seconds).

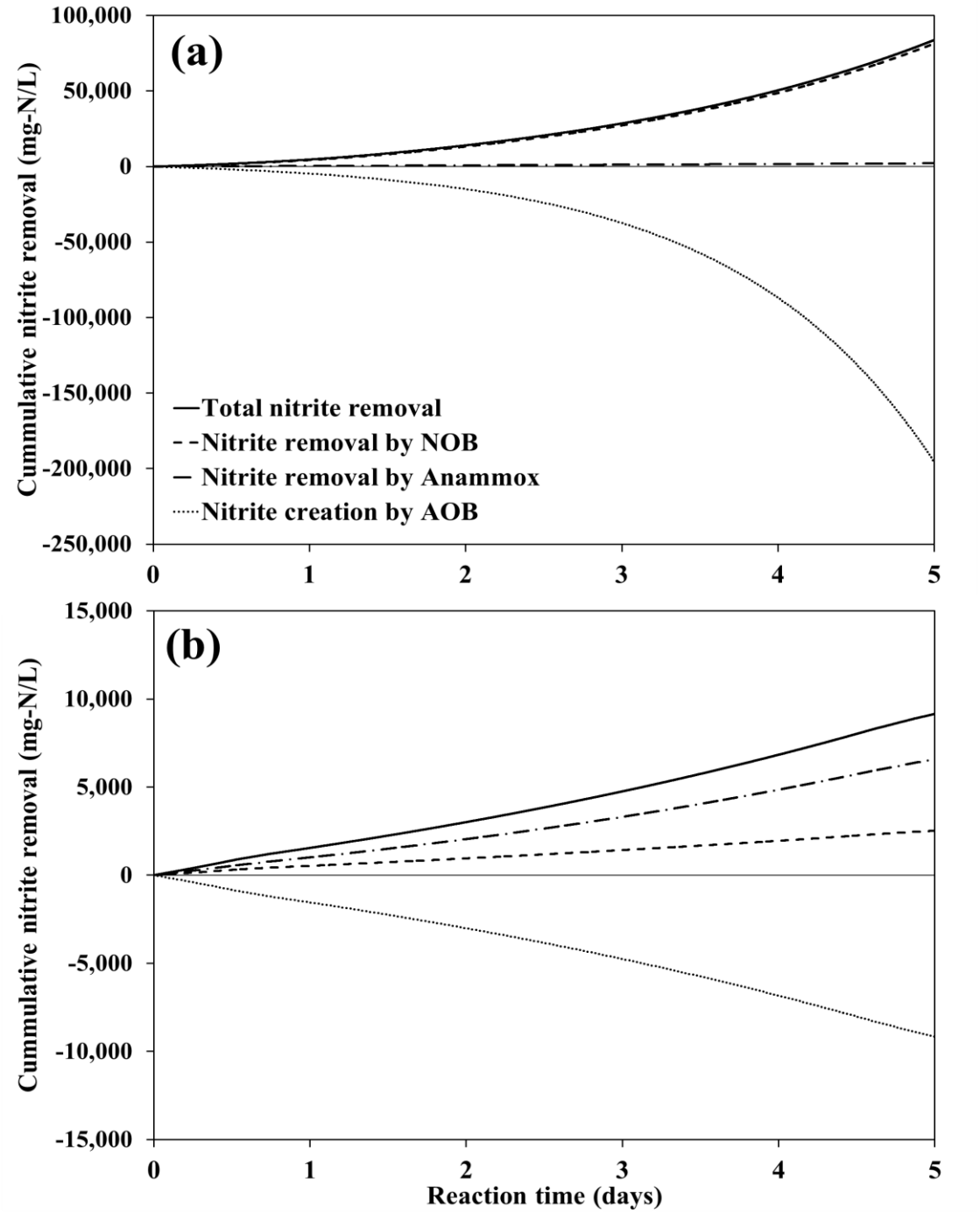

Fig. 4.10. Total nitrite removal, nitrite removal by X_{NOB}, nitrite removal by X_{ANA} and nitrite creation by X_{AOB} under: (a) continuous aeration, and (b) real-time aeration. (Simulation conditions are mentioned in Table 4.1 and 4.2, real-time aeration is: If $S_{NO_2} \leq 0.05 \rightarrow$ DO = 0.5 mg-O_2/L for 10 seconds and If $S_{NO_2} > 0.05 \rightarrow$ DO = 0 for 10 seconds). Negative values mean creation of nitrite by X_{AOB}.

Nitrite removal by X_{ANA} was the dominant nitrite removal mechanism under the real-time aeration scheme (Fig. 4.10b) because there was no competition between X_{NOB} and X_{ANA} for nitrite while oxygen was limited. Based on the model simulation results, 72% of the total removed nitrite (9.2 g-N/L) was removed by X_{ANA}while 27% was consumed by X_{NOB} and the rest was removed by heterotrophs under real-time aeration scheme. On the other hand, 84 g-N/L of nitrite was removed under continuous aeration scheme (Fig. 4.10a) where 97% of nitrite was removed by X_{NOB} and the rest was utilized by X_{ANA}, confirming that X_{NOB} was the dominant microorganism in nitrite removal when oxygen was available. Although 195 g-N/L of nitrite was created by X_{AOB} under continuous aeration scheme (Fig. 4.10a), only 43% of this created nitrite (84 g-N/L) was oxidized by X_{NOB} because the maximum specific growth rate constant of X_{AOB} (μ_{AOB}) was higher than μ_{NOB} and the oxygen half saturation constant of X_{AOB} ($K_{O_2}^{AOB}$) was lower than $K_{O_2}^{NOB}$ (Table 4.1), resulting in higher activity of X_{AOB} over X_{NOB}. This simulation result is consistent with the results of previous nitrogen removal studies (Blackburne et al., 2008; Ma et al., 2016; Ma et al., 2017; Val de Rio et al., 2019; Zhang et al., 2019), confirming the superiority of X_{AOB} on X_{NOB} in consuming oxygen.

4.4 Conclusions

A non-steady state mathematical model was developed and calibrated using experimental results from previous lab-scale Anammox studies. Based on the simulation results of the calibrated model, moderate dissolved oxygen (DO ≅ 0.10 mg-O_2/L) was important for high ammonia removal by X_{ANA} as moderate DO created a balance between ammonia oxidation into nitrite by X_{AOB} and ammonia removal by X_{AOB} using the

produced nitrite and remaining ammonia. Although low oxygen concentration (DO ≅ 0.01 mg-O_2/L) resulted in slow overall ammonia removal because of the limited growth of X_{AOB} under limited DO conditions, ammonia removal by X_{ANA} was considerable. On the other hand, ammonia removal by X_{ANA} was limited at high oxygen concentration (DO ≅ 1.0 mg-O_2/L) because high DO inhibited the Anammox bacterial growth while the total ammonia removal rate was the highest due to sufficient growth of X_{AOB}.

It was also observed that the required time for 90% ammonia removal increased with the increasing initial ammonia concentration and the decreasing dissolved oxygen concentration. For the low and moderate DO concentrations, the ammonia removal by $X_{ANA}$was enhanced with the increasing initial nitrite concentration because the availability of nitrite stimulated the growth of X_{ANA} without a competition with X_{AOB} and X_{NOB} under limited oxygen condition. Therefore, it is highly recommended to maintain moderate oxygen concentration to allow complete ammonia removal with a balance between aerobic ammonia oxidation into nitrite by X_{AOB} and Anammox bacterial growth.

In the nitrite-based real-time aeration, it was found that the ammonia removal rate by $X_{ANA}$was enhanced with the decreasing nitrite threshold concentration because the nitrite-based schematic aeration decreased the activity of X_{AOB}, resulting in a dominance of X_{ANA} both for the low and high-strength wastewater scenarios. Also, X_{ANA} was dominant over X_{NOB} in nitrite utilization under the nitrite-based aeration because this aeration scheme prevented an outgrowth of X_{AOB} and X_{NOB}, providing more favorable conditions for the growth of Anammox bacteria. In the simulation results of the real-time

monitoring of the bulk concentration, it was found that the ammonia removal by $X_{ANA}$was enhanced with the nitrite-based aeration compared to the continuous aeration scheme because the correlation between the aeration scheme and nitrite concentration controlled the activity of X_{NOB}. Therefore, it is highly recommended to implement the real-time monitoring of nitrite concentration for broad Anammox bacteria applications in cost-efficient biological wastewater treatment.

References

Agrawal, S., Seuntjens, D., De Cocker, P., Lackner, S., Vlaeminck, S.E., 2018. Success of mainstream partial nitritation/anammox demands integration of engineering, microbiome and modeling insights. Current Opinion in Biotechnology. 50, 214–221.

Akgul, D., Aktan, C.K, Yapsakli, K., Mertoglu, B., 2013. Treatment of landfill leachate using UASB-MBR-SHARON–Anammox configuration. Biodegradation. 24, 399–412.

Ali, M., Okabe, S., 2015. Anammox-based technologies for nitrogen removal : Advances in process start-up and remaining issues. Chemosphere. 141, 144–153.

Azari, M., Lübken, M., Denecke, M., 2017. Simulation of simultaneous anammox and denitrification for kinetic and physiological characterization of microbial community in a granular biofilm system. Biochemical Engineering Journal. 127, 206–216.

Baeten, J.E., Batstone, D.J., Schraa, O.J., van Loosdrecht, M.C.M., Volcke, E.I.P., 2019. Modelling anaerobic, aerobic and partial nitritation-anammox granular sludge reactors - A review. Water Research. 149, 322–341.

Beun, J.J., van Loosdrecht, M.C.M., Heijnen, J.J., 2002. Aerobic granulation in a sequencing batch airlift reactor. Water Research. 36, 702–712.

Bi, Z., Takekawa, M., Park, G., Soda, S., Zhou, J., Qiao, S., Ike, M., 2015. Effects of the C/N ratio and bacterial populations on nitrogen removal in the simultaneous anammox and heterotrophic denitrification process : Mathematic modeling and batch experiments. Chemical Engineering Journal. 280, 606–613.

Blackburne, R., Yuan, Z., Keller, Ã., 2008. Demonstration of nitrogen removal via nitrite in a sequencing batch reactor treating domestic wastewater. Water Research. 42, 2166–2176.

Cao, Y., van Loosdrecht, M.C.M., Daigger, G.T., 2017. Mainstream partial nitritation – anammox in municipal wastewater treatment : status, bottlenecks, and further studies. Applied Microbiology and Biotechnology. 101, 1365–1383.

Carvajal-Arroyo, J.M., Puyol, D., Li, G., Lucero-Acuňa, A., Sierra-Álvarez, R., Field, J.A., 2013. Pre-exposure to nitrite in the absence of ammonium strongly inhibits anammox. Water Research. 48, 52 – 60.

Chaali, M., Naghdi, M., Brar, K., 2018. A review on the advances in nitrifying biofilm reactors and their removal rates in wastewater treatment. Journal of Chemical Technology and Biotechnology. 93, 3113–3124.

Chapra, S.C., Canale, P.R., 1998. Numerical Methods for Engineers with Software and Programming Applications, third Ed. McGrawHill, America.

Chen, H., Ma, C., Yang, G., Wang, H., Yu, Z., Jin, R., 2014. Floatation of flocculent and granular sludge in a high-loaded anammox reactor. Bioresource Technology. 169, 409–415.

Chen, C., Sun, F., Zhang, H., Wang, J., Shen, Y., Liang, X., 2016. Evaluation of COD effect on anammox process and microbial communities in the anaerobic baffled reactor (ABR). Bioresource Technology. 216, 571–578.

Chen, R., Ji, J., Chen, Y., Takemura, Y., Liu, Y., Kubota, K., Ma, H., Li, Y., 2019. Successful operation performance and syntrophic micro-granule in partial nitritation and anammox reactor treating low-strength ammonia wastewater. Water Research. 155, 288–299.

Chen, G., Zhang, Y., Wang, X., Chen, F., Lin, L., Ruan, Q., Wang, Y., Wang, F., Cao, W., Chiang, P., 2020. Optimizing of operation strategies of the single-stage partial nitrification-anammox process. Journal of Cleaner Production. 256, 120667.

Cho, S., Fujii, N., Lee, T., Okabe, S., 2011. Development of a simultaneous partial nitrification and anaerobic ammonia oxidation process in a single reactor. Bioresource Technology. 102(2), 652–659.

Connan, R., Dabert, P., Khalil, H., Bridoux, G., Béline, F., Magrí, A., 2016. Batch enrichment of anammox bacteria and study of the underlying microbial community dynamics. Chemical Engineering Journal. 297(3), 217–228.

Conthe, M., Lycus, P., Arntzen, M.Ø., Ramos, A., Frostegård, Å., Bakken, L.R., Kleerebezem, R., van Loosdrecht, M.C.M., 2019. Denitrification as an N_2O sink. Water Research. 151, 381–387.

Corbalá-Robles, L., Picioreanu, C., van Loosdrecht, M.C.M., 2016. Analysing the effects of the aeration pattern and residual ammonium concentration in a partial nitritation-anammox process. Environmental Technology. 37(6), 694–702.

Cui, B., Yang, Q., Liu, X., Wu, W., Liu, Z., Gu, P., 2020. Achieving partial denitrification-anammox in biofilter for advanced wastewater treatment. Environment International. 138, 105612.

Du, R., Peng, Y., Cao, S., Wang, S., Wu, C., 2015. Advanced nitrogen removal from wastewater by combining anammox with partial denitrification. Bioresource Technology. 179, 497–504.

Du, R., Peng, Y., Ji, J., Shi, L., Gao, R., Li, X., 2019. Partial denitrification providing nitrite : Opportunities of extending application for anammox. Environment International. 131, 105001.

Elsayed, A., Hurdle, M., Kim, Y., 2021. Comprehensive model applications for better understanding of pilot-scale membrane-aerated biofilm reactor performance. Journal of Water Process Engineering. 40, 101894.

Eskicioglu, C., Galvagno, G., Cimon, C., 2018. Approaches and processes for ammonia removal from side-streams of municipal effluent treatment plants. Bioresource Technology. 268, 797–810.

Ge, C., Dong, Y., Li, H., Li, Q., Ni, S., Gao, B., 2019. Nitritation-anammox process – A realizable and satisfactory way to remove nitrogen from high saline wastewater. Bioresource Technology, 275, 86–93.

Gilbert, E.M., Agrawal, S., Schwartz, T., Horn, H., Lackner, S., 2015. Comparing different reactor configurations for Partial Nitritation/Anammox at low temperatures. Water Research, 81, 92–100.

Gilmore, K.R., Terada, A., Smets, B.F., Love, N.G., Garland, J.L., 2013. Autotrophic Nitrogen Removal in a Membrane-Aerated Biofilm Reactor Under Continuous Aeration: A Demonstration, Environmental Engineering Science. 30(1), 38–45.

Gong, Z., Yang, F., Liu, S., Bao, H., Hu, S., Furukawa, K., 2007. Feasibility of a membrane-aerated biofilm reactor to achieve single-stage autotrophic nitrogen removal based on Anammox. Chemosphere. 69, 776–784.

Graham, D.M., Jolis, D., 2017. Pilot-Scale Evaluation of pH-Based Control of Single Stage Deammonification Processes for Sidestream Treatment. Water Environment Research. 89 (2), 99–104.

Guo, Y., Chen, Y., Webeck, E., Li, Y., 2020. Towards more efficient nitrogen removal and phosphorus recovery from digestion effluent : Latest developments in the

anammox-based process from the application perspective. Bioresource Technology. 299, 122560.

Hao, X., Heijnen, J.J., van Loosdrecht, M.C.M., (2002). Sensitivity Analysis of a Biofilm Model Describing a One-Stage Completely Autotrophic Nitrogen Removal (CANON) Process. Biotechnology and Bioengineering. 77(3), 266–277.

Hauck, M., Maalcke-luesken, F.A., Jetten, M.S.M., Huijbregts, M.A.J., 2016. Removing nitrogen from wastewater with side stream anammox : What are the trade-offs between environmental impacts . Resources, Conservation and Recycling. 107, 212–219.

He, S., Chen, Y., Qin, M., Mao, Z., Yuan, L., Niu, Q., Tan, X., 2018. Effects of temperature on anammox performance and community structure. Bioresource Technology. 260, 186–195.

Henze, M., Gujer, W., Mino, T., van Loosdrecht, M.C.M., 2000. Activated Sludge Models ASM1, ASM2, ASM2d and ASM3. IWA Scientific and Technical Report No. 9, London, UK.

Hoekstra, M., Geilvoet, S.P., Hendrickx, T.L. G., Kip, C.S.V.E.T, Kip, Kleerebezem, R., van Loosdrecht, M.C.M., 2019. Towards mainstream anammox : lessons learned from pilot-scale research at WWTP Dokhaven. Environmental Technology. 40 (13), 1721–1733.

Jia, M., Solon, K., Vandeplassche, D., Venugopal, H., Volcke, E.I.P., 2020. Model-based evaluation of an integrated high-rate activated sludge and mainstream anammox system. Chemical Engineering Journal. 382, 122878.

Jiang, H., Liu, G., Ma, Y., Xu, X., Chen, J., Yang, Y., Liu, X., Wang, H., 2018. A pilot-scale study on start-up and stable operation of mainstream partial nitrification-anammox biofilter process based on online pH-DO linkage control. Chemical Engineering Journal. 350, 1035–1042.

Joss, A., Derlon, N., Cyprien, C., Burger, S., Szivak, I., Traber, J., Siegrist, H., Morgenroth, E., 2011. Combined Nitritation-Anammox : Advances in Understanding Process Stability. Environmental Science and Technology. 45, 9735–9742.

Joss, A., Salzgeber, D., Eugster, J., König, R., Rottermann, K., Burger, S., Fabijan, P., Leumann, S., Mohn, J., Siegrist, H., 2009. Full-Scale Nitrogen Removal from Digester Liquid with Partial Nitritation and Anammox in One SBR. Environmental Science and Technology. 43 (14), 5301–5306.

Kanders, L., Beier, M., Nogueira, R., Nehrenheim, E., 2018. Sinks and sources of anammox bacteria in a wastewater treatment plant – screening with qPCR. Water Science and Technology. 78.2, 441–451.

Keluskar, R., Nerurkar, A., Desai, A., 2013. Development of a simultaneous partial nitrification, anaerobic ammonia oxidation and denitrification (SNAD) bench scale process for removal of ammonia from effluent of a fertilizer industry. Bioresource Technology. 130, 390–397.

Koch, G., Egli, K., Meer, J.R. Van Der, Siegrist, H., 2000. Mathematical modeling of autotrophic denitrification in a nitrifying biofilm of a rotating biological contactor. Water Science and Technology. 41 (4-5), 191–198.

Lackner, S., Terada, A., Smets, B.F., 2008. Heterotrophic activity compromises autotrophic nitrogen removal in membrane-aerated biofilms : Results of a modeling study. Water Research. 42(3), 1102–1112.

Lackner, S., Gilbert, E.M., Vlaeminck, S.E., Joss, A., Horn, H., van Loosdrecht, M.C.M., 2014. Full-scale partial nitritation/anammox experiences - An application survey. Water Research, 55, 292–303.

Laureni, M., Falås, P., Robin, O., Wick, A., Weissbrodt, D.G., Lund, J., Ternes, T.A., Morgenroth, E., Joss, A., 2016. Mainstream partial nitritation and anammox : long-term process stability and effluent quality at low temperatures. Water Research. 101, 628–639.

Li, X., Sun, S., Badgley, B.D., Sung, S., Zhang, H., He, Z., 2016. Nitrogen removal by granular nitritation-anammox in an upflow membrane-aerated biofilm reactor. Water Research. 94, 23–31.

Li, J., Zhang, L., Peng, Y., Zhang, Q., 2017a. Effect of low COD/N ratios on stability of single-stage partial nitritation/anammox (SPN/A) process in a long-term operation. Bioresource Technology. 244, 192–197.

Li, X., Sun, S., Yuan, H., Badgley, B.D., He, Z., 2017b. Mainstream upflow nitritation-anammox system with hybrid anaerobic pretreatment : Long-term performance and microbial community dynamics. Water Research. 125, 298–308.

Li, J., Li, J., Gao, R., Wang, M., Yang, L., Wang, X., Zhang, L., 2018. A critical review of one-stage anammox processes for treating industrial wastewater : Optimization strategies based on key functional microorganisms. Bioresource Technology. 265, 498–505.

Li, J., Peng, Y., Zhang, L., Li, X., Zhang, Q., Yang, S., Gao, Y., Li, S., 2020. Improving Efficiency and Stability of Anammox through Sequentially Coupling Nitritation and

Denitritation in a Single-Stage Bioreactor. Environmental Science and Technology. 54, 10859–10867.

Li, J., Peng, Y., Zhang, Q., Li, X., Yang, S., Li, S., 2021. Rapid enrichment of anammox bacteria linked to floc aggregates in a single-stage partial nitritation-anammox process : Providing the initial carrier and anaerobic microenvironment. Water Research. 191, 116807.

Lin, H., Tsao, H., Huang, Y., Wang, Y., Yang, K., Yang, Y., Wang, W., Wen, C., Chen, S., Cheng, S., 2014. Removal of nitrogen from secondary effluent of a petrochemical industrial park by a hybrid biofilm-carrier reactor with one-stage ANAMMOX. Water Science and Technology. 69.12, 2526–2532.

Liu, Y., Niu, Q., Wang, S., Ji, J., Zhang, Y., Yang, M., Hojo, T., 2017a. Upgrading of the symbiosis of Nitrosomanas and anammox bacteria in a novel single-stage partial nitritation–anammox system : Nitrogen removal potential and Microbial characterization. Bioresource Technology. 244, 463–472.

Liu, T., Ma, B., Chen, X., Ni, B., Peng, Y., Guo, J., 2017b. Evaluation of mainstream nitrogen removal by simultaneous partial nitrification, anammox and denitrification (SNAD) process in a granule-based reactor. Chemical Engineering Journal. 327, 973–981.

Liu, T., Guo, J., Hu, S., Yuan, Z., 2020. Model-based investigation of membrane biofilm reactors coupling anammox with nitrite/nitrate-dependent anaerobic methane oxidation. Environment International. 137, 105501.

Lotti, T., Van Der Star, W. R. L., Kleerebezem, R., Lubello, C., van Loosdrecht, M.C.M., 2012. The effect of nitrite inhibition on the anammox process. Water Research. 46(8), 2559–2569.

Lotti, T., Kleerebezem, R., Lubello, C., van Loosdrecht, M.C.M., 2014. Physiological and kinetic characterization of a suspended cell anammox culture. Water Research. 60, 1–14.

Ma, B., Bao, P., Wei, Y., Zhu, G., Yuan, Z., Peng, Y., 2015. Suppressing Nitrite-oxidizing Bacteria Growth to Achieve Nitrogen Removal from Domestic Wastewater via Anammox Using Intermittent Aeration with Low Dissolved Oxygen. Scientific Reports. 5:13048, 1–9.

Ma, B., Wang, S., Cao, S., Miao, Y., Jia, F., Du, R., Peng, Y., 2016. Biological nitrogen removal from sewage via anammox : Recent advances. Bioresource Technology. 200, 981–990.

Ma, Y., Domingo-fe, C., Gy, B., Smets, B. F., 2017. Intermittent Aeration Suppresses Nitrite-Oxidizing Bacteria in Membrane-Aerated Biofilms : A Model-Based Explanation. Environmental Science and Technology. 51, 6146–6155.

Ma, B., Xu, X., Wei, Y., Ge, C., Peng, Y., 2020. Recent advances in controlling denitritation for achieving denitritation/anammox in mainstream wastewater treatment plants. Bioresource Technology. 299, 122697.

Miao, Y., Zhang, L., Li, B., Zhang, Q., Wang, S., Peng, Y., 2017. Enhancing ammonium oxidizing bacteria activity was key to single- stage partial nitrification-anammox system treating low-strength sewage under intermittent aeration condition. Bioresource Technology. 231, 36–44.

Miao, Y., Peng, Y., Zhang, L., Li, B., Li, X., Wu, L., Wang, S., 2018. Partial nitrification-anammox (PNA) treating sewage with intermittent aeration mode : Effect of influent C/N ratios. Chemical Engineering Journal. 334, 664–672.

Moussa, M.S., Hooijmans, C.M., Lubberding, H.J., Gijzen, H.J., 2005. Modelling nitrification, heterotrophic growth and predation in activated sludge. Water Research. 39, 5080–5098.

Mozumder, M.S.I., Picioreanu, C., van Loosdrecht, M.C.M., Volcke, E.I.P., 2014. Effect of heterotrophic growth on autotrophic nitrogen removal in a granular sludge reactor. Environmental Technology. 35(8), 1027–1037.

Munz, G., Lubello, C., Oleszkiewicz, J.A., 2011. Factors affecting the growth rates of ammonium and nitrite oxidizing bacteria. Chemosphere. 83(5), 720–725.

Ni, S., Sung, S., Yue, Q., Gao, B., 2012. Substrate removal evaluation of granular anammox process in a pilot-scale upflow anaerobic sludge blanket reactor. Ecological Engineering. 38(1), 30–36.

Ni, B., Smets, B.F., Yuan, Z., Pellicer-Nàcher, C., 2013. Model-based evaluation of the role of Anammox on nitric oxide and nitrous oxide productions in membrane aerated biofilm reactor. Journal of Membrane Science. 446, 332–340.

Ni, B., Joss, A., Yuan, Z., 2014. Modeling nitrogen removal with partial nitritation and anammox in one floc-based sequencing batch reactor. Water Research. 67, 321–329.

Niu, Q., He, S., Zhang, Y., Zhang, Y., Yang, M., Li, Y., 2015. Bio-kinetics evaluation and batch modeling of the anammox mixed culture in UASB and EGSB reactors: batch performance comparison and kinetic model assessment. RSC Advances. 6(5), 3487–3500.

Pellicer-Nàcher, C., Franck, S., Ruscalleda, M., Terada, A., Al-soud, A., Hansen, M.A., Søren, J., Smets, B.F., 2013. Sequentially aerated membrane biofilm reactors for

autotrophic nitrogen removal : microbial community composition and dynamics. Microbial Biotechnology. 7, 32–43.

Pereira, A.D., Cabezas, A., Etchebehere, Chernicharo, C.A.D.L., Araújo, J.C.D, 2017. Microbial communities in anammox reactors : a review. Environmental Technology Reviews. 6(1), 74–93.

Pérez, J., Lotti, T., Kleerebezem, R., Picioreanu, C., van Loosdrecht, M.C.M., 2014. Outcompeting nitrite-oxidizing bacteria in single- stage nitrogen removal in sewage treatment plants : A model-based study. Water Research. 66, 208–218.

Qian, W., Ma, B., Li, X., Zhang, Q., Peng, Y., 2019. Long-term effect of pH on denitrification : High pH benefits achieving partial-denitrification. Bioresource Technology. 278, 444–449.

Regmi, P., Miller, M.W., Holgate, B., Bunce, R., Park, H., Chandran, K., Wett, B., Murthy, S., Bott, C.B., 2014. Control of aeration, aerobic SRT and COD input for mainstream nitritation/denitritation. Water Research. 57, 162–171.

Soliman, M., Eldyasti, A., 2018. Ammonia-Oxidizing Bacteria (AOB): opportunities and applications — a review. Reviews in Environmental Science and Biotechnology. 17, 285–321.

Strous, M., Heijnen, J.J., Kuenen, J.G., Jetten, M.S.M., 1998. The sequencing batch reactor as a powerful tool for the study of slowly growing anaerobic ammonium-oxidizing microorganisms. Applied Microbial Biotechnology. 50, 589–596.

Strous, M., Kuenen, J. G., Jetten, M.S.M., 1999. Key Physiology of Anaerobic Ammonium Oxidation. Applied and Environmental Microbiology. 65(7), 3248–3250.

Udert, K. M., Kind, E., Teunissen, M., Jenni, S., Larsen, T.A., 2008. Effect of heterotrophic growth on nitritation/anammox in a single sequencing batch reactor. Water Science and Technology. 58.2, 277–284.

Val de Rio, A., Campos, J.L., Da Silva, C., Pedrouso, A., Mosquera-Corral, A., 2019. Nitrite-oxidizing bacteria in granular and flocculent sludge. Separation and Purification Technology. 213, 571–577.

Van der Star, W.R.L. Miclea, A.I., van Dongen, U.G.J.M., Muyzer, G., Picioreanu, C., van Loosdrecht, M.C.M., 2008. The Membrane Bioreactor : A Novel Tool to Grow Anammox Bacteria as Free Cells. Biotechnology and Bioengineering. 101(2), 286–294.

Van Hulle, S.W.H., Vandeweyer, H.J.P., Meesschaert, B.D., Vanrolleghem, P.A., Dejans, P., Dumoulin, A., 2010. Engineering aspects and practical application of autotrophic

nitrogen removal from nitrogen rich streams. Chemical Engineering Journal. 162(1), 1–20.

Volcke, E.I.P., Picioreanu, C., De Baets, B., van Loosdrecht, M.C.M., 2010. Effect of granule size on autotrophic nitrogen removal in a granular sludge reactor. Environmental Technology. 31:11, 1271–1280.

Wang, H., Xu, G., Qiu, Z., Zhou, Y., Liu, Y., 2019. NOB suppression in pilot-scale mainstream nitritation-denitritation system coupled with MBR for municipal wastewater treatment. Chemosphere. 216, 633–639.

Wang, W., Li, D., Li, S., Zeng, H., Zhang, J., 2021. Characteristics and formation mechanism of hollow Anammox granular sludge in low-strength ammonia sewage treatment. Chemical Engineering Journal. 421, 127766.

Wiesmann, U., 1994. Biological nitrogen removal from wastewater. Advances in Biochemical Engineering & Biotechnology. 51, 113–154.

Wyffels, S., Boeckx, P., Pynaert, K., Zhang, D., van Cleemput, O., Chen, G., 2018. Nitrogen removal from sludge reject water by a two-stage oxygen-limited autotrophic nitrification denitrification process. Water Science and Technology. 49(5-6), 57–64.

Xu, G., Zhou, Y., Yang, Q., Lee, Z.M., 2015. The challenges of mainstream deammonification process for municipal used water treatment. Applied Microbial Biotechnology. 99, 2485–2490.

Yang, J., Trela, J., Zubrowska-sudol, M., Plaza, E., 2015. Intermittent aeration in one-stage partial nitritation/anammox process. Ecological Engineering. 75, 413–420.

You, Q., Wang, J., Qi, G., Zhou, Y., 2020. Anammox and partial denitrification coupling : a review. RSC Advances. 12554–12572.

Yue, X., Yu, G., Lu, Y., Liu, Z., Li, Q., Tang, J., Liu, J., 2018. Effect of dissolved oxygen on nitrogen removal and the microbial community of the completely autotrophic nitrogen removal over nitrite process in a submerged aerated biological filter. Bioresource Technology. 254, 67–74.

Zekker, I., Kiviru, A., Mandel, A., Jaagura, M., Tenno, T., 2019. Enhanced Efficiency of Nitritating-Anammox Sequencing Batch Reactor Achieved at Low Decrease Rates of Oxidation–Reduction Potential. Environmental Engineering Science. 36(3), 1–11.

Zhang, L., Narita, Y., Gao, L., Ali, M., Oshiki, M., Okabe, S., 2017. Maximum specific growth rate of anammox bacteria revisited. Water Research. 116, 296–303.

Zhang, M., Wang, S., Ji, B., Liu, Y., 2019. Towards mainstream deammonification of municipal wastewater : Partial nitrification-anammox versus partial denitrification-anammox. Science of the Total Environment. 692, 393–401.

Zhang, Z., Zhang, Y., Chen, Y., 2020a. Recent advances in partial denitrification in biological nitrogen removal : From enrichment to application. Bioresource Technology. 298, 122444.

Zhang, X., Liu, Y., Zhang, J., Chen, Y., Wang, Q., 2020b. Impact of COD/N on anammox granular sludge with different biological carriers. Science of the Total Environment. 728, 138557.

5. Sensitivity analysis on important kinetic constants in Anammox bacteria enrichment process using a mathematical model

Anaerobic ammonia oxidation (Anammox) is a promising alternative for conventional activated sludge for nitrogen removal without additional organic carbon supply and high aeration demands. However, the growth of Anammox bacteria is relatively slow and Anammox bacteria are sensitive to various operational conditions (e.g., temperature and oxygen concentration). Moreover, the competition between Anammox and nitrite oxidizing bacteria is a key challenge on successful Anammox enrichment process. Granulation is an innovative solution to limit this microbial competition and reduce the oxygen mass transfer for better Anammox bacteria growth. Therefore, a one-dimensional mathematical model was developed and calibrated using previous Anammox studies to estimate the important model parameters and assess the effect of operational conditions (e.g., liquid film thickness and granule diameter) on the granulation process of Anammox bacteria.

This paper is prepared for future journal publication.

- Elsayed, A., Kim, Y. Sensitivity analysis on important kinetic constants in Anammox bacteria enrichment process using a mathematical model.

The co-author’s contributions include:

- Funding acquisition.
- Supervision and technical support.
- Manuscript review and revision.

Abstract

Granulation is an efficient approach for anaerobic ammonia oxidation (Anammox) bacteria enrichment to limit the growth of ammonia oxidizing bacteria (X_{AOB}) and nitrite oxidizing bacteria (X_{NOB}). However, the sensitivity of Anammox population to the kinetic constants of the involved microorganisms (i.e., X_{AOB}, X_{NOB} and X_{ANA}) represents a critical challenge for better understanding of Anammox bacteria enrichment in granules. In this study, a one-dimensional steady-steady state mathematical model based on spherical coordinates was developed and calibrated using previous Anammox studies to estimate the kinetic constants of Anammox bacteria, liquid film thickness and diffusion coefficient of soluble components in the granules. Based on the model simulation results, it was found that the Anammox population is insensitive to the kinetic constants of X_{AOB} and X_{NOB} at extremely low dissolved oxygen (DO) concentration (e.g., 0.01 mg-O_2/L) while they are important on Anammox bacteria enrichment at moderate DO (e.g., 0.10 mg-O_2/L) because they can control the competition between X_{AOB} and X_{ANA} for ammonia, and X_{ANA} and X_{NOB} for nitrite. At moderate DO concentration, the maximum specific growth rate constant (μ_{ANA}) and oxygen half saturation constant ($K_{O_2}^{ANA}$) of X_{ANA} governed the Anammox bacteria enrichment while the decay rate constant (b_{ANA}) had a negligible effect for the enrichment. For the kinetic constants of X_{AOB}, low maximum specific growth rate (μ_{AOB}) and high oxygen half saturation constant ($K_{O_2}^{AOB}$) of X_{AOB} increased the Anammox population because they limited the competition between X_{AOB} and X_{ANA} for ammonia. Moreover, it was found that the maximum specific growth rate constant (μ_{NOB}) and oxygen half saturation

constant ($K_{O_2}^{NOB}$) of X_{NOB} showed dominant effects on the Anammox population in the granules, highlighting the importance of X_{NOB} suppression during Anammox granulation. Regarding the mass transport parameters, large granules (i.e., granule diameter > 1000 µm) were preferred because thick anaerobic layer in the granule allowed better growth of Anammox bacteria. The main findings of this study can be used for implementing the granulation processes on large-scale Anammox enrichment applications.

Keywords

Anaerobic ammonia oxidation; Anammox bacteria enrichment; granulation; mathematical model calibration; competition; Dissolved oxygen concentration.

5.1 Introduction

Anaerobic ammonia oxidation (Anammox) is an innovative technology for nitrogen removal by converting ammonia and nitrite into nitrogen gas without expensive aeration systems (Hauck et al., 2016; Yue et al., 2018; You et al., 2020). Anammox process is considered as a promising alternative for conventional nitrification and denitrification in the municipal wastewater treatment (Du et al., 2015; Eskicioglu et al., 2018; Cui et al., 2020) as Anammox process requires less aeration cost, less footprint for wastewater treatment facilities and no organic carbon for complete nitrogen removal (Ali and Okabe et al., 2015; Chen et al., 2016; Tang et al., 2017). Also, the Anammox technology has a less sludge production rate coupled with minimal disposal cost and less greenhouse gases emissions (e.g., nitric oxide) compared to the conventional activated sludge (Gilbert et al., 2015; Rodriguez-Sanchez et al., 2016; Conthe et al., 2019). However, the growth of

Anammox bacteria is relatively slow where the doubling time can be as long as 10 to 20 days depending on the temperature and substrate conditions (Isanta et al., 2015; Lotti et al., 2015; Marie et al., 2015), resulting in long operational time for successful Anammox bacteria enrichment. Also, the competition between Anammox bacteria (X_{ANA}) and ammonia oxidizing bacteria (X_{AOB}) for ammonia, and nitrite oxidizing bacteria (X_{NOB}) for nitrite is a key challenge on the enrichment of Anammox bacteria. Therefore, the main scope of this study is oriented towards the determination of dominant parameters on efficient Anammox enrichment processes.

Many previous Anammox process studies investigated the enrichment of Anammox bacteria using granules (Vlaeminck et al., 2010; Wang et al., 2020; Li et al., 2021), biofilms (Gilmore et al., 2013; Lotti et al., 2014; Zhang et al., 2014), attached growth systems (Wang et al., 2009; Hu et al., 2010; Zhang et al., 2017) and batch systems (Connan et al., 2016). Granulation is considered as one of the most innovative solutions to limit the activity of X_{AOB} and X_{NOB} coupled with providing a sufficient retention time for the growth of Anammox bacteria (Laureni et al., 2015; Lin and Wang, 2017; Xu et al., 2019). Granulation processes also allow shorter start-up and easier control compared to other enrichment techniques (Gonzalez-Gil et al., 2015; Song et al., 2017; Adams et al., 2020). In the Anammox granular enrichment, ammonia oxidizing bacteria grow at the outer layer of the granules where dissolved oxygen is provided from the bulk solution. On the other hand, Anammox bacteria grow at the inner layer of the granules where the oxygen mass transfer is limited near the core of granules.

Operational conditions play a dominant role in Anammox bacteria enrichment using granules. In previous experimental Anammox studies, it was observed that

dissolved oxygen concentration is an important parameter on the enrichment of Anammox bacteria as low oxygen concentration is required for better growth of Anammox bacteria (Perez et al., 2014; Lin et al., 2014; Zekker et al., 2018). It was also found in previous Anammox studies that the granule diameter can control the Anammox bacteria enrichment (Liu et al., 2017; Luo et al., 2017; Chen et al., 2019). C/N ratio (carbon-to-nitrogen) and influent COD concentration are also two dominant parameters on the Anammox bacteria enrichment process as they affect the competition between Anammox bacteria and heterotrophic bacteria for nitrite (Ni et al., 2012; Li et al., 2017; Zhang et al., 2020). The competition between Anammox bacteria and other involved microorganisms (i.e., nitrifiers and heterotrophs) can also control the performance of Anammox bacteria enrichment (Pellicer-Nacher et al., 2014; Cao et al., 2017; Wang et al., 2017). However, there are no systematic investigations on the effect of mixing conditions (i.e., liquid film thickness) on the enrichment of Anammox bacteria.

Mathematical modeling is an important tool to describe the competition between X_{AOB} and X_{ANA} for ammonia, X_{AOB} and X_{NOB} for DO and X_{ANA} and X_{NOB} for nitrite under various operational conditions during the Anammox enrichment processes (Volcke et al., 2012; Vannecke et al., 2015). Also, mathematical models can be implemented for determining the governing microorganisms and kinetic constants on the Anammox enrichment processes. Mathematical modeling, including various microorganisms (i.e., nitrifiers, heterotrophs and Anammox bacteria), is essential to detect the complicated correlations between the process parameters (e.g., microbes and operational conditions) during the enrichment process (Corbala-Robles et al., 2016; Baeten et al., 2019). Mathematical models can be addressed to describe the failure of Anammox enrichment

due to the domination of nitrite oxidizing bacteria with a comprehensive analysis of the failure mechanisms, including rapid growth rate of X_{NOB} compared to X_{ANA} and substrate mass transport to the granule (e.g., granule diameter and liquid film thickness). However, there are no reported mathematical modeling studies to determine the role of kinetic constants of the involved microorganisms on the difficulty of Anammox enrichment processes.

In this study, the main objectives are to: (1) develop a mathematical model to simulate the enrichment of Anammox bacteria using granules; (2) calibrate the mathematical model using previous Anammox studies to determine the important model parameters; (3) apply a sensitivity analysis on the microbial kinetic constants to assess their effect on the competition between the microorganisms and the Anammox population; and (4) evaluate the effect of operational conditions (e.g., dissolved oxygen concentration and granule diameter) on the enrichment of Anammox bacteria.

5.2 Numerical model development and calibration

5.2.1 Biological reaction kinetics and mass transport

A one-dimensional steady state model was developed to simulate the mass transport in a spherical Anammox granule and the biological reactions driven by Anammox, ammonia oxidizing, nitrite oxidizing and heterotrophic bacteria. The model was used to simulate the Anammox bacteria enrichment based on IWA-ASM3 (International Water Association Activated Sludge Model No.3) (Henze et al., 2000) and the biological reactions of Anammox bacteria from previous model studies (Lackner et al., 2008; Ni et al., 2013). For the biological reactions of nitrogenous compounds in the granule,

ammonia (S_{NH_4}) was oxidized by Anammox bacteria (X_{ANA}) and ammonia oxidizing bacteria (X_{AOB}), nitrite (S_{NO_2}) was oxidized into nitrate (S_{NO_3}) by X_{ANA} and nitrite oxidizing bacteria (X_{NOB}) and denitrification was performed by heterotrophic bacteria (X_H) (Table C1). Soluble COD (S_{COD}) was utilized by X_H and particulate COD (X_S) was hydrolyzed into S_{COD} for the carbonaceous compounds (Table C1). Microbial decay reactions were also assumed for the particulate components (X_{ANA} ,X_{AOB} , X_{NOB} and X_H) (Table C1).

In the steady state model, the biological reaction kinetics and diffusive mass transport in the granules were included (Table 5.1), assuming non-homogenous granules in the reactor. In a single granule, the soluble components ($S_{NH_4}, S_{NO_2}, S_{NO_3}$, S_{O_2} and S_{COD}) were mobile by diffusion from the bulk solution to the granule through the liquid film where biological reactions were assumed to be negligible; however, the particulate components were assumed to be immobile. At the center of granule (r= 0), it was assumed that there was no flux for each of the soluble components (Eq. 5.1).

$$\left.\frac{dS_i}{dr}\right|_{r=0} = 0 \qquad (Eq\ 5.1)$$

where S_i is an individual soluble component and r is the distance from the granule center.

5.2.2 Numerical solution methods

In the steady state model, the ten mass balance equations for individual soluble and particulate components were discretized using the finite difference method (Table C1) (Chapra and Canale, 1998). In the finite difference method, the granule was evenly

divided into twenty grids regardless of the granule size (diameter). The 200 discretized mass-balance equations (20 grids × 10 components) were solved simultaneously by the fixed-point iteration approach (Chapra and Canale, 1998) with a relative tolerance of 0.0001.

5.2.3 Model calibration using literature simulation results

The steady state granule model for Anammox bacteria enrichment was calibrated using simulation results from previous Anammox process model studies (Corbalá-Robles et al., 2016; Liu et al., 2017; Hao et al., 2002) to estimate the kinetic constants of Anammox bacteria, the diffusion coefficient of soluble components in the granule and liquid film thickness (Table 5.2). In the model calibration, the simulation conditions (e.g., soluble components concentration) were assumed based on the mentioned simulation conditions in each study (Table 5.2). The simulation results in the literature papers were digitized and extracted to prepare the concentration profiles of soluble and particulate components within an Anammox granule.

5.2.4 Relative sensitivity analysis

Relative sensitivity analysis (RSA) was performed on the kinetic constants of X_{AOB}, X_{NOB} and X_{ANA} to evaluate their effect on the Anammox population (X_{ANA}) and determine the important kinetics on the Anammox bacteria enrichment. In the sensitivity analysis, a 10% change in a given kinetic constant was applied and the effect of this change on the Anammox population was evaluated for each discretized grid (20 grids). The average relative sensitivity function (f_{RS}) for a given kinetic constant was described

by the rate of change in the Anammox population ($\partial X_{ANA}(r)$) with space (r) normalized by the rate of change in the kinetic constant (∂k) and the median value of the kinetic constant (k) normalized by the Anammox population (X_{ANA}) corresponding to k (Eq. 5.2) for each grid (Salatul Islam Mozumder et al., 2014). The finite difference method was used to discretize the rate of change in the Anammox population with respect to the rate of change in the kinetic constant (Eq. 5.3) (Chapra and Canale, 1998).

$$f_{RS} = \frac{\sum_{r=0}^{r=n} \frac{\partial X_{ANA}(r)}{\partial k} \cdot \frac{k}{X_{ANA}}}{n} \qquad (Eq\ 5.2)$$

$$\frac{\partial X_{ANA}(r)}{\partial k} = \frac{X_{ANA}(r, k + \Delta k) - X_{ANA}(r, k - \Delta k)}{2\Delta k} \qquad (Eq\ 5.3)$$

where n is the number of discretized grids in r direction (n = 20 grids) and Δ is the change in the median of a kinetic constant (Δ = 10%).

Table 5.1 Model parameters and calibration targets at T = 20°C and pH = 7.0.

Model Parameter	Symbol	Study A	Study B	Study C	Baseline of this study	Reference
Heterotrophic Bacteria (X_H)						
Maximum specific growth rate (1/d)	μ_H	6.0	6.0	6.0	6.0	Henze et al., 2000
Maximum endogenous respiration rate (1/d)	b_H	0.4	0.4	0.4	0.4	Henze et al., 2000
Anoxic reduction factor for μ_H (-)	η_d	0.8	0.8	0.8	0.8	Henze et al., 2000
Oxygen saturation constant (mg-O_2/L)	$K_{O_2}^H$	0.2	0.2	0.2	0.2	Henze et al., 2000
Substrate saturation constant (mg-COD/L)	K_{COD}^H	20	20	20	20	Henze et al., 2000
Ammonium saturation constant (mg-N/L)	$K_{NH_4}^H$	0.05	0.05	0.05	0.05	Henze et al., 2000
Nitrite saturation constant (mg-N/L)	$K_{NO_2}^H$	0.5	0.5	0.5	0.5	Henze et al., 2000
Nitrate saturation constant (mg-N/L)	$K_{NO_3}^H$	0.5	0.5	0.5	0.5	Henze et al., 2000
Ammonia Oxidizing Bacteria (X_{AOB})						
Maximum specific growth rate (1/d)	μ_{AOB}	2.05	2.05	2.05	2.05	Wiesmann et al., 1994
Maximum endogenous respiration rate (1/d)	b_{AOB}	0.13	0.13	0.13	0.13	Wiesmann et al., 1994
Oxygen saturation constant (mg-O_2/L)	$K_{O_2}^{AOB}$	0.6	0.6	0.6	0.6	Wiesmann et al., 1994
Ammonium saturation constant (mg-N/L)	$K_{NH_4}^{AOB}$	2.4	2.4	2.4	2.4	Wiesmann et al., 1994
Nitrite Oxidizing Bacteria (X_{NOB})						
Maximum specific growth rate (1/d)	μ_{NOB}	1.45	1.45	1.45	1.45	Wiesmann et al., 1994
Maximum endogenous respiration rate (1/d)	b_{NOB}	0.06	0.06	0.06	0.06	Wiesmann et al., 1994
Oxygen saturation constant (mg-O_2/L)	$K_{O_2}^{NOB}$	1.0	1.0	1.0	1.0	Moussa et al., 2005
Ammonium saturation constant (mg-N/L)	$K_{NH_4}^{NOB}$	0.20	0.20	0.20	0.20	Ma et al., 2017
Nitrite saturation constant (mg-N/L)	$K_{NO_2}^{NOB}$	0.50	0.50	0.50	0.50	Volcke et al., 2010
Anammox Bacteria (X_{ANA})						
Maximum specific growth rate (1/d)	μ_{ANA}	0.10	0.033	0.08	0.10	This study.
Maximum endogenous respiration rate (1/d)	b_{ANA}	0.003	0.003	0.003	0.003	This study.
Oxygen saturation constant (mg-O_2/L)	$K_{O_2}^{ANA}$	0.10	0.10	0.10	0.10	This study.
Ammonium saturation constant (mg-N/L)	$K_{NH_4}^{ANA}$	0.07	0.07	0.07	0.07	This study.
Nitrite saturation constant (mg-N/L)	$K_{NO_2}^{ANA}$	0.05	0.05	0.05	0.05	This study.
Hydrolysis						
Hydrolysis rate constant (1/d)	q_H	3	3	3	3	Henze et al., 2000
Saturation constant for particulate COD (g-X_S/ g-X_H)	K_X	0.1	0.1	0.1	0.1	Henze et al., 2000
Anoxic reduction for q_H (-)	η_H	0.6	0.6	0.6	0.6	Henze et al., 2000
Stoichiometric Parameters						
Yield of X_H on substrate (g-COD/g-COD)	Y_H	0.63	0.63	0.63	0.63	Henze et al., (2000)
Yield of X_{AOB} on ammonium (g-COD/g-N)	Y_{AOB}	0.15	0.15	0.15	0.15	Wiesmann et al., 1994
Yield of X_{NOB} on nitrite (g-COD/g-N)	Y_{NOB}	0.041	0.041	0.041	0.041	Wiesmann et al., 1994
Yield of X_{ANA} on nitrite (g-COD/g-N)	Y_{ANA}	0.159	0.159	0.159	0.159	Lackner et al., 2008
Nitrogen content in biomass (g-N/g-COD)	i_{NBM}	0.07	0.07	0.07	0.07	Henze et al., 2000
Inert content in lysis biomass (g-COD/g-COD)	f_l	0.1	0.1	0.1	0.1	Henze et al., 2000

Table 5.2. Summary of simulation conditions and calibration targets of the calibrated model and previous Anammox studies.

Figure	Fig. 5.1	Fig. C1	Fig. C2	Table 5.3
Reference	Corbalá-Robles et al., 2016	Liu et al., 2017	Hao et al., 2002	Baseline of this study
S_{NH_4} in the bulk solution (mg-N/L)	1850 ± 100	50	80	500
S_{NO_2} in the bulk solution (mg-N/L)	N/A	N/A	0	10
S_{NO_3} in the bulk solution (mg-N/L)	N/A	N/A	0	10
S_{COD} in the bulk solution (mg-COD/L)	600 ± 30	20	0	0
S_{O_2} in the bulk solution (mg-O_2/L)	0.25	0.3	0.6	0.10
Granule diameter/biofilm thickness (µm)	1100	600	700	1000
Liquid film thickness (µm)	100	100	100	200
Diffusivity of S_{COD} in biofilm × 10^{-4} (m^2/day)	0.15	0.35	0.10	0.15
Diffusivity of S_{O2} in biofilm × 10^{-4} (m^2/day)	0.60	1.45	0.30	0.60
Diffusivity of S_{NH4} in biofilm × 10^{-4} (m^2/day)	0.65	1.35	0.10	0.55
Diffusivity of S_{NO2} in biofilm × 10^{-4} (m^2/day)	0.60	1.30	0.05	0.50
Diffusivity of S_{NO3} in biofilm × 10^{-4} (m^2/day)	0.40	1.20	0.03	0.50
Reaction media	granule	granule	biofilm	granule

5.3 Results and discussion

5.3.1 Model calibration with literature simulation results

The kinetic constants of Anammox bacteria, liquid film thickness (i.e., mixing conditions) and diffusion coefficient of soluble components were determined by calibrating the mathematical model using the simulation results of previous Anammox studies (Hao et al., 2002; Corbalá-Robles et al., 2016; Liu et al., 2017) (Fig. 5.1, C1, C2 and Table 5.2). The simulation results were compared with the simulation results of previous Anammox studies to capture the same trend and values of the concentration profiles of soluble (e.g., ammonia and DO) and particulate (e.g., X_{ANA} and X_{AOB}) components. The range of the maximum specific growth rate constant of X_{ANA} (μ_{ANA}) was 0.033 to 0.10 d^{-1} while the Anammox bacteria decay rate constant (b_{ANA}) was 0.003 d^{-1}, oxygen half saturation constant of X_{ANA} ($K_{O_2}^{ANA}$) was 0.10 mg-O_2/L, ammonia half saturation constant ($K_{NH_4}^{ANA}$) was 0.07 mg-N/L and nitrite half saturation constant ($K_{NO_2}^{ANA}$) was 0.05 mg-N/L. The determined kinetic constant ranges of X_{ANA} are consistent with those mentioned or estimated in previous Anammox studies (Strous et al., 1998; Koch et al., 2000; Hao et al., 2002; Lackner et al., 2008; Volcke et al., 2010; Ni et al., 2013; Mozumender et al., 2014; Ni et al., 2014; Bi et al., 2015; Corbalá-Robles et al., 2016; Zhang et al., 2017; Liu et al., 2020). The calibrated liquid film thickness (approximately 100 µm) was also consistent with the assumed values in previous mathematical model studies (Bishop et al., 1997; Wäsche et al., 2002; Matsumoto et al., 2007; Martin et al., 2017; Li et al., 2018a). Based on the mathematical model calibration, the diffusion coefficient of soluble components were estimated to be 0.10 – 0.35 × 10^{-4} m^2/day for S_{COD}, 0.30 – 1.45 × 10^{-4}

m^2/day for S_{O_2}, 0.10 – 1.35 × 10^{-4} m^2/day for S_{NH_4}, 0.05 – 1.30 × 10^{-4} m^2/day for S_{NO_2} and 0.03 – 1.20 × 10^{-4} m^2/day for S_{NO_3}. The determined diffusion coefficients are comparable with those used or mentioned in previous biofilm model studies (Stewart 1998; Stewart 2003; Elsayed et al., 2021).

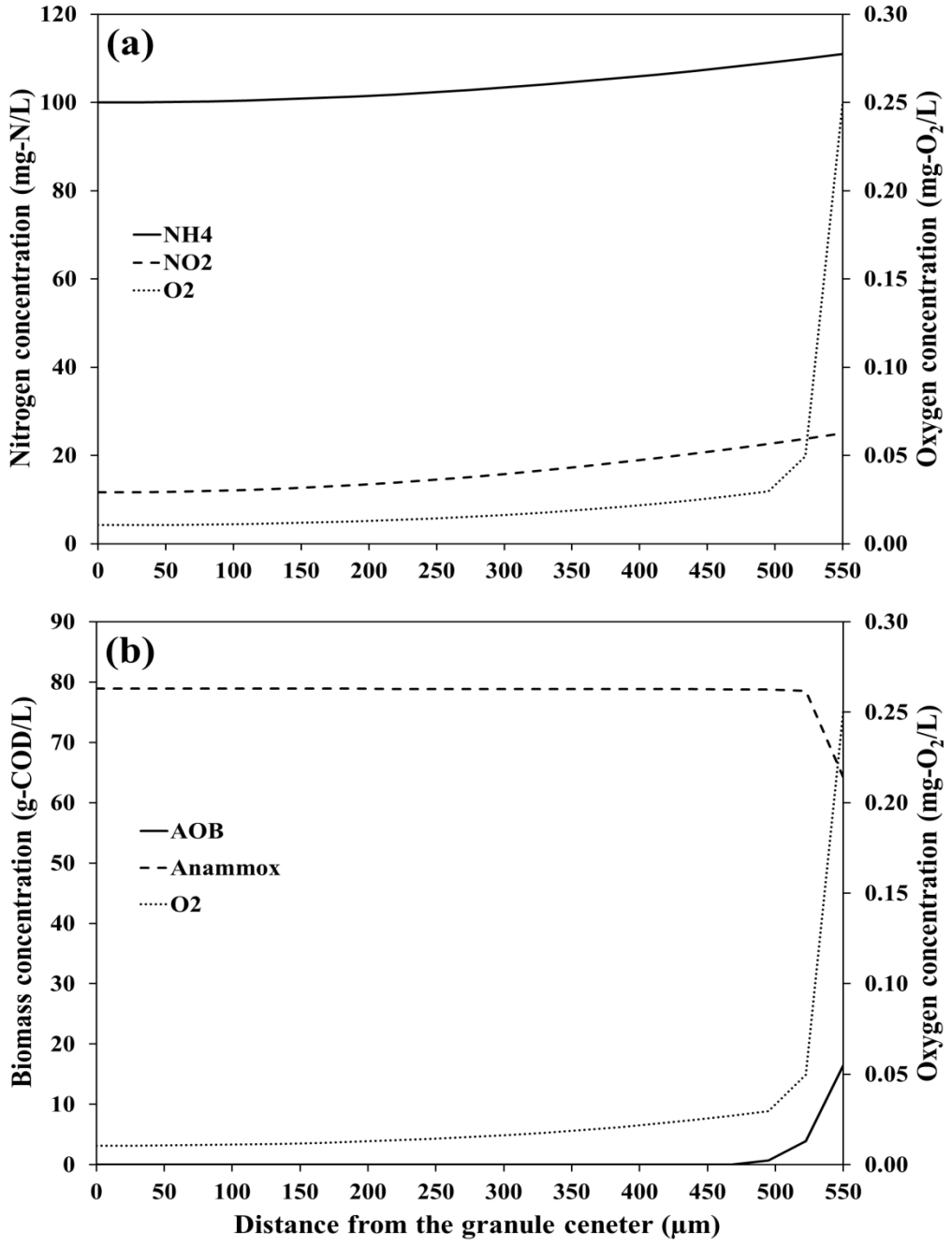

Fig. 5.1. Simulation results of the model calibration using study A (Corbalá-Robles et al., 2016): (a) soluble components concentration profiles (i.e., ammonia, nitrite and oxygen) and, (b) particulate components concentration profiles (i.e., X_{AOB} ,X_{ANA}) and oxygen concentration profile. (Simulation conditions are summarized in Table 5.1 and 5.2).

5.3.2 Growth kinetics on Anammox bacteria (X_{ANA}) enrichment

Based on the results of the kinetic constants of X_{ANA} sensitivity analysis, it was found that μ_{ANA} is important in Anammox bacteria enrichment while the Anammox population was not significantly affected by the decay rate constant (b_{ANA}) (Table 5.3). This model simulation result is consistent with the results of other Anammox studies (Perez et al., 2014; Zhang et al., 2017), reflecting the importance of μ_{ANA} on the Anammox bacteria enrichment. The Anammox population was positively correlated with μ_{ANA} because high μ_{ANA} enhanced the ammonia and nitrite utilization by X_{ANA}, resulting in better Anammox bacteria enrichment. It was also noticed that the Anammox population was positively correlated with the oxygen half saturation constant of X_{ANA} ($K_{O_2}^{ANA}$) because high $K_{O_2}^{ANA}$ resulted in less inhibition to Anammox bacteria by oxygen concentration. However, the Anammox population and b_{ANA} were in a negative correlation as high b_{ANA} caused high lysis rate of Anammox bacterial cells, resulting in insufficient Anammox bacteria enrichment.

At low oxygen concentration (DO = 0.01 mg-O_2/L), the effect of $K_{O_2}^{ANA}$ on the Anammox population was negligible compared to higher oxygen concentration (DO = 0.1 and 1.0 mg-O_2/L) because limited oxygen concentration had no inhibition to X_{ANA}, preventing oxygen toxicity to Anammox bacteria enrichment. The kinetic constants of Anammox bacteria did not affect the Anammox population under various ammonia concentrations because ammonia was not the rate limiting parameter on Anammox

bacteria growth at moderate oxygen concentration (i.e., DO = 0.1 mg-O_2/L). It was also found that the Anammox population was insensitive to the liquid film thickness because nitrite, the rate-limiting substrate on X_{ANA}, was created in the granule without diffusion from the bulk solution, resulting in negligible effect of the resistive liquid film on the Anammox bacteria enrichment at moderate oxygen concentration. Also, the Anammox population was increased with the increasing μ_{ANA} for large granule size (i.e., granule diameter = 2000 µm) because large granules allowed thick anaerobic layer in the granule, causing better Anammox bacteria growth compared to smaller sizes (i.e., granule diameter = 100 and 1000 µm).

5.3.3 Competition between X_{ANA} and X_{AOB}

For the kinetic constants of X_{AOB}, the maximum specific growth rate constant of X_{AOB} (μ_{AOB}) was dominant on the Anammox bacteria enrichment with a negative correlation because it represented the competition between X_{AOB} and X_{ANA} on ammonia (Table 5.3). Also, μ_{AOB} controlled the interdependence relation between X_{AOB} and X_{ANA} where X_{ANA} utilized the produced nitrite from aerobic ammonia oxidation by X_{AOB}. However, μ_{AOB} had no effect on the Anammox population at low oxygen concentration (DO = 0.01 mg-O_2/L) because limited oxygen prevented the aerobic oxidation of ammonia by X_{AOB}. The oxygen half saturation constant ($K_{O_2}^{AOB}$) and the decay rate constant (b_{AOB}) of X_{AOB} were positively correlated with the Anammox population as high $K_{O_2}^{AOB}$ and lysis rate decreased the activity of X_{AOB}, decreasing the competition between X_{AOB} and X_{ANA}.

For the three kinetic constants of X_{AOB}, it was observed that high oxygen concentration (DO = 1.0 mg-O_2/L) resulted in less effect on the Anammox bacteria

enrichment compared to lower oxygen concentrations (DO = 0.01 and 0.10 mg-O_2/L) because high oxygen inhibited the Anammox bacteria growth, showing the toxic influence of high oxygen on the Anammox population. This finding is consistent with the previous Anammox studies (Udert et al., 2008; Liu et al., 2017; Hoekstra et al., 2018), highlighting the negative effect of high oxygen concentration on X_{ANA}. It was also found that the Anammox bacteria enrichment was sensitive to thin liquid film (i.e., L_f = 100 μm) at low oxygen concentration because thin liquid film allowed rapid diffusion of ammonia from the bulk solution, resulting in high nitrite creation rate by X_{AOB}coupled with high X_{ANA} growth rate. The X_{AOB} kinetics had a minor effect on the Anammox population for small granule size (i.e., granule diameter = 100 μm) because the anaerobic layer in the granule was narrow to allow sufficient Anammox bacteria enrichment.

5.3.4 Competition between X_{ANA} and X_{NOB}

Based on the results of the sensitivity analysis on the kinetics of X_{NOB}, it was found that the maximum specific growth rate constant of X_{NOB} (μ_{NOB}) was negatively correlated with the Anammox population while the oxygen half saturation constant ($K_{O_2}^{NOB}$) and decay rate constant (b_{NOB}) of X_{NOB} were positively correlated with the Anammox bacteria enrichment (Table 5.3). Therefore, maintaining low activity of X_{NOB} by low μ_{NOB} or high $K_{O_2}^{NOB}$ and b_{NOB} resulted in high Anammox population, confirming that X_{NOB} should be suppressed for better Anammox bacteria enrichment process. This result is consistent with the results of previous Anammox studies (Mozumder et al., 2014; Cao et al., 2017; Li et al., 2018b) where it was demonstrated that controlling the competition between X_{NOB} and X_{ANA} was dominant for the Anammox bacteria enrichment process.

At high oxygen concentration (DO = 1.0 mg-O_2/L), the Anammox population was insensitive to the kinetics of X_{NOB} because oxygen toxicity prevented the competition between X_{NOB} and X_{ANA}on nitrite, resulting in low activity of X_{ANA}. Although nitrite was created in the granule by X_{AOB}, the Anammox population was enhanced by thick liquid film (i.e., L_f = 300 µm) because the oxygen mass transfer was limited through the diffusive liquid film, resulting in low X_{NOB} growth rate. It was also found that there was a minor effect of X_{NOB} kinetic constants on the Anammox population at small granule size (granule diameter = 100 µm) because the granule was totally penetrated by oxygen, resulting in narrow anaerobic layer in the granule for the Anammox bacteria enrichment. This finding is consistent with the previous biofilm studies (Wang et al., 2016; Kinh et al., 2017; Elsayed et al., 2021) where the range of the oxygen penetration depth was 50 - 600 µm based on the oxygen concentration and diffusivity.

Table 5.3. Effect of X_{ANA} ,X_{AOB} and X_{NOB} kinetic constants on Anammox population (X_{ANA}) during the enrichment process (Baseline conditions are summarized in Table 5.1 and 5.2).

Kinetic constant	DO (mg-O_2/L)			NH_4 (mg-N/L)			Liquid film thickness (µm)			Granule diameter (µm)		
	0.01	0.10	1.0	100	500	1000	100	200	300	100	1000	2000
μ_{ANA}	0.99	1.03	1.00	1.02	1.03	1.02	1.01	1.03	1.02	1.05	1.03	1.79
K_{O2}^{ANA}	0.10	0.31	0.27	0.30	0.31	0.30	0.29	0.31	0.29	0.30	0.31	0.29
b_{ANA}	-0.03	-0.04	-0.04	-0.04	-0.04	-0.04	-0.04	-0.04	-0.04	-0.04	-0.04	-0.02
μ_{AOB}	0	-2.15	-0.82	-3.29	-2.15	-1.41	-2.48	-2.15	-1.98	-1.42	-2.15	-2.92
K_{O2}^{AOB}	0	0.37	0.32	0.77	0.37	0.13	0.56	0.37	0.31	0.26	0.37	0.46
b_{AOB}	0	3.02	0.98	2.99	3.02	2.99	3.68	3.02	1.92	0.47	3.02	3.18
μ_{NOB}	0	-3.03	-0.13	-3.09	-3.03	-2.29	-3.34	-3.03	-2.33	-0.59	-3.03	-3.13
K_{O2}^{NOB}	0	1.75	0.11	1.98	1.75	1.63	2.44	1.75	0.62	0.58	1.75	1.95
b_{NOB}	0	1.10	0.61	1.53	1.10	1.18	2.99	1.10	0.87	0.53	1.10	1.28

5.4 Conclusions

A steady-state mathematical model was developed and calibrated using simulation results from previous Anammox studies to determine the kinetics of Anammox bacteria, liquid film thickness and diffusion coefficient of soluble components in the granule for Anammox bacteria enrichment process. Based on the simulation results of the calibrated model, it was found that the maximum specific growth rate constant of X_{ANA} (μ_{ANA}) was dominant on the Anammox population as high μ_{ANA} enhanced the ammonia and nitrite utilization by X_{ANA}, resulting in better Anammox bacteria enrichment. On the other hand, the decay rate constant (b_{ANA}) of X_{ANA} did not significantly affect the Anammox bacteria enrichment process. It was also noticed that Anammox population was enhanced with high oxygen half saturation constant of X_{ANA} ($K_{O_2}^{ANA}$) because high $K_{O_2}^{ANA}$ decreased the inhibition of Anammox bacteria to oxygen concentration.

For the kinetic constants of X_{AOB}, the maximum specific growth rate constant of X_{AOB} (μ_{AOB}) was important on the Anammox bacteria enrichment because it controlled the competition between X_{AOB} and X_{ANA} on ammonia utilization. Based on the sensitivity analysis results, it was found that high oxygen half saturation constant ($K_{O_2}^{AOB}$) and decay rate constant (b_{AOB}) of X_{AOB} enhanced the Anammox bacteria enrichment as high $K_{O_2}^{AOB}$ and b_{AOB} decreased the activity of X_{AOB}, providing favorable growth conditions for X_{ANA}.

Based on the simulation results of the steady-state model, the competition between nitrite oxidizing and Anammox bacteria for nitrite was critical in Anammox bacteria enrichment. It was also noticed that the maximum specific growth rate constant of X_{NOB} (μ_{NOB}) was negatively correlated with the Anammox population, reflecting the importance of X_{NOB} suppression for

efficient Anammox bacteria enrichment. However, the oxygen half saturation constant ($K_{O_2}^{NOB}$) and decay rate constant (b_{NOB}) of X_{NOB} were positively correlated with Anammox enrichment where high $K_{O_2}^{NOB}$ and b_{NOB} enhanced the growth rate of Anammox bacteria.

Based on the model simulation results, it was emphasized that extremely low dissolved oxygen (DO ≅ 0.01 mg-O_2/L) resulted in insensitivity of Anammox bacteria enrichment process to the kinetic constants of X_{AOB} and X_{NOB} because both of them cannot grow under limited DO concentration. Also, Anammox bacteria enrichment was insensitive to the kinetic constants of X_{AOB} and X_{NOB} at high dissolved oxygen (DO ≅ 1.0 mg-O_2/L) because high DO concentration inhibited the growth of Anammox bacteria, providing favorable conditions for the growth of X_{AOB} and X_{NOB}. On the other hand, enrichment of Anammox bacteria was sensitive to the kinetic constants of X_{AOB} and X_{NOB} at moderate DO (DO ≅ 0.10 mg-O_2/L) due to the competition between X_{AOB} and X_{ANA} for ammonia, X_{AOB} and X_{NOB} for DO and X_{ANA} and X_{NOB} for nitrite. It was also found that ammonia concentration has a negligible effect on the Anammox bacteria enrichment; however, nitrite concentration is the rate-limiting parameter on the Anammox population. Based on the sensitivity analysis results, liquid film thickness was dominant on the Anammox bacteria enrichment as the oxygen mass transfer to the granule was controlled by the resistive liquid film, affecting the Anammox bacteria growth under oxygen inhibition conditions. It was also found that large granules (granule diameter = 2000 μm) are recommended for better Anammox bacteria enrichment because large granules contained sufficient anaerobic layer for Anammox bacteria growth.

References

Adams, M., Xie, J., Kabore, J., Xie, J., Guo, M., Chen, C., 2020. Technology Research advances in anammox granular sludge : A review. Critical Reviews in Environmental Science and Technology. 1–44.

Ali, M., Okabe, S., 2015. Anammox-based technologies for nitrogen removal : Advances in process start-up and remaining issues. Chemosphere. 141, 144–153.

Baeten, J.E., Batstone, D.J., Schraa, O.J., van Loosdrecht, M.C.M., Volcke, E.I.P., 2019. Modelling anaerobic, aerobic and partial nitritation-anammox granular sludge reactors - A review. Water Research. 149, 322–341.

Bi, Z., Takekawa, M., Park, G., Soda, S., Zhou, J., Qiao, S., Ike, M., 2015. Effects of the C/N ratio and bacterial populations on nitrogen removal in the simultaneous anammox and heterotrophic denitrification process : Mathematic modeling and batch experiments. Chemical Engineering Journal. 280, 606–613.

Bishop, P.L., Gibbs, J.T., Cunningham, B.E., 1997. Relationship between concentration and hydrodynamic boundary layers over biofilms. Environmental Technology. 18, 375- 385.

Cao, Y., van Loosdrecht, M.C.M., Daigger, G.T., 2017. Mainstream partial nitritation – anammox in municipal wastewater treatment : status, bottlenecks, and further studies. Applied Microbiology and Biotechnology. 101, 1365–1383.

Chapra, S.C., Canale, P.R., 1998. Numerical Methods for Engineers with Software and Programming Applications, third Ed. McGrawHill, America.

Chen, C., Sun, F., Zhang, H., Wang, J., Shen, Y., Liang, X., 2016. Evaluation of COD effect on anammox process and microbial communities in the anaerobic baffled reactor (ABR). Bioresource Technology. 216, 571–578.

Chen, R., Ji, J., Chen, Y., Takemura, Y., Liu, Y., Kubota, K., Ma, H., Li, Y., 2019. Successful operation performance and syntrophic micro-granule in partial nitritation and anammox reactor treating low-strength ammonia wastewater. Water Research. 155, 288–299.

Connan, R., Dabert, P., Khalil, H., Bridoux, G., Béline, F., Magrí, A., 2016. Batch enrichment of anammox bacteria and study of the underlying microbial community dynamics. Chemical Engineering Journal. 297(3), 217–228.

Conthe, M., Lycus, P., Arntzen, M.Ø., Ramos, A., Frostegård, Å., Bakken, L.R., Kleerebezem, R., van Loosdrecht, M.C.M., 2019. Denitrification as an N_2O sink. Water Research. 151, 381–387.

Corbalá-Robles, L., Picioreanu, C., van Loosdrecht, M.C.M., 2016. Analysing the effects of the aeration pattern and residual ammonium concentration in a partial nitritation-anammox process. Environmental Technology. 37(6), 694–702.

Cui, B., Yang, Q., Liu, X., Wu, W., Liu, Z., Gu, P., 2020. Achieving partial denitrification-anammox in biofilter for advanced wastewater treatment. Environment International. 138, 105612.

Du, R., Peng, Y., Cao, S., Wang, S., Wu, C., 2015. Advanced nitrogen removal from wastewater by combining anammox with partial denitrification. Bioresource Technology. 179, 497–504.

Elsayed, A., Hurdle, M., Kim, Y., 2021. Comprehensive model applications for better understanding of pilot-scale membrane-aerated biofilm reactor performance. Journal of Water Process Engineering. 40, 101894.

Eskicioglu, C., Galvagno, G., Cimon, C., 2018. Approaches and processes for ammonia removal from side-streams of municipal effluent treatment plants. Bioresource Technology. 268, 797–810.

Gilbert, E.M., Agrawal, S., Schwartz, T., Horn, H., Lackner, S., 2015. Comparing different reactor configurations for Partial Nitritation/Anammox at low temperatures. Water Research, 81, 92–100.

Gilmore, K.R., Terada, A., Smets, B.F., Love, N.G., Garland, J.L., 2013. Autotrophic Nitrogen Removal in a Membrane-Aerated Biofilm Reactor Under Continuous Aeration: A Demonstration, Environmental Engineering Science. 30(1), 38–45.

Gonzalez-Gil, G., Sougrat, R., Behzad, A.R., 2015. Microbial Community Composition and Ultrastructure of Granules from a Full-Scale Anammox Reactor. Microbial Ecology. 70, 118–131.

Hao, X., Heijnen, J.J., van Loosdrecht, M.C.M., 2002. Sensitivity Analysis of a Biofilm Model Describing a One-Stage Completely Autotrophic Nitrogen Removal (CANON) Process. Biotechnology and Bioengineering. 77(3), 266–277.

Hauck, M., Maalcke-luesken, F.A., Jetten, M.S.M., Huijbregts, M.A.J., 2016. Removing nitrogen from wastewater with side stream anammox : What are the trade-offs between environmental impacts . Resources, Conservation and Recycling. 107, 212–219.

Henze, M., Gujer, W., Mino, T., van Loosdrecht, M.C.M., 2000. Activated Sludge Models ASM1, ASM2, ASM2d and ASM3. IWA Scientific and Technical Report No. 9, London, UK.

Hoekstra, M., Geilvoet, S.P., Hendrickx, T.L. G., Kip, C.S.V.E.T, Kip, Kleerebezem, R., van Loosdrecht, M.C.M., 2019. Towards mainstream anammox : lessons learned from pilot-scale research at WWTP Dokhaven. Environmental Technology. 40 (13), 1721–1733.

Hu, B., Zheng, P., Tang, C., Chen, J., van Der Biezen, E., Zhang, L., Ni, B., Jetten, M.S.M., Yan, J., Yu, H., & Kartal, B., 2010. Identification and quantification of anammox bacteria in eight nitrogen removal reactors. Water Research, 44(17), 5014–5020.

Isanta, E., Bezerra, T., Fernández, I., Suárez-Ojeda, M.E., Pérez, J., Carrera, J., 2015. Microbial community shifts on an anammox reactor after a temperature shock using 454-pyrosequencing analysis. Bioresource Technology, 181, 207–213.

Kinh, C.T., Suenaga, T., Hori, T., Riya, S., Hosomi, M., Smets, B.F., Terada, A., 2017.Counter-diffusion biofilms have lower N2O emissions than co-diffusion biofilms during simultaneous nitrification and denitrification: Insights from depth-profile analysis. Water Research. 124, 363-371.

Koch, G., Egli, K., Meer, J.R. Van Der, Siegrist, H., 2000. Mathematical modeling of autotrophic denitrification in a nitrifying biofilm of a rotating biological contactor. Water Science and Technology. 41 (4-5), 191–198.

Lackner, S., Terada, A., Smets, B.F., 2008. Heterotrophic activity compromises autotrophic nitrogen removal in membrane-aerated biofilms : Results of a modeling study. Water Research. 42(3), 1102–1112.

Laureni, M., Weissbrodt, D.G., Sziv, I., Robin, O., Lund, J., Morgenroth, E., Joss, A., 2015. Activity and growth of anammox biomass on aerobically pre-treated municipal wastewater. Water Research. 80, 325–336

Li, J., Zhang, L., Peng, Y., Zhang, Q., 2017. Effect of low COD/N ratios on stability of single-stage partial nitritation/anammox (SPN/A) process in a long-term operation. Bioresource Technology. 244, 192–197.

Li, M., Du, C., Liu, J., Quan, X., Lan, M., 2018a. Mathematical modeling on the nitrogen removal inside the membrane- aerated biofilm dominated by ammonia-oxidizing archaea (AOA): Effects of temperature, aeration pressure and COD/N ratio. Chemical Engineering Journal. 338, 680–687.

Li, J., Li, J., Gao, R., Wang, M., Yang, L., Wang, X., Zhang, L., 2018b. A critical review of one-stage anammox processes for treating industrial wastewater : Optimization strategies based on key functional microorganisms. Bioresource Technology. 265, 498–505.

Li, J., Peng, Y., Zhang, Q., Li, X., Yang, S., Li, S., 2021. Rapid enrichment of anammox bacteria linked to floc aggregates in a single-stage partial nitritation-anammox process : Providing the initial carrier and anaerobic microenvironment. Water Research. 191, 116807.

Lin, H., Tsao, H., Huang, Y., Wang, Y., Yang, K., Yang, Y., Wang, W., Wen, C., Chen, S., Cheng, S., 2014. Removal of nitrogen from secondary effluent of a petrochemical industrial park by a hybrid biofilm-carrier reactor with one-stage ANAMMOX. Water Science and Technology. 69.12, 2526–2532.

Lin, X., Wang, Y., 2017. Microstructure of anammox granules and mechanisms endowing their intensity revealed by microscopic inspection and rheometry. Water Research. 120, 22–31.

Liu, T., Ma, B., Chen, X., Ni, B., Peng, Y., Guo, J., 2017. Evaluation of mainstream nitrogen removal by simultaneous partial nitrification, anammox and denitrification (SNAD) process in a granule-based reactor. Chemical Engineering Journal. 327, 973–981.

Liu, T., Guo, J., Hu, S., Yuan, Z., 2020. Model-based investigation of membrane biofilm reactors coupling anammox with nitrite/nitrate-dependent anaerobic methane oxidation. Environment International. 137, 105501.

Lotti, T., Kleerebezem, R., Lubello, C., van Loosdrecht, M.C.M., 2014. Physiological and kinetic characterization of a suspended cell anammox culture. Water Research. 60, 1–14.

Lotti, T., Kleerebezem, R., Abelleira-Pereira, J.M., Abbas, B., van Loosdrecht, M.C.M., 2015. Faster through training : The anammox case. Water Research, 81, 261–268.

Luo, J., Chen, H., Han, X., Sun, Y., Yuan, Z., Guo, J., 2017. Microbial community structure and biodiversity of size-fractionated granules in a partial nitritation – anammox process. FEMS Microbiology Ecology. 93, 1–10.

Ma, Y., Domingo-fe, C., Gy, B., Smets, B. F., 2017. Intermittent Aeration Suppresses Nitrite-Oxidizing Bacteria in Membrane-Aerated Biofilms : A Model-Based Explanation. Environmental Science and Technology. 51, 6146–6155.

Marie, P.S, Pumpel, T., Markt, R., Murthy, S., Bott, C., Wett, B., 2015. Comparative evaluation of multiple methods to quantify and characterise granular anammox biomass. Water Research. 68, 194–205.

Martin, K., Sathyamoorthy, S., Houweling, D., Long, Z., Peeters, J., Snowling, S., 2017. A Sensitivity Analysis of Model Parameters Influencing the Biofilm Nitrification Rate :

Comparison between the Aerated Biofilm Reactor (MABR) and Integrated Fixed Film Activated Sludge (IFAS) Process. Water Environment Federation, 257-265.

Matsumoto, S., Terada, A., Tsuneda, S., 2007. Modeling of membrane-aerated biofilm : Effects of C/N ratio, biofilm thickness and surface loading of oxygen on feasibility of simultaneous nitrification and denitrification. Biochemical Engineering Journal. 37, 98–107.

Moussa, M.S., Hooijmans, C.M., Lubberding, H.J., Gijzen, H.J., 2005. Modelling nitrification, heterotrophic growth and predation in activated sludge. Water Research. 39, 5080–5098.

Mozumder, M.S.I., Picioreanu, C., van Loosdrecht, M.C.M., Volcke, E.I.P., 2014. Effect of heterotrophic growth on autotrophic nitrogen removal in a granular sludge reactor. Environmental Technology. 35(8), 1027–1037.

Ni, S., Sung, S., Yue, Q., Gao, B., 2012. Substrate removal evaluation of granular anammox process in a pilot-scale upflow anaerobic sludge blanket reactor. Ecological Engineering. 38(1), 30–36.

Ni, B., Smets, B.F., Yuan, Z., Pellicer-Nàcher, C., 2013. Model-based evaluation of the role of Anammox on nitric oxide and nitrous oxide productions in membrane aerated biofilm reactor. Journal of Membrane Science. 446, 332–340.

Ni, B., Joss, A., Yuan, Z., 2014. Modeling nitrogen removal with partial nitritation and anammox in one floc-based sequencing batch reactor. Water Research. 67, 321–329.

Pellicer-Nàcher, C., Franck, S., Ruscalleda, M., Terada, A., Al-soud, A., Hansen, M.A., Søren, J., Smets, B.F., 2013. Sequentially aerated membrane biofilm reactors for autotrophic nitrogen removal : microbial community composition and dynamics. Microbial Biotechnology. 7, 32–43.

Pérez, J., Lotti, T., Kleerebezem, R., Picioreanu, C., van Loosdrecht, M.C.M., 2014. Outcompeting nitrite-oxidizing bacteria in single- stage nitrogen removal in sewage treatment plants : A model-based study. Water Research. 66, 208–218.

Rodriguez-Sanchez, A., Purswani, J., Lotti, T., van Loosdrecht, M.C.M., Vahala, R., Gonzalez-Martinez, A., 2016. Distribution and microbial community structure analysis of a single-stage partial nitritation / anammox granular sludge bioreactor operating at low temperature. Environmental Technology, 37(18), 2281–2291.

Salatul Islam Mozumder, M., Goormachtigh, L., Garcia-Gonzalez, L., De Wever, H., Volcke, E.I.P., 2014. Modeling pure culture heterotrophic production of polyhydroxybutyrate (PHB). Bioresource Technology. 155, 272–280.

Song, Y., Liao, Q., Yu, C., Xiao, R., Tang, C., 2017. Physicochemical and microbial properties of settled and floating anammox granules in upflow reactor. Biochemical Engineering Journal. 123, 75–85.

Stewart, P. S., 1998. A Review of Experimental Measurements of Effective Diffusive Permeabilities and Effective Diffusion Coefficients in Biofilms. Biotechnology and Bioengineering. 59 (3), 261 -272.

Stewart, P.S., 2003. Diffusion in Biofilms. Journal of bacteriology. 185 (5), 1485–1491.

Strous, M., Heijnen, J.J., Kuenen, J.G., Jetten, M.S.M., 1998. The sequencing batch reactor as a powerful tool for the study of slowly growing anaerobic ammonium-oxidizing microorganisms. Applied Microbial Biotechnology. 50, 589–596.

Tang, C., Duan, C., Yu, C., Song, Y., 2017. Removal of nitrogen from wastewaters by anaerobic ammonium oxidation (ANAMMOX) using granules in upflow reactors. Environmental Chemistry Letters. 15(2), 311–328.

Udert, K. M., Kind, E., Teunissen, M., Jenni, S., Larsen, T.A., 2008. Effect of heterotrophic growth on nitritation/anammox in a single sequencing batch reactor. Water Science and Technology. 58.2, 277–284.

Vannecke, T.P.W., Wells, G., Hubaux, N., Morgenroth, E., Volcke, E.I.P., 2015. Considering microbial and aggregate heterogeneity in biofilm reactor models : how far do we need to go ?. Water Science and Technology. 72.10, 1692–1699.

Vlaeminck, S.E., Terada, A., Smets, B.F., Clippeleir, D., Schaubroeck, T., Bolca, S., Demeestere, L., Mast, J., Boon, N., Carballa, M., Verstraete, W., 2010. Aggregate Size and Architecture Determine Microbial Activity Balance for One-Stage Partial Nitritation and Anammox. Applied and Environmental Microbiology. 76(3), 900–909.

Volcke, E.I.P., Picioreanu, C., De Baets, B., van Loosdrecht, M.C.M., 2010. Effect of granule size on autotrophic nitrogen removal in a granular sludge reactor. Environmental Technology. 31:11, 1271–1280.

Wäsche, S., Horn, H., Hempel, D.C., 2002. Influence of growth conditions on biofilm development and mass transfer at the bulk/biofilm interface. Water Research. 36 (19), 4775–4784.

Wang, T., Zhang, H., Yang, F., Liu, S., Fu, Z., Chen, H., 2009. Start-up of the Anammox process from the conventional activated sludge in a membrane bioreactor. Bioresource Technology. 100(9), 2501–2506.

Wang, R., Xiao, F., Wang, Y., Lewandowski, Z., 2016. Determining the optimal trans-membrane gas pressure for nitrification in membrane-aerated biofilm reactors based on oxygen profile analysis. Applied Microbiology and Biotechnology. 100, 7699–7711.

Wang, Y., Chen, J., Zhou, S., Wang, X., Chen, Y., Lin, X., Yan, Y., Ma, X., Wu, M., 2017. 16S rRNA gene high-throughput sequencing reveals shift in nitrogen conversion related microorganisms in a CANON system in response to salt stress. Chemical Engineering Journal. 317, 512–521.

Wang, X., Yang, H., Su, Y., Liu, X., 2020. Characteristics and mechanism of anammox granular sludge with different granule size in high load and low rising velocity sewage treatment. Bioresource Technology. 312, 123608.

Wiesmann, U., 1994. Biological nitrogen removal from wastewater. Advances in Biochemical Engineering & Biotechnology. 51, 113–154.

Xu, D., Kang, D., Yu, T., Ding, A., Lin, Q., Zhang, M., Hu, Q., Zheng, P., 2019. A secret of high-rate mass transfer in anammox granular sludge : "Lung-like breathing". Water Research. 154, 189–198.

You, Q., Wang, J., Qi, G., Zhou, Y., 2020. Anammox and partial denitrification coupling : a review. RSC Advances. 12554–12572.

Yue, X., Yu, G., Lu, Y., Liu, Z., Li, Q., Tang, J., Liu, J., 2018. Effect of dissolved oxygen on nitrogen removal and the microbial community of the completely autotrophic nitrogen removal over nitrite process in a submerged aerated biological filter. Bioresource Technology. 254, 67–74.

Zekker, I., Kiviru, A., Mandel, A., Jaagura, M., Tenno, T., 2019. Enhanced Efficiency of Nitritating-Anammox Sequencing Batch Reactor Achieved at Low Decrease Rates of Oxidation–Reduction Potential. Environmental Engineering Science. 36(3), 1–11.

Zhang, X., Li, D., Liang, Y., Zeng, H., He, Y., Zhang, Y., Zhang, J., 2014. Performance and microbial community of completely autotrophic nitrogen removal over nitrite (CANON) process in two membrane bioreactors (MBR) fed with different substrate levels. Bioresource Technology. 152, 185–191.

Zhang, L., Narita, Y., Gao, L., Ali, M., Oshiki, M., Okabe, S., 2017. Maximum specific growth rate of anammox bacteria revisited. Water Research. 116, 296–303.

Zhang, X., Liu, Y., Zhang, J., Chen, Y., Wang, Q., 2020. Impact of COD/N on anammox granular sludge with different biological carriers. Science of the Total Environment. 728, 138557.

6. Conclusions and future work

This thesis presents the importance of applying mathematical models in wastewater treatment processes to test novel technologies for nitrogen and MP removal. Mathematical models were developed and calibrated to describe MABR and Anammox processes as innovative technologies for efficient nitrogen removal during wastewater treatment processes. Also, MP degradation using hydrolytic enzymes was investigated using mathematical model calibration with experimental results. Therefore, mathematical models are effective tools for better understanding of removal mechanisms, determining the optimal operational conditions for efficient removal rate and implementing novel technologies on large scale nitrogen and MP removal applications.

6.1 Chapter 2: nitrogen removal using membrane aerated biofilm reactor (MABR)

A comprehensive MABR model was developed and calibrated with a pilots-scale operation data to simulate the mass transport and biological reactions in the MABR biofilm, bulk solution and the oxygen partial pressure along the MABR membrane fibers. In the pilot operation, it was found that the increasing influent ammonia loading rate and oxygen supply rate enhanced the ammonia removal rate; however, the influent C/N ratio hardly affected the ammonia removal rate. The model simulation results showed that the bulk ammonia concentration is a dominant parameter on efficient nitrification in the MABR biofilm for municipal wastewater while it has a negligible effect on nitrification for high-strength wastewater. Also, limited soluble COD can negatively affect the denitrification in the MABR biofilm. Based on the numerical simulation

results, the biofilm thickness should be kept at 600 µm or thicker to house both the aerobic and anoxic zones in the biofilm for simultaneous nitrification and denitrification. It was also found that the liquid film thickness is not an important factor for nitrification; however, thick liquid films limit denitrification because of the slow transport of soluble COD through the liquid film. The C/N ratio is a dominant parameter in MABR operation only for high-strength wastewater due to the competition between X_H and X_{AOB} for oxygen.

In this study, a linear change in the oxygen partial pressure was assumed to estimate the oxygen concentration at the membrane side. However, micro-sensors can be used for observing the oxygen concentration for more accurate calibration process. Also, the biofilm thickness was assumed to be constant along the membrane height and over the pilot operation; however, accurate measurement of biofilm thickness is required for better estimation of the model calibration targets. The attachment and detachment mechanisms between the biofilm and bulk solution can be included in the mathematical model.

6.2 Chapter 3: microplastic (MP) removal using hydrolytic enzymes

Lab-scale experiments were conducted to estimate the kinetic constants for polyethylene MP degradation using hydrolytic enzymes at different temperature and enzyme dose conditions. It was found that protease was the most effective enzyme on MP reduction while lipase was the least efficient enzyme. Based on the experimental results, the increasing enzyme concentration and temperature enhanced the reduction of MP. In a 3-day batch experiment, most of MP beads were degraded in the first seven hours of operation while the removal rate was negligible after 24

hours of the experiment. The effect of repeated doses of protease and multiple enzymes on the removal of MP was investigated.

A non-steady state mathematical model was developed and calibrated using the lab-scale experimental results to estimate the kinetic constant of MP reduction by an enzyme ($k_{1,i}$) and the enzyme self-decay constant ($k_{2,ii}$). The mathematical model was also applied to simulate the multiple enzymes batch experiment, considering the interaction between the two enzymes using an interactive-decay constant ($k_{2,CP}$). The calibrated model kinetic constants were used to approximate the MP removal in anaerobic digestion process where it was found that the retention time is the most important parameter on MP degradation.

For the future work, additional experimental work can be conducted to quantify the MP degradation in anaerobic digestion where hydrolytic enzymes are rich in concentration. The experimental results can be compared with the model simulation results, confirming the validity of kinetic constants in anaerobic digestion applications. Moreover, additional sets of experimental work can be performed to assess the effect of pH, particle diameter of MP beads and MP material type on the MP removal and the reaction kinetic constants.

6.3 Chapter 4: nitrogen removal by anaerobic ammonia oxidation (Anammox) process

A non-steady state mathematical model was developed and calibrated using experimental results from previous lab-scale Anammox studies. Based on the simulation results of the calibrated model, moderate dissolved oxygen concentration was required for maintain successful

nitrogen removal by Anammox bacteria. Moreover, nitrite concentration is a governing parameter on nitrogen removal by Anammox bacteria. It was also found that the nitrite-based real-time aeration is an effective technique to limit the growth of nitrite oxidizing bacteria in low and high-strength wastewater, providing favorable conditions for Anammox process. Therefore, it is highly recommended to apply a real-time monitoring of nitrite concentration for broad Anammox bacteria applications in cost-efficient biological wastewater treatment.

In this study, lab-scale experimental results from previous Anammox studies were used for model calibration; however, more experimental work can be performed to cover other operational conditions (e.g., bulk pH and temperature) and assess their effect on the kinetic constants of Anammox bacteria. Also, additional experimental work can be conducted to simulate the real-time aeration based on nitrite concentration, validating the mathematical model results. Different aeration schemes based on real-time monitoring of bulk concentration can be implemented to optimize the nitrogen removal with high contribution of Anammox process coupled with less aeration cost.

6.4 Chapter 5: enrichment of anaerobic ammonia oxidation (Anammox) bacteria

A steady-state mathematical model was developed and calibrated using previous Anammox studies to determine the kinetics of Anammox bacteria, liquid film thickness and diffusion coefficient of soluble components in the granule during Anammox bacteria enrichment process. Based on the simulation results of the calibrated model, it was found that the maximum specific growth rate constant (μ_{ANA}) and oxygen half saturation constant of X_{ANA} ($K_{O_2}^{ANA}$) of

X_{ANA} were dominant parameters on the Anammox population while the decay rate constant (b_{ANA}) of X_{ANA} did not significantly affect the Anammox bacteria enrichment process.

Moreover, the competition between X_{AOB} and X_{ANA} for ammonia and X_{ANA} and X_{NOB} for nitrite has an important role on Anammox granulation process. It was also found that the Anammox population is more sensitive to the kinetic constants of X_{AOB} and X_{NOB} at moderate DO concentration; however, either extremely low or high DO resulted in insensitivity of Anammox bacteria enrichment process to these kinetic constants. Based on the sensitivity analysis results, liquid film thickness was an important parameter on the Anammox bacteria granules as the oxygen mass transfer to the granule was controlled by the resistive liquid film. It was also found that large granules (granule diameter > 1000 μm) are recommended for better Anammox granulation.

In this study, previous Anammox model studies were used for model calibration; however, experimental work is essential to investigate the actual mechanisms of Anammox granulation and the governing parameters on the enrichment process. For example, liquid film thickness and diffusion coefficient of soluble components can be estimated by calibrating the mathematical model with lab-scale/pilot-scale experimental results.

Appendix A: Supplementary information for chapter 2

Comprehensive model applications for better understanding of pilot-scale membrane-aerated biofilm reactor performance

Table A1. The statistical parameters of ammonia, nitrate and COD removal rate of the pilot operation.

Statistical parameter	Ammonia removal rate (kg-N/day)	Nitrate removal rate (kg-N/day)	COD removal rate (kg-COD/day)
Average (Ẋ)	4.0	0.36	11.1
Median (M)	3.8	1.0	10.3
First quartile ($\boldsymbol{Q_1}$)	3.2	-1.86	5.8
Third quartile ($\boldsymbol{Q_3}$)	4.4	2.3	15.5
Upper fence ($\boldsymbol{U_f}$)	6.3	8.5	30
Lower fence ($\boldsymbol{L_f}$)	1.3	-8.0	-8.8

Table A2. Matrix of the stoichometrices and process rate for the biological reactions (Adopted from Matsumoto et al., 2007).

Process	S_{O_2}	S_{COD}	S_{NH_4}	S_{NO_2}	S_{NO_3}	X_H	X_{AOB}	X_{NOB}	X_S	Process rate (g-COD/(m^3 day))
Heterotrophic Bacteria										
Aerobic growth	$-(1-Y_H)/Y_H$	$-1/Y_H$	$-i_{NBM}$			1				$\mu_H \left(\frac{S_{COD}}{K_{COD}^H + S_{COD}}\right)\left(\frac{S_{O_2}}{K_{O_2}^H + S_{O_2}}\right)\left(\frac{S_{NH_4}}{K_{NH_4}^H + S_{NH_4}}\right) X_H$
Anoxic growth (NO_2)		$-1/Y_H$	$-i_{NBM}$	$-(1-Y_H)/1.71Y_H$		1				$\mu_H \eta_d \left(\frac{S_{COD}}{K_{COD}^H + S_{COD}}\right)\left(\frac{S_{NO_2}}{K_{NO_2}^H + S_{NO_2}}\right)\left(\frac{K_{O_2}^H}{K_{O_2}^H + S_{O_2}}\right)\left(\frac{S_{NH_4}}{K_{NH_4}^H + S_{NH_4}}\right) X_H$
Anoxic growth (NO_3)		$-1/Y_H$	$-i_{NBM}$		$-(1-Y_H)/2.86Y_H$	1				$\mu_H \eta_d \left(\frac{S_{COD}}{K_{COD}^H + S_{COD}}\right)\left(\frac{S_{NO_3}}{K_{NO_3}^H + S_{NO_3}}\right)\left(\frac{K_{O_2}^H}{K_{O_2}^H + S_{O_2}}\right)\left(\frac{S_{NH_4}}{K_{NH_4}^H + S_{NH_4}}\right) X_H$
Aerobic endogenous respiration	$-(1-f_i)$					-1			$1-f_i$	$b_H \left(\frac{S_{O_2}}{K_{O_2}^H + S_{O_2}}\right) X_H$
Anoxic endogenous respiration (NO_2)				$-(1-f_i)/1.71$		-1			$1-f_i$	$b_H \eta_H \left(\frac{S_{NO_2}}{K_{NO_2}^H + S_{NO_2}}\right)\left(\frac{K_{O_2}^H}{K_{O_2}^H + S_{O_2}}\right) X_H$
Anoxic endogenous respiration (NO_3)					$-(1-f_i)/2.86$	-1			$1-f_i$	$b_H \eta_H \left(\frac{S_{NO_3}}{K_{NO_3}^H + S_{NO_3}}\right)\left(\frac{K_{O_2}^H}{K_{O_2}^H + S_{O_2}}\right) X_H$
AOB										
Aerobic growth	$-(3.43-Y_{AOB})/Y_{AOB}$		$-1/Y_{AOB} - i_{NBM}$	$1/Y_{AOB}$			1			$\mu_{AOB} \left(\frac{S_{O_2}}{K_{O_2}^{AOB} + S_{O_2}}\right)\left(\frac{S_{NH_4}}{K_{NH_4}^{AOB} + S_{NH_4}}\right) X_{AOB}$
Aerobic endogenous respiration	$-(1-f_i)$						-1		$1-f_i$	$b_{AOB} \left(\frac{S_{O_2}}{K_{O_2}^{AOB} + S_{O_2}}\right) X_{AOB}$
Anoxic endogenous respiration (NO_2)				$-(1-f_i)/1.71$			-1		$1-f_i$	$b_{AOB} \eta_H \left(\frac{S_{NO_2}}{K_{NO_2}^{AOB} + S_{NO_2}}\right)\left(\frac{K_{O_2}^{AOB}}{K_{O_2}^{AOB} + S_{O_2}}\right) X_{AOB}$
Anoxic endogenous respiration (NO_3)					$-(1-f_i)/2.86$		-1		$1-f_i$	$b_{AOB} \eta_H \left(\frac{S_{NO_3}}{K_{NO_3}^{AOB} + S_{NO_3}}\right)\left(\frac{K_{O_2}^{AOB}}{K_{O_2}^{AOB} + S_{O_2}}\right) X_{AOB}$
NOB										
Aerobic growth	$-(1.14-Y_{NOB})/Y_{NOB}$		$-i_{NBM}$	$-1/Y_{NOB}$	$1/Y_{NOB}$			1		$\mu_{NOB} \left(\frac{S_{O_2}}{K_{O_2}^{NOB} + S_{O_2}}\right)\left(\frac{S_{NH_4}}{K_{NH_4}^{NOB} + S_{NH_4}}\right)\left(\frac{S_{NO_2}}{K_{NO_2}^{NOB} + S_{NO_2}}\right) X_{NOB}$
Aerobic endogenous respiration	$-(1-f_i)$							-1	$1-f_i$	$b_{NOB} \left(\frac{S_{O_2}}{K_{O_2}^{NOB} + S_{O_2}}\right) X_{NOB}$
Anoxic endogenous respiration (NO_2)				$-(1-f_i)/1.71$				-1	$1-f_i$	$b_{NOB} \eta_H \left(\frac{S_{NO_2}}{K_{NO_2}^{NOB} + S_{NO_2}}\right)\left(\frac{K_{O_2}^{NOB}}{K_{O_2}^{NOB} + S_{O_2}}\right) X_{NOB}$
Anoxic endogenous respiration (NO_3)					$-(1-f_i)/2.86$			-1	$1-f_i$	$b_{NOB} \eta_H \left(\frac{S_{NO_3}}{K_{NO_3}^{NOB} + S_{NO_3}}\right)\left(\frac{K_{O_2}^{NOB}}{K_{O_2}^{NOB} + S_{O_2}}\right) X_{NOB}$
Hydrolysis										
Hydrolysis		1							-1	$q_H \left(\frac{X_S/X_H}{K_X + X_S/X_H}\right) X_H$

Table A3. Monthly average wastewater temperature, ammonia, nitrate and COD removal rate for the pilot operation data.

Month	**Wastewater temperature (°C)**	**Ammonia removal rate (kg-N/day)**	**Nitrate removal rate (kg-N/day)**	**COD removal rate (kg-COD/day)**
February	13.1 ± 0.08	2.34 ± 0.50	-0.60 ± 0.23	9.36 ± 3.47
March	13.0 ± 0.01	4.81 ± 0.35	-2.35 ± 1.01	4.31 ± 2.03
April	12.8 ± 0.01	4.17 ± 0.24	-3.81 ± 0.79	10.06 ± 7.52
May	14.3 ± 0.55	4.31 ± 0.96	-2.50 ± 1.02	8.28 ± 4.60
June	17.1 ± 0.53	4.16 ± 0.46	-3.46 ± 0.61	4.24 ± 4.83
July	18.8 ± 0.45	3.92 ± 0.63	-1.95 ± 1.43	5.31 ± 3.14
August	20.1 ± 0.25	4.73 ± 1.02	-0.35 ± 2.03	11.40 ± 7.21
September	20.5 ± 0.30	4.09 ± 0.52	1.57 ± 2.34	13.93 ± 6.13
October	20.1 ± 0.44	3.94 ± 0.64	2.30 ± 0.58	14.45 ± 6.69
November	17.8 ± 0.73	3.49 ± 0.67	1.82 ± 0.59	12.69 ± 4.67
December	16.0 ±0.60	3.21 ± 0.31	2.27 ± 0.63	13.42 ± 7.96
January	13.1 ±0.87	3.14 ± 0.79	1.35 ± 2.10	7.83 ± 5.29
February	12.9 ± 0.30	2.72 ± 0.68	1.25 ± 0.93	13.03 ± 6.90
March	12.3 ± 0.32	3.65 ± 0.47	0.63 ± 0.79	11.61 ± 4.50

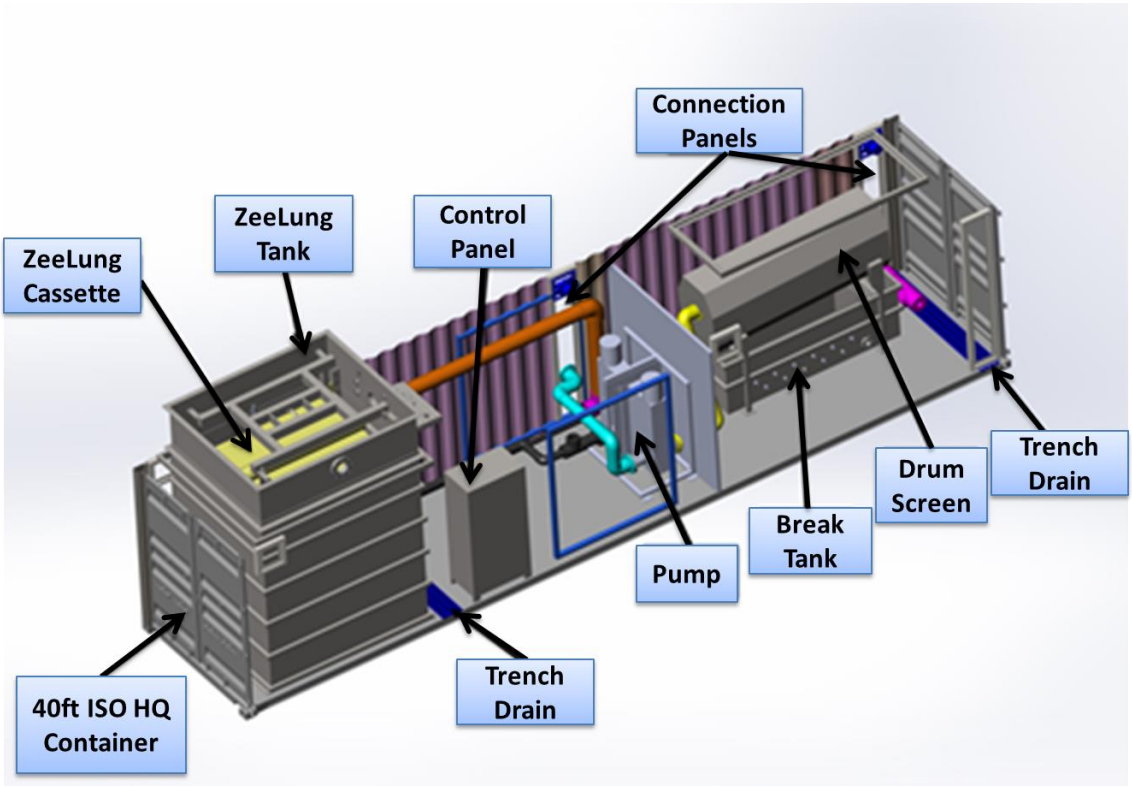

Fig. A1. Schematic diagram of Zeelung MABR pilot system that was installed and operated at a local wastewater treatment plant (SUEZ Water Technologies and Solutions)

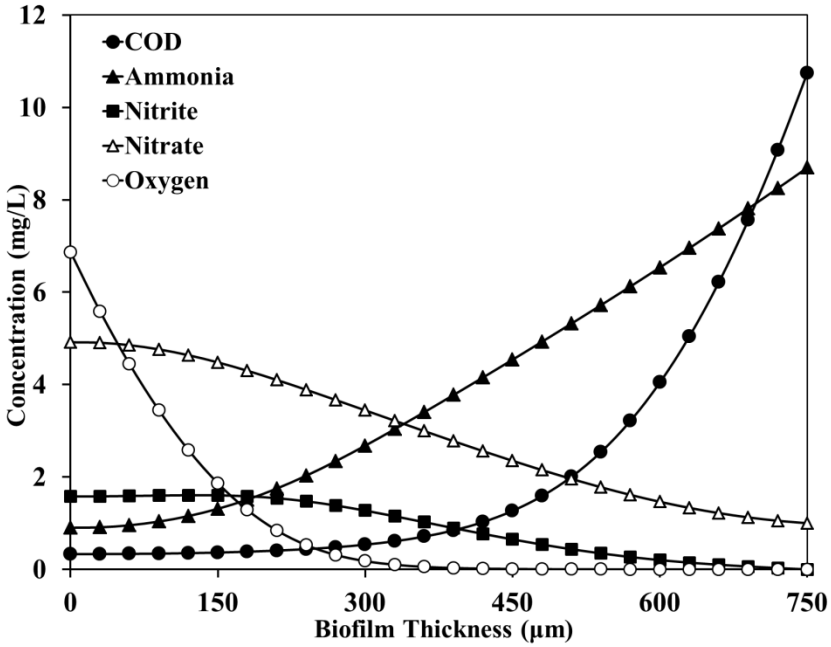

Fig. A2. Concentration profiles of soluble components within the biofilm thickness. This figure is identical to Fig. 2b in a previous MABR study (Matsumoto et al., 2007) and was used for validating the numerical simulation results of the proposed one-dimensional scale MABR steady state model in our study.

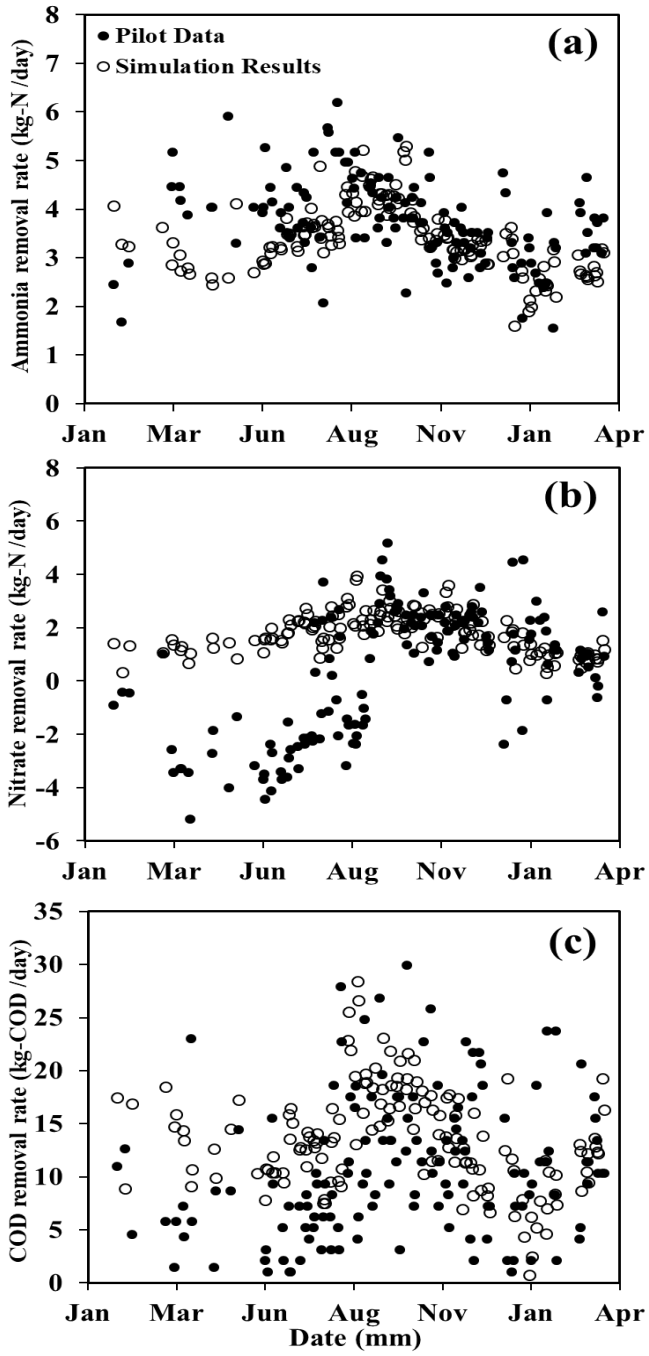

Fig. A3. Comparison between pilot operational data and the model simulation results: (a) ammonia removal, (b) nitrate removal and (c) COD removal. (Simulation conditions: biofilm thickness = 1000 μm, liquid film thickness = 250 μm, other conditions were assumed based on parameters in Tables 1, 2 and 3. The simulation results included the biological reactions in the biofilm and the bulk solution.

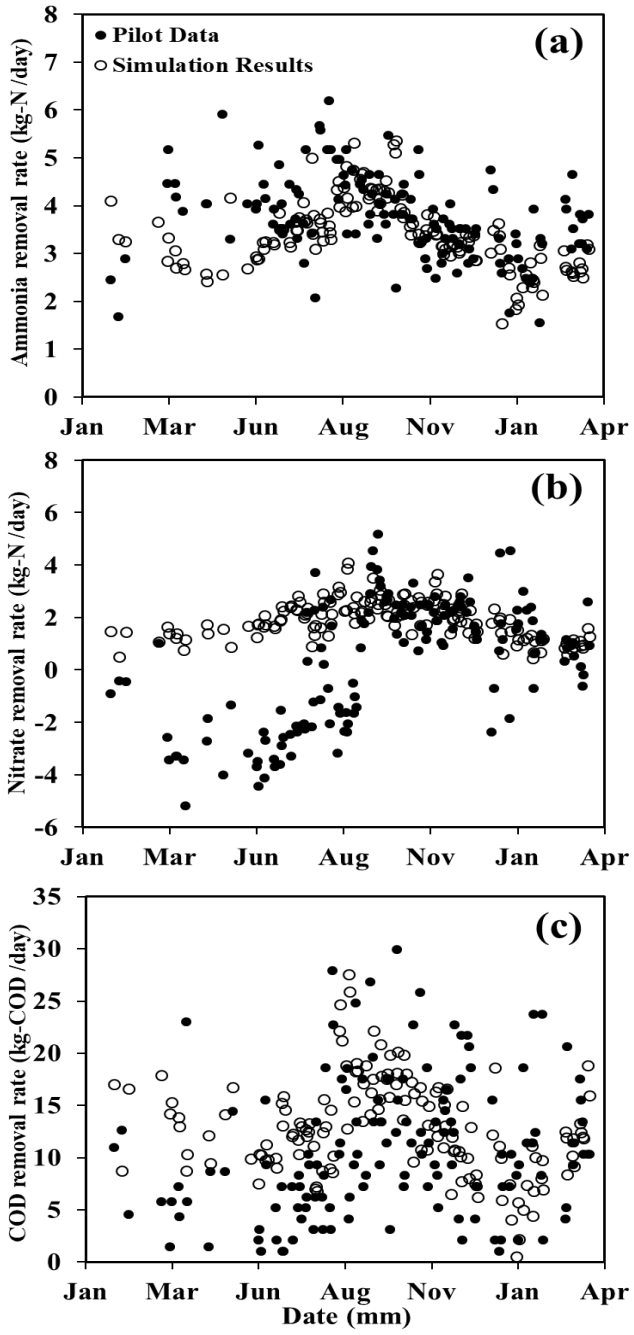

Fig. A4. Comparison between pilot operational data and the model simulation results: (a) ammonia removal, (b) nitrate removal and (c) COD removal. (Simulation conditions: biofilm thickness = 1250 μm, liquid film thickness = 250 μm, other conditions were assumed based on parameters in Tables 1, 2 and 3. The simulation results included the biological reactions in the biofilm and the bulk solution.

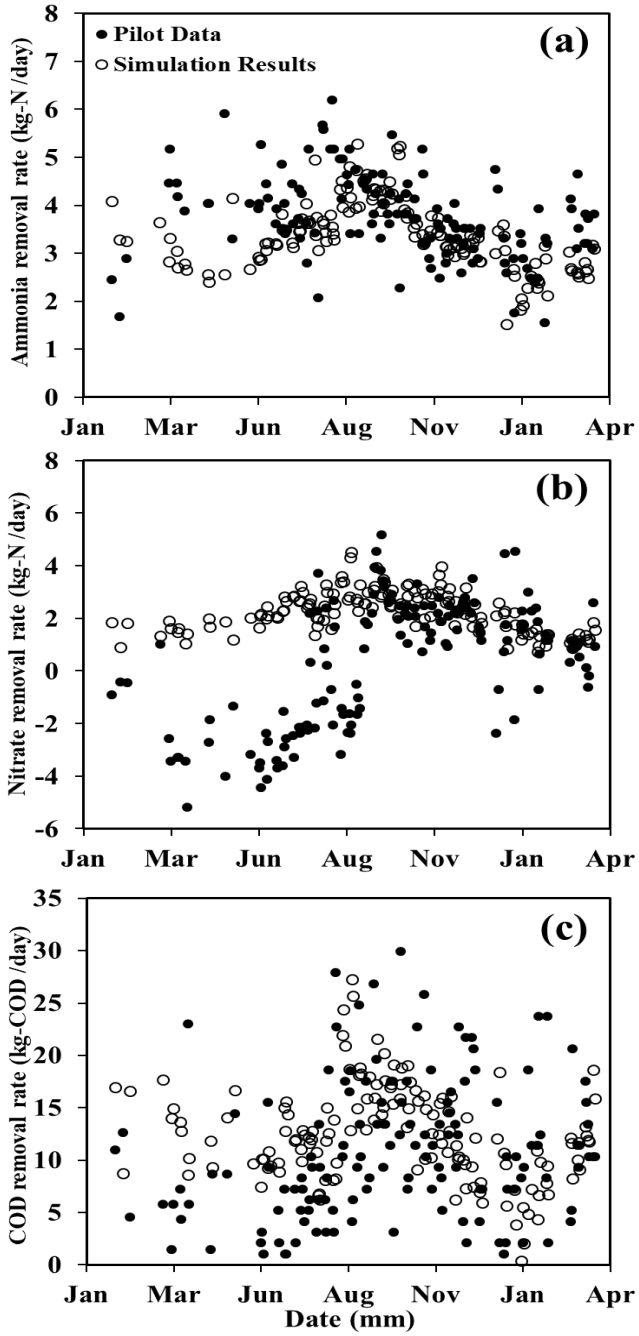

Fig. A5. Comparison between pilot operational data and the model simulation results: (a) ammonia removal, (b) nitrate removal and (c) COD removal. (Simulation conditions: biofilm thickness = 1750 μm, liquid film thickness = 250 μm, other conditions were assumed based on parameters in Tables 1, 2 and 3. The simulation results included the biological reactions in the biofilm and the bulk solution.

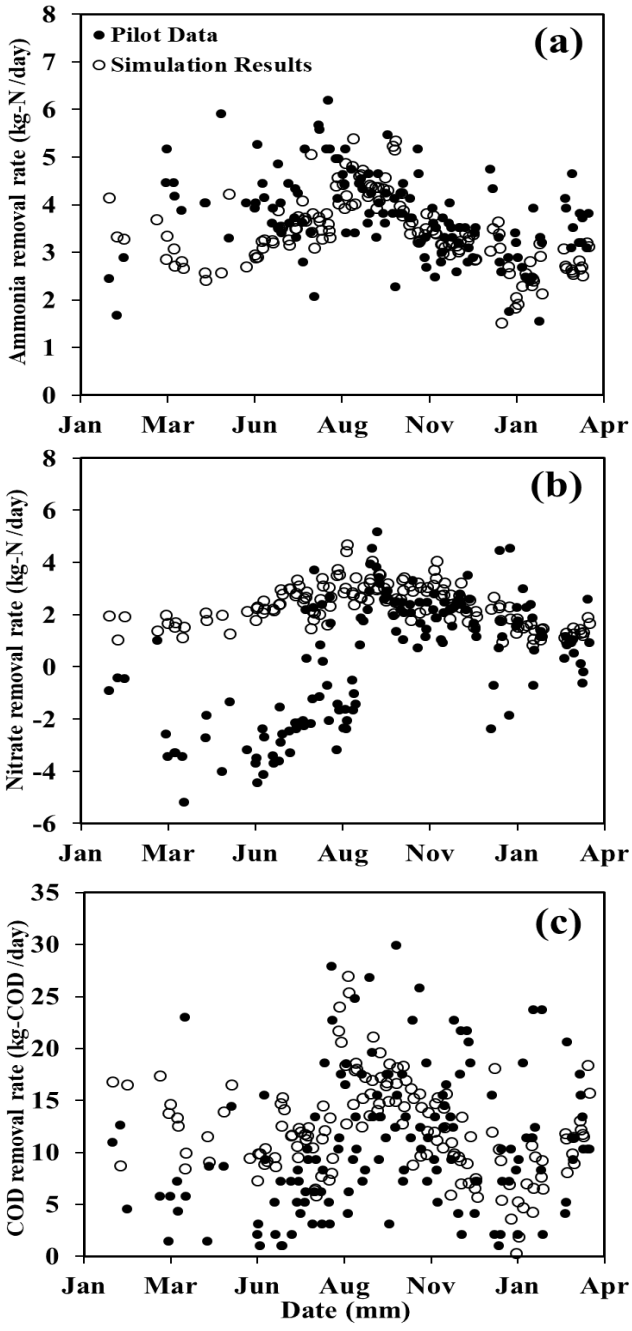

Fig. A6. Comparison between pilot operational data and the model simulation results: (a) ammonia removal, (b) nitrate removal and (c) COD removal. (Simulation conditions: biofilm thickness = 2000 μm, liquid film thickness = 250 μm, other conditions were assumed based on parameters in Tables 1, 2 and 3. The simulation results included the biological reactions in the biofilm and the bulk solution.

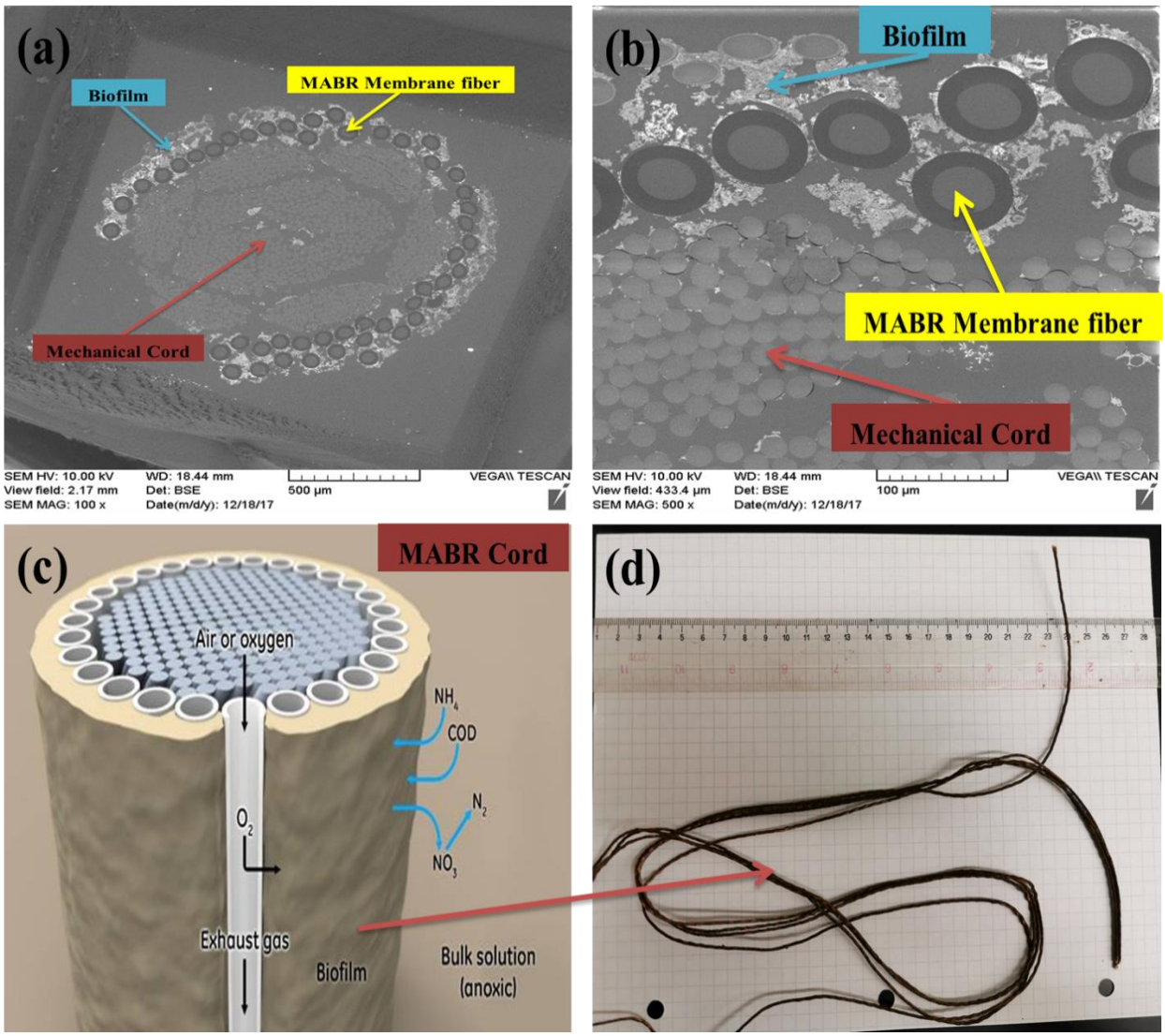

Fig. A7. Detailed description of the MABR cord (mechanical cord, MABR membrane fibers and the attached biofilm on the membrane surface): (a), (b) SEM image of the MABR cord, (c) schematic image of the MABR cord and (d) photograph of the MABR cord. Note that the biofilm was shrank and partially fell off while the membrane sample was dried and processed for the SEM analysis. The biofilm was initially much thicker when the sample was still wet.

References

Matsumoto, S., Terada, A., Tsuneda, S., 2007. Modeling of membrane-aerated biofilm : Effects of C/N ratio, biofilm thickness and surface loading of oxygen on feasibility of simultaneous nitrification and denitrification. Biochemical Engineering Journal. 37, 98–107.

Appendix B: Supplementary information for chapter 4

Mathematical model application for real-time aeration based on nitrite level in Anammox process

Table B1. Matrix of the stoichometrices and process rate for the biological reactions.

Process	S_{O_2}	S_{COD}	S_{NH_4}	S_{NO_2}	S_{NO_3}	X_H	X_{AOB}	X_{NOB}	X_{ANA}	X_S	Process rate (g-COD/(m^3 day))
Heterotrophic Bacteria											
Aerobic growth	$-(1-Y_H)/Y_H$	$-1/Y_H$	$-i_{NBM}$			1					$\mu_H \left(\frac{S_{COD}}{K^H_{COD}+S_{COD}}\right)\left(\frac{S_{O_2}}{K^H_{O_2}+S_{O_2}}\right)\left(\frac{S_{NH_4}}{K^H_{NH_4}+S_{NH_4}}\right)X_H$
Anoxic growth (NO_2)		$-1/Y_H$	$-i_{NBM}$	$-(1-Y_H)/1.71Y_H$		1					$\mu_H\,\eta_d \left(\frac{S_{COD}}{K^H_{COD}+S_{COD}}\right)\left(\frac{S_{NO_2}}{K^H_{NO_2}+S_{NO_2}}\right)\left(\frac{K^H_{O_2}}{K^H_{O_2}+S_{O_2}}\right)\left(\frac{S_{NH_4}}{K^H_{NH_4}+S_{NH_4}}\right)X_H$
Anoxic growth (NO_3)		$-1/Y_H$	$-i_{NBM}$		$-(1-Y_H)/2.86Y_H$	1					$\mu_H\,\eta_d \left(\frac{S_{COD}}{K^H_{COD}+S_{COD}}\right)\left(\frac{S_{NO_3}}{K^H_{NO_3}+S_{NO_3}}\right)\left(\frac{K^H_{O_2}}{K^H_{O_2}+S_{O_2}}\right)\left(\frac{S_{NH_4}}{K^H_{NH_4}+S_{NH_4}}\right)X_H$
Decay						-1				$1-f_l$	$b_H X_H$
AOB Bacteria											
Aerobic growth	$-(3.43-Y_{AOB})/Y_{AOB}$		$-1/Y_{AOB}-i_{NBM}$	$1/Y_{AOB}$			1				$\mu_{AOB}\left(\frac{S_{O_2}}{K^{AOB}_{O_2}+S_{O_2}}\right)\left(\frac{S_{NH_4}}{K^{AOB}_{NH_4}+S_{NH_4}}\right)X_{AOB}$
Decay							-1			$1-f_l$	$b_{AOB}\,X_{AOB}$
NOB Bacteria											
Aerobic growth	$-(1.14-Y_{NOB})/Y_{NOB}$		$-i_{NBM}$	$-1/Y_{NOB}$	$1/Y_{NOB}$			1			$\mu_{NOB}\left(\frac{S_{O_2}}{K^{NOB}_{O_2}+S_{O_2}}\right)\left(\frac{S_{NH_4}}{K^{NOB}_{NH_4}+S_{NH_4}}\right)\left(\frac{S_{NO_2}}{K^{NOB}_{NO_2}+S_{NO_2}}\right)X_{NOB}$
Decay								-1		$1-f_l$	$b_{NOB}\,X_{NOB}$
Anammox Bacteria											
Anoxic growth (NO_2)			$-1/Y_{ANA}-i_{NBM}$	$-1/Y_{ANA}-1/1.14$	$1/1.14$				1		$\mu_{ANA}\left(\frac{S_{NH_4}}{K^{ANA}_{NH_4}+S_{NH_4}}\right)\left(\frac{S_{NO_2}}{K^{ANA}_{NO_2}+S_{NO_2}}\right)\left(\frac{K^{ANA}_{O_2}}{K^{ANA}_{O_2}+S_{O_2}}\right)X_{ANA}$
Decay									-1	$1-f_l$	$b_{ANA}\,X_{ANA}$
Hydrolysis											
Hydrolysis		1								-1	$q_H\left(\frac{X_S/X_H}{K_X+X_S/X_H}\right)X_H$

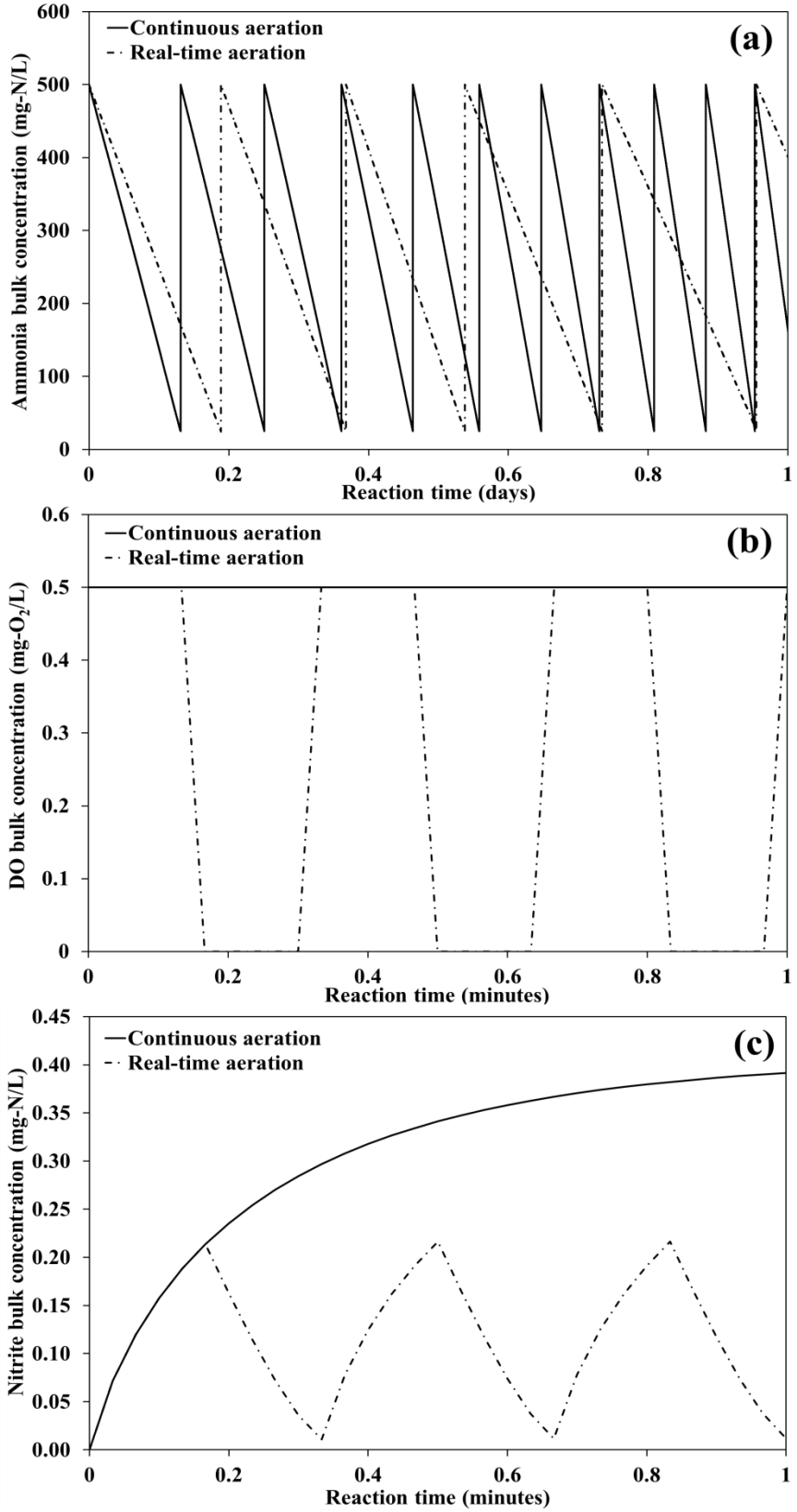
(a)
Continuous aeration
Real-time aeration
Ammonia bulk concentration (mg-N/L)
Reaction time (days)
(b)
Continuous aeration
Real-time aeration
DO bulk concentration (mg-O2/L)
Reaction time (minutes)
(c)
Continuous aeration
Real-time aeration
Nitrite bulk concentration (mg-N/L)
Reaction time (minutes)

Fig. B1. Comparison between the effect of continuous and real-time aeration on: (a) ammonia concentration, (b) DO concentration, and (c) nitrite concentration. (Simulation conditions are mentioned in Table 1 and 2, nitrite-based aeration is: If $S_{NO_2} \leq 0.05 \rightarrow$ DO = 0.5 mg-O_2/L for 10 seconds and If $S_{NO_2} > 0.05 \rightarrow$ DO = 0 for 10 seconds).

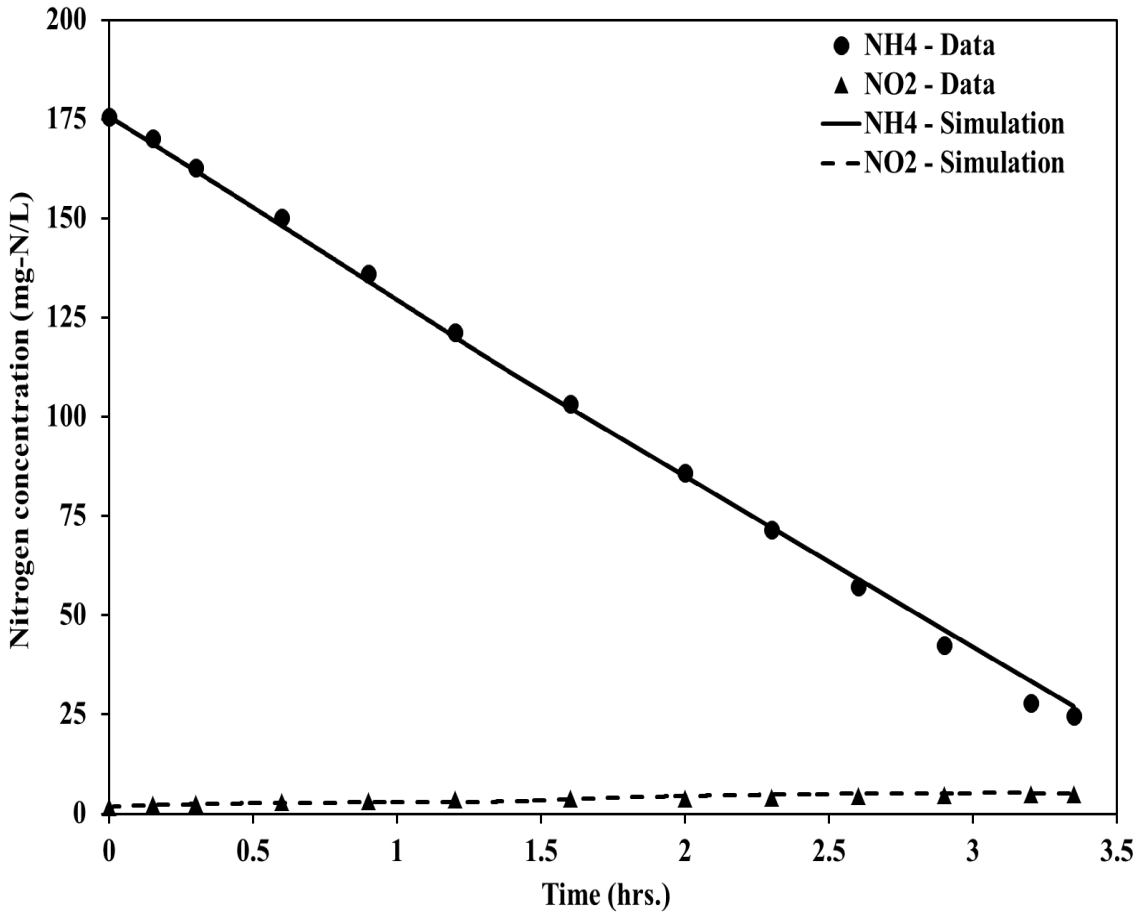

Fig. B2. Comparison between the simulation results of the non-steady state model and the experimental data of study B (Ni et al., 2014) for model calibration. (Simulation conditions are mentioned in Table 1 and 2).

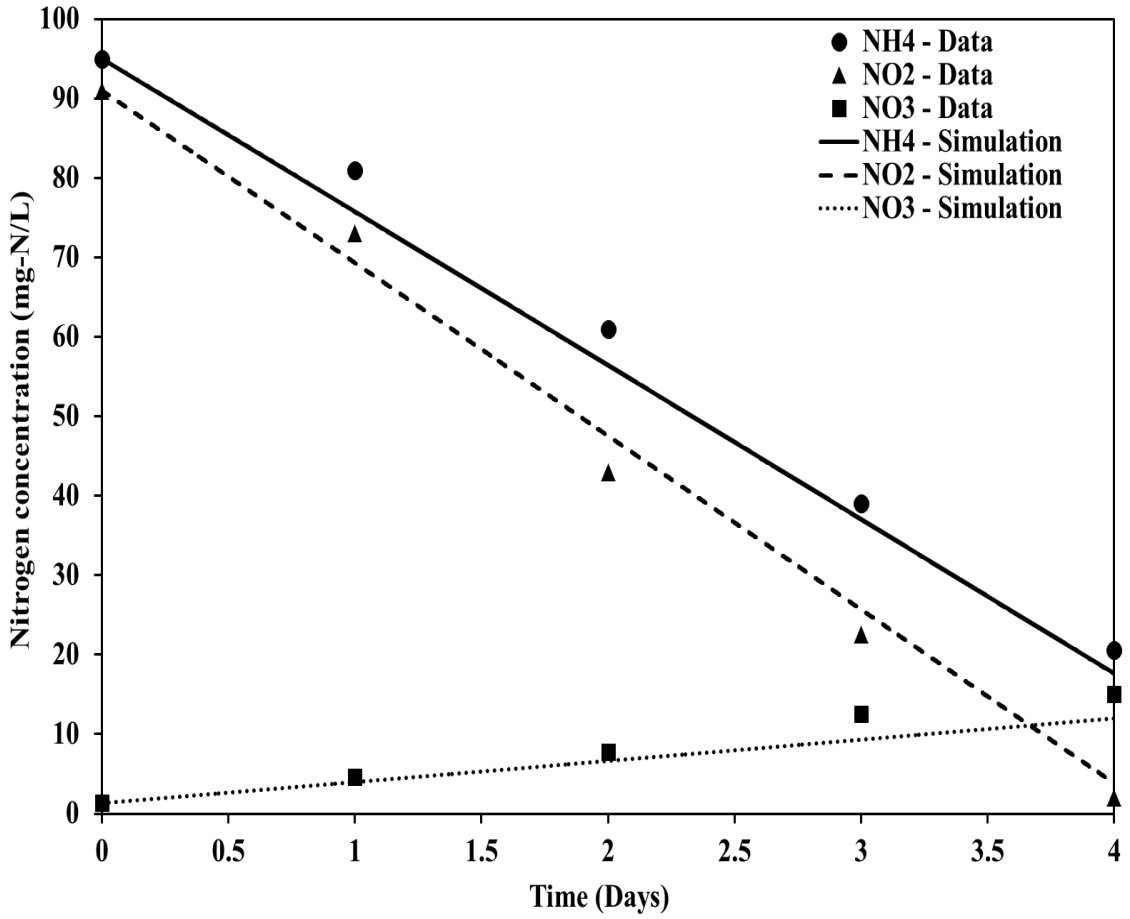

Fig. B3. Comparison between the simulation results of the non-steady state model and the experimental data of study C (Gong et al., 2007) for model calibration. (Simulation conditions are mentioned in Table 1 and 2).

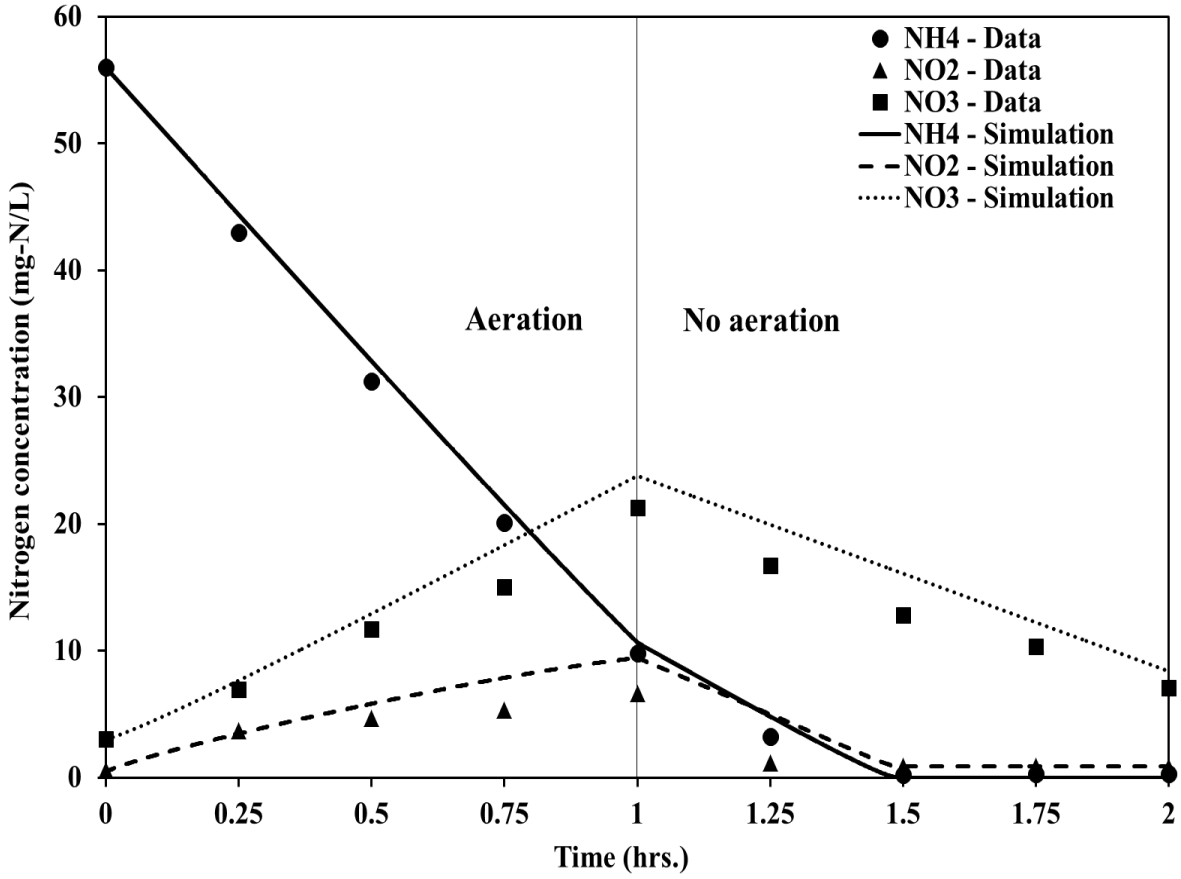

Fig. B4. Comparison between the simulation results of the non-steady state model and the experimental data of study D (Li et al., 2020) for model calibration. (Simulation conditions are mentioned in Table 1 and 2).

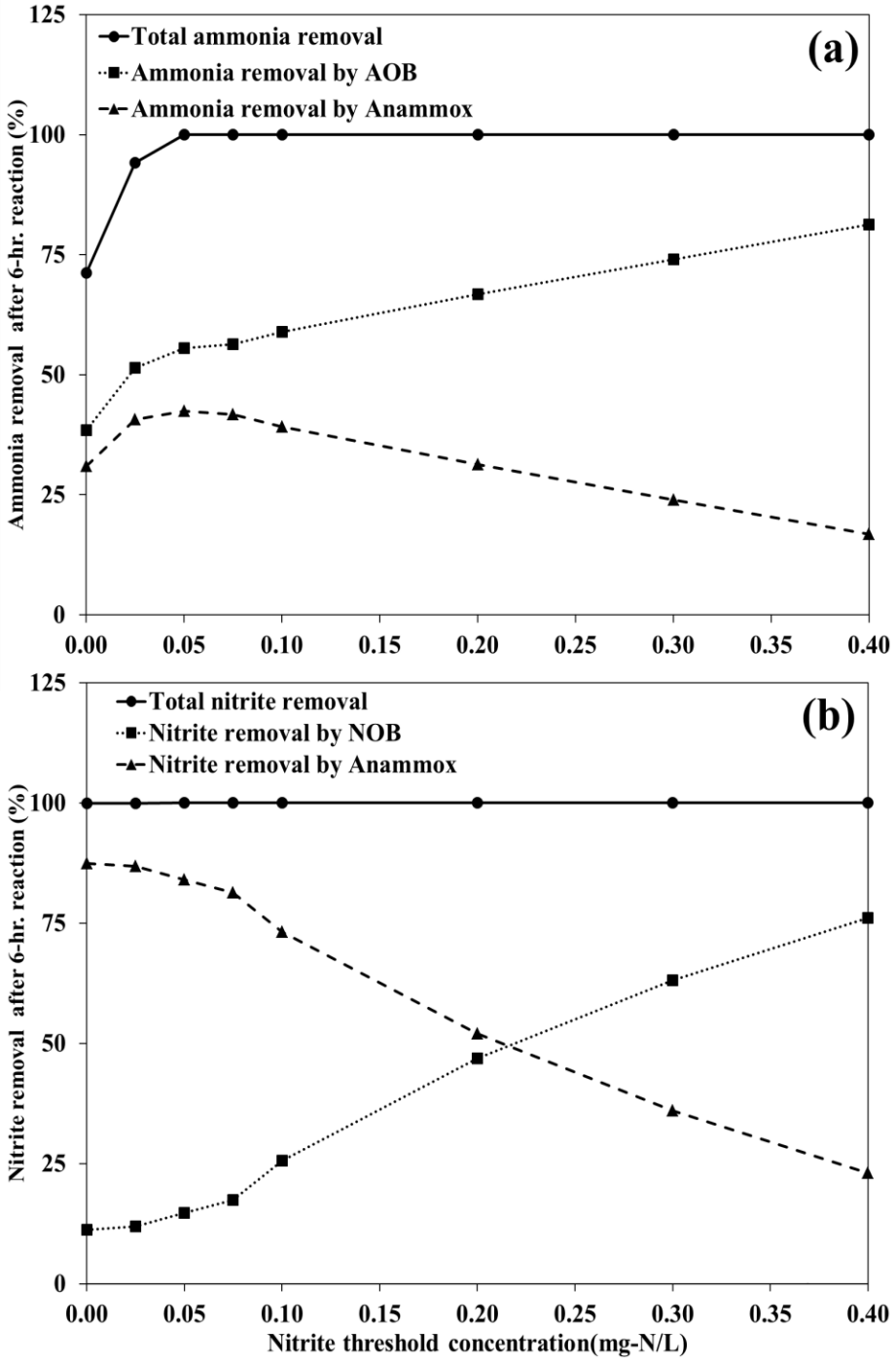

Fig. B5. Effect of the nitrite threshold concentration ($S_{NO_2}\big|_{ON}$) for high-strength wastewater on the contribution of: (a) X_{AOB} and X_{ANA} in the ammonia removal, (b) X_{NOB} and X_{ANA} in the nitrite removal. (Simulation conditions are mentioned in Table 1 and 2, real-time aeration is: If $S_{NO_2} < S_{NO_2}\big|_{ON}$ → DO = 0.5 mg-O_2/L and If $S_{NO_2} > S_{NO_2}\big|_{ON}$ → DO = 0).

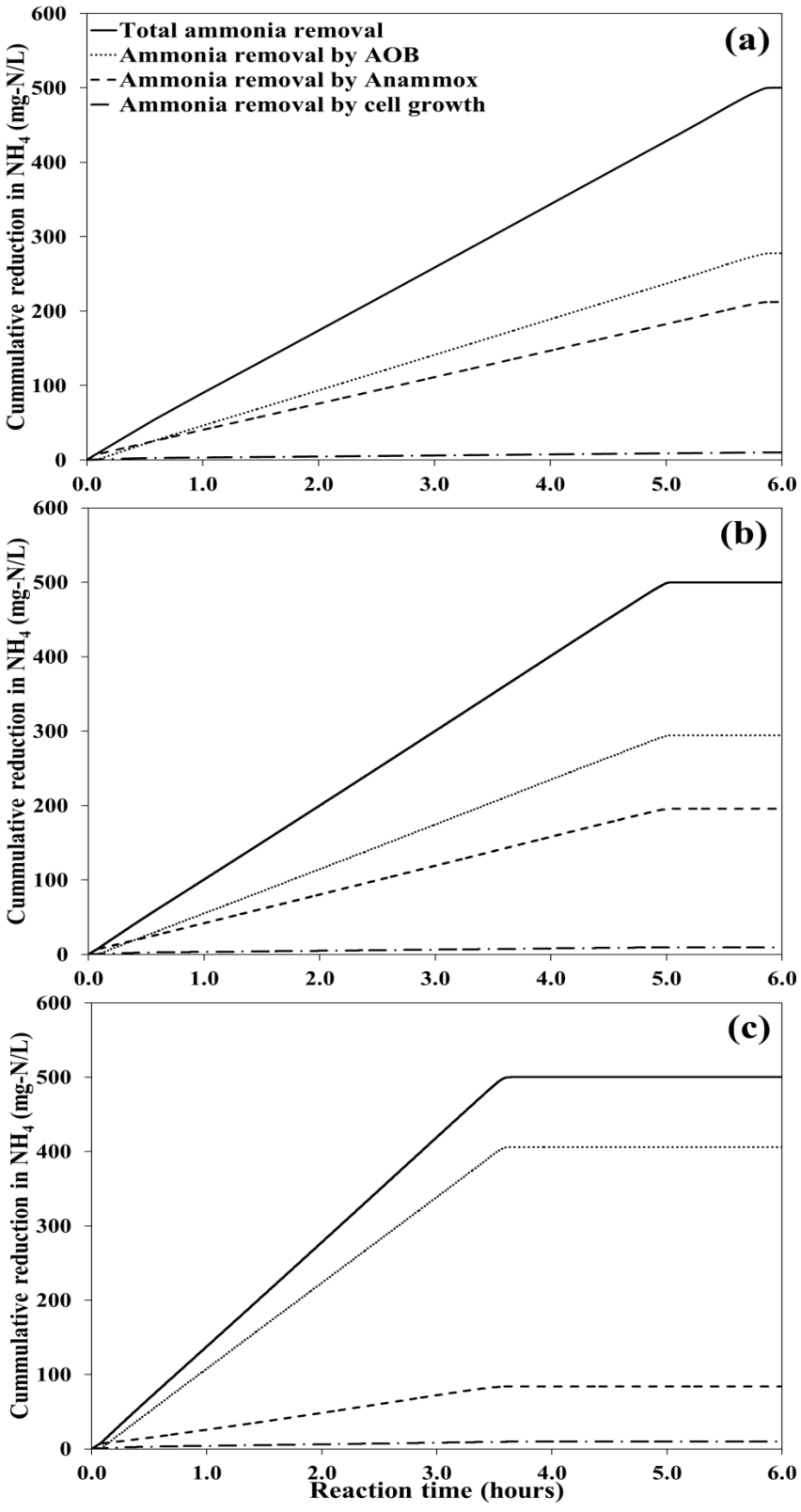
Total ammonia removal
Ammonia removal by AOB
Ammonia removal by Anammox
Ammonia removal by cell growth
(a)
(b)
(c)
Cummulative reduction in NH4 (mg-N/L)
Reaction time (hours)
0
100
200
300
400
500
600
0.0
1.0
2.0
3.0
4.0
5.0
6.0

Fig. B6. Effect of the nitrite threshold concentration ($S_{NO_2}\big|_{ON}$) on the contribution of X_{AOB}, X_{ANA} and cell growth in the cumulative removal of ammonia concentration for high-strength wastewater at nitrite threshold of: (a) 0.05 mg-N/L, (b) 0.10 mg-N/L, and (c) 0.40 mg-N/L. (Simulation conditions are mentioned in Table 1 and 2, real-time aeration is: If $S_{NO_2} < S_{NO_2}\big|_{ON}$ → DO = 0.5 mg-O_2/L and If $S_{NO_2} > S_{NO_2}\big|_{ON}$ → DO = 0).

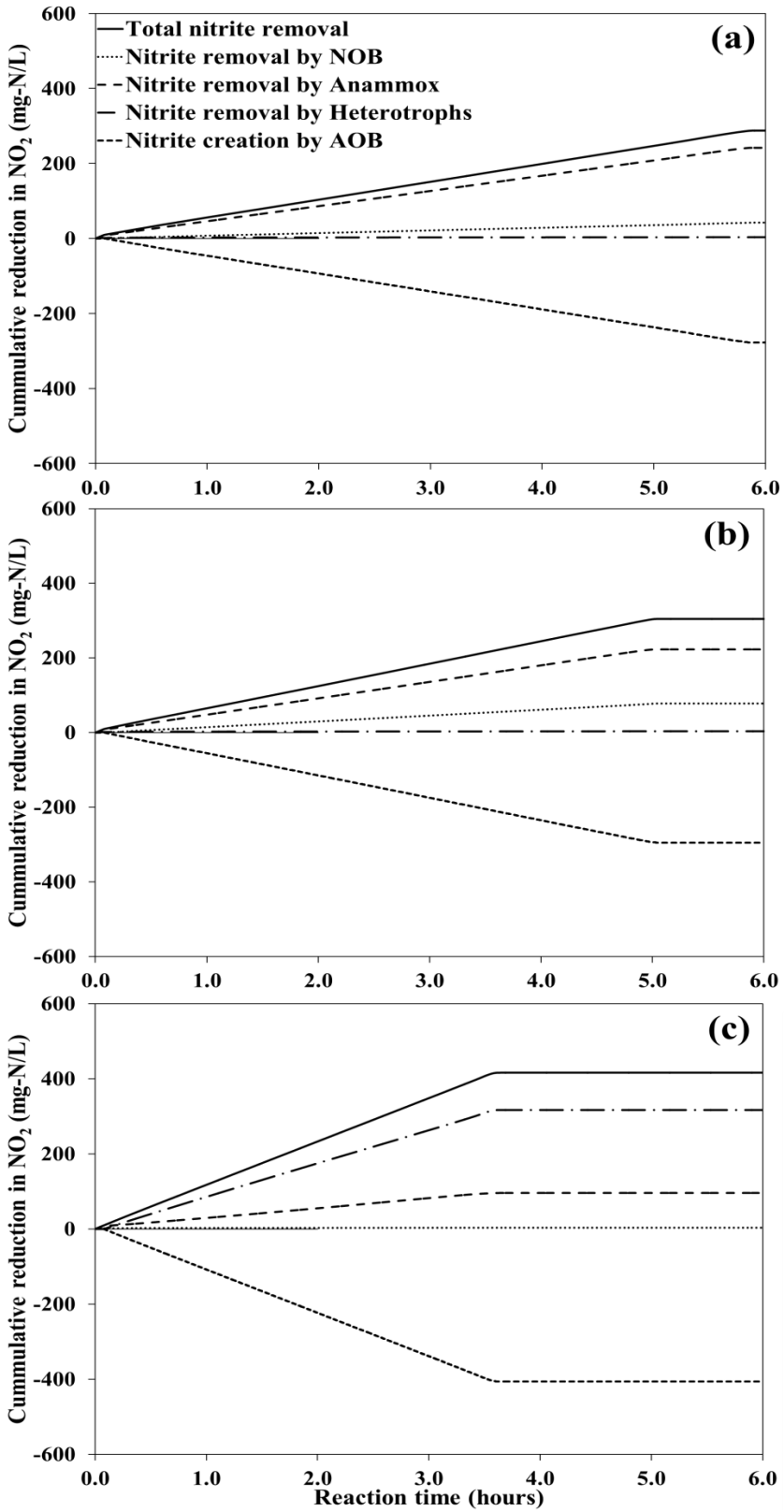
(a)
(b)
(c)
Total nitrite removal
Nitrite removal by NOB
Nitrite removal by Anammox
Nitrite removal by Heterotrophs
Nitrite creation by AOB
Cummulative reduction in NO2 (mg-N/L)
Reaction time (hours)
600
400
200
0
-200
-400
-600
0.0
1.0
2.0
3.0
4.0
5.0
6.0

Fig. B7. Effect of the nitrite threshold concentration ($S_{NO_2}\big|_{ON}$) on the contribution of X_{NOB}, $X_{ANA}$and heterotrophs in the cumulative removal of nitrite concentration for high-strength wastewater at nitrite threshold of: (a) 0.05 mg-N/L, (b) 0.10 mg-N/L, and (c) 0.40 mg-N/L. (Simulation conditions are mentioned in Table 1 and 2, real-time aeration is: If $S_{NO_2} < S_{NO_2}\big|_{ON}$ → DO = 0.5 mg-O_2/L and If $S_{NO_2} > S_{NO_2}\big|_{ON}$ → DO = 0). Negative values mean creation of nitrite by X_{AOB}.

References

Gong, Z., Yang, F., Liu, S., Bao, H., Hu, S., Furukawa, K., 2007. Feasibility of a membrane-aerated biofilm reactor to achieve single-stage autotrophic nitrogen removal based on Anammox. Chemosphere. 69, 776–784.

Li, J., Peng, Y., Zhang, L., Li, X., Zhang, Q., Yang, S., Gao, Y., Li, S., 2020. Improving Efficiency and Stability of Anammox through Sequentially Coupling Nitritation and Denitritation in a Single-Stage Bioreactor. Environmental Science and Technology. 54, 10859–10867.

Ni, B., Joss, A., Yuan, Z., 2014. Modeling nitrogen removal with partial nitritation and anammox in one floc-based sequencing batch reactor. Water Research. 67, 321–329.

Appendix C: Supplementary information for chapter 5

Sensitivity analysis on important kinetic constants in Anammox bacteria enrichment process using a mathematical model

Table C1. Matrix of the stoichometrices and process rate for the biological reactions.

Process	S_{O_2}	S_{COD}	S_{NH_4}	S_{NO_2}	S_{NO_3}	X_H	X_{AOB}	X_{NOB}	X_{ANA}	X_S	Process rate (g-COD/(m^3 day))
Heterotrophic Bacteria											
Aerobic growth	$-(1-Y_H)/Y_H$	$-1/Y_H$	$-i_{NBM}$			1					$\mu_H \left(\frac{S_{COD}}{K^H_{COD}+S_{COD}}\right)\left(\frac{S_{O_2}}{K^H_{O_2}+S_{O_2}}\right)\left(\frac{S_{NH_4}}{K^H_{NH_4}+S_{NH_4}}\right)X_H$
Anoxic growth (NO_2)		$-1/Y_H$	$-i_{NBM}$	$-(1-Y_H)/1.71Y_H$		1					$\mu_H\,\eta_d \left(\frac{S_{COD}}{K^H_{COD}+S_{COD}}\right)\left(\frac{S_{NO_2}}{K^H_{NO_2}+S_{NO_2}}\right)\left(\frac{K^H_{O_2}}{K^H_{O_2}+S_{O_2}}\right)\left(\frac{S_{NH_4}}{K^H_{NH_4}+S_{NH_4}}\right)X_H$
Anoxic growth (NO_3)		$-1/Y_H$	$-i_{NBM}$		$-(1-Y_H)/2.86Y_H$	1					$\mu_H\,\eta_d \left(\frac{S_{COD}}{K^H_{COD}+S_{COD}}\right)\left(\frac{S_{NO_3}}{K^H_{NO_3}+S_{NO_3}}\right)\left(\frac{K^H_{O_2}}{K^H_{O_2}+S_{O_2}}\right)\left(\frac{S_{NH_4}}{K^H_{NH_4}+S_{NH_4}}\right)X_H$
Decay						-1				$1-f_l$	$b_H X_H$
AOB Bacteria											
Aerobic growth	$-(3.43-Y_{AOB})/Y_{AOB}$		$-1/Y_{AOB}-i_{NBM}$	$1/Y_{AOB}$			1				$\mu_{AOB}\left(\frac{S_{O_2}}{K^{AOB}_{O_2}+S_{O_2}}\right)\left(\frac{S_{NH_4}}{K^{AOB}_{NH_4}+S_{NH_4}}\right)X_{AOB}$
Decay							-1			$1-f_l$	$b_{AOB}\,X_{AOB}$
NOB Bacteria											
Aerobic growth	$-(1.14-Y_{NOB})/Y_{NOB}$		$-i_{NBM}$	$-1/Y_{NOB}$	$1/Y_{NOB}$			1			$\mu_{NOB}\left(\frac{S_{O_2}}{K^{NOB}_{O_2}+S_{O_2}}\right)\left(\frac{S_{NH_4}}{K^{NOB}_{NH_4}+S_{NH_4}}\right)\left(\frac{S_{NO_2}}{K^{NOB}_{NO_2}+S_{NO_2}}\right)X_{NOB}$
Decay								-1		$1-f_l$	$b_{NOB}\,X_{NOB}$
Anammox Bacteria											
Anoxic growth (NO_2)			$-1/Y_{ANA}-i_{NBM}$	$-1/Y_{ANA}-1/1.14$	$1/1.14$				1		$\mu_{ANA}\left(\frac{S_{NH_4}}{K^{ANA}_{NH_4}+S_{NH_4}}\right)\left(\frac{S_{NO_2}}{K^{ANA}_{NO_2}+S_{NO_2}}\right)\left(\frac{K^{ANA}_{O_2}}{K^{ANA}_{O_2}+S_{O_2}}\right)X_{ANA}$
Decay									-1	$1-f_l$	$b_{ANA}\,X_{ANA}$
Hydrolysis											
Hydrolysis		1								-1	$q_H\left(\frac{X_S/X_H}{K_X+X_S/X_H}\right)X_H$

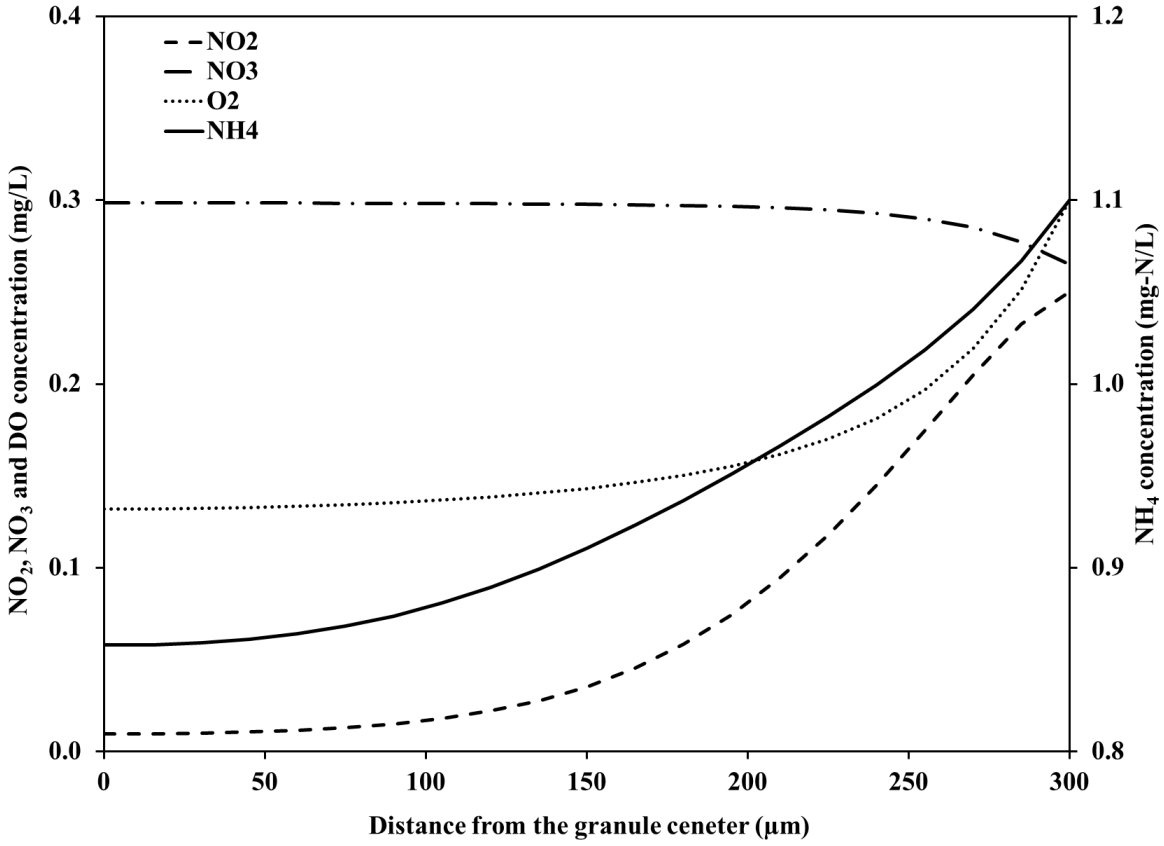

Fig. C1. Simulation results of the soluble components concentration profiles using the steady state granule model for Anammox bacteria enrichment, simulating the numerical simulation results of study B (Liu et al., 2017) for model calibration. (Simulation conditions are mentioned in Table 1 and 2).

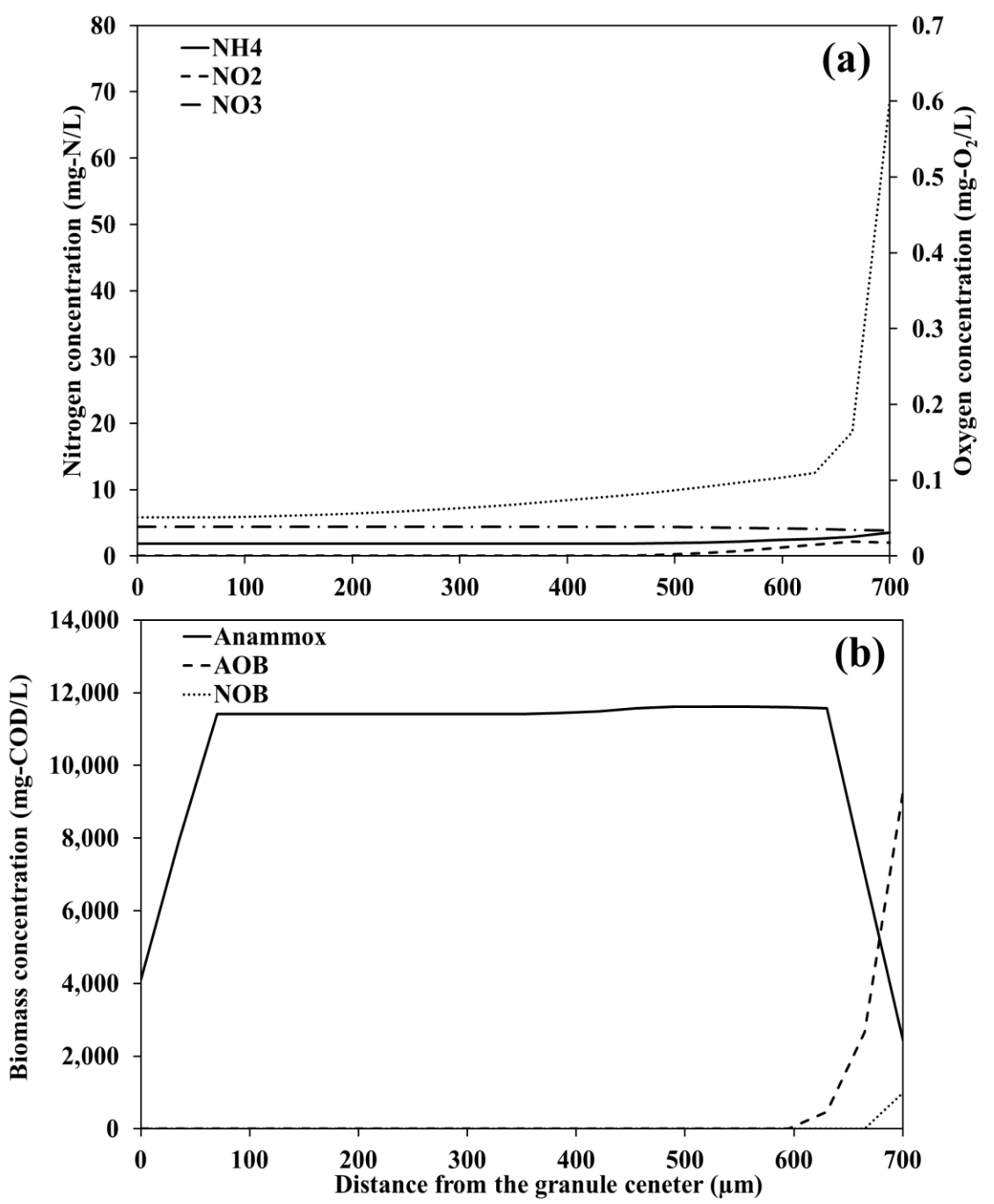

Fig. C2. Simulation results using the steady state granule model for Anammox bacteria enrichment, simulating the numerical simulation results of study C (Hao et al., 2002) for model calibration: (a) soluble components concentration profiles (i.e., ammonia, nitrite, nitrate and oxygen) and, (b) particulate components concentration profiles (i.e., X_{ANA} ,X_{AOB} and ,X_{NOB}). (Simulation conditions are mentioned in Table 1 and 2).

References

Hao, X., Heijnen, J.J., van Loosdrecht, M.C.M., 2002. Sensitivity Analysis of a Biofilm Model Describing a One-Stage Completely Autotrophic Nitrogen Removal (CANON) Process. Biotechnology and Bioengineering. 77(3), 266–277.

Liu, T., Ma, B., Chen, X., Ni, B., Peng, Y., Guo, J., 2017. Evaluation of mainstream nitrogen removal by simultaneous partial nitrification, anammox and denitrification (SNAD) process in a granule-based reactor. Chemical Engineering Journal. 327, 973–981.